Proceedings of the

Forty-Fifth
DOE Solar Photochemistry
P.I. Meeting

DoubleTree by Hilton DC North/Gaithersburg
Gaithersburg, Maryland
June 3-5, 2024

Chemical Sciences, Geosciences, and Biosciences Division
Office of Basic Energy Sciences
Office of Science
U.S. Department of Energy

FOREWORD

The 45th Department of Energy Solar Photochemistry Principal Investigators' Meeting, sponsored by the Chemical Sciences, Geosciences, and Biosciences Division of the Office of Basic Energy Sciences (BES), is being held June 3-5, 2024, at the DoubleTree by Hilton DC North/Gaithersburg in Gaithersburg, Maryland. These proceedings include the meeting agenda, abstracts of the formal presentations and posters, and a list of participants.

The Solar Photochemistry Program supports fundamental, molecular-level research on solar energy capture and conversion in the condensed phase and at interfaces. This conference is the annual meeting of the PIs who conduct research with support from this Program. The gathering is intended to facilitate the exchange of scientific ideas and foster collaboration among researchers.

We would like to express our thanks to Teresa Crockett of Basic Energy Sciences, as well as Paul Hudson and his colleagues at the Oak Ridge Institute for Science and Education for their assistance with meeting logistics. Finally, we are grateful to all of the participants in this meeting who have contributed so much to the continued success of the Solar Photochemistry Program.

Chris Fecko and Jennifer Roizen
Chemical Sciences, Geosciences,
and Biosciences Division
Office of Basic Energy Sciences

TABLE OF CONTENTS

Abstracts of Oral Presentations

Session I – Opening Session

Session II – Photochemistry of Photosensitizers

Session III – Semiconductor Architectures to Direct Photochemistry

Session IV – New Photoelectrodes

Session V – Photoinduced Charge Separation

Session VI – Probing Energy and Carrier Dynamics

Session VII – Molecular Catalysts for Solar Fuels Generation

Session VIII – Nitrogen Reduction

Session IX – Light-driven Dynamics in Linked Systems

Session X – Particle-based Photocatalysis

Session XI – Semiconductor Surface Phenomena

Abstracts of Poster Presentations

45th DOE SOLAR PHOTOCHEMISTRY PI MEETING

June 3-5, 2024

DoubleTree by Hilton Washington DC North / Gaithersburg MD

PROGRAM

Monday Morning, June 3

7:30 a.m.	Breakfast

SESSION I
Opening Session
Jenny Roizen, Chair

8:30 a.m.	News from DOE-BES Chemical Sciences, Geosciences, and Biosciences Division **Gail McLean**, DOE Office of Basic Energy Sciences
9:00 a.m.	Optical Generation and Manipulation of Spin Qubits **Martin L. Kirk**, University of New Mexico **David A Shultz**, North Carolina State University
9:30 a.m.	Multiproton-Coupled Electron Transfer (MPCET) in Artificial Photosynthetic Systems **Ana Moore**, Arizona State University
10:00 a.m.	Break

SESSION II
Photochemistry of Photosensitizers
Lisa Olshansky, Chair

10:30 a.m.	Fundamental Studies of the Vibrational, Electronic, and Photophysical Properties of Tetrapyrrolic Architectures **Dewey Holten**, Washington University
11:00 a.m.	Sensitizers for Solar Fuels Production: Group 4, 11 and 12 Metal Complexes **Stephen Bradforth** and **Mark Thompson**, University of Southern California

11:30 a.m. Heteroleptic Copper(I) Charge-Transfer Photosensitizers Supported by β-Diketiminates
Thomas S. Teets, University of Houston

11:45 a.m. Unlocking the Secrets of Intersystem Crossing in Photoexcited Lewis Acid Appended Mn(IV)-Oxo Complexes
Megan Lazorski, Metropolitan State University of Denver

12:00 p.m. Working Lunch (*Discussions about formulating a PIER Plan*)

Monday Afternoon, June 3

3:15 p.m. Solar Photochemistry Comments
Chris Fecko and Jenny Roizen, DOE Office of Basic Energy Sciences

SESSION III

Semiconductor Architectures to Direct Photochemistry

Erin Ratcliff, Chair

3:30 p.m. Symmetry Breaking in Semiconductor Nanocrystals for Controlling Charge Carrier and Spin Dynamics
Matthew C. Beard, National Renewable Energy Laboratory

4:00 p.m. Understanding Chiral-Induced Spin-Selectivity Effect for Solar Energy Conversion
Jing Gu, San Diego State University

4:15 p.m. When the Whole is Greater than the Sum of Its Parts: Understanding Photocatalytic Hydrogen Evolution in CdS Quantum Dots (QDs) vs. QD gels
Stephanie Brock, Wayne State University

4:30 p.m. Light-Controlled Multi-Electron Catalysis Coordinated across Time and Space
Junko Yano, Lawrence Berkeley National Laboratory

4:45 p.m. Break

SESSION IV

New Photoelectrodes

Rob Coridan, Chair

5:00 p.m. Development of Multicomponent Photoelectrodes for Solar Fuel Production
Kyoung-Shin Choi, University of Wisconsin-Madison

5:30 p.m. Multilayered Nanoporous Photoanodes of Mixed-Metal Oxides for Solar Water Splitting
Matt Law, University of California, Irvine

5:45 p.m. Molecularly Defined Multi-Metal Clusters for Solar Energy Conversion
Alex B.F. Martinson, Argonne National Laboratory

Monday Evening, June 3

6:00 p.m. Working Dinner (*Poster Preview Talks*)

7:30 p.m. Posters (*Odd numbers*)

Tuesday Morning, June 4

7:30 a.m. Breakfast

SESSION V

Photoinduced Charge Separation

Matt Bird, Chair

8:30 a.m. The Impact of Electric Fields on Electron Transfer at Metal Oxide-Electrolyte Interfaces
Gerald J. Meyer, University of North Carolina at Chapel Hill

9:00 a.m. Organic, Nanoscale, and Self-Assembled Structures Relevant to Solar Energy Conversion
Michael J. Therien, Duke University

9:30 a.m. Charge Generation in Mixed-Dimensionality Nanoscale Heterojunctions
Jeffrey L. Blackburn, National Renewable Energy Laboratory

10:00 a.m. Break

SESSION VI
Probing Energy and Carrier Dynamics
Justin Johnson, Chair

10:30 a.m. Identification of Nuclear Coordinates Driving Solar Energy Conversion Processes using Ultrafast Raman Techniques
Renee R. Frontiera, University of Minnesota

11:00 a.m. Spin Chemistry of Photoinduced Charge Separation
Jens Niklas, Argonne National Laboratory

11:30 a.m. Pulse Radiolysis Investigations of Excess Charges in Conjugated Molecules and Mechanisms of CO_2 Reduction Catalysis
David C. Grills, Brookhaven National Laboratory

12:00 p.m. Use of Carbonyl as an Infrared Reporter for Probing the Nature of Charges in Oligo- and Poly-(p-phenylene)s
Juchao Yan, Eastern New Mexico University

12:15 p.m. Spontaneous Enthalpy-Uphill Charge Separation – a Potential Way to Minimize Energy Loss for Charge Separation
Wai-Lun Chan, University of Kansas

12:30 p.m. Working Lunch (*Discussions about formulating a Data Management Plan*)

Tuesday Afternoon, June 4

SESSION VII
Molecular Catalysts for Solar Fuels Generation
Louise Berben, Chair

3:15 p.m. Ligand-based CO_2 Reduction and Water Oxidation: Can We Replace Ru with First-row Transition Metals within the Same Ligand Framework?
Javier J. Concepcion, Brookhaven National Laboratory

3:45 p.m. Solar-energy-driven Interfacial Multi-Electron-Transfer Catalytic Systems for Fuels
Djamaladdin G. Musaev, **Tianquan Lian**, and **Craig L. Hill**, Emory University

4:15 p.m. Kinetic Barriers to Metal Hydride Complex Formation in Fuel-forming Catalysis
Jillian L. Dempsey, University of North Carolina

4:45 p.m. Break

SESSION VIII
Nitrogen Reduction
Tom Hamann, Chair

5:00 p.m. Mechanism of Photochemical N_2 Reduction
Paul W. King, National Renewable Energy Laboratory

5:30 p.m. A Programmable, Non-Equilibrium Electrified Ammonia Synthesis for Efficient Hydrogen Storage
Yiguang Ju, Princeton University

5:45 p.m. Understanding Interfacial Phenomena for Solar H_2 Production and N_2 Reduction
Adam C. Nielander, SLAC National Accelerator Laboratory

Tuesday Evening, June 4

6:00 p.m. Working Dinner (*Poster Preview Talks*)

7:30 p.m. Posters (*Even numbers*)

Wednesday Morning, June 5

7:30 a.m. Breakfast

SESSION IX
Light-driven Dynamics in Linked Systems
Karen Mulfort, Chair

8:30 a.m. Reversible Photoinduced Ligand Detachment from CdSe Quantum Dots
John B. Asbury, Pennsylvania State University

9:00 a.m. Time-Resolved Studies of Photodynamic Metal Organic Frameworks
Amanda J. Morris, Virginia Tech

9:30 a.m. Light Harvesting, Energy Transport, and Energy Conversion with Molecular Frameworks
Joseph T. Hupp, Northwestern University

10:00 a.m. Break

SESSION X
Particle-based Photocatalysis
Shane Ardo, Chair

10:30 a.m. Dye-Sensitized Semiconductor Photoelectrodes and Z-Schemes for Solar Water Splitting
Thomas E. Mallouk, University of Pennsylvania

11:00 a.m. High-Resolution Nanoelectrochemical Studies of Photoelectrocatalytic Processes
Michael V. Mirkin, Queens College-CUNY

11:30 a.m. Non-contact Probes and Mechanism of Interface Charge-carrier Selectivity and Photovoltage Generation in Semiconductor Photocatalyst Particles
Shannon Boettcher, University of Oregon and University of California, Berkeley

12:00 p.m. Working Lunch (*Discussions about new directions for the field*)

Wednesday Afternoon, June 5

SESSION XI
Semiconductor Surface Phenomena
Mike Rose, Chair

1:15 p.m. Exploring the Connection between Electronic States and Surface Chemistry Using Photoelectron Spectroscopy
Sylwia Ptasinska, University of Notre Dame

1:45 p.m. Enhancing the Durability and Efficiency of III-V Photoelectrodes and Structured Cu_2O Photocathodes for Solar Fuels Production
Nathan S. Lewis, California Institute of Technology

2:15 p.m. Closing Comments
Chris Fecko and Jenny Roizen, DOE Office of Basic Energy Sciences

2:30 p.m. Adjourn

Optical Generation and Manipulation of Spin Qubits

Martin L. Kirk,[a] Anil Reddy Marri,[b] David A Shultz,[b] and Art van der Est[c]
[a]Department of Chemistry and Chemical Biology, University of New Mexico, Albuquerque, NM 87131-0001
[b]Department of Chemistry, North Carolina State University, Raleigh, NC 27695-8204
[c]Department of Chemistry, Brock University, St. Catharines, Ontario L2S 3A1 Canada

Stable spin-½ organic radicals that are covalently attached to a variety of chromophoric platforms represent an important class of open-shell molecules for understanding complex spin interactions in excited state (ES) processes. In particular, spin-orbit coupling, ES magnetic exchange interactions, vibronic spin-orbit coupling, intersystem crossing and internal conversion can all be controlled via the nature of the radical-chromophore coupling. Critical to quantum information science (QIS) applications, we have shown electron spin polarization (ESP) of both ground- and ESs, resulting in important structure-property relationships for controling both the sign and magnitude of the ESP.

Electron spin polarization is critical for the preparation of specific quantum states but also for signal enhancement. The latter is important in QIS applications since it reduces the need for ultra-high magentic fields or ultra-low temperatures. Our efforts continue to focus on square-planar (R-CAT)Pt(bpy) and related complexes comprised of a diamagnetic d^8 Pt(II) ion coordinated by catecholate (CAT) donor- and bipyridine (bpy) acceptor ligands that are elaborated by attaching an organic radical to the CAT or bpy ligands directly or via an organic bridge fragment (*e.g.*, **1-NN**, *Figure 1A*).

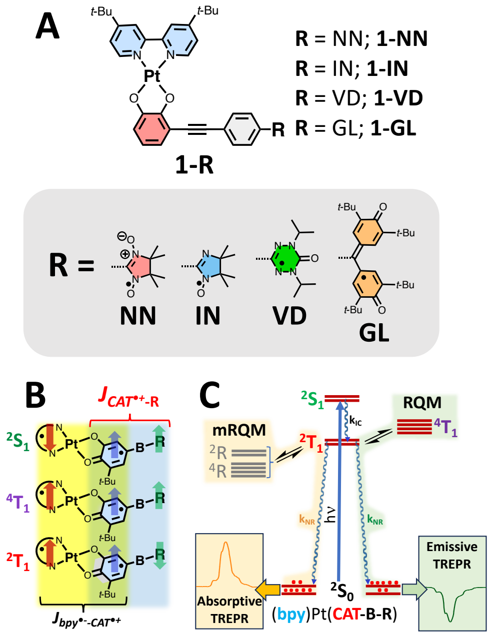

Figure 1. (A) Examples of radical-elaborated LL'CT chromophores. (B) Three electronic states that comprise the excited LL'CT manifold. (C) Reversed- and modified reversed quartet mechanisms.

These chromophoric (CAT)Pt(bpy) component of these complexes exhibit a low-energy CAT → bpy ligand-to-ligand charge transfer (LL'CT) transition that results in a charge-separated ES which possesses ~90% biradical character. This LL'CT band in the visible region of the spectrum with an energy that can be both synthetically and solvatochromatically tuned. When a single stable radical is attached to the LL'CT chromophore, the ES manifold is comprised of the singlet and triplet states of the chromophore being exchange coupled to the radical spin to yield $^2S_1$ (sing-doub), $^2T_1$ (trip-doub), and $^4T_1$ (quartet) states, *Figure 1B,C.*

The covalent attachment of a stable radical to the LL'CT chromophore is critical, since in the absence of the radical these complexes undergo rapid charge recombination back to the ground state (GS) in <1 ns. Covalent attachment of a stable radical is accompanied by fast charge recombination to the GS, but not before exchange-enhanced chromophoric intersystem crossing occurs from the initial photoexcited $^2S_1$ state to the $^2T_1$, which is followed by equilibration of $^2T_1$

with $^4T_1$ and/or localized radical excited states (*Figure C*). Equilibration pathways are enabled by zero-field splitting, energy transfer, or spin-vibronic coupling, and result in non-Boltzmann populations ("spin polarization") of the $^2T_1$ m_s-levels. Since the $^2T_1$ lifetimes are all shorter than the spin-lattice relaxation times of the stable radical, charge recombination delivers the ESP to the GS where it can be recorded using transient EPR spectroscopy, *Figure 1C*.

We have made substantial progress in understanding the ES electronic structure of these complexes, the mechanisms for generating GS and ES ESP in these systems, the polarization of multiple spin qubits and how the ES manifold of the LL'CT complexes is further altered by appending more than one radical spin to the LL'CT chromophore (*Figure 2A-E*). This presentation will highlight our future plans to use the (CAT)Pt(bpy) chromophore for polarizing stable radicals other than **NN**, to spin polarize multiple radicals, and to develop a detailed electronic structure description of the ESP mechanism as it pertains to QIS applications.

Our future plans are also geared to address both magnetic field and magnetic exchange effects on electron spin relaxation in biradicals. Here, we use pulsed EPR spectroscopy to understand how the pairwise magnetic exchange interaction in coupled biradical qubits contributes to spin relaxation (*Figure 3*) and loss of coherence. Variable-field and variable-temperature pulsed EPR experiments will be used to understand how intramolecular exchange coupling in biradical qubits affects spin relaxation, with the goal of increasing the knowledge base for the use of exchange coupled molecular spins in a variety of QIS applications.

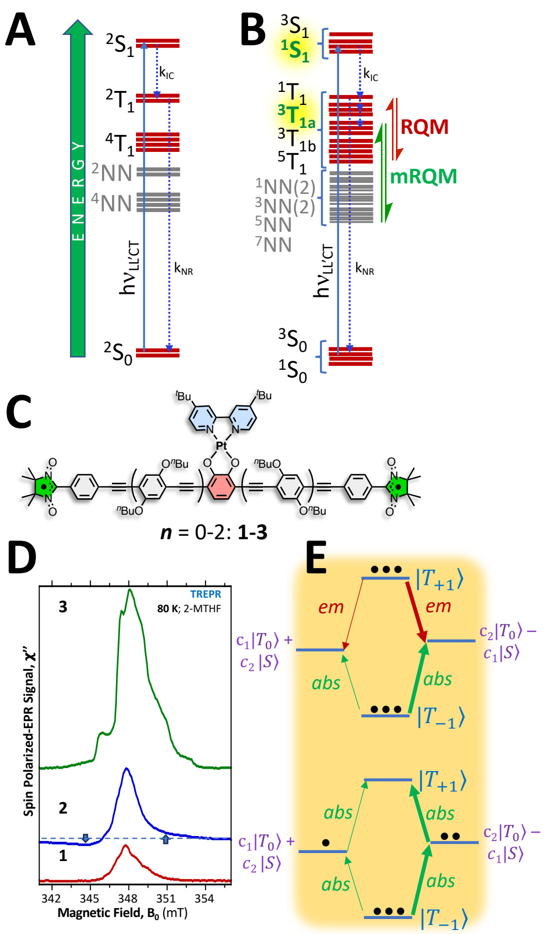

Figure 2. (A) State diagram for mono-radical elaborated LL'CT complexes, (B) state diagram for bi-radical elaborated LL'CT complexes, (C) change in ESP as a function of chromophore-radical exchange coupling, (E) mechanism for generating both net and multiplet ESP when $\boldsymbol{J} \sim \boldsymbol{D}$ ($\boldsymbol{D}$ = axial zero-field splitting).

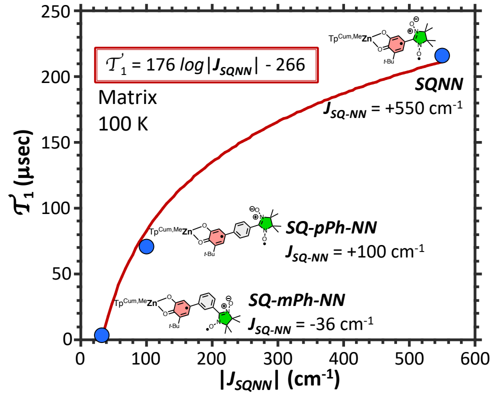

Figure 3. Relative TREPR intensities vs. $J_{SQ\text{-}bridge\text{-}NN}$ for $Tp^{Cum,Me}Zn$(SQ-N), $Tp^{Cum,Me}Zn$(SQ-*p*Ph-NN) and $Tp^{Cum,Me}Zn$(SQ-*m*Ph-NN).

DOE Solar Photochemistry Sponsored Publications 2021-2024

1. “Metal Ion Control of Photoinduced Electron Spin Polarization in Electronic Ground States,” Kirk, M. L.; Shultz, D. A.; Chen, J.; Hewitt, P.; Daley, D.; Paudel, S.; van der Est, A. *J. Am. Chem. Soc.* **2021**, *143*, 10519-10523.
2. “Chromophore-Radical Excited State Antiferromagnetic Exchange Controls the Sign of Photoinduced Ground State Spin Polarization,” Kirk, M. L.; Shultz, D. A.; Hewitt, P.; Stasiw, D. E.; Chen, J.; van der Est, A. *Chem. Sci.* **2021**, *12*, 13704-13710.
3. “Excited State Exchange Control of Photoinduced Electron Spin Polarization in Electronic Ground States,” Kirk, M. L.; Shultz, D. A.; Hewitt, P.; van der Est, A. *J. Phys. Chem. Lett.* **2022**, *13*, 872-878.
4. “Excited State Magneto-Structural Correlations Related to Photoinduced Electron Spin Polarization,” Kirk, M. L.; Shultz, D. A.; Hewitt, P.; Chen, J.; van der Est, A. *J. Am. Chem. Soc.* **2022**, *144*, 12781–12788.
5. “Single-Photon-Induced Electron Spin Polarization of Two Exchange-Coupled Stable Radicals,” Kirk, M. L.; Shultz, D. A.; Marri, A. R.; Hewitt, P.; van der Est, A. *J. Am. Chem. Soc.* **2022**, *144*, 21005–21009.
6. “Origin of Ferromagnetic Exchange Coupling in Donor-Acceptor Biradical Analogs of Charge Separated Excited States,” Chen, J.; Yang, J.; Yadav, M.; Shultz, D. A.; Kirk, M. L. *Inorg. Chem.* **2023**, *62*, 739–747.
7. †“Dinuclear Ligand-to-Ligand Charge Transfer Complexes,” Shultz, D. A.; Stephenson, R.; Kirk, M. L. *Dalton Trans.* **2023**, *52*, 1970-1976.
8. “Competitive Reversed Quartet Mechanisms for Photogenerated Ground State Electron Spin Polarization,” Kirk, M. L.; Shultz, D. A.; Hewitt, P.; Marri, A. R.; van der Est, A. *Chem. Sci.* **2023**, *14*, 9689–9695 (Pick of the Week).
9. “Photoinduced Magnetic Exchange-Jump Promotes Ground State Biradical Electron Spin Polarization,” Kirk, M. L.; Shultz, D. A.; Marri, A. R.; van der Est, A. *J. Am. Chem. Soc.* **2024**, *146*, 9285-9292.

Multiproton-Coupled Electron Transfer (MPCET) in Artificial Photosynthetic Systems

E. J. Gonzalez,[1] R. E. Dominguez,[1] D. A. Heredia,[1] D. Nishiori,[1] G. F. Moore,[1]
S. Hammes-Schiffer,[2] G. R. Fleming,[3] T. A. Moore,[1] and A. L. Moore[1]

[1]School of Molecular Sciences, Arizona State University, Tempe, Arizona 85287-1604.
[2] Department of Chemistry, Princeton University, Princeton, New Jersey 08544.
[3] Department of Chemistry, University of California Berkeley, Berkeley California 94720.

Our approach to engineering the essential proton management features of photosynthesis into artificial photosynthetic constructs is to design a series of bioinspired, MPCET-driven proton wires. Importantly, expanding the one-proton translocation of PCET to MPCET provides a mechanism to transport protons away from a redox site to a location for the generation of proton motive force (proton chemical potential – the organizing principle of bioenergetics and a driving force in artificial photosynthetic constructs that will use bioinspired synthesis, molecular motors, and gradients to transform solar energy to meet human needs). In our artificial systems, the redox process is either an electrochemically or photochemically driven one-electron oxidation of a bioinspired Tyr$_Z$-His190 redox relay of Photosystem II. It consists of a benzimidazole phenol (BIP) coupled to a variable-length Grotthuss-type polybenzimidazole-based proton wire capable of translocating protons up to ~16 Å.[1-2] The function of these constructs is described as an EnPT process where one-electron oxidation of the phenol drives the translocation of n protons (n = 1–4 to date) over the proton wire to the terminal proton acceptor (TPA). The phenol/phenoxy radical E_{mid} was found to be a function of the pK_a of the terminal proton acceptor (TPA) and the number of benzimidazoles units in the hydrogen-bonded network; it becomes less positive (i.e., a weaker oxidant) as the number of bridging benzimidazoles increases. Fortunately, substituting the benzimidazole-based bridge with electron-withdrawing groups (e.g., trifluoromethyl groups) maintains the high redox potential for oxidative processes relevant to artificial photosynthesis, e.g., water oxidation. Such substitutions increase the midpoint potential of the phenoxyl radical/phenol couple so that proton translocations over ~11 Å become thermodynamically comparable to that of an unsubstituted system where one proton is transferred over ~2.5 Å. This indicates that the polybenzimidazole wire is a non-innocent participant in the redox process.[3-4]

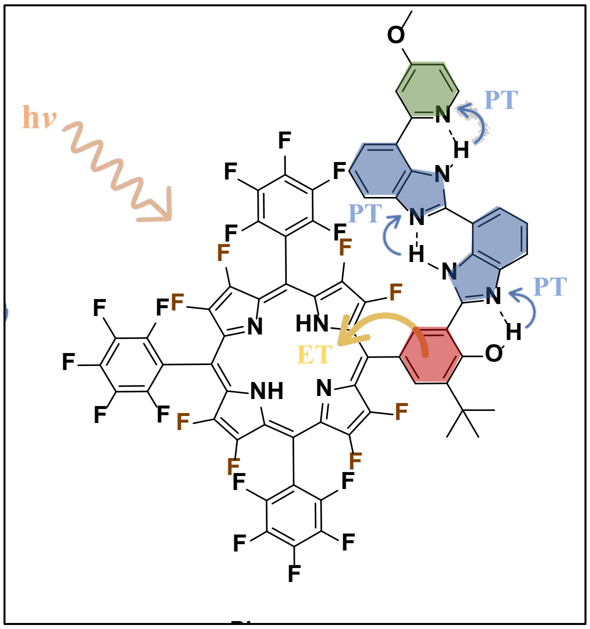

We studied a photochemically driven E1PT process with a BIP covalently attached to a tripentafluorophenylporphyrin (BIPPF$_{15}$).[5] Two-dimensional electronic-vibrational spectroscopy (2DEV) showed that PCET takes place on two time scales: 1) an ultrafast process from the unrelaxed S$_1$ state, and 2) a slower process on the time scale of a few hundred ps arising from the relaxed S$_1$ state. The ultrafast process enables the observation of the initial F-C state evolving to charge separation on the 120 fs time scale via the development of a dipole moment resulting from a dihedral twisting between the BIP and the macrocycle. On the 120 fs time scale, the proton simultaneously arrived on the benzimidazole and the electron on the porphyrin. With the BIP of $BIPPF_{15}$ substituted by a pyridine derivative TPA, we explored the dynamics of a photoinduced E2PT process.[6] Analysis of the evolution of the IR signals for the proton on the TPA and electron on the porphyrin from the 2D Center Line Slope and Excitation Profile data showed that a low-frequency mode predicted by Hammes-Schiffer promotes the proton and electron transfers and are concerted to within ~ 24 fs. To increase the driving force of the PCET/MPCET process so that it can take place in non-polar solvents, where disruption of the hydrogen bond network is unlikely, a porphyrin fluorinated at the *beta*-positions, see the Figure for an E3PT system, was employed. The infrared spectroelectrochemical spectrum (IRSEC) indicates the protonation of the TPA upon electrochemical oxidation of the phenol. Preliminary photophysical characterization shows that the fluorescence of the porphyrin is highly quenched, and transient absorption measurements on the 150 fs time scale in the visible show a broad signal with maxima at ~680 nm and ~ 610 nm raising in ~1 ps and decaying in ~30 ps. These transient absorption bands coincide with the visible spectroelectrochemical data and are consistent with the one-electron reduction of the porphyrin. Experiments are being conducted in Fleming's lab to confirm proton translocation to the TPA and measure the dynamics of the MPCET process in this photochemically driven E3PT system.

DOE Solar Photochemistry Sponsored Publications 2021-2024

1. Odella, E.; Secor, M.; Elliott, M.; Groy, T. L.; Moore, T. A.; Hammes-Schiffer, S.; Moore, A. L., Multi PCET in Symmetrically Substituted Benzimidazoles. *Chem. Sci.* **2021,** *12* (38), 12667-12675. DOI:10.1039/D1SC03782J

2. Guerra, W. D.; Odella, E.; Urrutia, M. N.; Liddell, P. A.; Moore, T. A.; Moore, A. L., Models to Study Photoinduced Multiple Proton Coupled Electron Transfer Processes. *JPP* **2021,** *25* (07n08), 674-682. DOI: 10.1142/S1088424621500577

3. Odella, E.; Secor, M.; Reyes Cruz, E. A.; Guerra, W. D.; Urrutia, M. N.; Liddell, P. A.; Moore, T. A.; Moore, G. F.; Hammes-Schiffer, S.; Moore, A. L., Managing the Redox Potential of PCET in Grotthuss-Type Proton Wires. *J. Am. Chem. Soc.* **2022,** *144* (34), 15672-15679. DOI: 10.1021/jacs.2c05820

4. Odella, E.; Moore, T. A.; Moore, A. L., Tuning the Redox Potential of Tyrosine-Histidine Bioinspired Assemblies. *Photosynth. Res.* **2022,** *151* (2), 185-193. DOI: 10.1007/s11120-020-00815-x

5. Yoneda, Y.; Mora, S. J.; Shee, J.; Wadsworth, B. L.; Arsenault, E. A.; Hait, D.; Kodis, G.; Gust, D.; Moore, G. F.; Moore, A. L.; Head-Gordon, M.; Moore, T. A.; Fleming, G. R., Electron-Nuclear Dynamics Accompanying Proton-Coupled Electron Transfer. *J. Am. Chem. Soc.* **2021,** *143* (8), 3104-3112. DOI: 10.1021/jacs.0c10626

6. Arsenault, E. A.; Guerra, W. D.; Shee, J.; Reyes Cruz, E. A.; Yoneda, Y.; Wadsworth, B. L.;

Odella, E.; Urrutia, M. N.; Kodis, G.; Moore, G. F.; Head-Gordon, M.; Moore, A. L.; Moore, T. A.; Fleming, G. R., Concerted Electron-Nuclear Motion in Proton-Coupled Electron Transfer-Driven Grotthuss-Type Proton Translocation. *J. Phys. Chem. Lett.* **2022,** *13* (20), 4479-4485. DOI: 10.1021/acs.jpclett.2c00585

7. Ravensbergen, J.; Pillai, S.; Méndez-Hernández, D. D.; Frese, R. N.; van Grondelle, R.; Gust, D.; Moore, T. A.; Moore, A. L.; Kennis, J. T. M., Dual Singlet Excited-State Quenching Mechanisms in an Artificial Caroteno-Phthalocyanine Light Harvesting Antenna. *ACS Phys. Chem. Au* **2022,** *2* (1), 59-67. DOI: 10.1021/acsphyschemau.1c00008

8. Lewis, C. M.; Flory, J. D.; Moore, T. A.; Moore, A. L.; Rittmann, B. E.; Vermaas, W. F. J.; Torres, C. I.; Fromme, P., Electrochemically Driven Photosynthetic Electron Transport in Cyanobacteria Lacking Photosystem II. *J. Am. Chem. Soc.* **2022,** *144* (7), 2933-2942. DOI: 10.1021/jacs.1c09291

9. Williams, J. C.; Faillace, M. S.; Gonzalez, E. J.; Dominguez, R. E.; Knappenberger, K.; Heredia, D. A.; Moore, T. A.; Moore, A. L.; Allen, J. P., Mn-Porphyrins in a Four-Helix Bundle Participate in Photo-Induced Electron Transfer with a Bacterial Reaction Center. *Photosynth Res* **2023**. DOI: 10.1007/s11120-023-01051-9

10. Petropoulos, V.; Rukin, P.; Quintela, F.; Russo, M.; Moretti, L.; Moore, A. L.; Moore, T. A.; Gust, D.; Prezzi, D.; Scholes, G. D.; Molinari, E.; Cerullo, G.; Troiani, F.; Rozzi, C. A.; Maiuri, M., Vibronic Coupling Drives the Ultrafast Internal Conversion in a Functionalized Free Base Porphyrin. *J. Phys. Chem. Lett.* **2024**. DOI: 10.1021/acs.jpclett.4c00372

Fundamental Studies of the Vibrational, Electronic, and Photophysical Properties of Tetrapyrrolic Architectures

David F. Bocian,[1] Dewey Holten,[2] Christine Kirmaier,[2] and Jonathan S. Lindsey[3]

[1]Department of Chemistry, University of California Riverside, Riverside, CA 92521
[2]Department of Chemistry, Washington University, St. Louis, MO 63130
[3]Department of Chemistry, North Carolina State University, Raleigh, NC 27695

A long-term objective of our program is to design, synthesize, and characterize tetrapyrrole-based molecular architectures that absorb sunlight across the visible and near-infrared spectrum, funnel energy, and separate charge (hole, electron) with high efficiency and in a manner compatible with current and future solar-energy conversion schemes. Here, two areas of progress over the past two years are highlighted.

Electronic-vibrational coherences have been observed in photosynthetic antennas and reaction centers. Unanswered is the extent to which the rate of energy/electron transfer is enhanced by such coherences. We have studied the rate of energy transfer in a series of well-characterized bacteriochlorin dyads in which the donor–acceptor excited-state energy gap is varied from ~200 cm^{-1} to ~1100 cm^{-1}. The results on the dyads in toluene at 295 K are published. We have extended studies and Förster analysis to the dyads in 2-methyltetrahydrofuran at 295 and 77 K. The measured energy-transfer time constants deviate no more than ~3-fold from (A) a trend-line vs. donor–acceptor excited-state energy gap (figure top panel) and (B) values predicted by Förster theory (bottom panel). The small deviations do not correlate with the density of vibrations at the donor-acceptor energy gap.

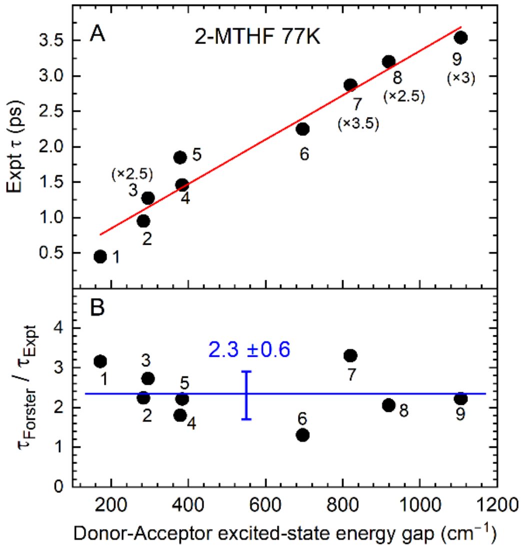

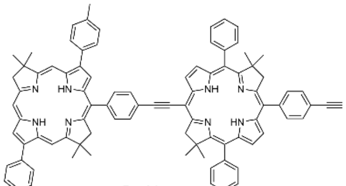
Dyad 1

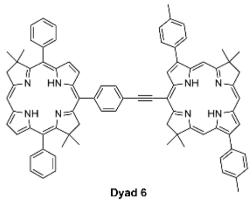
Dyad 6

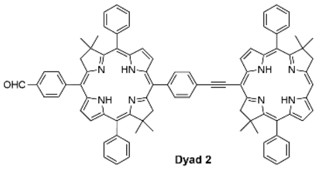

Dyad 2

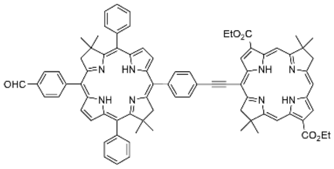

Dyad 7

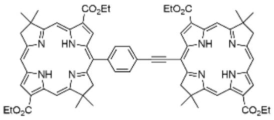

Dyad 3

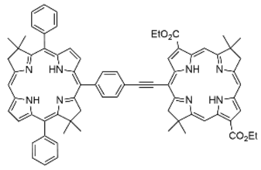

Dyad 8

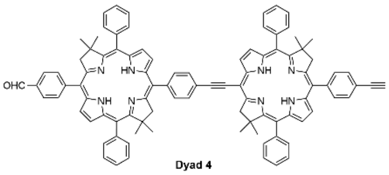

Dyad 4

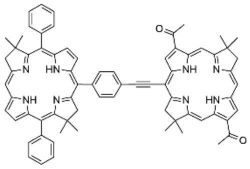
Dyad 9

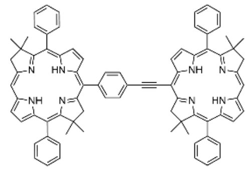
Dyad 5

A second area of progress is design, synthesis and characterization of annulated bacteriochlorins that extend tetrapyrrole absorption further into the NIR-II spectral region (>1000 nm). New annulated bacteriochlorin Phen^{2,1}-BC (red structure) has the $S_0 \rightarrow S_1(0,0)$ transition at 1292 nm (0.96 eV). Prior isomer Phen-BC (blue, 912 nm) differs in attachment sites to the naphthalene. Surprising for Phen^{2,1}-BC are (1) the weak $S_0 \rightarrow S_1$ oscillator strength (0.23) vs. that for Phen-BC (1.1), and (2) significant intensity in $S_0 \rightarrow S_1$ vibronic overtones that reflect vibronic coupling. Phen^{2,1}-BC has a very short S_1 excited-state lifetime (~0.5 ps) dominated by $S_1 \rightarrow S_0$ internal conversion. The internal-conversion rate constant (point 16D in middle-right figure) is near the blue energy-gap-law trend-line for bacteriochlorins that employ β-meso annulation. The red trend-line for non-annulated analogs predicts ~70 ps for Phen^{2,1}-BC. Phen^{2,1}-BC also has angle $\theta_{12} = 39°$ between transition-dipole moments for $S_0 \rightarrow S_1$ and $S_0 \rightarrow S_2$ (panel F at lower-left). This is much smaller than the typical $\theta_{12} \sim 90°$ for simple non-annulated analogs (panel A), implying significant mixing of normal x-polarized ($S_0 \rightarrow S_2$) and y-polarized ($S_0 \rightarrow S_1$) transitions. However, Phen^{2,1}-BC has MOs similar to those for the four-orbital model. An empirical x-y mixing parameter (lower right) shows that even though Phen^{2,1}-BC has $\theta_{12} = 39°$, the electronic structure (*e.g.*, MOs) retains ~80% of the character in the absence of the mixing. The x-y electronic mixing and vibronic mixing for Phen^{2,1} BC that affect the $S_0 \rightarrow S_1$ oscillator strength and S_1 lifetime are a consequence of reduced symmetry resulting from the annulation motif employed. Collectively, the results suggest a heuristic for the molecular design of tetrapyrrole chromophores for deep penetration into the relatively unutilized NIR-II region. The results also have implications for understanding characteristics of the natural photosynthetic pigments and the design of synthetic analogs for solar-energy conversion.

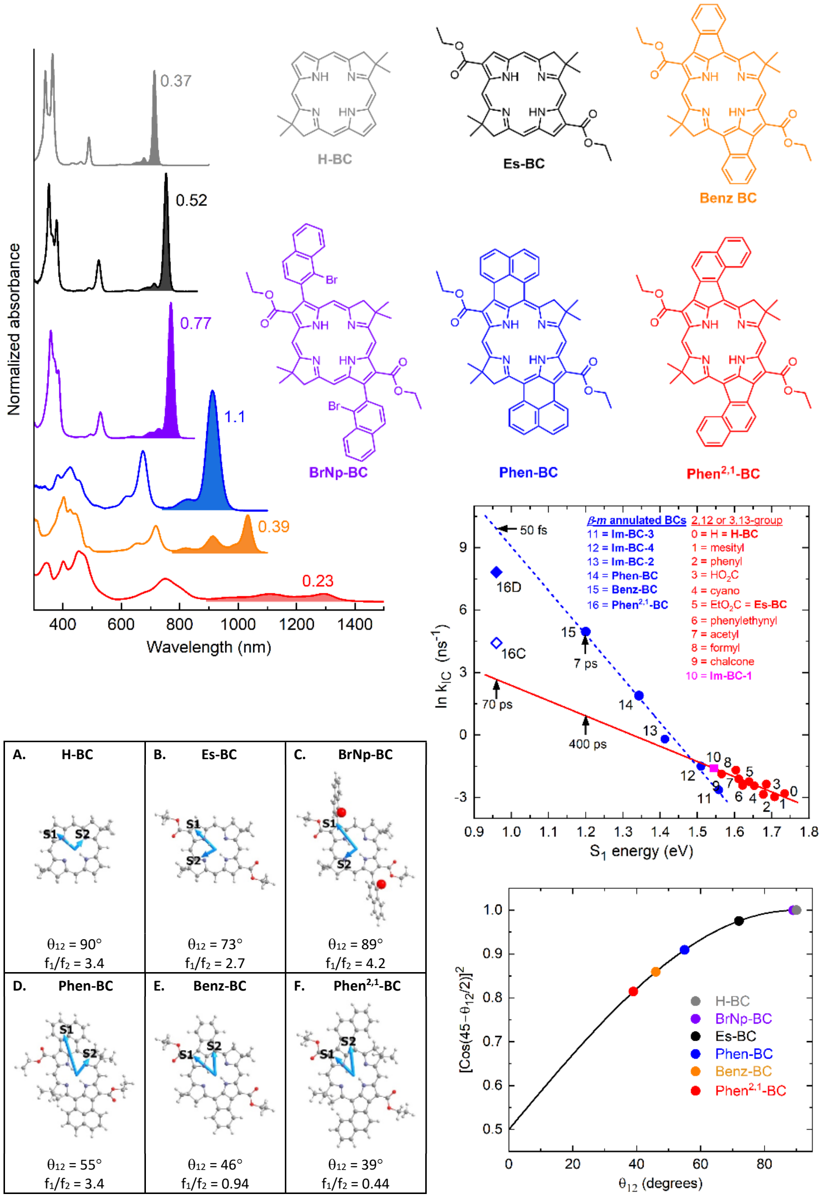

DOE Solar Photochemistry Sponsored Publications 11/2021-4/2024

1. “Beyond Green with Synthetic Chlorophylls – Connecting Structural Features with Spectral Properties,” Taniguchi, M.; Bocian, D. F.; Holten, D.; Lindsey, J. S. *J. Photochem. Photobiol. C: Photochem. Rev.* **2022**, *52*, 100513.
2. “Synthesis of Bacteriochlorins Bearing Diverse β-Substituents,” Jing, H.; Wang, P.; Chen, B.; Jiang, J.; Vairaprakash, P.; Liu, S.; Rong, J.; Chen, C.-Y.; Nalaoh, P.; Lindsey, J. S. *New J. Chem.* **2022**, *46*, 5534–5555.
3. “Meso Bromination and Derivatization of Synthetic Bacteriochlorins,” Jing, H.; Liu, S.; Jiang, J.; Tran, V.-P.; Rong, J.; Wang, P.; Lindsey, J. S. *New J. Chem.* **2022**, *46*, 5556–5572.
4. “De Novo Synthesis of Bacteriochlorins Bearing Four Trideuteriomethyl Groups,” Jing, H.; Tang, Q.; Bocian, D. F.; Lindsey, J. S. *Organics* **2022**, *3*, 22–37.
5. “Simple Dipyrrin Analogues of Prodigiosin for use as Colistin Adjuvants,” Siwawannapong, K.; Nemeth, A. M.; Melander, R. J.; Rong, J.; Davis, J. R.; Taniguchi, M.; Carpenter, M. C.; Lindsey, J. S.; Melander, C. *ChemMedChem* **2022**, e202200286.
6. “Dihydrooxazine Byproduct of a McMurry-Melton Reaction En Route to a Synthetic Bacteriochlorin,” Tran, V.-P.; Matsumoto, N.; Nalaoh, P.; Jing, H.; Chen, C.-Y.; Lindsey, J. S. *Organics* **2022**, *3*, 262–274.
7. “Probing the Effects of Electronic-Vibrational Resonance on the Rate of Excited-State Energy Transfer in Bacteriochlorin Dyads,” Magdaong, N. C. M.; Jing, H.; Diers, J. R.; Kirmaier, C.; Lindsey, J. S.; Bocian, D. F.; Holten, D. *J. Phys. Chem. Lett.* **2022**, 13, 7906–7910.
8. “Digital Database of Absorption Spectra of Diverse Flavonoids Enables Structural Comparisons and Quantitative Evaluations,” Taniguchi, M.; LaRocca, C.; Bernat, J. D.; Lindsey, J. S. *J. Nat. Prod.* **2023**, *86*, 1087–1119.
9. “Balancing Panchromatic Absorption and Multistep Charge Separation in a Compact Molecular Architecture,” Roy, A.; Magdaong, N. C. M.; Jing, H.; Rong, J.; Diers, J. R.; Kang, H. S.; Niedzwiedzki, D. M.; Taniguchi, M.; Kirmaier, C.; Lindsey, J. S.; Bocian, D. F.; Holten, D. *J. Phys. Chem. A* **2022**, 126, 9353–9365.
10. “Panchromatic Absorbers Tethered for Bioconjugation or Surface Attachment,” Liu, R.; Rong, J.; Wu, Z.; Taniguchi, M.; Bocian, D. F.; Holten, D.; Lindsey, J. S. *Molecules* **2022**, *27*, 6501.
11. “Dyads with Tunable Near-Infrared Donor–Acceptor Excited-State Energy Gaps: Molecular Design and Förster Analysis for Ultrafast Energy Transfer,” Jing, H.; Magdaong, N. C. M.; Diers, J. R.; Kirmaier, C.; Bocian, D. F.; Holten, D.; Lindsey, J. S. *Phys. Chem. Chem. Phys.* **2023**, *25*, 1827–1847.
12. “Investigation of a Bacteriochlorin-containing Pentad for Panchromatic Light-Harvesting and Charge Separation,” Jing, H.; Magdaong, N. C. M.; Diers, J. R.; Kirmaier, C.; Bocian, D. F.; Holten, D.; Lindsey, J. S. *Phys. Chem. Chem. Phys.* **2023**, *25*, 1781–1798.
13. “Porphyrin Building Blocks Bearing Two or Four Divergent Ethynes,” Cao, P.-L. D.; Wu, Z.; Rong, J.; Lindsey, J. S. *J. Porphyrins Phthalocyanines* **2023**, *27*, 1049–1058.
14. “Rapid Screening of Dyes for Self-Aggregation, Adsorption, and Metabolic Integrity – Quantitative Metrics as a Prelude to Biological Studies,” Liu, Q.; Taniguchi, M.; Goel, S.; Lindsey, J. S. *Dyes Pigments* **2024**, *223*, 111914.
15. “Chlorin–Dextran Conjugates for Brightness Enhancement in Water,” Liu, S.; Lindsey, J. S.; Taniguchi, M. *Proc. SPIE* **2024**, *12862*, 128620A.

16. “Light-Scattering in Absorption Spectra: A Literature Survey of Examples and Corrections,” Taniguchi, M.; Lindsey, J. S.; *Proc. SPIE* **2024**, *12862*, 128620B.

17. “Extension of Nature’s NIR-I Chromophore into the NIR-II Region,” Siwawannapong, K.; Diers, J. R.; Magdaong, N. C. M.; Nalaoh, P.; Kirmaier, C.; Lindsey, J. S.; Holten, D.; Bocian, D. F. *Phys. Chem. Chem. Phys.* **2024**, *XX*, *in press*.

Sensitizers for Solar Fuels Production: Group 4, 11 and 12 Metal Complexes

Stephen Bradforth, Mark Thompson, Austin Mencke, Michael Kellogg, Kelly Biv,
D. Allen Shariaty, Thabassum A. N. Kallungal, Nina Baluyot-Reyes,

Department of Chemistry, University of Southern California, Los Angeles, CA 90089

Generating a sustainable fuel from sunlight plays an important role in meeting the energy demands of the modern age. In our talk we will discuss our work with two-coordinate carbene-metal-amide (cMa, M = Cu(I) and Au(I)) complexes[1,2,5] as well as Zr and Zn complexes with chelating donor-acceptor ligands, exploring them as sensitizers for driving electrocatalytic reactions. The complexes studied here absorb visible photons ($\varepsilon_{vis} > 10^3$ $M^{-1}cm^{-1}$), maintain long excited state lifetimes ($\tau \sim 0.5$-15 μs) and are predicted to have high excited state reducing potential. We have demonstrated hydrogen production with gold and copper cMa's when combined in homogenous solution with standard cobalt electrocatalysts.[3]

The principal goal of our work is to develop efficient sensitizers that utilize earth abundant elements. Our talk will focus on three topics. The first topic is the study of complexes of two very abundant metals: zirconium and zinc-based complexes, comparing properties to the Group 11 complexes that we have already thoroughly spectroscopically characterized.[1] These d^0 and d^{10} Zr and Zn complexes, respectively, utilize donor-acceptor chelating ligands, leading to excited states that are effectively interligand charge transfers. While the metal ions bridge the donor and acceptor, we believe the principal interactions are through space interactions between the donor and acceptor components of the ligands. The excited state lifetimes of these new Zn and Zr materials are in the microsecond regime, with quantum efficiencies as high as 0.4 for the best performing materials. Emission in these materials is via thermal promotion for the dark T_1 to the bright S_1 (TADF). Our measurements suggest that the Zn complexes have very small energy gaps between their S_1 and T_1 states (*i.e.* < 10 meV). In contrast, we have found that coinage metals have 25 – 100 meV. The longer excited state lifetimes for Zn complexes are thus not due to slow ISC ($T_1 \rightarrow S_1$), but to low oscillator strengths for their S_1 states.

The second topic we will cover involves our efforts to shift the absorption profile of the cMa complexes to cover the visible part of the solar spectrum. Our best performing cMa complexes (longest excited state lifetime) absorb principally in the blue end of the spectrum. Shifting from an interligand charge transfer (ICT) excited state to one that has mixed ICT and ligand localized character markedly enhances the lifetimes of these materials, pushing them into the 10-15 μs regime. The long lifetimes may eliminate a problem we have identified using these cMa sensitizers for reduction reactions. Our initial studies of cMa complexes as sensitizers coupled with a cobalt-bisglyoxime catalyst for water reduction showed good turnover numbers based on sensitizer, but a high concentration of sacrificial reductant (SAC) was required to efficiently capture the excited state, leading to cMa^- formation.[3] This was due to the lifetime of 250 ns for the chosen cMa in THF solution. The problem with this is that the reduced cMa appears to degrade forming colloidal metal particles. Increasing the excited state lifetime into the 10's of μs regime will allow us to use conditions where the electrocatalyst is directly reduced by cMa*, leading to formation of cMa^+, which is stable under the reactions conditions and can be subsequently reduced by an electrode or sacrificial agent to regenerate the neutral cMa.

The third topic involves another strategy to direct reduction by cMa*. We will show ultrafast

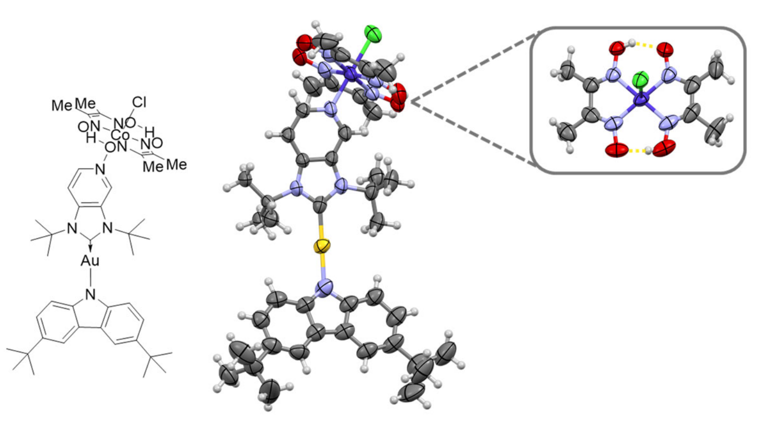

Coupled cMa sensitizer and cobalt-bisglyoxime catalyst used in TA studies.

studies of electron transfer from an excited cMa to a pendent electrocatalyst (see Figure). By binding the sensitizer and cataylst together we can get around the diffusion limit for electron transfer from the sensitizer to the catalyst potentially eliminating the need for high SAC concentration or large extension to the excited state lifetime. In this case a carbene ligand is used with free pyridyl nitrogen in the ligand framework. We have isolated the cMa with this pyridyl nitrogen coordinate to a cobalt bisglyoxime water reduction catalyst. Ultrafast studies of this complex show very rapid formation of the charge separated state $[L_2(Cl)Co^{\ominus}\text{-cMa}^{\oplus}]$. We have also investigated a derivative that has an electronically isolated pyridyl-Co(Cl)L_2 catalyst and will discuss our ultrafast studies of the two complexes.

DOE Solar Photochemistry Sponsored Publications 2021-2024.[1-6]

1. Kellogg, M. S.; Mencke, A. R.; Muniz, C. N.; Nattikallungal, T. A.; Cardoso-Delgado, F.; Baluyot-Reyes, N.; Sewell, M.; Bird, M. J.; Bradforth, S. E.; Thompson, M. E., Intra- and Intermolecular Charge-Transfer Dynamics of Carbene–Metal–Amide Photosensitizers. *The Journal of Physical Chemistry C* **2024**, DOI: 10.1021/acs.jpcc.4c01994

2. Li, T. Y.; Zheng, S. J.; Djurovich, P. I.; Thompson, M. E., Two-Coordinate Thermally Activated Delayed Fluorescence Coinage Metal Complexes: Molecular Design, Photophysical Characters, and Device Application. *Chem Rev* **2024,** *124* (7), 4332-4392, DOI: 10.1021/acs.chemrev.3c00761

3. Muniz, C. N.; Archer, C. A.; Applebaum, J. S.; Alagaratnam, A.; Schaab, J.; Djurovich, P. I.; Thompson, M. E., Two-Coordinate Coinage Metal Complexes as Solar Photosensitizers. *Journal of the American Chemical Society* **2023,** *145* (25), 13846-13857, DOI: 10.1021/jacs.3c02825

4. Ma, J.; Schaab, J.; Paul, S.; Forrest, S. R.; Djurovich, P. I.; Thompson, M. E., Luminescent Bimetallic Two-Coordinate Gold(I) Complexes Utilizing Janus Carbenes. *Journal of the American Chemical Society* **2023,** *145* (36), 20097-20108, DOI: 10.1021/jacs.3c07743

5. Muniz, C. N.; Schaab, J.; Razgoniaev, A.; Djurovich, P. I.; Thompson, M. E., Π-Extended Ligands in Two-Coordinate Coinage Metal Complexes. *Journal of American Chemical Society* **2022,** *144* (39), 17916-17928, DOI: 10.1021/jacs.2c06948

6. Estergreen, L.; Mencke, A. R.; Cotton, D. E.; Korovina, N. V.; Michl, J.; Roberts, S. T.; Thompson, M. E.; Bradforth, S. E., Controlling Symmetry Breaking Charge Transfer in Bodipy Pairs. *Accounts of Chemical Research* **2022,** *55* (11), 1561-1572, DOI: 10.1021/acs.accounts.2c00044

Heteroleptic Copper(I) Charge-Transfer Photosensitizers Supported by β-Diketiminates

Dooyoung Kim and Thomas S. Teets
Department of Chemistry
University of Houston
Houston, TX 77204-5003

Molecular photosensitizers composed of earth-abundant materials are critical for large-scale development of chemical processes that use solar energy as an input. It is challenging to simultaneously optimize the light absorption, lifetime of the charge-separated state, and redox potentials of a photosensitizer, particularly true in earth-abundant analogues. For metal-based photosensitizers complexes of copper(I) have emerged at the forefront, in large part because their d^{10} configuration obviates deleterious excited-state deactivation pathways that plague charge-transfer chromophores of other redox-active base metals. Our program is developing new classes of heteroleptic copper(I) charge-transfer chromophores, which enable judicious and independent control of frontier orbital energies and the associated redox potentials and engender long-range charge separation in the low-energy excited states. This talk will describe our early efforts in this area.

The first class of compounds we investigated are four-coordinate compounds of the general formula Cu(NacNac)(N^N), where NacNac is a substituted β-diketiminate and N^N is a diimine ligand from the 1,10-phenanthroline or 2,2′-biquinoline families (Figure 1). In these compounds the HOMO is primarily localized on the NacNac ligand (with some delocalization on copper), and the LUMO is localized almost exclusively on the diimine. This spatial separation of the frontier orbitals allows independent control of their energies and results in low-energy charge-transfer absorption bands that can be tuned throughout the visible to near-infrared regions, making these compounds superior light harvesters compared to most copper(I) charge-transfer chromophores. However, their excited-state lifetimes are short, with sterically crowding substituents on both ligands having a large impact but still only resulting in lifetimes that maximize at 2 ns, obviating any photocatalytic reactivity.

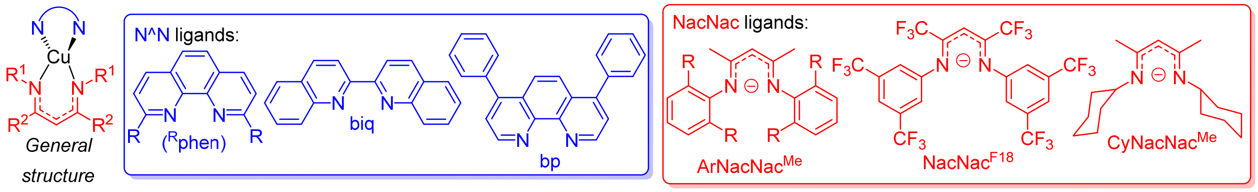

Figure 1. General structures of four-coordinate heteroleptic complexes.

The majority of this talk will focus on more recent efforts investigating an alternative design, where the N^N ligand in the four-coordinate compounds is replaced with an aryl isocyanide, furnishing the three-coordinate complexes summarized in Figure 2. Two of these compounds feature pyrene-substituted isocyanides and are thus bichromophoric in nature, taking advantage of the “triplet reservoir” effect to increase the lifetime of the charge-transfer state. The photoluminescence of these compounds shows three distinct behaviors, also included in Figure 2. The parent compound with 2,6-dimethylphenyl isocyanide (**Cu1**) exhibits charge-transfer (^{3}CT) phosphorescence with a short excited-state lifetime of 9.3 ns. In the opposite extreme, pyrene-substituted **Cu3** exhibits phosphorescence that originates from a triplet excited state localized on the pyrene moiety (abbreviated as the ^{3}py state), which results in a very long excited-state lifetime of 1.7 ms. Finally, **Cu2** represents an interesting intermediate case, where the ^{3}CT and ^{3}py states are nearly isoenergetic and reversible triplet-triplet energy transfer occurs. This results in ^{3}CT phosphorescence at room temperature, but the equilibrium with ^{3}py lengthens the excited-state lifetime to 3.9 μs. At 77 K the ^{3}CT state is destabilized and the phosphorescence originates from ^{3}py.

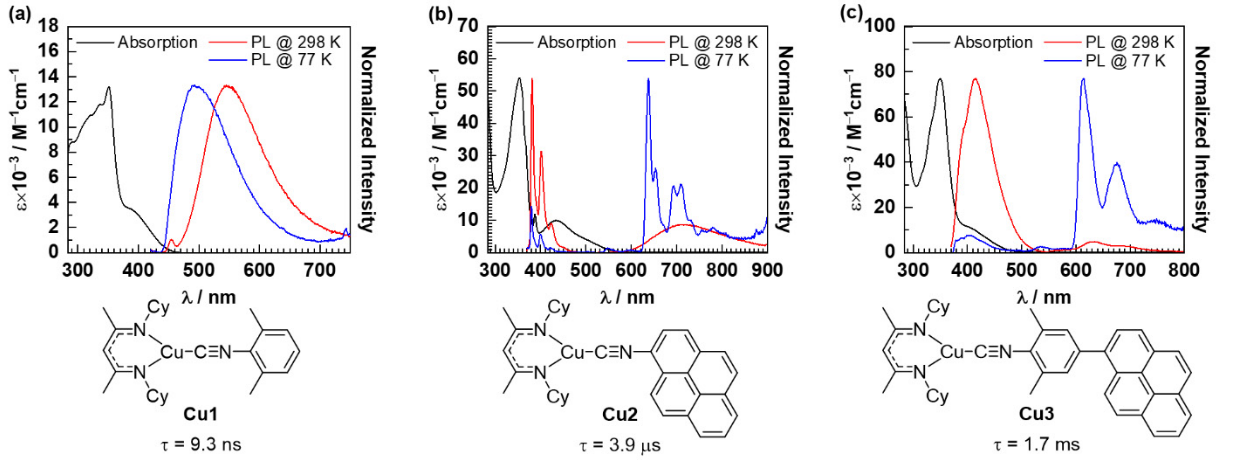

Figure 2. Overlaid UV–vis absorption and photoluminescence spectra (at 298 K and 77 K) of (a) **Cu1**, (b) **Cu2**, and (c) **Cu3**, recorded in toluene.

All three compounds are active in photocatalytic transformations with blue or green-light irradiation. They promote photocatalytic isomerization of (*E*)-stilbene, a common test reaction for triplet energy-transfer catalysis, with **Cu2** and **Cu3** resulting in faster conversion on account of their longer excited-state lifetimes. All three compounds are predicted to be strong photoreductants, and **Cu3** was also screened in select photoredox transformations. It is capable of promoting aryl bromide hydrodehalogenation and ketone reduction reactions relevant to organic synthesis, and ether C–O bond cleavage reactions relevant to lignin biomass degradation.

DOE Solar Photochemistry Sponsored Publications

1. Kim, D.; Rosko, M. C.; Dang, V. Q.; Castellano, F. N.; Teets, T. S. "Sterically Encumbered Heteroleptic Copper(I) β-Diketiminate Complexes with Extended Excited-State Lifetimes." *Inorg. Chem.* **2023**, *62*, 16759–16769. https://doi.org/10.1021/acs.inorgchem.3c02042

2. Kim, D.; Teets, T. S. "A Series of Four-Coordinate Heteroleptic Copper(I) Complexes with Diimine and β-diketiminate Ligands." *Polyhedron* **2024**, *248*, 116748. *Invited contribution for "Emerging Investigators in Inorganic Chemistry" special issue.* https://doi.org/10.1016/j.poly.2023.116748

3. Kim, D.; Dang, V. Q.; Teets, T. S. "Improved Transition Metal Photosensitizers to Drive Advances in Photocatalysis." *Chem. Sci.* **2024**, *15*, 77–94. https://doi.org/10.1039/D3SC04580C

4. Kim, D.; Rosko, M. C.; Castellano, F. N.; Gray, T. G.; Teets, T. S. "Long Excited-State Lifetimes in Three-Coordinate Copper(I) Complexes via Triplet–Triplet Energy Transfer to Pyrene-Decorated Isocyanides." *Submitted for publication.*

Unlocking the Secrets of Intersystem Crossing in Photoexcited Lewis Acid Appended Mn(IV)-Oxo Complexes

Jesus Paredes, Kelly Penley, Nicolette Couture, Gage Leach, Luis Milan, Melissa Gish, David Mulder, Wade Braunecker, Shailesh Ambre, and Megan Lazorski
Department of Chemistry and Biochemistry
Metropolitan State University of Denver
Denver, CO 80033

This project expands the energy sciences frontier in two critical dimensions: (1) probing the use of spin-selectivity to extend the lifetime of photosensitizers based on manganese - a cheap, earth-abundant first-row transition metal (FRTM), and (2) increasing the representation of historically underrepresented and minoritized (URM) groups in STEM.

Photosensitizers are compounds that absorb energy from light and convert that into chemical potential, which can be used to overcome energetic barriers and/or photocatalyze difficult chemical transformations. The overarching scientific goal of this project is to investigate ways to control the properties of earth abundant FRTM photosensitizer complexes such that they compete with or outperform the historical benchmarks based on rare, expensive metals such as ruthenium. This work seeks to understand how intrinsic electronic and spin properties of earth-abundant FRTM complexes can be tuned to capitalize on new modes of photoactivity as a potential avenue for design of photosensitizers or photocatalytic solar fuel production schemes.

Specifically, this project focuses on Lewis Acid (LA) appended non-heme (nH) manganese(IV)-oxo complexes ($[(nH)Mn^{4+}O]^{z+}$-LA), one of which can perform benzene hydroxylation via oxidative photoinduced electron transfer (PET). In these complexes, the LA binding event provides a new electronic pathway in a photoexcited *d-d* state by facilitating intersystem crossing (ISC) to an excited state with a different spin. The ISC step forces the photoexcited electron to take a spin-forbidden relaxation pathway to the ground state, which impacts how long the absorbed light-energy is stored for later use, i.e., the lifetime (τ). In one of the two literature investigations on photoactive $[(nH)Mn^{4+}O]^{z+}$-LAs, the photoinduced lifetime changes by nearly 1 μs when the LA is changed from $[Sc(OTf)_3]^{3+}$ to $[Sc(NO_3)_3]^{3+}$ but with the same nH ligand. In contrast, many *ground state* studies on $[(nH)Mn^{4+}O]^{z+}$-LA complexes suggest that LA binding *and* the nH ligand impact the frontier orbital energies. Therefore, differences in the nH ligand are also likely to impact the photoinduced mechanism. Herein, the excited state energetics and dynamics are probed by synthesizing series' of $[(nH)Mn^{4+}O]^{z+}$-LA complexes with systematic changes in LA and nH ligand designs. These data are used to determine how each factor, independently and together, influences the rate of ISC (k_{ISC}).

The three primary objectives of this research aim to elucidate how photophysical properties and mechanisms of ISC in these complexes are influenced by LA binding properties, various nH ligand architectures, and dipolar properties in the complexes. More specifically, steady state and transient spectroscopic techniques are used to assess: (1) changes in frontier orbital potential energy surfaces as a function of $Mn^{4+}=O$ bond distance upon LA binding, (2) how nH ligand flexibility impacts excited state vibronic spin-orbit coupling (SOC), (3) how the σ-donor strength of the nH ligand's axial donor atom and field strength of equatorial donor atoms impact excited state energetics, and (4) how changes in LA properties and ligand characteristics affect the molecular dipole moment, photoinduced transition dipole moment, and polarizability volume of the complex in the ground and excited states. By understanding these properties, the mechanism of excited state k_{ISC} modulation can ultimately be controlled. This information will provide the fundamental underpinnings that could enable earth abundant FRTM complexes to compete with or replace the historical benchmark photosensitizers/catalysts that rely on unsustainable 4d/5d transition metals.

Aligning with our scientific work that seeks to define the next wave of useful light harvesting complexes, we define new models for *REaching a New Energy sciences Workforce (RENEW)*. Our work intentionally addresses obvious and invisible barriers for scientists from URM groups such that equitable opportunities to compete and perform in STEM are created where the historical benchmarks limited participation. Toward both goals, resources at Metropolitan State University of Denver (MSU Denver), a primarily undergraduate Hispanic Serving Institution, and National Renewable Energy Laboratory (NREL) are combined to perform this work. Undergraduate, postbaccalaureate, and postdoctoral students from URM groups are recruited via URM specific programs at MSU Denver: the Wilton Flemon Postdoctoral Teaching Fellowship and two newly developed post-baccalaureate bridge programs. These programs include multi-tiered mentorship, competitive pay, benefits, community-building and networking activities, and long-term, immersive research experiences. A manuscript has been submitted to the Journal of Chemical Education on our program which pioneers a model for students from URM groups seeking equitable post-graduation employment in the chemical sciences rather than graduate school. Scaffolded research teams of post-baccalaureate and undergraduate students will be co-led by a postdoc and project PIs. This structure allows students and researchers to engage in high-impact research, expand their skillset, and build their STEM identity in an inclusive, safe community. As such, we capitalize on the strengths of both MSU Denver and NREL to provide transformational opportunities in the energy sciences workforce.

Currently, five undergraduate students have begun work on this project from three fronts. Two students are synthesizing nH ligands at MSU Denver, two students are training on transient absorption (TA) and electron paramagnetic resonance (EPR) instrumentation at NREL, and one student is synthesizing the $[(nH)Mn^{4+}O]^{z+}$-LA inorganic complexes and performing steady state spectroscopic characterization techniques. Two nH ligands have been successfully synthesized and additional nH ligand syntheses have begun. These nH ligands will soon be used to synthesize the $[(nH)Mn^{4+}O]^{z+}$ complexes and appended with a series of LAs to yield the $[(nH)Mn^{4+}O]^{z+}$-LAs. By that time, the students working on TA and EPR will be ready to start spectroscopic characterization. As our postbaccalaureate programs launch in the Fall of 2024, this spring has been dedicated to creating the application materials, creating the website as a platform for recruitment and an application portal, defining the process for hiring postdoctoral students, advertising to a broad network of students from URM groups, and attending to the myriad details accompanying the creation of two completely non-traditional, inter-institutional bridge programs. At present, postbaccalaureate candidates are being interviewed and will be selected right before the application deadline for the postdoctoral fellows’ approaches. As the postdoctoral fellows play an integral role in the postbaccalaureate programs, they will start work in the summer of 2024.

Symmetry breaking in Semiconductor Nanocrystals for controlling charge carrier and spin dynamics

Matthew C. Beard,[1] Marissa Martinez,[1] Yifan Dong,[1] Zhiyuan Huang,[1] TK Kluherz,[1] Mikhail Zamkov,[2] Jacob Shelton,[1] William Griten,[1,3] Todd Krauss,[3] Peter Sercel[1]
1.Chemical and Nanoscience Center, National Renewable Energy Laboratory
Golden, Co, 80004
2. Center for Photochemical Sciences, Bowling Green State University
Bowling Green, Ohio, 43403
3. Department of Chemistry, University of Rochester
Rochester, New York, 14627

Symmetry breaking is a necessary condition of any photoconversion process, e.g., charges must be directed to opposite ends of a solar cell in order to generate a photovoltage and photocurrent. For solar cells this is typically done using bulk heterostructures i.e., semiconductor/metal, semiconductor/semiconductor junctions, in the case of organic PV a blend of donor and acceptor molecules that forms a bulk heterostructure ensure charge separation. Local symmetry breaking, i.e., at the molecular level, leads to a variety of novel phenomena, including ferroelectricity, bulk photovoltaic effect, even-order non-linear optics etc., and when spin orbit coupling is also present leads to bulk spin-orbit effects such as Rashba/Dresselhaus spin splitting and other novel spin-to-charge conversion processes such as the chiral induced spin selectivity (CISS) effect. Thus, control over symmetry breaking enables control over charge and spin degrees of freedom in semiconductor systems and can be utilized in a variety of energy conversion approaches.

Low dimensional semiconductors such as 2D semiconductors, nanowires, semiconductor nanocrystals and layered hybrid organic/inorganic semiconductors offer unique ways to control symmetry breaking via nanochemistry methods. We have explored three different types of symmetry breaking motifs in nanocrystalline systems, that I will discuss here. (1) We have developed methods to break symmetry in nanostructures by taking advantage of the inorganic/organic nature of colloidal nanocrystals, specifically, organic ligands attached to the surface of inorganic semiconductor nanocrystals, or quantum dots (QDs), that help to define and determine their physicochemical properties. We discovered that dipolar ligands undergo a cooperative ligand exchange process because they exhibit strong ligand-ligand interactions when oriented on the nanocrystal surfaces and when the interaction energy is less than $-0.45k_bT$ a phase transition occurs, yielding the ability to construct Janus-ligand shells. Janus-ligand shells describe a situation where one side of the NCs have one type of ligand and the other side another type. We used that to transform spherically symmetric QDs to ones that exhibit spontaneous polarization, breaking the symmetry of the QDs. The spontaneous polarization arises from the asymmetric Janus ligand shell which renders a dipole moment to the symmetric QD building blocks, while the spherical and colloidal nature of the QDs allows for close packing in films and arrays. We demonstrate this by aligning the QDs in an electric field and showing that they exhibit the pyroelectric effect. We also formed QDs with hydrophobic and hydrophilic ligands that form optically active Pickering emulsions.

Strong electronic coupling between the QD core and the surface bound ligands can also break the symmetry inherent in the PbS and PbSe electronic structure. One limit on the efficiency of multiple exciton generation (MEG) in PbSe and PbS QDs is the symmetric nature of the conduction and valence bands. Optically active ligands attached to QD surfaces breaks that symmetry by injecting electrons from the S1 state of the dye directly into the conduction band of PbS QDs. We found that such a synergistic process increases the MEG energy efficiency by almost a factor of two in the hybrid system.

(2) The composition of the nanostructures can also be used to break symmetry. Janus nanoparticles can be constructed by taking advantage of asymmetric cation exchange and the resulting PbS/CdS heterostructures also show an increase in the MEG efficiency. Quantum dots with quantum well shells can be used to break symmetry and allow for novel photophysical phenomena. We have studied charge and spin dynamics in novel CdS/CdSe/CdS/ZnS core/shell/shell/shell structures, where the CdS/CdSe/CdS forms a quantum well that localizes the hole within the CdSe region. As a results, the electron and hole are separated with resulting biexciton lifetimes lengthened into the nanosecond timescale, yet the PLQY remains high. We used ultrafast time-resolved circular dichroism and polarized pump and probe transient absorption spectroscopy to determine the excitation intensity dependent spin lifetime. Due to the low defect density and the charge separated nature of the carriers the spin lifetime is lengthened at room temperature to a >3 ns at low fluences. Lowering the bandgap of the CdSe shell opens up possibility to promote multiple exciton generation because the offset energy between the barrier and well can be > 2x the bandgap of the well.

The metal lone-pair electrons can induce local symmetry breaking and may underpin many of the interesting photophysical properties of the inorganic halide perovskite family of semiconductors. Recently, a stable low-temperature monoclinic polar phase was predicted for $CsSnBr_3$ and $CsSnI_3$, opening the possibility of direct investigation of a ferroelectric distorted structure in the presence of spin-orbit effects and quantum confinement. To date there are no reports of such a structure in $CsSnI_3$, and a known low-temperature monoclinic structure in $CsSnBr_3$ remains unexplored. We have found optical evidence of a polar transformation occurring around 240 K in $CsSnI_3$ nanocrystals, with several changes in optical behavior below this transition point, including possible high-energy photoluminescence indicating slowed charge carrier cooling. Slowed cooling offers the possibility of hot-carrier solar energy conversion and enhanced MEG, both reported phenomena in halide perovskite systems. Discovery of a stable ferroelectric structures semiconductor NCs opens many new potential directions for further research in e.g. Rashba excitons. We have studied the carrier dynamics above and below the symmetry breaking phase transition.

Finally, (3) introducing chirality into the structures ensures symmetry breaking. Chiral structures lack both inversion and mirror symmetry elements and recently chiral semiconductors have been shown to enable control over charge and spin populations at room temperature without the incorporation of magnetic elements or use of magnetic fields through the CISS effect. Control over spin and charge at room temperature may enable advances in solar photoconversion processes with particular impact on water oxidation and CO_2 reduction photoinduced reactions. Introducing chirality in nanoscale semiconductors can be accomplished either through organic/inorganic interactions, i.e., chiral ligands on achiral nanocrystals and.or through constructing morphological chiral superstructures, i.e, twisted nanocrystal wires, helical stacked layers, ect. We have developed a single step synthesis of chiral CdSe nanoplatelets in organic solvents resulting in highly emissive nanoplatelets with 3 monolayers. The resulting nanoplateletes were studied using CD, time resolved CD and PL. We have also developed a novel ultrafast probe of CISS and if time permits, I will discuss these results.

DOE Solar Photochemistry Sponsored Publications 2021-2024

1. R. Fei, M. Hautzinger, A. Rose, Y. Dong, I.I. Smalyukh, M. C. Beard, J. vd Lagamaat, “Controlling exciton/exciton recombination in 2-D perovskite using exciton polariton coupling”, *J. Phys. Chem. Lett.*, **2024,** 15, 1748-1754 **,** doi: 10.1021/acs.jpclett.3c03452

2. M. S. Martinez, M. Nolen, N. Pompetti, L. J. Richter, R. Li, C. Farberow, J. C. Johnson, and M. C. Beard, “Controlling Electronic Coupling of Acene Chromophores on QD Surfaces through Variable Concentration Ligand Exchange”, *ACS Nano*, 17, 14916-14929, **2023,** doi: 10.1021/acsnano.3c03498

3. J. Crassous, M. Fuchter, D. Freedman, N.A. Kotov, M.C. Beard, S. Feldman, “Emerging materials for chiral light control” *Nat. Rev. Mat*er, **2023,** doi: 10.1038/s41578-023-00543-3

4. Q. Hu, H. Hu, L. Cui, Z. Li, D. Svedruzic, J. Blackburn, M.C. Beard, W. Xiong, X. Gao, X. Chen., “Charge Transfer Mechanism in Au–Cyanobacteria Hybrid for Solar to Chemical Production”, *ACS Energy Lett*, 8, 1, 677-684, **2023,** doi: 10.1021/acsenergylett.2c02707

5. Z. Huang, J. Koubek, A. Sellinger, M.C. Beard, “Pickering Emulsions of Self-Assembled Lead Sulfide Quantum Dots with Janus-Ligand Shells as Nanoreactors for Photocatalytic Reactions”, *ACS Applied Nano Materials*, 5, 3, 3183-3187, **2022,** doi: 10.1021/acsanm.2c00341

6. S.K. Bera, M. Shrivastava, K. Bramhachari, H. Zhang, A.K. Poonia, D. Mandal, E.M. Miller, M.C. Beard, A. Agarwal, K.V. Adarsh, “Atom like interaction and optically tunable giant bandgap renormalization in large area atomically thin MoS_2”, *Phys. Rev. B*, 104, L201404, **2021,** doi: 10.1103/PhysRevB.104.L201404

7. Lisa, J. Blackburn, M.C. Beard, J.C. Johnson, “Interlayer Triplet Sensitized Luminescence in Layered 2-Dimensional Hybrid Metal-Halide Perovskites”, *ACS Energy Lett*, 6, 4079-4096, **2021,** doi: 10.1021/acsenergylett.1c02011

8. E. R. Kennehan, K. T. Munson, C. Grieco, G. S. Doucette, A. R. Marshall, M. C. Beard, J. B. Asbury, “Exciton-Phonon Coupling and Carrier Relaxation in PbS Quantum Dots – the case of carboxylate ligands”, *J. Phys. Chem. C*, 125, 41, 22622-22629, **2021,** doi: 10.1021/acs.jpcc.1c05803

9. M. S. Martinez, A. J. Nozik, Matthew C. Beard, "Size Dependent Janus-Ligand Shell Formation on PbS Quantum Dots”, *J. Phys. Chem. C*, 125,39, 21729-21739, **2021**, doi:10.1021/acs.jpcc.1c06713

10. Eric R. Kennehan, Kyle T. Munson, Christopher Grieco, Grayson S. Doucette, Ashley R. Marshall, M. C. Beard, John B. Asbury “Influence of Ligand Structure on Excited State Surface Chemistry of PbS Quantum”, *J. Am. Chem. Soc.*, 143, 34, 13824-13834, **2021**, doi: 10.1021/jacs.1c06248

11. Z. Huang, J. Hao, J. Blackburn, M.C. Beard, “Pyroelectricity of PbS Quantum Dot films induced by Janus-Ligand Shells”, *ACS Nano*, 15, 9, 14965-14971, **2021,** doi: 10.1021/acsnano.1c05185

12. G. M. Carroll, R. Limpens, G. Pach, Y. Zhai, M. C. Beard, and N. R. Neale “Suppressing

Biexciton Auger Recombination in Colloidal Silicon Nanocrystals with Hole Traps", *J. Phys. Chem. C.*, 125, 4, 2565-2574, **2021,** doi: 10.1021/acs.jpcc.0c11388

13. U. Banin, N. Waiskopf, L. Hammerstrom, G. Boschloo, M. Freitag, E.M.J. Johansson, J. Sa, H. Tian, M.B. Johnston, L.M. Herz, R.L. Milot, M.G. Kanatzidis, W.Ke, I. Spanopoulous, K.L. Kohlstedt, G.C. Schatz, N. Lewis, T. Meyer, A.J. Nozik, M.C. Beard, C.F. Megarity, F. Armstrong, C.A. Schmuttenmaer, V.S. Batista, G.W. Brudvig, "Nanotechnology for Catalysis and Solar Energy Conversion" *Nanotechnology*, 32, 042003, **2021,** doi: 10.1088/1361-6528/abbce8

Understanding Chiral-Induced Spin-Selectivity Effect for Solar Energy Conversion

Fan He, Jackie Johnson, Yong Yan, Matthew C. Beard, Jing Gu
Department of Chemistry & Biochemistry
San Diego State University
San Diego, CA

The discovery of chiral-induced spin selectivity (CISS) revealed the ability of chiral molecules to act as a spin filter, resulting in the alignment of the spin orientation of electrons when electrons transmit through the oriented chiral system. Recently, CISS has been explored for solar energy conversion, especially the oxygen evolution reaction (OER). For instance, recent research has shown that coating chiral molecules on a TiO_2 photoanode can significantly reduce the overpotential of OER. Furthermore, researchers revealed that the triplet ground state of oxygen prefers the formation of triplet ·OH. Therefore, when a spin-polarized ·OH intermediate is formed on the electrode surface in the presence of chiral molecules, the selectivity and activity of OER improves, manifested as low overpotential and high current density. Despite those great accomplishments, the role of chiral molecules in impacting charge separation, recombination, and charger transfer in photoelectrochemical systems is still vague. Thus, the FAIR project aims to understand the CISS effect in impacting charge separation, recombination, and transfer in

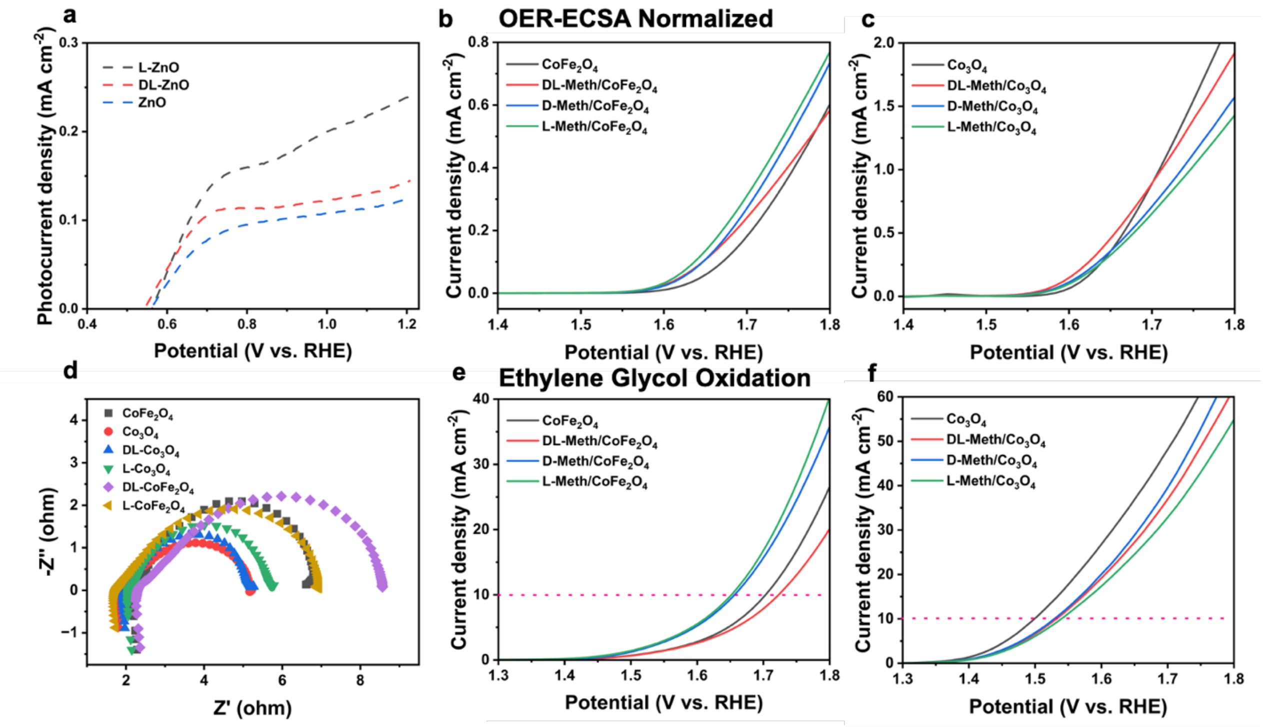

Fig 1. **a**. Linear Sweep Voltammetry (LSV) curves for chiral and achiral ZnO photoanodes. ECSA normalized OER LSV for chiral and non-chiral **b.** $CoFe_2O_4$ and **c.** Co_3O_4. **d.** Impedance measurements on chiral and non-chiral $CoFe_2O_4$ and Co_3O_4. LSV curves for ethylene glycol oxidation on chiral and non-chiral **e.** $CoFe_2O_4$ and **f.** Co_3O_4.

photoelectrochemical systems to shed light on the non-innocent role of chiral molecules in photosynthesis.

To differentiate the CISS effect between chiral materials with a helical structure and surface-bound chiral molecules on a semiconductor surface, we synthesized chiral ZnO photoanodes by using an amino acid-induced self-assembly method. Herein, L-ZnO crystals assemble into helically bent nanoplates in a left-handed direction while DL-ZnO forms a non-helical structure. The photocurrent density of chiral L-ZnO (0.26 mA/cm^2) doubles (under 0.5 M Na_2SO_4) compared to achiral DL-ZnO photoanode (0.13 mA/cm^2) at 1.23 V vs. RHE under OER condition (**Fig. 1a**). To understand the charge transport effect between photoelectrode and catalysts, $CoFe_2O_4$ (Ferromagnetic) and Co_3O_4 (paramagnetic) with different magnetic properties were synthesized and studied under electrochemical conditions in 1.0 M KOH (**Fig.1b-f**). We postulate that the inclusion of chiral molecules could potentially boost the OER performance of $CoFe_2O_4$, much like when exposed to a magnetic field. In contrast, Co_3O_4 should show minimum OER performance improvement. As expected, when a layer of L-(or D) methionine is drop cast on $CoFe_2O_4$, a positive shift of onset potential is observed (**Fig.1b**). Interestingly, a reverse effect with a negative onset potential shift is noticed on Co_3O_4 (**Fig.1c**). Similar onset potential shift trends are observed in ethylene glycol oxidation reaction (**Fig. 1e-f**). To avoid any onset potential shifts originating from chiral molecules affecting charge transfer or blocking active sites, impedance and electrochemical active surface area (ECSA) measurements were conducted (**Fig.1 d**). Both measurements demonstrate the presence of chiral molecules has a minimum impact on charge transfer or active site numbers. Future ultrafast spectroscopy will provide more insight into how CISS will impact light generation, charge separation, and charge transfer.

.

.

When the whole is greater than the sum of its parts: Understanding photocatalytic hydrogen evolution in CdS quantum dots (QDs) vs. QD gels

Vinicius Alevato[1], Daniel Streater[2], Joseph Frimpong[1], Moses Adeyemo[1], Cole Premtaj[1],
Zhenfei Liu[1], Jier Huang[2,3], Stephanie Brock[1]

[1]Department of Chemistry, Wayne State University, Detroit, MI 48202
[2]Department of Chemistry, Marquette University, Milwaukee, WI 53201
[3]Department of Chemistry and Schiller Institute for Integrated Science and Society, Boston College, Chestnut Hill, MA 02467

Quantum dot (QD) nanoparticles are promising systems for solar fuels generation because of their unique and tunable photophysical characteristics, with Cd chalcogenide systems the most extensively explored due to favorable band alignment for processes like water splitting. However, single Cd chalcogenide QDs suffer from instability due to photocorrosion and are, on their own, incapable of driving the complex series of events needed to enable efficient photocatalysis. Accordingly, we seek to establish methods to enable *selective* and *tunable* assembly of different functional nanoparticles, including QDs, into a 3-D macroscopic architecture capable of regulating the flow of energy and carriers while preserving access to the active surface of the constituent nanoparticles via an inter-connected pore network. Our initial target is to establish the relationship between the properties of individual QDs/catalyst moieties and their integrated composites, with a specific emphasis on how geometry, domain size, and interfacial linkers dictate exciton formation/delocalization, charge separation, charge transport, charge transfer, and catalysis within the ensemble. Our DOE Solar Photochemistry-supported multi-PI efforts incorporate QD gel network synthesis, modification, and catalytic testing (Brock), photophysics and transport evaluation using time resolved spectroscopies (Huang), and computational modeling of band structures, alignments, and optical properties of QDs and QD assemblies (Liu).

We started our investigation by addressing the question: How does the behavior of CdS quantum dots differ when incorporated into a 3-D porous network linked by endogenous disulfide bonds vs. when discrete and ligand capped, and what role does native structure (zincblende vs.

Figure 1. (a) H_2 production rate for CdS QDs and AGs (aerogels) as a function of structure (zinc blende, *zb*, vs. wurtzite, *w*); (b) effect of AG annealing on H_2 evolution; (c) TEM image of *w*CdS QDs and AG; (d) femtosecond transient absorption (fs-TA) of AGs; (e) effect of AG annealing on fs-TA

(b)

Catalyst	H_2 rate (μmol h^{-1} g^{-1})
*zb*CdS QD	1458
*zb*CdS AG	6650
*w*CdS QD	1221
*w*CdS AG	3325

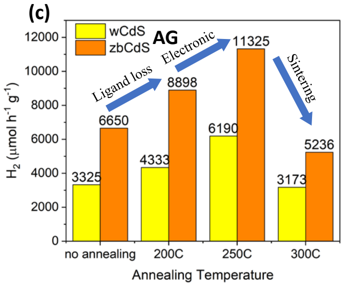

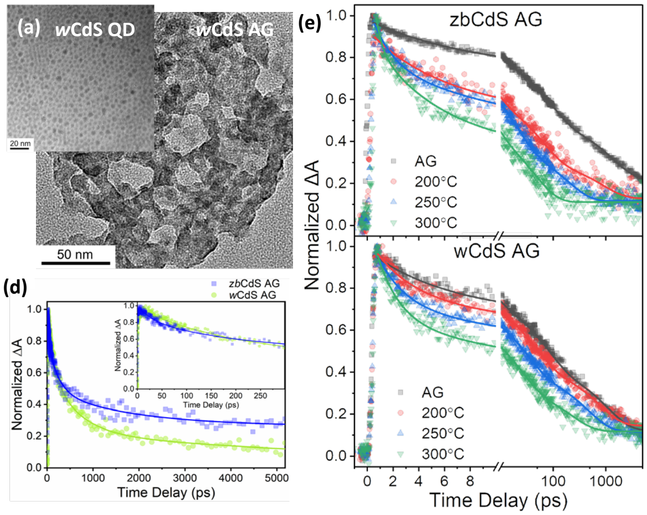

wurtzite) play? To answer this question, we prepared ~3.3 nm diameter CdS QDs adopting zincblende (*zb*) and wurtzite (*w*) structures and prepared aerogel (AG) structures with surface areas of ~ 200 m^2/g by oxidative assembly of thiolate-capped QDs followed by supercritical CO_2 drying. TEM images of starting QDs and AGs are shown in Figure 1(a). Photocatalytic water reduction was conducted using 1.0 mg catalyst in 50 mL of aqueous Na_2SO_3 (1.05M) + Na_2S (0.75M) with a 300 W Xe light source and a 425 nm cutoff filter. As shown in Figure 1(b), AGs exhibit 3-4 times the activity of QDs, and *zb* is more active than *w*. Annealing of AGs up to 250 ºC results in an enhancement of H_2 production rate, whereas further heating to 300 ºC results in deactivation (Figure 1(c)). The initial enhancement upon annealing is attributed to the loss of residual ligands in the aerogel, exposing more surface sites for catalysis, and possibly better electronic communication. Evaluation of 300 ºC samples reveals a decrease in the bandgap accompanied by an increase in the crystallite size and a decrease in the surface area, suggesting sintering is occurring, reducing the activity. Femtosecond transient absorption (fs-TA) spectroscopy of unannealed AGs (Figure 1(d)) reveal 2.5x longer lived excitons are present in the *zb*CdS AG relative to *w*CdS AG, indicative of a structural effect underlying the difference in activities. Fs-TA of annealed AGs (Figure 1(e)) suggests that the annealing process uniformly decreases the exciton lifetimes with increasing annealing temperature, likely due to the introduction of trap states. We hypothesize that excitonic lifetimes and consequent activity can be increased by effective passivation of trap states without loss of active sites (or, better yet, by introduction of co-catalysts to house the active sites). In furtherance of this goal, we have been computationally modeling the electronic effects of surface ligands as related to passivation (Figure 2).

Using first-principles approach, we studied the effect of ligand exchange on CdS QD facets, and found that one needs a combination of L-type (donating electron pairs to the surface) and X-type (forming covalent bonds with the surface) ligands to fully passivate the CdS surface (Figure 2). The precise combination of these two types of ligands can be determined based on an electron counting argument. These results provide guidelines for passivating surface defects that are prevalent in these materials. Furthermore, many-body perturbation theory calculations show that ligands can be used to tune the band edge energies without altering the intrinsic optical excitations of CdS. Our next steps will involve experimental validation of the computational results by introduction of specific ligand types and combinations to annealed AGs, and evaluation of their photodynamic and photocatalytic behavior.

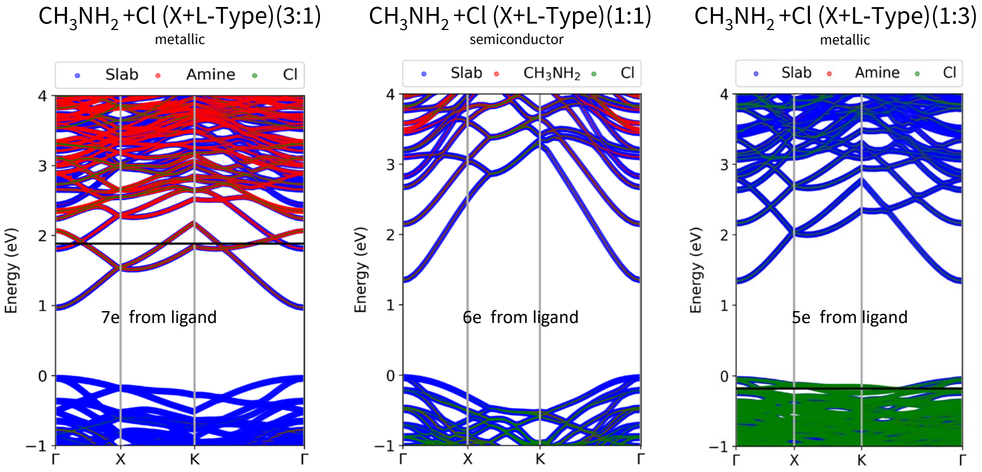

Figure 2. Effect of ligand type on surface passivation of (111) facets of zbCdS QDs. Six electrons are needed from the ligands to passivate the surface without introduction of mid-gap states. Addition of more or fewer electrons shifts the Fermi level up or down, respectively

DOE Solar Photochemistry Sponsored Publications

1. N. Behera, D. Gunasekera, J. P. Mahajan, J. Frimpong, Z.-F. Liu, and L. Luo, “Electrochemical hydrogen isotope exchange of amines controlled by alternating current frequency”, *Faraday Discuss.* 247, 45 (2023).

2. V. Alevato.; D. Streater, J. Huang, and S. L. Brock, “Effect of Crystal Structure on Aggregation of CdS Quantum Dots: Consequences for Photophysical Properties and Photocatalytic Hydrogen Evolution Activity”, *submitted*

3. J. Frimpong, S. Aryal, T. Karun, and Z.-F. Liu, “Understanding the ligand exchange in CdS quantum dots from first principles”, *manuscript in preparation*

4. V. Alevato, D. Streater, C. Premtaj, J. Huang, and S. L. Brock, “CdS Quantum Dot Aerogels for Photocatalytic Hydrogen Evolution” *manuscript in preparation*

Light-Controlled Multi-Electron Catalysis coordinated across Time and Space

Peter Agbo, Joel Ager, Frances Houle, Philipp Simon, Junko Yano
Chemical Sciences Division, Material Sciences Division, Molecular Biophysics and Integrated Bioimaging Division
Lawrence Berkeley National Laboratory
Berkeley, CA 94702

Artificial photosynthetic system designs have deep roots in our understanding of how natural photosynthesis works, borrowing key elements such as the energetic z-scheme, and coupling water oxidation to CO_2 reduction chemistry. Natural systems take advantage of catalytic cascades to build complex molecules from simple building blocks, and using cascades is a logical step to improve the efficiency and selectivity of conversion of solar energy into complex chemicals in artificial systems. The chemical reactions used for such conversion involve multi-electron/proton processes for making new bonds and molecules, and require the precise control of flow of charges and molecular reactants to be selective. A current bottleneck to the implementation of many of those reactions is a lack of product specificity due to the limited control of the reaction pathways. Research programs targeting the realization of artificial photosynthesis have contended with the challenges posed by reaction pathways that require many electrons and protons to make even the simplest compounds that meet practical energy density requirements. It has become clear that a single catalyst is not the best route to selectively and efficiently produce a specific product from CO_2 that requires more than 2 electrons, whether electrochemical or photoelectrochemical. To overcome this limitation, catalytic cascades are recognized as a key strategy for artificial photosynthesis (**Figure 1**). Our goal in this proposal is to master control over these reactions, directing charges and molecules to the catalytic sites throughout their lengthy reaction sequences.

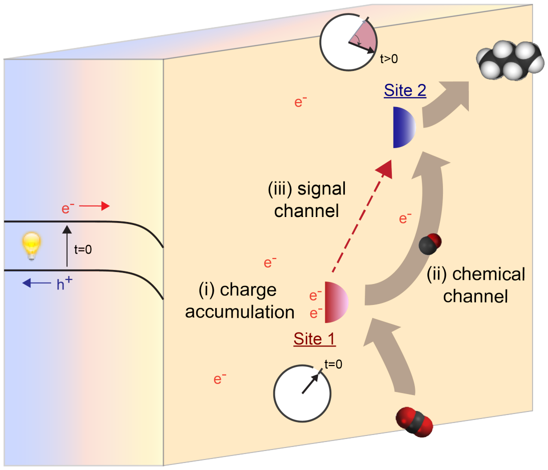

Figure 1: Signaling and chemical channels in multielectron PEC reaction using CO_2 reduction as an example. Control of charge accumulation at Site 1 **(i)** enables the first step of the cascade to occur at a specific time. Substrate channeling **(ii)** ensures that the intermediate formed at Site 1 arrives at Site 2 with high probability. Signaling from site 1 **(iii)** controls the timing of the second conversion step. In this way, the state of Site 1 is communicated to Site 2 when the reactive intermediate arrives, and the catalytic rates of two sites are matched for efficient

A fundamental challenge of controlling reaction sequence is that progress in the reaction relies on stochastic events, and electron transfers leading to charge accumulation at catalytic sites are random in time on heterogeneous surfaces. As a result, cascaded catalysts operate "open loop": the chemical activity of the second site in the cascade is uncoordinated with that of the first. The fundamental scientific questions raised are (1) *how can molecular-level processes initiated by multiple types of energy carriers - photons, electrons and holes, present at the same time and each with characteristic transport rates - be tightly coordinated, and* (2) *how can photo-driven catalytic sequences be actively controlled to ensure that only the desired products are formed.*

Signaling and chemical channels in multielectron Photoelectrochemical Reaction: Cascade catalysis (Abstract by Ager et al.) and multiple strategies to control substrate transport and timing of charge flow is a design that enables multielectron catalysis in natural enzymes. Our simulation results show that simple proximity of catalytic sites will not drive a controlled cascade, and entry of substrates into a connecting channel via isotropic diffusion is inherently inefficient. Using signaling methods to open a gate with charge pulses and controlling the timing to reset catalysts to their resting state will be an essential element.

We are exploring an architecture that includes a tunneling structure and pulsed circuitry to time charge injection. Such system will allow us to use experiment and computational methods to investigate charge injection rate vs turnover rate and the influence of pulse rate and charges on the catalyst and the chemical reactions.

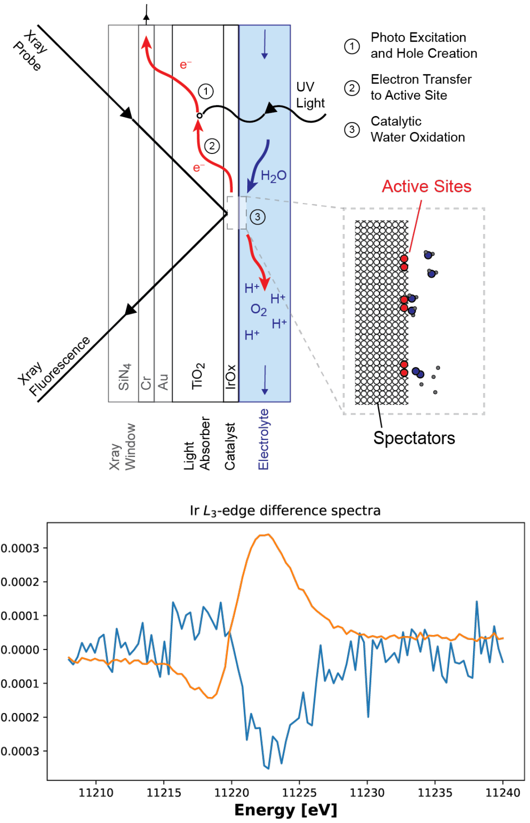

Figure 2: Photoabsorber TiO_2 with attached Ir oxide water oxidation catalyst. *(Top)* Experimental setup. *(Bottom)* Ir L_3-edge XAS difference spectra collected at BL 15-2 in SSRL under light (blue) and applied potential (orange).

Detecting chemical changes with temporal and spatial sensitivity: To follow chemical changes (charge accumulation and structural changes) at local active site(s) on heterogeneous surfaces during electrochemical and photoelectrochemical reactions, one needs to suppress dark signals that arise from dark spectator atoms. We are developing X-ray spectroscopy methods with modulation excitation in collaboration with Stanford Synchrotron Radiation Lightsource to effectively and uniquely detect signals from active catalytic sites. In **Figure 2**, we are working on this method using the water oxidation reaction with IrO_2 grown on TiO_2 substrate. We are also applying this method to characterize the electrocatalytic conversion of CO_2 on Cu under operation conditions (in collaboration with Liquid Sunlight Alliance). Stochastic kinetics simulations of the chemistry as a function of modulation frequency will enable both the X-ray data to be interpreted and the details of the theory used to construct the mechanisms to be examined more fully.

DOE Solar Photochemistry Sponsored Publications

1. Houle, F. A.; Yano, J.; Ager, J. W. Hurry Up and Wait: Managing the Inherent Mismatches in Time Scales in Natural and Artificial Photosynthetic Systems. *ACS Catal.* **2023**, *13* (11), 7139–7158. https://doi.org/10.1021/acscatal.3c00355.

2. Kim, C.; Govindarajan, N.; Hemenway, S.; Park, J.; Zoraster, A.; Kong, C. J.; Prabhakar, R. R.; Varley, J. B.; Jung, H.-T.; Hahn, C.; Ager, J. W. Importance of Site Diversity and Connectivity in Electrochemical CO Reduction on Cu. *ACS Catal.* **2024**, *14* (5), 3128–3138. https://doi.org/10.1021/acscatal.3c05904.

Development of Multicomponent Photoelectrodes for Solar Fuel Production

Daye Seo,[1] Andrew Grieder,[2] Andjela Radmilovic,[1] Yuan Ping,[2] and Kyoung-Shin Choi[1]
[1]Department of Chemistry
[2]Department of Materials Science and Engineering
University of Wisconsin-Madison
Madison, WI 53706

The overall objective of our project is to understand and control factors that affect the photoelectrochemical properties of multicomponent and multilayer oxide photoelectrodes for use in photoelectrochemical cells to produce fuels and chemicals. Our motivation to study multicomponent photoelectrodes is that the structural and compositional diversity of multicomponent photoelectrodes (e.g., ternary or quaternary oxide photoelectrodes) increase the chance of designing a photoelectrode with desired band positions, charge transport properties, and solution compatibility. Our motivation to study multi-layer photoelectrodes is that even when a promising photoelectrode is developed, it needs to be optimally interfaced with appropriate catalyst, buffer, and protection layers to most effectively and stably utilize surface-reaching charge carriers for desired redox reactions. In this presentation, we will discuss atomic doping of $BiFeO_3$ to produce p-type $BiFeO_3$ that can serve as a photocathode. We demonstrate how it can be used for solar O_2 reduction to H_2O_2 when coupled with an appropriate catalyst.

Bismuth iron oxide ($BiFeO_3$) is a semiconductor with an ABO_3-type perovskite structure in which Bi^{3+} occupying the A site is dodecahedrally coordinated by 12 O^{2-} and Fe^{3+} occupying the B site is octahedrally coordinated by 6 O^{2-}. Unlike the ideal perovskite (**Fig. 1a**), $BiFeO_3$ has a non-centrosymmetric structure caused by a rhombohedral distortion (**Fig. 1b**), and the resulting ferroelectricity has motivated the intensive investigation of $BiFeO_3$ for applications in electronics. Recently, $BiFeO_3$ has also been investigated as a photoelectrode for solar water splitting. It has a relatively narrow bandgap of ~2.2 eV and conduction band minimum (CBM) and valence band maximum (VBM) positions that straddle the water reduction and oxidation potentials, all of which are very favorable characteristics for a photoelectrode for use in a water-splitting or related photoelectrochemical cell.

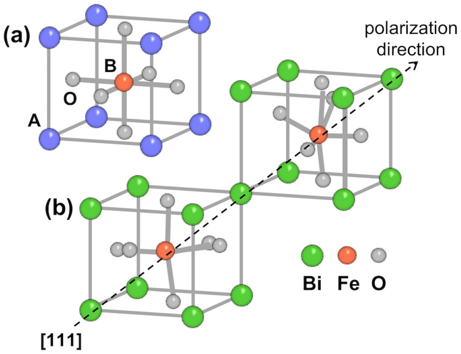

Fig. 1. (a) Ideal ABO_3 perovskite structure and (b) rhombohedrally distorted $BiFeO_3$.

Previous studies have shown that both n-type and p-type $BiFeO_3$ can be obtained without intentional doping. This means that both donor and acceptor-type defects can form readily and the dominant defect type can vary depending on the synthesis conditions. The defects that can serve as donors and induce n-type behavior include oxygen vacancies, while the defects that can serve as acceptors and induce p-type behavior include Bi vacancies. Since both donor- and acceptor-type defects can readily form and coexist in $BiFeO_3$, the concentration of the majority carrier in n-type or p-type $BiFeO_3$ formed without intentional doping is not considerably higher than that of the minority carrier. These lightly doped $BiFeO_3$ photoelectrodes are not optimal for evaluating the advantages and limitations of $BiFeO_3$ as a photoanode or a photocathode material.

In our recent study, we presented a new electrodeposition-based synthesis method to prepare $BiFeO_3$ electrodes. In this method, Bi and Fe metals are co-electrodeposited with a Bi:Fe ratio of 1:1 and then oxidized by thermal annealing in air to produce $BiFeO_3$ electrodes. The $BiFeO_3$ electrodes prepared by this method are n-type, meaning that under these synthesis conditions, more donor-type defects formed than acceptor-type defects. For the reason explained above, these n-type $BiFeO_3$ electrodes obtained without intentional doping are very lightly doped. In order to increase the free electron concentration, we additionally annealed the n-type $BiFeO_3$ electrodes under a N_2 environment to introduce more oxygen vacancies that can serve as donors. Using the resulting electrodes, we were able to evaluate the photoelectrochemical properties of $BiFeO_3$ photoanodes.

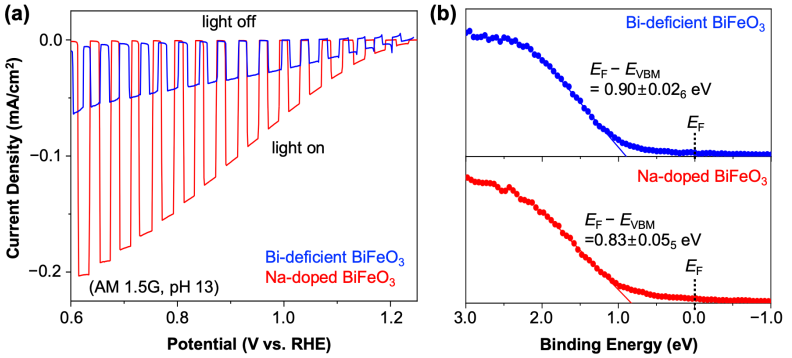

Fig. 2. (a) LSVs of Bi-deficient (blue) and Na-doped (red) $BiFeO_3$ photoelectrodes for O_2 reduction. (b) Valence band (E_F–E_{VBM}) spectra of Bi-deficient (blue) and Na-doped (red) $BiFeO_3$.

When it comes to p-type $BiFeO_3$, all reported $BiFeO_3$ photocathodes were prepared by intrinsic doping where Bi or Fe vacancies were created during synthesis either intentionally or unintentionally. However, to our best knowledge, extrinsic doping (i.e, introducing an impurity atom via substitutional doping to create acceptor levels), which may more methodically increase the hole concentration, has not been attempted to enhance the p-type behavior of $BiFeO_3$.

In this presentation, we report combined experimental and theoretical investigations on the substitutional doping of Na^+ at the Bi^{3+} site, which can considerably enhance p-type behavior of $BiFeO_3$. We prepared two different p-type $BiFeO_3$ electrodes, one with intrinsic doping (i.e., Bi vacancy, V_{Bi}) and the other with extrinsic doping (i.e., Na-doping at the Bi site, Na_{Bi}), while keeping other factors (e.g., film thickness and morphology) comparable. By comparing photoelectrochemical properties of these photoelectrodes (**Fig. 2**) and relating experimental and computational results (e.g., formation energy and the ionization energy of V_{Bi} and Na_{Bi}) (**Fig. 3**), we elucidate the difference between intrinsic doping and extrinsic doping and offer an atomic level understanding of their effects on the photoelectrochemical properties of p-type $BiFeO_3$. Furthermore, using the Na-doped $BiFeO_3$ photocathode decorated with a Ag nanoparticle catalyst, we demonstrate solar O_2 reduction to H_2O_2, which provides an energy-efficient and environmentally benign route for H_2O_2 production.

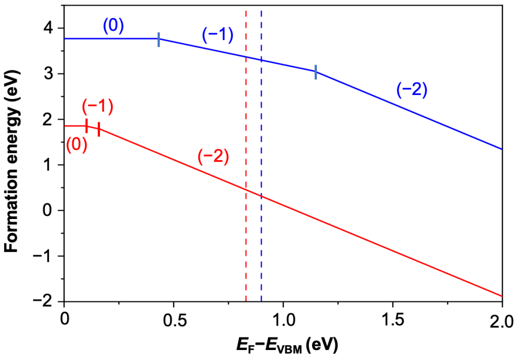

Fig. 3. Defect formation energy and charge transition levels of V_{Bi} (blue) and Na_{Bi} (red). The stable charge states as a function of E_F for each defect are denoted in the parenthesis. The dashed lines represent the experimentally determined E_F–E_{VBM} of Bi-deficient BiFeO (blue) and Na-doped $BiFeO_3$ (red).

DOE Solar Photochemistry Sponsored Publications 2023-2024

1. Wi, D. H.; Lumley, M. A.; Xi, Z.; Liu, M.; Choi, K.-S. “Investigation of Electron Extraction and Protection Layers on Cu_2O Photocathodes” *Chem. Mater.* **2023**, *35*, 4385–4392.
2. Kim, H. E.; Wi, D. H.; Lee, J. S.; Choi, K.-S. “Photoelectrochemical Nitrate and Nitrite Reduction Using Cu_2O Photocathodes” *ACS Energy Lett.* **2024**, *9*, 1993–1999.
3. Yuan, X.; Bender, M. T.; Choi, K.-S. “What the Nernst Equation Does Not Teach You about Water Reduction and Oxidation under Mild pH Conditions” *Nat. Catal.* **2024***,* Under review.
4. Seo, D.; Grieder, A.; Radmilovic, A.; Alamudun, S. F.; Yuan, X.; Ping, Y.; Choi, K.-S. “Atomic Doping to Enhance the p-type Behavior of $BiFeO_3$ Photoelectrodes for Solar H_2O_2 Production” **2024**, To be submitted.
5. Seo, D.; Somjit, V.; Galli, G.; Choi, K.-S. “Properties of $BiVO_4$ Photocathodes” **2024**, Manuscript in preparation.
6. Wang, W.; Zhou, C.; Hilbrands, A.; Chen, E.; Liu, M.; Choi, K.-S.; Galli, G. “Strategies and Open Questions in the Study of Photoactive Materials in Solar Water Splitting” **2024**, Manuscript in preparation.

Multilayered Nanoporous Photoanodes of Mixed-Metal Oxides for Solar Water Splitting

Logan Brennan, Jan Ragadi, Ivy Wang, Samuel Austin, Matt Law
Department of Chemistry
University of California, Irvine
Irvine, CA. 92617

The lack of efficient, stable, and low-cost materials for water oxidation is a major barrier to the development of a photoelectrochemical (PEC) water splitting technology that can meet the U.S. Hydrogen Shot goal of producing green hydrogen at a cost of less than $1/kg H_2 within the next decade. Many new materials for PEC water oxidation have been identified by calculations or high-throughput combinatorial discovery campaigns, yet detailed fundamental studies of these materials are needed to understand and control the factors that govern their water oxidation performance (efficiency and stability) and develop suitable photoanode architectures for practical PEC water splitting.

The goal of this new project is to combine studies of high-quality bulk single crystals and nanostructured films to understand the properties and photoelectrochemical behavior of several promising oxide semiconductors for solar-driven water oxidation and to test new concepts and strategies to enhance solar-to-hydrogen efficiency and durability (Figure 1). High-quality single crystals grown by the flux method will be used to establish the optical and electronic properties of each material, the impact of dopants on charge transport and oxygen evolution reaction (OER) photoactivity, and the corrosion pathways and kinetics of the main crystal surfaces, and to develop surface coatings that afford high OER activity and stability. The surface coatings, dopants, and optoelectronic insights from the single crystal work will be iteratively implemented in a novel class of nanoporous films made by our group that have a suitable architecture for high-performance,

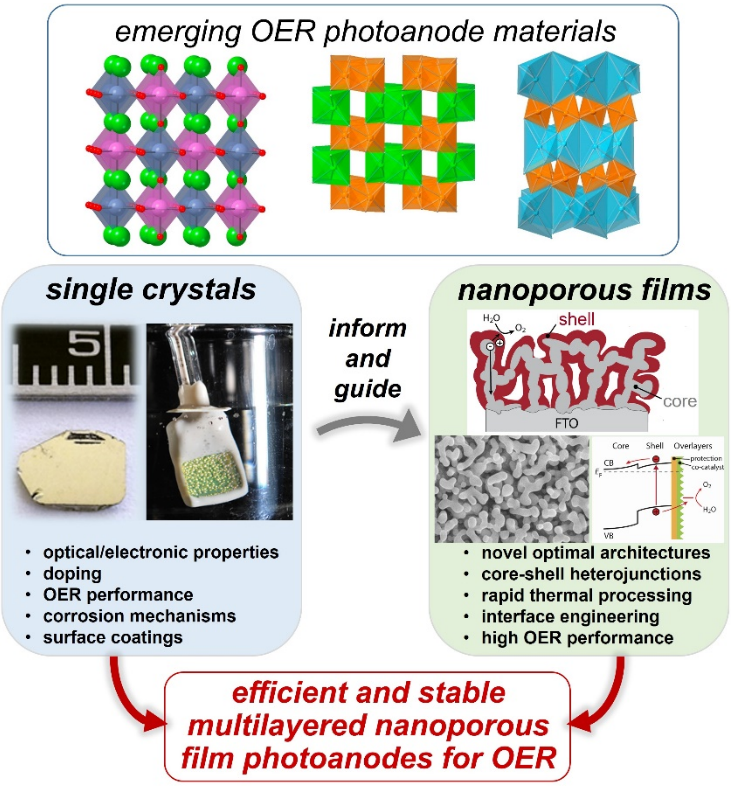

Figure 1. Project overview. Optoelectronic and photoelectrochemical studies of single crystals and nanostructured films will be used to determine the optoelectronic properties, OER activity, and corrosion mechanisms of new photoanode materials, develop surface coatings that afford high OER activity and stability, and guide the creation of multilayered nanoporous film photoanodes with optimal morphologies, compositions, and surface coatings for efficient and stable solar-driven water oxidation.

practical water oxidation. The nanoporous film morphology orthogonalizes the directions of light absorption in the semiconductor and hole delivery to the electrolyte to enable efficient light absorption and charge carrier utilization. These films are made by a scalable solution-phase method that offers independent control of nanocrystal composition and size, film porosity, and film thickness and provide a versatile experimental platform for developing solar fuels electrodes.

The first six months of the project have focused on the synthesis of single crystals and nanoporous films of the target phases. Small crystals of the most synthetically challenging of the target compounds were grown in CsI flux at 800 °C. Efforts to grow crystals of sufficient size for the proposed studies (> 3 mm) are ongoing. After discussing our latest single crystal results, I will demonstrate that our nanoporous film synthesis is a general way to fabricate phase-pure nanostructured films of a wide variety of binary and mixed-metal oxides, including $BiVO_4$, $Mn_2V_2O_7$, $BiFeO_3$, $FeWO_4$, WO_3, Fe_2O_3, and TiO_2 (e.g., Figure 2). Some of these compounds (e.g., $BiVO_4$, WO_3, and TiO_2) are intended for use as the core material of core-shell nanoporous films that feature a distributed *n-n* heterojunction between the core and shell materials with a type-II (staggered) band offset to force photogenerated electrons into the core and holes into the shell, greatly reducing recombination and improving OER efficiency. Plans to determine the electronic and optical properties and corrosion mechanisms of the target phases, identify the factors that govern the OER efficiency and durability of single-component nanoporous films of the target materials, develop effective passivation/protection/catalyst surface coatings to enhance OER performance, evaluate the ability of core-shell nanoporous films to improve charge separation and utilization close to thermodynamic limits, study rapid thermal processing as an approach for enhancing OER activity and stability by defect passivation and interface modification, and control morphology, composition, and surface coatings to demonstrate core-shell nanoporous films with record OER performance will be highlighted.

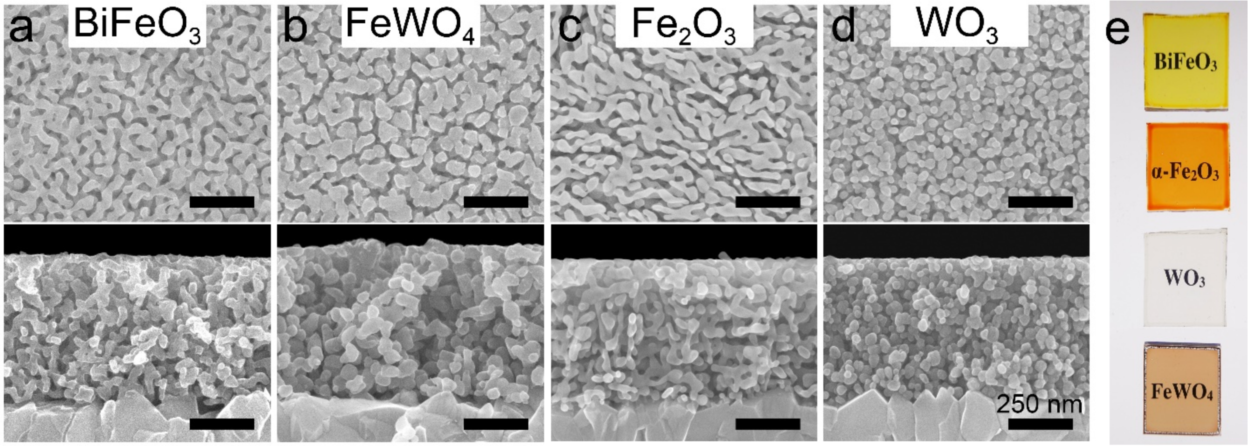

Figure 2. Nanoporous oxide films for photoanodes. (a-d) Plan-view and cross-section SEM images of nanoporous films of four different semiconductors. The films are 570 ± 30 nm thick and grown on 1-inch FTO-coated glass substrates. (e) Photographs of the films.

DOE Solar Photochemistry Sponsored Publications:

1. Brennan, L., Gargasya, Y., Law, M. A general solution route to nanoporous metal oxide films. *To be submitted.*

Molecularly Defined Multi-Metal Clusters for Solar Energy Conversion

Alex B.F. Martinson[1], Nuwanthaka Jayaweera[1], Shana Havenridge[2], Amelia M. Wheaton[2],
Colby S. Bell[2], Gethmini K. Jayasekara[2], Kihoon Kim[1], Cong Liu[2], Karen L. Mulfort[2]
[1]Materials Science and [2]Chemical Sciences and Engineering Divisions
Argonne National Laboratory, Lemont, IL 60439

Discrete, well-defined molecular-scale metal-containing clusters are ubiquitous in nature and accomplish many of the chemical transformations critical to sustaining life on earth. The goal of this program is to realize the potential of discrete metal clusters in the context of harvesting solar energy and light-initiated catalysis for fuels generation, Figure 1. We synthesize and characterize discrete atom-number metal-chalcogenide clusters of well-defined size and structure in order to tune visible light absorption, catalytic behavior, and environmental stability for comparison to zero-valent metal clusters whose light-harvesting and catalytic activity is limited by short excited state lifetimes and overall stability. Guided by computational analysis of thermodynamic stability and kinetic pathways, we leverage recent advances in emerging vapor-phase synthesis methods to pursue clusters whose structure we can tune by the identity of the metal centers, bridging anion, capping ligands, hetero-metal centers, and overall cluster size. We utilize a comprehensive suite of ground state and time-resolved characterization tools to uncover the light-driven behavior and role of localized electronic states resulting from unique metal-ligand and metal-metal interactions. We hypothesize that metal-chalcogenide clusters, although largely unexplored for solar energy harvesting, are superb candidates by which to understand effective light-harvesting and multi-electron transformations relevant to solar-driven fuels generation.

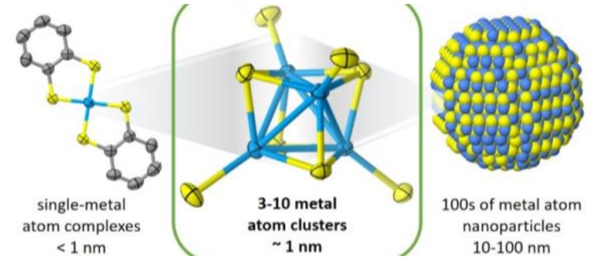

Figure 1. We investigate new molecularly-defined clusters that are fully computationally addressable and understandable.

We explore a new approach to discrete-atom-number metal chalcogenide cluster synthesis, via vapor phase methods related to atomic layer deposition (ALD). In ALD, alternating exposure of a planar surface to volatile and reactive metal- and sulfide-containing precursors enables deposition of metal sulfide thin films. In the limit of low ALD nucleation density, a 2D array of "islands" results that may eventually coalesce to a traditional thin film. We have previously shown that ALD of metal oxides *within* a polymer thin film, a process called Sequential Infiltration Synthesis (SIS), may seed inorganic deposition in a 3D array of few-atom metal-containing clusters. More recently, through this program, we have exerted careful control of the SIS process to grow a 3D array of In- and S-containing structures in polymethylmethacrylate (PMMA) that are consistent with atomically precise "magic-size" clusters. Across a range of polymers, temperatures, and SIS cycle number

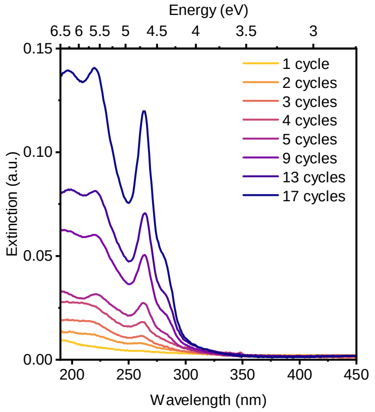

Figure 2. The optical absorption is largely independent of SIS cycle number.

we observe sharp optical absorption peaks that are characteristic of monodisperse few-atom clusters, Figure 2. We use first-principles computation to deduce one possible mechanism that leads to the formation of a $In_6S_6(CH_3)_6$ cluster that is simulated to be consistent with the experimental UV-Vis and infrared absorption spectra.

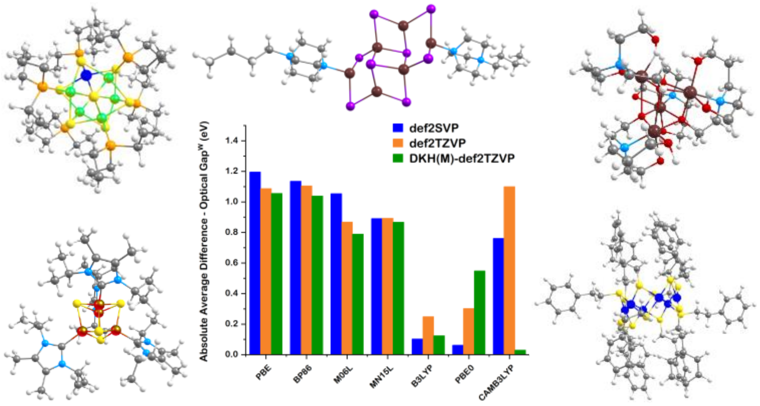

Figure 3. Optical gap differences between experiment and various levels of theory organized by basis set, for selected metal-chalcogenide clusters shown as DFT-minimized structures.

Computations can help synthetic procedures by aiding characterization through simulated absorption, infrared, and Raman spectroscopy, supplying reaction energies, and analyzing possible reaction mechanisms. In addition to providing experimental support, we have been exploring new model catalysts through computationally lead projects. Initially, as transition metal nanoclusters are often underrepresented in the literature, resulting in a lack of DFT benchmarking on the optical and photochemical properties, we have conducted a thorough benchmark on geometry, band, and optical gaps with different exchange-correlation functionals, Figure 3. Through this study, it was apparent that local interactions are important for ground state parameters, but exact Hartree-Fock exchange is needed for correct spin state and excited state properties.

More recently, we have been using this level of theory to analyze the potential for photocatalysis using nanoclusters of the general formula $Co_6E_8(PR_3)_6$ (E = S, Se; R = Et, Ph) (Figure 3, top left) and help guide experimental conditions for catalysis and synthetic modifications to the cluster. Previous work by other groups have shown that it is possible to remove a single PR_3 ligand from the clusters by application of heat or blue light, opening up an undercoordinated metal center that we propose will enable precise binding of small molecule substrates including H^+, H_2O, and CO_2. Further, we are computationally and experimentally evaluating synthesis routes for clusters of the general formula $Co_5M_1E_8(PR_3)_6$ where M is another first-row divalent transition metal to generate heterometallic clusters with asymmetric electronic structure with the potential to access preferential charge transfer pathways. We are also experimentally and computationally investigating how cluster oxidation state and ligand substitution impacts intra-cluster and cluster-to-ligand charge transfer transitions. Through this project, we aim to experimentally and computationally analyze how synthetic modifications influence cluster electronic structure and evaluate the energy barriers and mechanisms for photocatalytic HER and CO_2 reduction.

Future studies already in progress include expansion of the SIS methods for metal sulfide growth to include materials with greater visible light absorption including CdS-based clusters. Alternative SIS strategies will leverage alternative polymers or even small molecules to nucleate growth of clusters with superior uniformity and greater density. Ground state and time-resolved characterization tools will be used to investigate the role of localized electronic states that result from metal-ligand and metal-metal interactions.

DOE Solar Photochemistry Sponsored Publications

1. S. Havenridge, C. Liu. A “Theoretical Benchmark of the Geometric and Optical Properties for 3d Transition Metal Nanoclusters via Density Functional Theory.” *J. Phys. Chem. A* **2024**, *in revision*.
2. K. Kim, S. Havenridge, N. J. Zaluzec, D. Kang, N. Jayaweera, C. Liu, K. L. Mulfort, A. B. F. Martinson “Sequential infiltration synthesis of magic size indium sulfide clusters” **2024**, *in preparation.*

The Impact of Electric Fields on Electron Transfer at Metal Oxide-Electrolyte Interfaces

Quentin Loague, Matthew Goodwin, Hayden Mann, and Gerald J. Meyer

University of North Carolina at Chapel Hill, Department of Chemistry
Chapel Hill, NC 27599-3290

Our research focuses on the impact of electric fields on light driven interfacial electron transfer with molecular complexes at metal oxide interfaces [1-5]. One objective is to quantify the impact of electric fields on the absorption and photoluminescence spectra of transition metal complexes. Particular emphasis is placed on spin disallowed electronic transitions and those with large polarizability changes that serve as electric field reporters. A second objective involves determination of interfacial electron transfer kinetics to complexes located within the electric double layer of a transparent conductive oxide (TCO). Analysis of kinetic data measured as a function of the thermodynamic driving force with the Marcus-Gerischer theory allows determination of the fundamental electron transfer parameters necessary for predictive models.

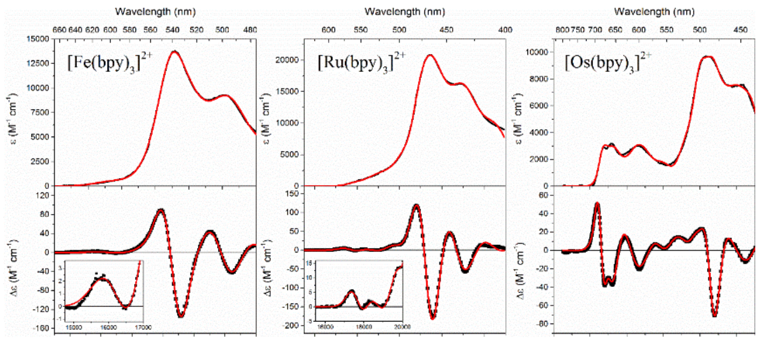

Figure 1. Absorbance (upper) and electroabsorption (lower) spectra of the indicated $[M(bpy)_3]^{2+}$ complexes measured at 77K in a butyronitrile glass. Insets for M = Fe, Ru are an expansion of the low energy region.

This presentation will begin with an overview of the two key objectives that include published and ongoing research. Figure 1 shows the absorption and electroabsorption spectra of $[M(bpy)_3]^{2+}$ complexes, where bpy is 2,2'-bipyridine and M = Fe, Ru, Os. Note the similarity of the metal-to-ligand charge-transfer (MLCT) absorption bands in the 350-550 nm range that differ significantly in the longer wavelength region. Indeed, a striking observation in these electroabsorption spectra are resolved features in the low energy region where $S_0 \rightarrow T_1$ transitions are expected and indeed observed when M = Os. The electroabsorption spectra appear to amplify transition(s) in this region and the most recent studies revealed a surprising sensitivity to the identity of the diimine ligands [5]. Liptay analysis indicated large 8-12 D excited state dipoles and a measurable change in the polarizability. As expected, the triplet charge transfer distances were significantly smaller than the singlet, although the difference was quite small for the iron complexes. Ongoing work seeks to more accurately quantify the polarizability changes with a new higher-order electroabsorption spectroscometer and to quantify excited state relaxation with a newly designed electrophotoluminescence apparatus.

The large dipole moments evident in Figure 1 indicate that these complexes are useful probes of the electric fields present at polarized metal oxide interfaces. Indeed, the physical location of electrons injected into core/shell SnO_2/TiO_2 nanostructures were probed with a $[Ru(bpy)_3]^{2+}$ complex that has phosphonic acid groups for surface attachment, abbreviated RuP = $[Ru(bpy)_2(4,4'-(PO_3H_2)_2-bpy)]^{2+}$ [3]. A comparative study of SnO_2, TiO_2 and SnO_2/TiO_2 core/shell materials, where the thickness of the TiO_2 shell was systematically varied, revealed that injected electrons reside within the SnO_2 core. The data indicates that the improved water oxidation yields reported for these core/shell materials emanate from slow electron tunneling through the TiO_2 shell. An interesting observation was that electric field magnitude was largest for SnO_2 and exceeded 1.2 MV/cm, behavior that was understood based on the small dielectric constant of SnO_2 (ε =10) relative to TiO_2 ($\varepsilon = 80$).

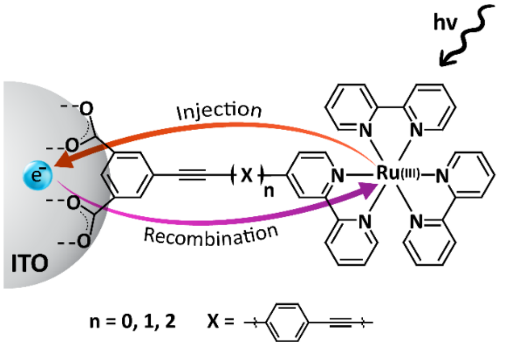

Figure 2. Excited state injection and interfacial charge recombination within the ITO electric double layer with rigid-rod complexes that bear 0, 1, or 2 phenylene ethynylene units.

The presentation will focus on the impact of molecular orientation and position on interfacial electron transfer kinetics within the electric double layer [1,2,4]. In collaboration with the Galoppini group, a series of three rigid-rod sensitizers based on phenylene ethynylene bridges were anchored to conductive tin-doped indium oxide (ITO), Figure 2. The visible absorption spectra and the formal potentials, $E^o(Ru^{III/II})$, of the surface anchored rigid-rods were insensitive to the presence of the phenylene ethynylene bridge units when measured in acetonitrile electrolytes. Both excited state injection and charge recombination kinetics were quantified as a function of the thermodynamic driving force, $-\Delta G^o$. Pseudo-rate constants for both electron transfer reactions were quantified and found to increase as the number of bridge units decreased at a fixed $-\Delta G°$. With the assumption that the reorganization energy, λ, and the electronic coupling matrix element, H_{ab}, were applied potential independent, Marcus-Gerischer analysis provided estimates of H_{ab} and λ. Interestingly, the data revealed that excited state injection involved the aromatic bridge units while charge recombination was through space, providing a new opportunity for vectoral electron transfer. The magnitude of λ values was found to increase with distance in qualitative agreement with dielectric continuum theory while H_{ab} decreased markedly with distance. The implications of these findings for applications in solar energy conversion will specifically be discussed.

DOE Solar Photochemistry Sponsored Publications 2021-2024

1. **Dye-Sensitized Solar Cells Strike Back**. Munoz-Garcia, A.; Benesperi, I.; Boschloo, G.; Concepcion, J.; Delcamp, J.; Gibson, E.; Meyer, G.J; Pavone, M.; Pettersson, H.; Hagfeldt, A.; Freitag, M. *Chem. Soc. Rev.* **2021**, *50*, 12450-12550.

2. **Reorganization Energies for Interfacial Electron Transfer Across Phenylene Ethynylene Rigid-rod Bridges.** Heidari, M.; Loague, Q.; Bangle, R.E.; Galoppini, E.; Meyer, G.J. *ACS Appl. Mater. Interfaces* **2022**, *14*, 35205-35214.

3. **Sensitizer Electroabsorption as a Probe of Electrons Injected into Nanocrystalline SnO_2/TiO_2 Core/Shell Thin Films.** James, E.M.; Bennett, M.T.; Meyer, G.J. *J. Phys. Chem. C* **2023**, *127*, 5904–5910.

4. **Impact of Molecular Orientation on Lateral and Interfacial Electron Transfer at Oxide Surfaces.** Loague, Q.; Keller, N.; Mueller, A.; Aramburu, B.; Bangle, R.; Schneider, J.; Polo, A.; Meyer, G.J. *ACS Appl. Mater. Interfaces* **2023**, *28*, 34249–34262.

5. **Impact of Diimine Ligands on Singlet-to-Triplet Charge-Transfer Electroabsorption in Iron and Ruthenium Complexes.** Maurer, A.B.; Loague, Q.R.; Goodwin, M.J.; Meyer, G.J. *J. Phys. Chem. A* **2024**, *in press.*

Organic, Nanoscale, and Self-Assembled Structures Relevant to Solar Energy Conversion

Michael J. Therien
Department of Chemistry
French Family Science Center, 124 Science Drive
Duke University
Durham, NC 27708-0354

Understanding the molecular-level principles by which complex chemical systems carry out photochemical charge separation and transport will impact the design of practical solar energy conversion and storage devices. Towards this goal, this program focuses on several broad themes, and aims to: (i) delineate new compositions of matter relevant to solar energy conversion, (ii) understand the basic photophysical properties of next-generation conjugated materials for excitonic solar cells, (iii) elucidate rules and principles that govern charge transfer, charge migration, the extent of charge and exciton delocalization, and exciton diffusion dynamics in structures and assemblies that enable light-driven energy transduction, (iv) probe and modulate the extent of electronic coupling between conjugated organic materials and nanoscale structures in both ground and excited states, (v) illuminate factors and design principles that regulate light-triggered charge carrier generation, and (vi) engineer high quantum yield electron-hole pair production from initially prepared excitonic states in hybrid compositions that feature nanoscale, electrooptically active components. Accomplishments over the current funding period include:

Regulating Electronically Excited Singlet-Triplet Energy Gaps through Substituent-Driven Modulation of the Exchange and Coulomb Interactions. Control of the singlet-triplet energy gap (ΔE_{ST}) is central to realizing productive energy conversion reactions, photochemical reaction trajectories, and emergent applications that exploit molecular spin physics. We have described a systematic method to tune ΔE_{ST} in simple molecular frameworks that holds chromophore size, and electronic structural parameters (such as the HOMO-LUMO gap) constant. Using a combination of molecular design, photophysical and potentiometric experiments, and quantum chemical analyses, we show that the degree of electron-electron

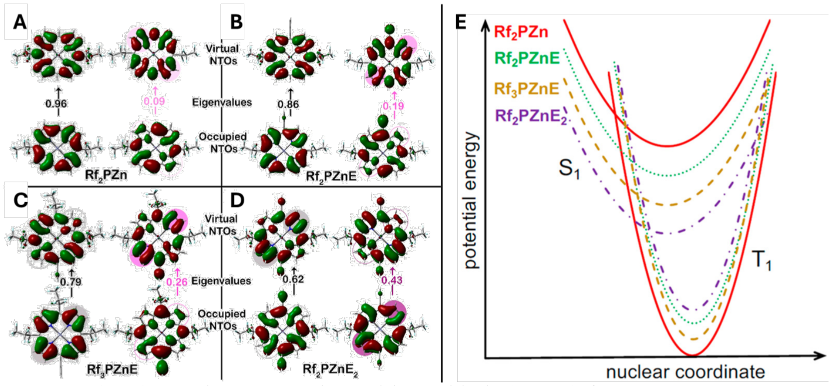

Figure 1. (A-E) Dominant natural transition orbitals (NTOs) for **Rf$_2$PZn**, **Rf$_2$PZnE**, **Rf$_3$PZnE**, and **Rf$_2$PZnE$_2$** (Rf = C_3F_7; E = ethyne) that contribute to the T_1 state wave functions computed at the S_1 state equilibrium geometry at the TD-MN15/TZVP level. The NTO pairs having the two largest eigenvalues in the transition density matrix are presented. Gray and pink shading emphasizes the extent of reduced electron density overlap at selected macrocycle locations in the occupied and virtual orbitals of these NTO pairs. Eigenvalues for the NTOs that describe the H→L (NTO$_1$) and H-1→L+1 (NTO$_2$) one electron transitions are highlighted in black and magenta respectively. (F) Schematic representation of S_1 and T_1 state potential energy surfaces for **Rf$_2$PZn**, **Rf$_2$PZnE**, **Rf$_3$PZnE**, and **Rf$_2$PZnE$_2$**, highlighting the dependence of absolute S_1 and T_1 energies and ΔE_{ST} upon the macrocycle substitution pattern. Note that the potentiometrically determined HOMO-LUMO (H-L) gaps (E_p; $E_{1/2}^{0/+}$ - $E_{1/2}^{-/0}$) for **Rf$_2$PZn**, **Rf$_2$PZnE**, **Rf$_3$PZnE**, and **Rf$_2$PZnE$_2$** are invariant (~2.27 eV).

repulsion in excited singlet and triplet states may be finely controlled through the substitution pattern of a simple porphyrin absorber, enabling regulation of relative S_1- and T_1-state energies by the designed restriction of the electron-electron Coulomb (J) and exchange (K) interaction magnitudes. This approach modulates ΔE_{ST} magnitude by controlling the densities of state in the occupied and virtual molecular orbital manifolds, natural transition orbital polarization, and the relative contributions of one electron transitions involving select natural transition orbital pairs. This roadmap, which regulates electron density overlaps in the occupied and virtual states that define the singlet and triplet wavefunctions of these chromophores enables new approaches to preserve excitation energy despite intersystem crossing (**Figure 1**).

Fluence Dependent Photoinduced Charge Transfer Dynamics in Polymer-Wrapped Semiconducting Single-Walled Carbon Nanotubes. Due to their spatial extent relative to single-walled carbon nanotube (SWNT) length scales, multiple excitons can coexist in a single tube. Multi-body interactions that involve excitons and charge carriers can therefore play key roles in the relaxation processes of SWNT charge separated states generated by optical excitation. We exploit a SWNT-molecular donor-acceptor hybrid system, *R*-PBN(b)-Ph_6PDI-[(6,5)SWNT], to elucidate how the ultrafast charge separation (CS) and thermal charge recombination (CR) dynamics that are triggered upon SWNT $E_{00} \rightarrow E_{11}$ excitation are affected by excitation fluence. Transient optical data that characterize these photoinduced CS and thermal CR reactions were acquired over optical excitation fluences that produce SWNT exciton densities ranging over ~0.7 –18 excitons (100 nm)$^{-1}$. These experiments distinguish four distinct pathways for decay of the ([SWNT$^{(\bullet+)n}$]-(PDI$^{-\bullet}$) CS state: classical thermal recombination between geminate (~10^1 ps time scale) and non-geminate SWNT hole polarons and PDI radical anions (~10^2 ps time scale), as well as two additional fluence-dependent processes involving these distinct charge separated states in which multi-body interactions impact relaxation dynamics. In these fluence-dependent reaction pathways, excess excitons which have not triggered a CS reaction are present; here, the combination of SWNT carrier diffusion time scales and the thermodynamic potential of the ^{1}[SWNT]$^{-/*}$ state drives relaxation of *R*-PBN(b)-Ph_6PDI-[(6,5)SWNT] charge separated states [[SWNT$^{(\bullet+)n}$]-(PDI$^{-\bullet}$)$_n$] to lower energy CS states characterized by hole (SWNT$^{(\bullet+)}$) and electron (SWNT$^{(\bullet-)}$) polarons ([SWNT $^{(-\bullet)n}$SWNT$^{(\bullet+)n}$]-(PDI)). When non-geminate SWNT$^{(\bullet+)}$ and SWNT$^{(\bullet-)}$ charge carriers are generated, CR dynamics depend on the migratory time scale of the solvated carbon nanotube polaron. For light-triggered charge transfer reactions involving SWNTs carried out under excitation conditions that lie outside of the dilute exciton regime, this work highlights that reactions driven by the carbon nanotube excited-state reduction ($^1E^{-/*}$) and excited-state oxidation ($^1E^{*/+}$) potentials can play a substantial role in determining the nature of the observed time-dependent charge transfer dynamics (**Figure 2**).

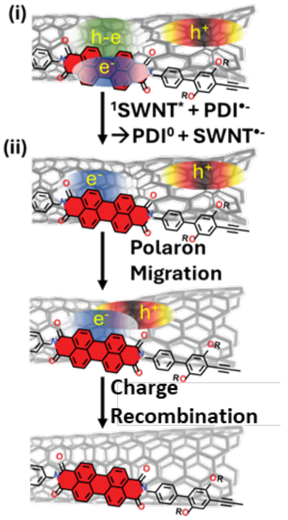

Figure 2. Schematic highlighting the reaction of persistent excitons with non-geminate charge separated (CS) states produced via photoinduced chare separation [^{1}SWNT*-(PDI)$_n$)] → [SWNT$^{(\bullet+)n}$]-(PDI$^{-\bullet}$)$_n$]. (i) Excess excitons react with PDI$^{\bullet-}$ [**^{1}SWNT* + PDI$^{\bullet-}$→PDI^0 + SWNT$^{\bullet-}$**] on the ps timescale, producing the PDI ground state and a SWNT electron polaron (**SWNT$^{\bullet-}$**). (ii) On a longer (100s of ps) timescale, SWNT electron and hole polarons recombine.

DOE Solar Photochemistry Sponsored Publications 2021-2024

1) EPR of Photoexcited Triplet State Acceptor Porphyrins, A. J. Redman, G. Moise, S. Richert, E. J. Peterson, W. K. Myers, M. J. Therien, and C. R. Timmel, *J. Phys. Chem. C* **2021**, *125*, 11782–11790. DOI: 10.1021/acs.jpcc.1c03278.

2) Excited State Dynamics and Nonlinear Optical (NLO) Properties of Hyperpolarizable Chromophores Based on Conjugated Bis(terpyridyl)Ru(II) and Palladium and Platinum Porphyrinic Components: Impact of Heavy Metals upon Supermolecular Electro-Optic Properties, A. Nayak, J. Park, K. De Mey, X. Hu, D. N. Beratan, K. Clays, and M. J. Therien, *Inorg. Chem.* **2021**, *60*, 15404−15412. DOI: 10.1021/acs.inorgchem.1c02041.

3) Spinning Molecules, Spinning Spins: Modulation of an Electron Spin Exchange Interaction in a Highly Anisotropic Hyperfine Field, A. M. Brugh, R. Wang, M. J. Therien, and M. D. E. Forbes, *ACS Omega* **2021**, *6*, 27865−27873. DOI: 10.1021/acsomega.1c03490.

4) Regulating Singlet-Triplet Energy Gaps through Substituent-Driven Modulation of the Exchange and Coulomb Interactions, E. J. Peterson, J. Rawson, D. N. Beratan, P. Zhang, and M. J. Therien, *J. Am. Chem. Soc.* **2022**, *144*, 15457−15461. DOI: 10.1021/jacs.2c06713.

5) Synthesis and Functionalization of Electron-deficient Perfluoroalkyl Porphyrin Building Blocks for Supermolecular Systems, R. Liu, J. Zhu, J. Rawson, L. R. Pederson, V. L. Cinnater, J. P. Mansergh, and M. J. Therien, *J. Porphyrins Phthalocyanines* **2023***, 27*, 741-756. DOI: 10.1142/S1088424623500451.

6) Light-driven Electron Transfer by Quantum Vibronic Ratcheting, P. P. Roy, Z. X. W. Widel, R. Liu, J. Valdiviezo, J. P. Mansergh, C. Leonardo, S. Chowdhary, D. N. Beratan, M. J. Therien, and G. R. Fleming, Manuscript in revision.

7) Fluence Dependent Photoinduced Charge Transfer Dynamics in Polymer-Wrapped Semiconducting Single-Walled Carbon Nanotubes, Z. X. W. Widel, J. A. Alatis, R. H. Stephenson, F. Mastrocinque, G. E. Bullard, J.-H. Olivier, Y. Bai, and M. J. Therien, Submitted.

8) Ultrafast, Photoinduced Proton-Coupled Electron Transfer Reactions that Exploit Electronically Excited Rylenes, R. Liu, Z. X. W. Widel, J. P. Mansergh, J. Zhu, A. R. Caplin, N. F. Polizzi, S. I. Mann, K. J. Pinnock, P. Zheng, W. F. DeGrado, D. N. Beratan, and M. J. Therien, Submitted.

Charge Generation in Mixed-Dimensionality Nanoscale Heterojunctions

Jeffrey L. Blackburn, Alejandra Hermosilla-Palacios, Alexis R. Myers, Justin D. Earley, Justin C. Johnson, Melissa K. Gish, Obadiah G. Reid, Andrew J. Ferguson, Garry Rumbles
Materials Chemistry and Computational Science Center
National Renewable Energy Laboratory
Golden, CO 80401

Free carrier generation mechanisms in low dielectric constant media, such as those used in organic solar cells, have been heavily debated for many years. While high dielectric constants of inorganic semiconductors facilitate electron-hole separation, low-dielectric organic semiconductors feature strong electrostatic interactions that bind electrons and holes in coulombically-bound carrier (CBC) states. Despite strong coulombic binding, many studies report substantial free carrier yields in solid-state organic materials. A range of hypotheses attempt to explain high free carrier yields in photoexcited and ground-state doped pi-conjugated semiconductors, including energetic disorder, carrier delocalization, electrostatic interactions, entropy, and carrier-carrier or Coulomb screening at relatively high carier concentration. Our group uses model systems to understand the roles of enthalpy, entropy, and molecular/interfacial structure on charge generation in nanoscale semiconductor architectures. This presentation will focus on two classes of "mixed-dimensionality" heterostructures that strategically pair 0D, 1D, and 2D semiconductors to reveal fundamental mechanisms of charge generation in both the excited state (e.g. donor/acceptor blends) and ground-state (e.g. redox-doped).

In the first topic, we demonstrate that mobile/conductive free charge carriers can be produced in chemically doped pi-conjugated semiconductors in low-dielectric environments, even at very low carrier density. Molecular redox doping has emerged as a useful strategy for improving organic solar cell efficiency, but fundamental mechanisms of redox doping in organic semiconductors are still debated. It is difficult to deconvolve structural, interfacial, and electronic structure heterogeneity impacts on charge generation in solid-state organic materials, blends, and heterostructures. Device measurements add extra uncertainties as to how doping modifies charge injection/extraction barriers. We simplify these variables in a model pi-conjugated electron donor/acceptor system by probing isolated, chemically-doped semiconducting single-walled carbon nanotubes (s-SWCNTs) in a low-dielectric constant solvent (toluene, $\varepsilon_r \approx 2.4$) to uncover the roles of dopant structure and local dielectric environment in free carrier generation. We intentionally employ this system and environment since traditional electrostatic models would predict no electronic conductivity in isolated organic host/dopant complexes in such conditions.

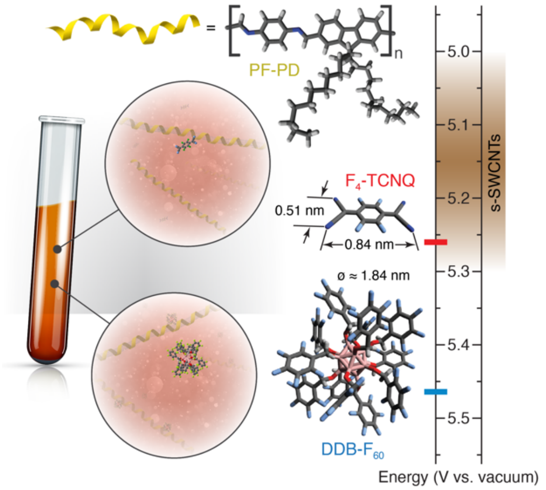

Figure 1. We use dielectric loss spectroscopy to measure the complex permittivity of redox-doped semiconducting SWCNTs in a low dielectric solvent. We find that dopant molecular structure and entropic stabilization play key roles in producing mobile charge carriers in this model system, providing general design rules for charge generation in pi-conjugated semiconductors.

Using dielectric loss spectroscopy, we demonstrate that large spherical (0D) molecular oxidants produce free charge carriers, substantial electronic conductivity, and an increase in the local dielectric constant, even at average dopant/carrier densities well below one hole per nanotube. A key to this result is the molecular structure of the dopant, which centers the electron transfer event onto a sterically isolated internal dodecaborane core, isolating the anion ~ 1 nm from the injected hole. Highly mobile free charge generation under these conditions requires a substantially lower CBC enthalpic stabilization than expected for a static low dielectric constant and/or entropic stabilization of free charges that can escape the CBC potential well, both of which have important and generalizable ramifications for understanding charge generation in organic pi-conjugated semiconductors.

In the second topic, I will discuss our development of rationally designed heterojunctions between 1D s-SWCNTs and 2D transition metal dichalcogenide (TMDC) monolayers to harvest visible/near-infrared photons and convert these excitations into long-lived charge-separated states. Energy harvesting applications rely critically upon the creation of tailored interfaces that enable the movement of energetic species (excitons, electrons, holes) in specified directions. We have demonstrated that Type-II heterojunctions between s-SWCNTs and TMDCs enable rapid exciton dissociation and microsecond charge-separated state lifetimes. Taking inspiration from the multistep charge transfer cascade found in the photosynthetic reaction center, we recently developed new TMDC/SWCNT/TMDC (2D/1D/2D) trilayer architectures that enable charge transfer cascades for improving charge separation yield and lifetime.

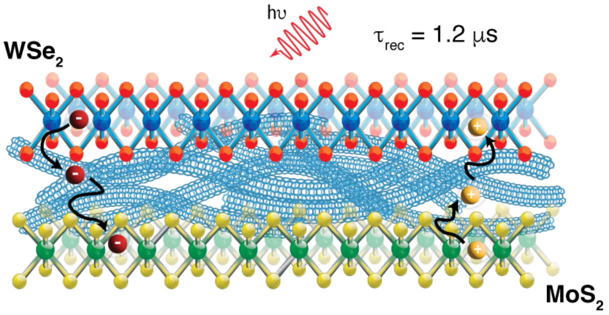

Figure 2. We utilize pump-probe spectroscopy to track exciton and charge dynamics in mixed-dimensionality heterostructures. Trilayer TMDC/s-SWCNT/TMDC heterostructures enable charge transfer cascade that increases charge generation yield and prolongs the lifetime of the resulting charge-separated state.

In this recent work, we prepare large-area MoS_2/SWCNT/WSe_2 trilayers and use selective excitation in pump-probe transient absorption spectroscopy to track exciton and charge dynamics. The charge transfer cascade in the trilayer roughly doubles the photoinduced charge yield and lifetime of the separated charges, relative to MoS_2/SWCNT bilayers. Interestingly, the trilayer architecture appears to facilitate ultrafast hole transfer to WSe_2 (<200 fs), a charge transfer reaction that is not efficient in the identically prepared WSe_2/SWCNT bilayer. The well-separated and narrow spectral features of each species in the trilayer also allow us to probe out-of-plane carrier diffusion in the nanotube layer and the degree to which bound interfacial excitons impact the photophysics in these mixed-dimensionality heterostructures. The behavior observed in these mixed-dimensionality heterostructures contrasts with the dominance of Coulomb-bound "interlayer" excitons in TMDC/TMDC heterobilayers or trilayers.

DOE Solar Photochemistry Sponsored Publications 2021-2024

1. Alexis R. Myers, Dana B. Sulas-Kern, Rao Fei, Debjit Ghoshal, M. Alejandra Hermosilla-Palacios, Jeffrey L. Blackburn. Quantifying Carrier Density in Monolayer MoS_2 by Optical Spectroscopy. **2024**, *Under Review*

2. Justin D. Earley, Obadiah G. Reid, Tucker L. Murrey, Evan A. Doud, Alexander M. Spokoyny, M. Alejandra Hermosilla-Palacios, Garry Rumbles, Andrew J. Ferguson, Jeffrey L. Blackburn. Efficient Free Carrier

Generation at Low Carrier Concentration in Chemically-doped Single-walled Carbon Nanotubes. **2024**, *Under Review*.

3. Kathyrn M. Neilson, Sarallah Hamtaei, Koosha Nassiri Nazif, Joshua M. Carr, Sepideh Rahimisheikh, Frederick U. Nitta, Guy Brammertz, Jeffrey L. Blackburn, Joke Hadermann, Krishna C. Saraswat, Obadiah G. Reid, Bart Vermang, Alwin Daus, Eric Pop. Toward Mass-Production of Transition Metal Dichalcogenide Solar Cells: Scalable Growth of Photovoltaic-Grade Multilayer WSe_2 by Tungsten Selenization. **2024**, *Under Review*. DOI: 10.48550/arXiv.2402.08534.

4. Daphné Lubert-Perquel, Jeffrey L Blackburn, Byeong Wook Cho, Young Hee Lee, Justin C Johnson. Modulating Resonant Electronic Coupling of Tungsten Diselenide Monolayers with Vanadyl Phthalocyanine for Spin-Valley Polarization Control. **2024**, *Under Review*. DOI: 10.48550/arXiv.2310.06979.

5. Alexis R Myers, Zhaodong Li, Melissa Gish, Justin Earley, Justin Johnson, M Alejandra Hermosilla-Palacios, Jeffrey Blackburn. Ultrafast Charge Transfer Cascade in a Mixed-Dimensionality Nanoscale Trilayer. *ACS Nano*, **2024**, *18*, 8190. DOI: 10.1021/acsnano.3c12179.

6. M Alejandra Hermosilla-Palacios, Marissa Martinez, Evan A Doud, Tobias Hertel, Alexander M Spokoyny, Sofie Cambré, Wim Wenseleers, Yong-Hyun Kim, Andrew J Ferguson, Jeffrey L Blackburn. Carrier density and delocalization signatures in doped carbon nanotubes from quantitative magnetic resonance. *Nanoscale Horizons* **2024**, *9*, 278. DOI: 10.1039/D3NH00480E

7. Gideon Oyibo, Thomas Barrett, Sharadh Jois, Jeffrey L. Blackburn, Ji Ung Lee. Measuring the Electronic Bandgap of Carbon Nanotube Networks in Non-ideal pn Diodes. **2024**, *Under Review.* DOI: 10.48550/arXiv.2212.05983

8. Tucker L. Murrey, Taylor J. Aubry, Omar Leon Ruiz, Kira A. Thurman, Klaus H. Eckstein, Evan A. Doud, Julia M. Stauber, Alexander M. Spokoyny, Benjamin J. Schwartz, Tobias Hertel, Jeffrey L. Blackburn, Andrew J. Ferguson. Tuning Counterion Chemistry to Reduce Carrier Localization in Doped Semiconducting Carbon Nanotube Networks. *Cell Reports Physical Science* **2023**, *4,* 101407. DOI: 10.1016/j.xcrp.2023.101407

9. Ivan Sudakov, Etienne Goovaerts, Wim Wenseleers, Jeffrey L. Blackburn, Juan G. Duque, Sofie Cambre. Chirality Dependence of Triplet Excitons in (6,5) and (7,5) Single-walled Carbon Nanotubes Revealed by Optically Detected Magnetic Resonance. ACS Nano **2023**, 17, 2190. DOI: 10.1021/acsnano.2c08392

10. Qiushi Hu, Haitao Hu, Lei Cui, Zhaodong Li, Drazenka Svedruzic, Jeffrey L. Blackburn, Matthew C. Beard, Wei Xiong, Xiang Gao, Xihan Chen. Ultrafast Electron Transfer in Au-Cyanobacteria Hybrid for Solar to Chemical Production. *ACS Energy Letters* **2023**, *8*, 677. DOI: 10.1021/acsenergylett.2c02707

11. Gideon Oyibo, Thomas Barrett, Sharadh Jois, Jeffrey L. Blackburn, Ji Ung Lee. All-Carbon Nanotube Solar Cell Devices Mimic Photosynthesis. *Nano Letters* **2022**, *22*, 9100. DOI: 10.1021/acs.nanolett.2c03544

12. Shai R. Vardeny, Alan Phillips, Kira A. Thurman, Z. Valy Vardeny, Jeffrey L. Blackburn. Amplitude-Mode Spectroscopy of Chemically Injected and Photogenerated Charge Carriers in Semiconducting Single-walled Carbon Nanotubes. *Nano Research* **2022**, DOI: 10.1007/s12274-022-5080-1

13. Bryon W. Larson, Kira A. Thurman, Hyun Suk Kang, Andrew J. Ferguson, Jeffrey L. Blackburn, Mark Steger. Arresting Photodegradation in Semiconducting Single-walled Carbon Nanotube Thin Films. *ACS Applied Nano Materials* **2022**, *5*, 3502 – 3511. DOI: 10.1021/acsanm.1c04140

14. Anna Zieleniewska, Fabian Lodermeyer, Maurizio Prato, Garry Rumbles, Dirk M. Guldi, Jeffrey L. Blackburn. Elucidating the Electronic Properties of Single-wall Carbon Nanohorns. *Journal of Materials Chemistry C* **2022**, *10*, 5783 – 5786. DOI: 10.1039/D2TC00179A

15. Zhaodong Li, Nuwan H. Attanayake, Jeffrey L. Blackburn, Elisa M. Miller. Carbon Dioxide and Nitrogen Reduction Reactions Using 2D Transition Metal Dichalcogenide (TMDC) and Carbide/Nitride (MXene) Catalysts. *Energy & Environmental Science* **2021**, *14*, 6242-6286. DOI: 10.1039/D1EE03211A

16. Zhiyuan Huang, Ji Hao, Jeffrey L. Blackburn, Matthew C. Beard. Pyroelectricity of Lead Sulfide (PbS) Quantum Dot Films Induced by Janus-Ligand Shells. *ACS Nano* **2021**, *15*, 14965-14971. DOI: 10.1021/acsnano.1c05185

17. Huize Wang, Simon Delacroix, Anna Zieleniewska, Jing Hou, Nadezda V. Tarakina, Daniel Cruz, Iver Lauermann, Andrew J. Ferguson, Jeffrey L. Blackburn, Volker Strauss. In Situ Synthesis of Molybdenum Carbide Nanoparticles Incorporated into Laser-Patterned Nitrogen-Doped Carbon for Room Temperature VOC Sensing. *Advanced Functional Materials* **2021**, *31*, 2104061. DOI: 10.1002/adfm.202104061

18. Noah J. Stanton, Rachelle Ihly, Brenna Norton-Baker, Andrew J. Ferbuson, Jeffrey L. Blackburn. Solution-phase p-type Doping of Highly Enriched Semiconducting Single-walled Carbon Nanotubes for Thermoelectric Thin Films. *Applied Physics Letters* **2021**, 119, 023302. DOI: 10.1063/5.0055837

19. Zhaodong Li, Chao Wu, Xian Gao, Bennett Addison, Xihan Chen, Jianping Yu, Drazenka Svedruzic, Jeffrey Blackburn, Wei Xiong. Exogenous Electricity Flowing Through Cyanobacterial Photosystem I Drives CO_2 Valorization with High Energy Efficiency. *Energy & Environmental Science* **2021**, *14*, 5480-5490. DOI: 10.1039/D1EE01526E
20. Dana B. Sulas-Kern, Hanyu Zhang, Zhaodong Li, Jeffrey L. Blackburn. Interplay Between Microstructure, Defect States, and Mobile Charge Generation in Transition Metal Dichalcogenide Heterojunctions. *Nanoscale* **2021**, *13*, 8188-8198. DOI: 10.1039/D1NR00384D
21. Hyun Suk Kang, Thomas J. Sisto, Samuel Peurifoy, Boyuan Zhang, Colin Nuckolls, Jeffrey L. Blackburn. Linking Optical Spectra to Free Charges in Donor/Acceptor Heterojunctions: Cross-Correlation of Transient Microwave and Optical Spectroscopy. *Materials Horizons* **2021**, *8*, 1509-1517. DOI: 10.1039/D0MH01810D
22. Henry V. Wladkowski, Julian Duarte, Shashank R. Nandyala, Joshua S. Walker, Subas Kattel, Jeffrey L. Blackburn, Jeffrey A. Fagan, Jon M. Pikal, William D. Rice. Polyvinyl Acetate-Based Polymer Host for Optical and Far-Infrared Spectroscopy of Individualized Nanoparticles. *Journal of Applied Physics* ***2021*** *129,* 034701. DOI: 10.1063/5.0033611

Identification of nuclear coordinates driving solar energy conversion processes using ultrafast Raman techniques

Margaret L. Clapham, Shahzad Alam, Polly G. Lynch, Aritra Das, Renee R. Frontiera
Department of Chemistry
University of Minnesota
Minneapolis, MN 55455

The goal of our DOE-sponsored research is to use advanced Raman spectroscopies to provide synthetic insight on molecular-based solar energy conversion systems. Specifically, we aim to identify certain nuclear coordinates and vibrational coherences which can be rationally modified in order to improve function. We make use of femtosecond stimulated Raman spectroscopy (FSRS), which monitors multidimensional structural changes on an ultrafast timescale, as well as resonance Raman intensity analysis, which provides structural information on the first tens of femtosecond following photoexcitation. Our group has made a number of technical advancements to the FSRS technique,[6] including incorporation of an optical microscope, development of spatially-offset FSRS, coherent control methods to identify driving from spectator modes, and development of methods to discriminate electronic from vibrational signatures. Here we have applied this expertise to the following DOE-sponsored projects in solar photochemistry:

In Figure 1, we depict our approach to quantifying the impact of specific nuclear coordinates on solar photochemistry. We use a double pulse excitation scheme in order to impulsively amplify mode-selective wavepackets on excited state potential energy surfaces. We then monitor the impact of this excitation on downstream processes with stimulated Raman probing. By comparing double pulse excitation with frequencies matched to all low frequency modes of the system, we are able to quantify the impacts of these specific nuclear coordinates on a photochemical process. We have applied this to several systems relevant to solar energy conversion, including metal-ligand charge

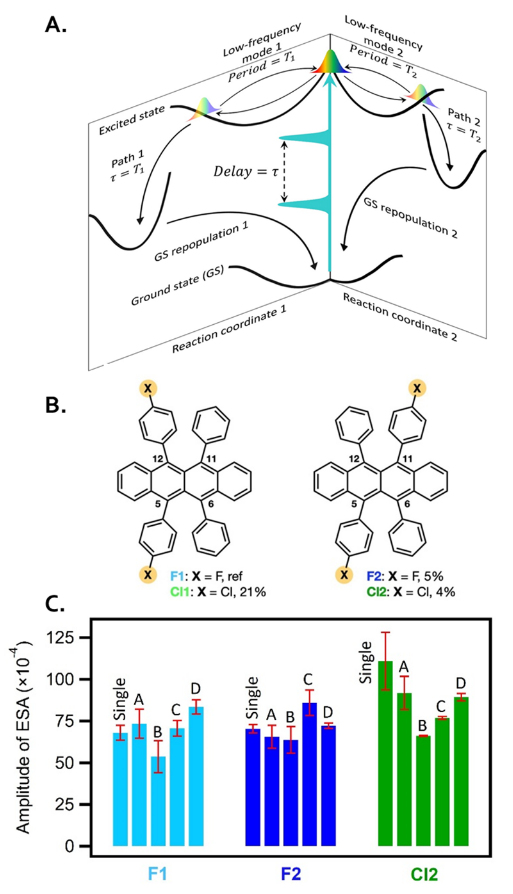

Figure 1. Mode-specific contributions to photochemistry as probed by double-pulse excitation femtosecond stimulated Raman spectroscopy. A. Depiction of double-pulse excitation, in which a single mode is coherently amplified and downstream photochemistry probed. B. Rubrene derivatives. C. Mode selective excitation impacts excited state absorption yields.

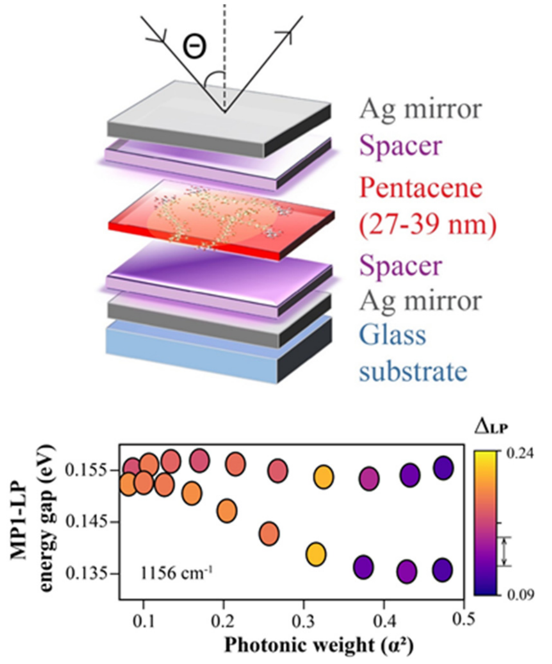

Figure 2. Resonance Raman intensity analysis quantifies dimensionless displacements (Δ) of excited state lower polaritonic potential energy surfaces in excitonic polarions.

transfer complexes from Professor Jim McCusker's group, pentacene dimers from Luis Campos and Matt Sfier's groups, and to derivatized rubrene samples (Figure 1B). In these samples we are able to distinguish driving from spectator modes through changes to photoproduct yields and amplitudes. In Figure 1C we show data from derivatized rubrene samples, where it is apparent that coherent excitation of low frequency mode B, a twisting of the edge phenyl rings,[3] results in suppression of photochemistry in a specific chlorinated derivative Cl2. Overall this work establishes a methodology to quantify the impact of all Raman-active low frequency modes on photochemical processes, and provides guidance for improved synthetic design.[2,6]

In an interrelated aim of this project, our objective is to map excitonic polariton potential energy surfaces along many nuclear degrees of freedom in order to optimize coupling of light to matter for photoinduced electron transfer. In Figure 2 we show our progress in this area, in which we are able to quantify the mode-specific displacements of the lower polaritonic surface relative to the molecular ground state. In this work we use resonance Raman intensity analysis to quantify the slope of the potential energy surface in the Franck-Condon region, which for polaritons is the most crucial as it is resonant with cavity excitation.

Additionally, we have constructed an *operando* femtosecond stimulated Raman apparatus (Figure 3) to track photoinduced dynamics under electrical bias with spectro-microscopy. Our initial results show variations in Raman frequencies as a function of spatial position, and our ongoing work will determine how these variations in local electric field interactions impact chemical reaction dynamics. Overall, our work provides quantitative insight as to how specific nuclear coordinates and vibronic degrees of freedom can be used to understand and control solar energy conversion.

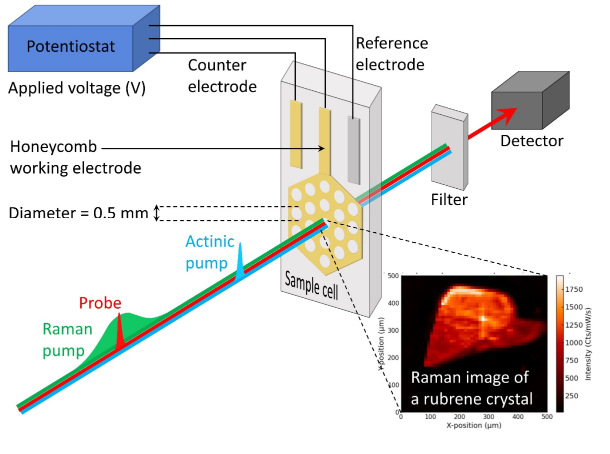

Figure 3. *Operando* femtosecond stimulated Raman spectroscopy probes photoinduced dynamics under electrical bias.

DOE Solar Photochemistry Sponsored Publications 2021-2024

1. Rich, C. C.; Frontiera, R. R. Vibronic Coupling and Exciton Chirality: Electronic and Structural Rearrangement between Helical to Zero Momentum Molecular Exciton States. *Journal of Physical Chemistry C* **2021**, *125* (39), 21511–21520. https://doi.org/10.1021/acs.jpcc.1c05827.

2. Bera, K.; Douglas, C. J.; Frontiera, R. R. Femtosecond Stimulated Raman Spectroscopy – Guided Library Mining Leads to Efficient Singlet Fission in Rubrene Derivatives. *Chemical Science* **2021**, *12* (41), 13825–13835. https://doi.org/10.1039/D1SC04251C.

3. Clapham, M. L.; Leighton, R. E.; Douglas, C. J.; Frontiera, R. R. Beyond Single Crystals: Imaging Rubrene Polymorphism across Crystalline Batches through Lattice Phonon Raman Microscopy. *The Journal of Chemical Physics* **2021**, *155* (23), 234703. https://doi.org/10.1063/5.0065496.

4. Clapham, M. L.; Frontiera, R. R.; Douglas, C. J. Mixed Rubrene Cocrystals Offer Insights into Intermolecular Interactions Influencing Crystal Packing. *Crystal Growth & Design* **2023**, *23* (6), 3942–3946. https://doi.org/10.1021/acs.cgd.3c00296.

5. Volek, T. S.; Armstrong, Z. T.; Sowa, J. K.; Wilson, K. S.; Bohlmann Kunz, M.; Bera, K.; Koble, M.; Frontiera, R. R.; Rossky, P. J.; Zanni, M. T.; Roberts, S. T. Structural Disorder at the Edges of Rubrene Crystals Enhances Singlet Fission. *Journal of Physical Chemistry Letters* **2023**, *14* (50), 11497–11505. https://doi.org/10.1021/acs.jpclett.3c02845.

6. Lynch, P. G.; Das, A.; Alam, S.; Rich, C. C.; Frontiera, R. R. Mastering Femtosecond Stimulated Raman Spectroscopy: A Practical Guide. *ACS Phys. Chem Au* **2024**, *4* (1), 1–18. https://doi.org/10.1021/acsphyschemau.3c00031.

Spin Chemistry of Photoinduced Charge Separation

Jens Niklas, Jasleen K. Bindra, Mandefro Y. Teferi, Karen L. Mulfort, Oleg G. Poluektov
Division of Chemical Sciences and Engineering
Argonne National Laboratory
Lemont, IL 60439

The goal of the Solar Photochemistry program in our group at Argonne is to uncover the fundamental atomic, electronic, and spin chemistry that can be used to link one-electron charge transfer states to the multi-electron charge accumulation that is essential for solar fuels catalysis. Molecular systems with their atomic scale precision provide an unparalleled opportunity to study how even small changes to the molecular structure can influence photochemical and catalytic activity. A highlight of this program is the interaction of synthesis with high-resolution physical characterization of the ground and excited states using a variety of techniques including transient optical spectroscopy, multifrequency EPR spectroscopy, X-ray absorption spectroscopy, and X-ray scattering. This talk will focus on research utilizing EPR spectroscopy and the deep insight into the electronic structure it provides. We are applying a suite of advanced EPR techniques, including ENDOR, ESEEM and DEER, to characterize in detail solar energy conversion systems. A specialty of our group is the application of time-resolved multifrequency EPR spectroscopy at X-band (9 GHz), Q-band (34 GHz), and D-band (130 GHz), which uses *in-situ* pulsed Laser excitation. Three topics will be discussed: 1) Singlet Fission (SF) in molecular systems containing pentacene and tetracene derivatives, 2) Light-induced spin dynamics in ZnO-quantum dot/organic molecule conjugates, and 3) Characterization of the microenvironment of molecular cobalt HER catalysts.

Singlet Fission. SF is a photophysical process in which a singlet exciton generated by light absorption of a ground state molecule interacts with a neighboring molecule in the ground state (Figure 1A). This interaction can create a correlated triplet pair in its singlet state ^{1}(TT), which is under certain conditions converted by coherent spin-mixing to the quintet state ^{5}(TT), potentially followed by decay to two independent triplets. One important question is how the generation of the correlated triplet pair and, therefore, the efficiency of SF can be improved. We have studied the spin dynamics of a variety of molecular pentacene and tetracene systems which demonstrate structure dependent efficiency of SF, intersystem crossing, and decay of the strongly coupled triplet pair to two weakly coupled triplets. Optical time-resolved spectroscopy can unravel photophysics and kinetics, but it cannot distinguish correlated and uncorrelated triplet pairs and reveal the spin dynamics of the spin-correlated states. In contrast, time-resolved EPR allows us to disentangle the spin dynamics and quantify the relative efficiency of SF processes in these complexes. The SF process can create multiple charge separated states from absorption of a single photon and potentially increases the power conversion efficiency of photovoltaic systems beyond the Shockley-Queisser

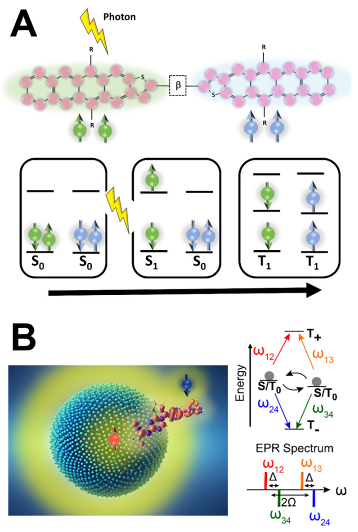

Figure 1. A) Singlet Fission (SF): Absorption of a photon results in a triplet pair in its singlet state ^{1}(TT), which can be converted to quintet state ^{5}(TT).
B) Light-induced Spin-Correlated Radical Pair (SCRP) in an organic dye/inorganic Quantum Dot (QD) system.

limit. Furthermore, these systems have gathered attention for potential use in Quantum Information Science (QIS), specifically quantum sensing and computation.

Light-Induced Spin Dynamics in ZnO-Quantum Dots. Photochemical charge separation in organic donor-acceptor systems and photosynthetic reaction center proteins can result in formation of spin-correlated radical pairs (SCRP), which is a crucial step in the chemical conversion of light energy. While organic donor-acceptor systems and photosynthetic reaction center proteins have been extensively studied, so far only very few EPR measurements of light-induced SCRPs in inorganic photocatalytic systems are reported. In this work, we study ZnO-quantum dots (QDs) connected to organic dye molecules (Figure 1B). The spin states of these systems can be probed and manipulated with microwave pulses using EPR techniques. The ZnO-QDs offer a flexible platform for studying electron spin-based qubit pairs owing to their size tunable electronic and spin properties, as well as their surface functionality. The spin states in QDs can have g-values distinctly different from those of organic molecules. This enables more straightforward spin specific addressability than what is available with fully organic systems, thus satisfying a key requirement of functional qubit systems. The wide choice of organic dyes allows to tailor optical absorption, energetics, kinetics and interaction strength between electron spins on donor and acceptor. This complementary approach opens the door to a deeper understanding of charge separation in organic molecule/inorganic QD complexes.

Microenvironment of Molecular Cobalt HER Catalysts. Natural photosynthetic systems provide valuable principles for highly efficient energy conversion of light to chemical fuels using molecular cofactors tailored to the specific utility of these organic and inorganic cofactors. Control over the cofactor microenvironment assists in stabilizing multiple oxidation and protonation states, and using these physical constructs allows to exert control over electronic structure and spin state. Previously, using multi-frequency EPR, we have studied in great detail the electronic structure of various cobalt complexes which are highly effective and stable H_2 evolution photocatalysts in near-neutral aqueous conditions, in a variety of solvents and solvent mixtures with a range of polarities. This enabled us to create correlation plots for magnetic resonance parameters which make it possible to understand the electronic structure and microenvironment of the molecular cobalt catalysts in diverse systems including natural, artificial and hybrid architectures. Recently, we synthesized a series of mononuclear Co(II)poly(pyridyl) complexes with well defined differences in their secondary coordination sphere, in particular with respect to the critical steps for proton management in molecular H_2 catalysis (Figure 2A). Using advanced pulsed EPR techniques such as Mims-type ^{1}H ENDOR (Figure 2B), we were able to identify different protonation sites at ~5 and ~3 Å from the Co(II) spin center, corresponding to protonation of the pyridine and bridging nitrogen, respectively. These experimental results will be complemented with synchrotron X-ray characterization and be supported with DFT calculations and molecular dynamics simulations.

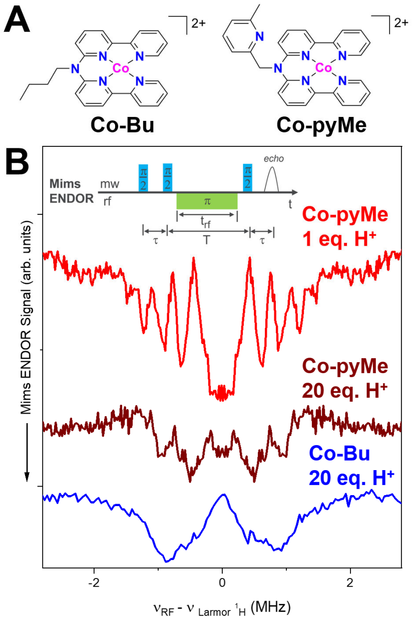

Figure 2. A) Structures of two Co(II)poly(pyridyl) HER catalysts. **B)** Mims-type ^{1}H X-band ENDOR difference spectra for Co-Bu and Co-pyMe in the presence of 1 or 20 equivalents of acid.

DOE Solar Photochemistry Sponsored Publications 2021-2024

1. M.Y. Teferi, A.Y. Lee, J. Niklas, T. Mani, J.H. Olshansky, O.G. Poluektov "Light-Induced Spin Qubit Pairs in Quantum Dot-organic Dyes Donor-Acceptor Hybrids – Size dependent properties of ZnO Quantum Dots" *in preparation* **(2024)**
2. J. Wong, M. Onizhuk, J. Nagura, A.S. Thind, J.K. Bindra, C. Wicker, G.D. Grant, Y. Zhang, J. Niklas, O.G. Poluektov, S. Guha, R.F. Klie, J. Zhang, G. Galli, F.J. Heremans, D.D. Awschalom, A.P. Alivisatos "Coherent Erbium Spin Defects in Collidal Nanocrystalline Hosts" *under review* **(2024)**
3. U. Kanbur, J.N. Hall, Y.L. Kim, J. Niklas, O.G. Poluektov, C. Liu, A.J. Kropf, M. Delferro, D.M. Kaphan "Supported Organochromium Ethylene Oligomerization Enabled by Surface Lithiation" *under review* **(2024)**
4. J. Zhang, G.D. Grant, I. Masiulionis, M.T. Solomon, J.K. Bindra, J. Niklas, A.M. Dibos, O.G. Poluektov, F.J. Heremans, S. Guha, D.D. Awschalom, "Optical and spin coherence of Er^{3+} in epitaxial CeO_2 on silicon" *under review* **(2024)**
5. G.D. Grant, J. Zhang, I. Masiulionis, S. Chattaraj , K.E. Sautter, S.E. Sullivan, R. Chebrolu, Y. Liu, J.B. Martins, J. Niklas, A.M. Dibos, S. Kewalramani, J.W. Freeland, J.G. Wen, O.G. Poluektov, F.J. Heremans, D.D. Awschalom, S. Guha "Optical and Microstructural Characterization of Er^{3+} Doped Epitaxial Cerium Oxide on Silicon" *APL Materials* 12, 021121 **(2024)** DOI: 10.1063/5.0181717
6. G. He, K.R. Parenti, P.J. Budden, J. Niklas, T. Macdonald, E. Kumarasamy, X. Chen, X. Yin, D.R. McCamey, O.G. Poluektov, L.M. Campos, M.Y. Sfeir "Unraveling Triplet Formation Mechanisms in Acenothiophene Chromophores" *Journal of the American Chemical Society* 145, 22058-22068 **(2023)** DOI: 10.1021/jacs.3c07082
7. X. Zheng, R. Reji, M.C. Drummer, H.Y. He, J. Niklas, N.P. Weingartz, I.L. Bolotin, L.X. Chen, O.G. Poluektov, P. Zapol, K.D. Glusac "Facile Optical Gap Tuning in Nanographene Metal-Organic Frameworks" *ACS Applied Optical Materials* 1, 1643-1650 **(2023)** DOI: 10.1021/acsaom.3c00220
8. Z.L. Xie, N. Gupta, J. Niklas, O.G. Poluektov, V.M. Lynch, K.D. Glusac, K.L. Mulfort "Photochemical charge accumulation in a heteroleptic copper(I)-anthraquinone molecular dyad via proton-coupled electron transfer" *Chemical Science* 14, 10219 - 10235 **(2023)** DOI: 10.1039/D3SC03428C
9. X. Zheng, M.C. Drummer, H.Y. He, T.M. Rayder, J. Niklas, N.P. Weingartz, I.L. Bolotin, V. Singh, B.V. Kramar, L.X. Chen, J.T. Hupp, O.G. Poluektov, O.K. Farha, P. Zapol, K.D. Glusac "Photoreactive Carbon Dioxide Capture by a Zirconium-Nanographene Metal-Organic Framework" *Journal of Physical Chemistry Letters* 14, 4334-4341 **(2023)** DOI: 10.1021/acs.jpclett.3c00049
10. A.Y. Lee, T.A. Colleran, A. Jain, J. Niklas, B.K. Rugg, T. Mani, O.G. Poluektov, J.H. Olshansky "Quantum dot-organic molecule conjugates as hosts for photo-generated spin qubit pairs" *Journal of the American Chemical Society* 145, 4372-4377 **(2023)** DOI: 10.1021/jacs.2c11952

11. K.E. McCullough, I.L. Peczak, R.M. Kennedy, Y.Y. Wang, J. Lin, X. Wu, A.L. Paterson, F.A. Perras, J. Hall, A.J. Kropf, R.A. Hackler, Y. Shin, J. Niklas, O.G. Poluektov, J. Wen, W. Huang, A.D. Sadow, K.R. Poeppelmeier, M. Delferro, M.S. Ferrandon "Synthesis of platinum nanoparticles on strontium titanate nanocuboids via surface organometallic grafting for the catalytic hydrogenolysis of plastic waste" *Journal of Materials Chemistry A* 11, 1216-1231 **(2023)** DOI: 10.1039/d2ta08133d
12. J. Niklas, L. Kohler, A.M. Potocny, K.L. Mardis, K.L. Mulfort, O.G. Poluektov "Electronic Structure of Molecular Cobalt Catalysts for H_2 Production Revealed by Multifrequency EPR" *Journal of Physical Chemistry* 126, 11889-11899 **(2022)** DOI: 10.1021/acs.jpcc.2c02576
13. A. Chapovetsky, R.M. Kennedy, R. Witzke, E.C. Wegener, F. Dogan, P. Patel, M. Ferrandon, J. Niklas, O.G. Poluektov, N. Rui, S.D. Senanayake, J.A. Rodriguez, N.J. Zaluzec, L. Yu, J.G. Wen, C. Johnson, C.J. Jenks, A.J. Kropf, C. Liu, M. Delferro, D.M. Kaphan "Lithium Ion Battery Materials as Tunable, Redox Non- Innocent Catalyst Supports" *ACS Catalysis* 12, 7233-7242 **(2022)** DOI: 10.1021/acscatal.2c00935
14. X.S. Liu, J.Z. Xie, J. Niklas, E.E. Turner, D.F. Yuan, J.S. Anderson, J.J. Rack, O.G. Poluektov, L. Yu "Donor-Acceptor Conjugated Copolymers Containing Transition-Metal Complex: Intrachain Magnetic Exchange Interactions and Magneto-Optical Activity" *Chemistry of Materials* 34, 5740-5747 **(2022)** DOI: 10.1021/acs.chemmater.2c01433
15. T. Ma, B.X. Dong, J.W. Onorato, J. Niklas, O. Poluektov, C.K. Luscombe, S.N. Patel "Correlating conductivity and Seebeck coefficient to doping within crystalline and amorphous domains in poly(3-(methoxyethoxyethoxy)thiophene)" *Journal of Polymer Science* 59, 2797-2808 **(2021)** DOI: 10.1002/pol.20210608
16. Y. Sha, X.M. Lin, J. Niklas, O.G. Poluektov, B.T. Diroll, Y. Lin, J. Wen, Z.D. Hood, A. Lei, E.V. Shevchenko "Insights into the Extraction of Photogenerated Holes from CdSe/CdS Nanorods for Oxidative Organic Catalysis" *Journal of Materials Chemistry A* 9, 12690-1299 **(2021)** DOI: 10.1039/d1ta01124c
17. B.X. Dong, C. Nowak, J.W. Onorato, T. Ma, J. Niklas, O.G. Poluektov, G. Grocke, M.F. DiTusa, F.A. Escobedo, C.K. Luscombe, P.F. Nealey, S.N. Patel "Complex Relationship between Side-Chain Polarity, Conductivity, and Thermal Stability in Molecularly Doped Conjugated Polymers" *Chemistry of Materials* 33, 741-753 **(2021)** DOI: 10.1021/acs.chemmater.0c04153
18. L. Kohler, A.M. Potocny, J. Niklas, M. Zeller, O.G. Poluektov, K.L. Mulfort "Replacing Pyridine with Pyrazine in Molecular Cobalt Catalysts: Effects on Electrochemical Properties and Aqueous H_2 Generation" *Catalysts* 11, 75 **(2021)** DOI: 10.3390/catal11010075

Pulse Radiolysis Investigations of Excess Charges in Conjugated Molecules and Mechanisms of CO_2 Reduction Catalysis

David C. Grills, Matthew J. Bird, Andrew R. Cook, John R. Miller, James F. Wishart
Chemistry Division
Brookhaven National Laboratory (BNL)
Upton, NY 11973-5000

The Electron- and Photo-Induced Processes (EPIP) program at BNL uses excitation by photons (in laser flash photolysis) or high-energy electrons (in pulse radiolysis), to investigate fundamental chemical problems relevant to the production and efficient use of solar energy. These include radiation chemistry in organic solvents, elucidating the primary radiolysis products, their relaxation dynamics and reactivity, and mastering their conversion into strong reductants or oxidants, to enable radiolysis studies of chemical reaction mechanisms. Radiolysis techniques provide unique insights into the redox thermodynamics and reactivity of transient species, which often cannot be obtained by conventional methods. Our work is carried out at the Accelerator Center for Energy Research (ACER) in BNL's Chemistry Division, which consists of two electron accelerators and two ^{60}Co gamma sources. These resources provide powerful and rare capabilities to BNL programs, as well as many external collaborators and users in energy research.

We have coupled nanosecond time-resolved mid-infrared spectroscopy (TRIR) with pulse radiolysis (PR), creating a unique capability (PR-TRIR) that provides improved characterization of radiolytically-generated transient species compared to conventional UV-Vis transient absorption spectroscopy, thus enabling a better mechanistic understanding of energy-related redox processes. We have applied PR-TRIR to a wide variety of systems in organic solvents, some of which are discussed here.

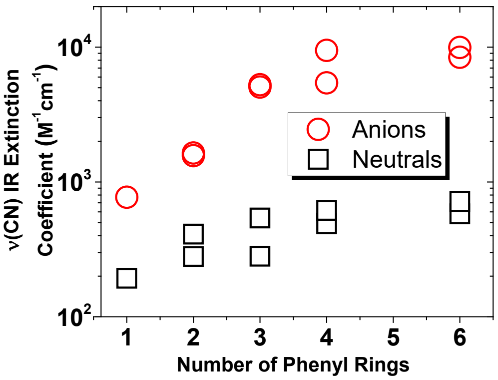

Probing the Nature of Excess Charges in Conjugated Molecules. Conjugated molecular chains have the potential to act as "molecular wires" in a variety of applications, including organic solar cells, catalysis, molecular electronics, and quantum information systems. In prior work, we showed that PR-TRIR can provide insight into the energetics and dynamics of excess charges in conjugated molecules due to the exquisite sensitivity of the ν(C≡N) IR frequencies of nitrile groups to the degree of electron delocalization and induced electric field. More recently,[7] employing a new series of ladder-type oligophenylenes, we have shown that the ν(C≡N) IR intensity and linewidth can also provide unique and complementary information on the nature of charges, with intensities revealing strong coupling to electronic structure, rising with excess charge and delocalization by >50× compared to the neutral monomer (see Figure above). This work was in collaboration with Prof. Tomoyasu Mani (University of Connecticut).

Understanding and Controlling Solvated Electrons and Radiolytic Radicals in Organic Solvents. Since PR acts on the solvent, creating a mix of solvated electrons (e_{solv}^{-}), protons, and various solvent-derived radicals, $R^{\bullet}$ (see Scheme below), it is critical that we understand and learn how to control these species, particularly when applying PR to mechanistic studies of catalysis. For example, we often employ formate anion (HCO_2^-) in acetonitrile (CH_3CN) to scavenge many of the deleterious solvent radicals, $R^{\bullet}$, via H-atom transfer, with the attendant generation of the useful reductant, $CO_2^{\bullet-}$. More recently, we used variable temperature PR to quantify the radiation yield, absorption spectrum, and equilibrium between the two forms (cavity electron and molecular dimer anion) of e_{solv}^- in CH_3CN.[12] This work furnished the previously lacking requisite data for fully quantitative PR investigations in CH_3CN. We also recently showed that tertiary amines, e.g., triethylamine (TEA), are oxidized following PR of a solution of TEA in CH_3CN.[18] This suppresses the formation of $R^{\bullet}$, and results in the generation of the useful reducing radical, $TEA^{\bullet}$, via a proton transfer between $TEA^{\bullet+}$ and TEA. This discovery allowed us to probe the elusive redox properties of the $TEA^{\bullet}$ radical, and the related triethanolamine radical, $TEOA^{\bullet}$. TEA and TEOA are ubiquitously used as sacrificial electron donors (SEDs) in photocatalytic CO_2 and proton reduction, as well as in a wide range of metallaphotoredox catalytic processes. However, the relative reducing powers of the $TEA^{\bullet}$ and $TEOA^{\bullet}$ radicals, which are always generated, were unknown. We established that, contrary to previous assumptions, $TEA^{\bullet}$ is a more potent reductant than $TEOA^{\bullet}$ by ~0.2 V, estimated using the Marcus cross relation. This knowledge will aid the design of photocatalytic systems involving SEDs. Current work is focused on determining the absolute redox potentials of these two radicals.

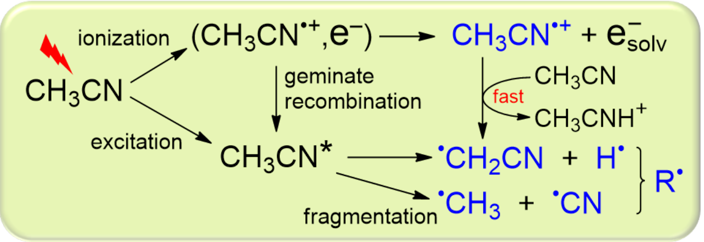

Application of Pulse Radiolysis to Mechanisms of CO_2 Reduction Catalysis. The knowledge gained from the fundamental radiation chemistry research described above has laid the foundation for our mechanistic PR investigations of CO_2 reduction catalysis. This work bridges the EPIP and Artificial Photosynthesis (AP) groups at BNL, and also involves various collaborators. Initial PR-TRIR work on the electrochemical CO_2 reduction pre-catalyst, $Mn(^tBu_2\text{-bpy})(CO)_3(HCO_2)$ ($^tBu_2$-bpy = 4,4′-$^tBu_2$-2,2′-bipyridine), identified all primary intermediates and monitored the kinetics of Mn-radical dimerization to $[Mn(^tBu_2\text{-bpy})(CO)_3]_2$. We have since applied PR-TRIR to probe the presence or absence of dimerization in various Mn-based catalytic systems, as well as the one-electron activation of Mn- and Re-based catalysts containing the electron-rich, non-innocent oxyquinolate ligand, in which subtle changes in the coordination environment were easily detected. In a recent study of the role of sterics and Lewis basicity in the 2nd coordination sphere,[9] we found that phenyl groups in the 6,6'-positions of a 2,2'-bipyridine ligand provide a 'sweet spot', offering sufficient steric bulk to hinder dimerization, but not too much so that the activation free energy for the rate-determining C–OH bond cleavage step remains low (see Figure right). Another powerful example of the utility of PR-TRIR was its use in fully characterizing every reaction step in the catalytic cycle of CO formation for the Co-macrocycle CO_2 reduction catalyst, $Co(HMD)^{2+}$ (HMD = 5,7,7,12,14,14-hexamethyl-1,4,8,11-tetraazacyclotetradeca-4,11-diene).[14]

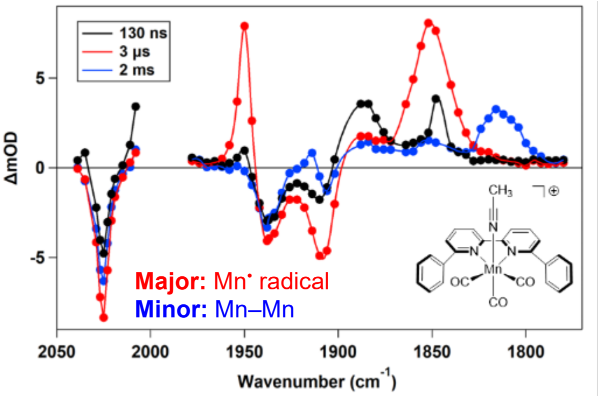

Future Work. We are collaborating with Prof. Juchao Yan (Eastern New Mexico University) to use carbonyl groups as IR probes of excess charges in oligo- and poly-(*p*-phenylenes). Current and future work on the fundamental radiation chemistry of organic solvents is focused on identifying more efficient scavengers of radiolytic solvent radicals that are also non-innocent in terms of their reactivity toward the solutes under investigation. We are also developing methods to investigate sequential reduction-protonation reactions by PR in CH_3CN. A new direction in the application of PR to understanding catalytic mechanisms is a focus on hydrogen atom transfer (HAT)-mediated CO_2 reduction to products other than CO, such as formate and methanol. We also plan to extend this work beyond CO_2 reduction, to more general mechanisms of photoredox catalysis that produce a variety of high-value organic chemicals.

DOE Solar Photochemistry Sponsored Publications 2021-2024

1. Dimarco, B. N.; Polyansky, D. E.; Grills, D. C.; Wang, P.; Kuwahara, Y.; Zhao, X.; Fujita, E. "Structural and Electronic Influences on Rates of Tertpyridine-Amine Co^{III}-H Formation During Catalytic H2 Evolution in an Aqueous Environment" *ChemPhysChem* **2021**, *22*, 1478-1487. doi:10.1002/cphc.202100295.
2. Rotundo, L.; Grills, D. C.; Gobetto, R.; Priola, E.; Nervi, C.; Polyansky, D. E.; Fujita, E. "Photochemical CO_2 Reduction Using Rhenium(I) Tricarbonyl Complexes with Bipyridyl-Type Ligands with and without Second Coordination Sphere Effects" *ChemPhotoChem* **2021**, *5*, 526-537. doi:10.1002/cptc.202000307.
3. Yan, J.; Wilson, R. W.; Buck, J. T.; Grills, D. C.; Reinheimer, E. W.; Mani, T. "IR linewidth and intensity amplifications of nitrile vibrations report nuclear-electronic couplings and associated structural heterogeneity in radical anions" *Chem. Sci.* **2021**, *12*, 12107-12117. doi:10.1039/d1sc03455c.
4. Blasczak, V.; Mckinnon, M.; Suntrup, L.; Aminudin, N. A.; Reed, B.; Groysman, S.; Ertem, M. Z.; Grills, D. C.; Rochford, J. "Steric and Lewis Basicity Influence of the Second Coordination Sphere on Electrocatalytic CO_2 Reduction by Manganese Bipyridyl Complexes" *Inorg. Chem.* **2022**, *61*, 15784-15800. doi:10.1021/acs.inorgchem.2c02586.
5. Fujita, E.; Grills, D. C.; Manbeck, G. F.; Polyansky, D. E. "Understanding the Role of Inter- and Intramolecular Promoters in Electro- and Photochemical CO_2 Reduction Using Mn, Re, and Ru Catalysts" *Acc. Chem. Res.* **2022**, *55*, 616-628. doi:10.1021/acs.accounts.1c00616.
6. Grills, D. C.; Layne, B. H.; Wishart, J. F. "Coupling Pulse Radiolysis with Nanosecond Time-Resolved Step-Scan Fourier Transform Infrared Spectroscopy: Broadband Mid-Infrared Detection of Radiolytically Generated Transients" *Appl. Spectrosc.* **2022**, *76*, 1142-1153. doi:10.1177/00037028221097429.
7. Grills, D. C.; Lymar, S. V. "Solvated Electron in Acetonitrile: Radiation Yield, Absorption Spectrum, and Equilibrium between Cavity- and Solvent-Localized States" *J. Phys. Chem. B* **2022**, *126*, 262-269. doi:10.1021/acs.jpcb.1c08946.
8. Polyansky, D. E.; Grills, D. C.; Ertem, M. Z.; Ngo, K. T.; Fujita, E. "Role of Bimetallic Interactions in the Enhancement of Catalytic CO_2 Reduction by a Macrocyclic Cobalt Catalyst" *ACS Catal.* **2022**, *12*, 1706-1717. doi:10.1021/acscatal.1c05043.
9. Carr, C. R.; Vrionides, M. A.; Grills, D. C. "Reactivity of radiolytically and photochemically generated tertiary amine radicals towards a CO_2 reduction catalyst" *J. Chem. Phys.* **2023**, *159*,

244503. doi:10.1063/5.0180065.

10. Henke, W. C.; Peng, Y.; Meier, A. A.; Fujita, E.; Grills, D. C.; Polyansky, D. E.; Blakemore, J. D. "Mechanistic roles of metal- and ligand-protonated species in hydrogen evolution with [Cp*Rh] complexes" *Proc. Natl. Acad. Sci. USA* **2023**, *120*, e2217189120. doi:10.1073/pnas.2217189120.
11. Blasczak, V.; Murphy, A.; Suntrup, L.; Ngo, K. T.; Reed, B.; Groysman, S.; Grills, D. C.; Rochford, J. “Structure activity relationships for second-coordination sphere functional group dependent CO_2 reduction by managanese bipyridyl electrocatalysts” *ChemCatChem* **2024**, *16*, e202301388 (cover article).
12. Pham, T-N.; Ertem, M. Z.; Grills, D. C.; Yap, G. P. A.; Rosenthal, J. “Synthesis, Characterization and Evaluation of a Non-Aromatic Fe(III) Isocorrole Complex for the Electrochemical Reduction of CO_2 to CO”, *Inorg. Chem.*, submitted.
13. Zhang, L; Muller A. V.; Grills, D. C.; Polyansky, D. E.; Sampaio, R. N.; Concepcion, J. J. “Control of Selectivity in Photochemical CO_2 Reduction with the Redox Potential of the Photosensitizers” *ACS Catal.* **2024**, submitted.

Use of carbonyl as an infrared reporter for probing the nature of charges in oligo- and poly-(*p*-phenylene)s

Juchao Yan,[1] Marat R. Talipov,[2] Sandra Biedron,[3] Tomoyasu Mani,[4] David C. Grills,[4] Xin Zhang[5]

[1] Department of Physical Sciences, Eastern New Mexico University, Portales, New Mexico 88130
[2] Department of Chemistry and Biochemistry, New Mexico State University, Las Cruces, New Mexico 88003
[3] Department of Electrical and Computer Engineering, University of New Mexico, Albuquerque, New Mexico 87131
[4] Chemistry Division, Brookhaven National Laboratory, Upton, New York 11973
[5] Physical Sciences Division, Pacific Northwest National Laboratory, Richland, Washington 99352

Although a record-high power conversion efficiency of ~19% has been achieved, there is still a long way to go for the ultimate commercialization of all-polymer solar cells. The bottleneck is due, in part, to the lack of understanding and control of the movement of localized electrons in donor-acceptor-type conjugated polymers.

In our prior work, we synthesized ladder-type, nitrile-functionalized oligo-(*p*-phenylene)s and used pulse radiolysis coupled with nanosecond time-resolved infrared spectroscopy (PR-TRIR) to probe electron delocalization. Although it offers a superb infrared reporter for probing electron delocalization, the nitrile group is not commonly incorporated into solar-relevant polymers. We have thus selected the carbonyl moiety as a new infrared reporter in ladder-type, oligo- and ploy-(*p*-phenylene)s for the same purpose. In this talk, we will talk about our molecular design and synthesis, theoretical calculations using density functional theory (DFT) for the structure-property relationships, as well as our electronic structure study by MeV ultrafast electron diffraction and optical-pump terahertz-probe spectroscopy in the near future.

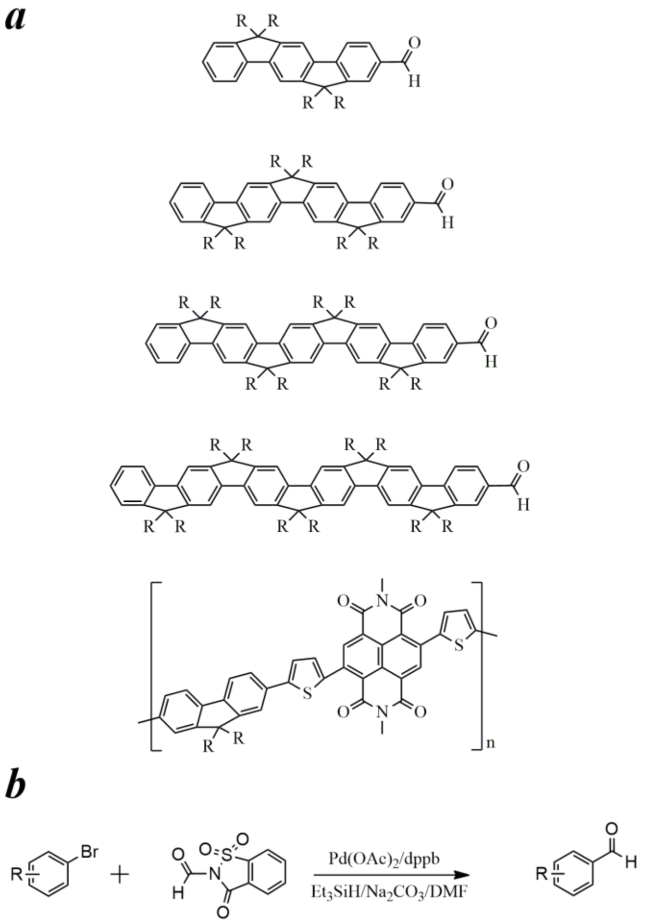

Scheme 1. (***a***) Molecular structures of the carbonyl-terminated oligo- and poly-(*p*-phenylene)s, and (***b***) the generic process for reductive carbonylation.

Scheme 1 illustrates the molecular structures for the title compounds and the reductive carbonylation for converting mono-brominated oligo(*p*-phenylene)s into carbonyl-terminated oligo(*p*-phenylene)s. The syntheses of mono-brominated oligo(*p*-phenylene)s generally include Suzuki cross coupling, cyclization, alkylation, and bromination.

DFT and multistate parabolic model (MPM) are used to evaluate the negative charge distributions for the anion radicals of a series of polyfluorenes (PF_n), ladder-type, oligo-(*p*-phenylene)s (L_n), and their derivatives with a carbonyl group at one terminus. Figure 1 shows the spatial distribution of spin density for the anion radicals of the oligomers. For oligomers terminated with hydrogens on both ends, the charge is predominantly localized in the middle of the chain, covering 7-8 units. For oligomers capped on one end with a carbonyl group, a dramatic shift of the charge is observed, towards the capped end. In future work, this will be probed experimentally using the PR-TRIR technique at Brookhaven National Laboratory.

Figure 1. Isovalue plots showing spatial distribution of spin density for the anion radical states of oligomers.

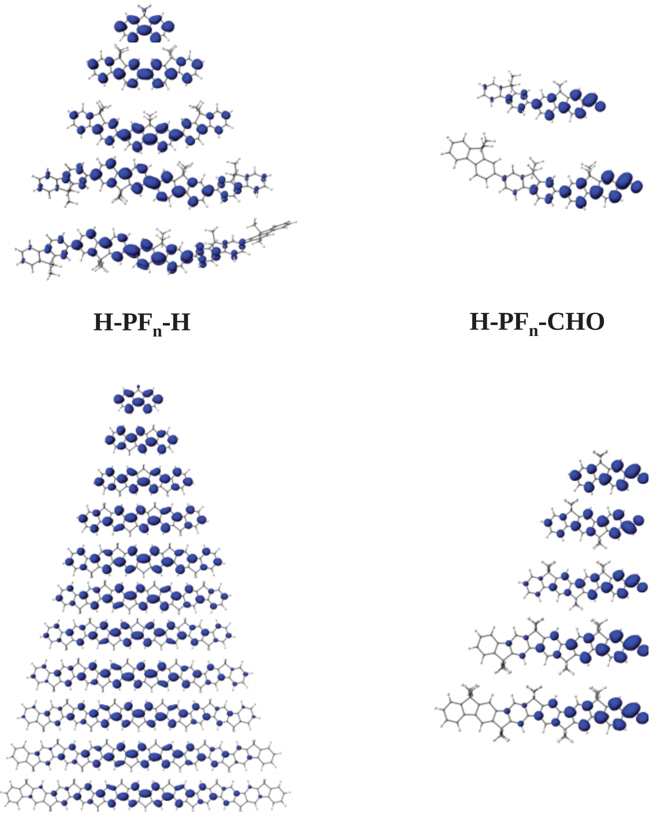

H-PF$_n$-H **H-PF$_n$-CHO**

H-L$_n$-H **H-L$_n$-CHO**

We thank the Department of Energy, Office of Science, Office of Basic Energy Sciences for funding via the Building EPSCoR-State/National Laboratory Partnerships program (award # DE-SC-0023329), and our students, both undergraduate and graduate, for their assistance.

DOE Solar Photochemistry Sponsored Publications

1. Talipov, M. R.; Brown, S.; Yan, J. C. Multistate Parabolic Model: A Unified Framework for Understanding Charge Distribution in π-Conjugated Oligomers. *J. Phys. Chem. C* (submitted).

Spontaneous Enthalpy-Uphill Charge Separation – a Potential Way to Minimize Energy Loss for Charge Separation

Kushal Rijal, Stephanie Amos, Neno Fuller, Hartwin Peelaers, Wai-Lun Chan
Department of Physics and Astronomy,
University of Kansas
Lawrence, KS 66045

Project Scope: Electron-and-hole pairs are bound together to form excitons in most molecular materials. For photo-to-electrical and photo-to-chemical energy conversions, these bound-excitons need to be separated into free carriers. This charge separation (CS) process often leads to energy losses, which has been known to limit the efficiency of organic photovoltaics (OPV). However, this paradigm changes with the recent development of non-fullerene acceptors (NFAs), in which free charges can be generated with a much lower energy loss. This project focuses on unveiling how electron delocalization, entropy, interfacial energetics, and structural anisotropy would enable such CS. The team uses ultrafast time-resolved spectroscopy and multi-scale modeling to investigate the CS mechanism in both model donor/acceptor (D/A) interfaces, and bulk heterojunctions (BHJs) used in high performance OPVs.

Recent Results:

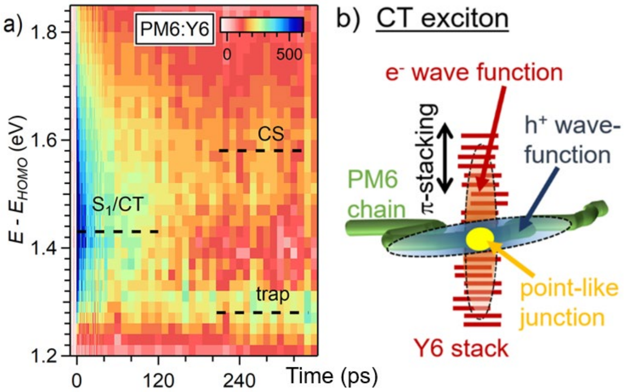

Fig. 1 a) The TPPE spectrum obtained from a PM6:Y6 film. b) A schematic illustrated the CT exciton.

1. <u>Spontaneous enthalpy-uphill CS in bulk heterojunctions</u> – By using time-resolved two photon photoemission spectroscopy (TR-TPPE), we found that at model ZnPc/F_8ZnPc D/A interfaces, enthalpy-uphill CS instead of hot-exciton cooling can occur spontaneously after photoexcitation. The CS state is populated from the charge transfer (CT) exciton state despite the electronic energy of the CS state being higher. We argue that the enthalpy-uphill CS is driven by entropy. By using a tight-binding model, we found that the entropic driving force is maximized when the delocalized electron and hole wavefunctions in the CT exciton intersect with each other via point-like junctions. The entropy-driven CS process can occur without a large energy-level offset at the interface, which can account for the low energy loss found in high performance NFA OPVs.

In light of this hypothesis, we studied the CS process in the high performance PM6:Y6 BHJs. Indeed, we found that a significant portion of the CT excitons converts spontaneously (in 10 – 100 ps) into free carriers (Fig. 1a) despite the CT exciton having a considerable binding energy of 0.15 eV. The structure of the PM6:Y6 BHJ is further characterized by atomic force microscope (AFM) and glazing incident X-ray scattering (GIXS). The measured morphology is consistent with our hypothesis, i.e., the enthalpy-uphill CS can occur in the presence of point-like junctions (Fig. 1b).

2. <u>The impact of interfacial energetics on CS</u> – NFAs such as Y6 have electron push-pull structures. It has been found that molecular quadrupoles associated with these structures can induce interfacial band bending that assists CS. Similar band bending and molecular quadrupoles can be found in our model ZnPc/F_8ZnPc D/A interface as well. Going beyond a tight-binding model, we studied

the interface using density functional theory (DFT) using the SCAN meta-GGA functional in combination with the Grimme D4 to explicitly include van der Waals interactions. We focused on interfaces of equal numbers of stacked ZnPc and F_8ZnPc molecules. We find that the electrostatic potential at each of the molecular sites is different, which can produce a band bending effect. The wavefunction localization also points out the importance of the interface. As shown in Fig. 2, while the HOMO and LUMO are fully localized on ZnPc or F_8ZnPc domains respectively, as expected from the band alignment, the wavefunction is not localized on the interface. For states below the HOMO and above the LUMO, the interface molecules also have far less wavefunction localization. These wavefunctions, combined with the calculated electrostatic potentials, indicate that an electron-hole pair located closer to the interface has a higher energy than a pair located farther away from the interface. This band bending effect can compensate the exciton binding energy. We plan to further quantify this effect and include it in a tight binding model so that we can study its effect on CS in a much larger simulation cell.

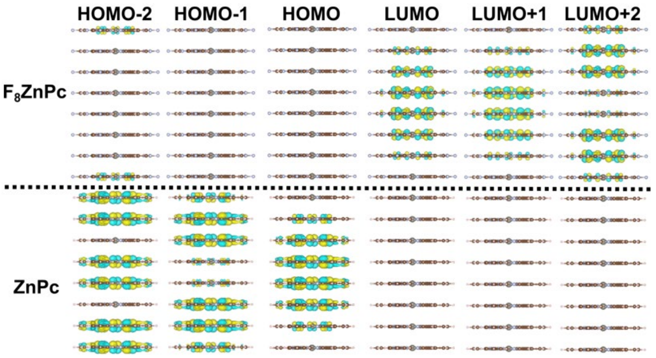

Fig. 2 HOMO/LUMO wavefunctions for a stack of F_8ZnPc/ZnPc molecules.

3. <u>Enthalpy-uphill CS observed in other hybrid interfaces</u> – We found that the enthalpy-uphill CS can also occur at hybrid organic/2D interfaces (F_8ZnPc/monolayer-WS_2). This result shows that our hypothesis can be applicable to interfaces beyond organic/organic interfaces.

Future Plans:

1. We will extend our TR-TPPE studies to various fullerene and NFA BHJs to find out whether the enthalpy-uphill CS occurs only in the high-performance NFA-based BHJs. Moreover, in collaboration with Dr. El-Khoury's group at PNNL, we aim to probe the nanoscale morphology of BHJs with tip-enhanced optical spectroscopy.

2. We will continue to use DFT to study interfacial effects and polaron formation in a stack of F_xZnPc molecules. This information will be fed into large-scale tight binding model and kinetic Monte Carlo simulation to understand their effects on CS.

3. For the experimental work on model interfaces, we will use F_4ZnPc/ZnPc to find out if the entropy-driven CS can still be effective when the interfacial energy offset is extremely small.

DOE Solar Photochemistry Sponsored Publications

1. K. Rijal, N. Fuller, F. Rudayni, N. Zhang, X. Zuo, C. L. Berrie, H. -L. Yip, W.-L. Chan, Endothermic Charge Separation Occurs Spontaneously in Non-Fullerene Acceptor/Polymer Bulk Heterojunction, *preprint - under review in Adv. Mater.*

2. W. -L. Chan, K. Rijal, Entropy-Driven Charge Separation: A Potential Explanation for the Low Energy Loss Found in OPVs with Non-fullerene Acceptors, J. Phys. Chem. C **128**, 687-696 (2024).

3. F. Rudayni, K. Rijal, N. Fuller, W. -L. Chan, Enthalpy-Uphill Exciton Dissociation at Organic/2D Heterostructures Promotes Free Carrier Generation, Mater. Horiz. **11**, 813-821 (2024).

Ligand-based CO_2 reduction and water oxidation: can we replace Ru with first-row transition metals within the same ligand framework?

M. Zahid Ertem, David C. Grills, Dmitry E. Polyansky, Gerald F. Manbeck, Javier J. Concepcion
Chemistry Division
Brookhaven National Laboratory
Upton, NY 11973

The goal of our research program is to gain a fundamental understanding of the processes involved in the chemical conversion of solar energy. The long-term storage of solar energy as fuels or valuable chemicals by Artificial Photosynthesis (AP) requires efficient coupling of light absorption, photo-induced charge separation and transfer processes, and catalytic chemical transformations, together with managing proton movement and charge leveling of catalysts. Tackling these challenges encompasses mechanistic investigations of catalysis for reductive and oxidative reactions. The development of catalytic systems for CO_2 reduction beyond CO and formate and ultimately to liquid fuels is pursued, together with the development of self-healing molecular catalysts for water oxidation based on first-row transition metal complexes. A new focus in our research is the transition from using precious metals to earth-abundant metals. This is particularly important for photosensitizers/light absorbers where coverage of large geographical areas will be required for efficient light capture. Our strategy is to develop synthetic procedures and perform mechanistic studies with the better-behaved and more easily tractable second and third row transition metal-based catalysts, and then use this knowledge with earth-abundant systems while keeping the same ligand frameworks or derivatives that might confer more stability on first row congeners, Figure 1. Our approach for addressing these challenging tasks relies on a multifaceted collaborative effort by a research team with expertise in synthesis, mechanistic studies, and computations. The use of pulse radiolysis, CFN and NSLSII as BNL-specific tools provides additional leverage for conducting in-depth mechanistic investigations.

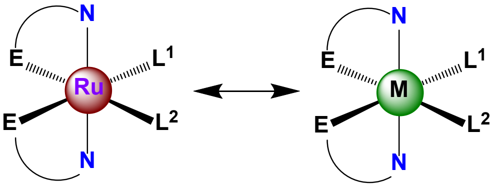

E : C, N; tunability of electron density at M
L^1 : "Catalytic center"
L^2 : Additional tunability

M: Fe, Co

Figure 1. Strategy for reductive catalysis

In this presentation, the use of ligand-based catalysis as a strategy that enables the transition to earth-abundant, first-row transition metals will be discussed. Two examples will be presented to showcase this strategy: one for CO_2 reduction and one for water oxidation. The photochemical reduction of CO_2 to formate with high selectivity using metal formyl intermediates as hydride donors will be demonstrated, Figure 2. To our knowledge, this is the first time that formyl intermediates have been invoked as the active form of the catalyst in hydride transfer to CO_2. Using N-heterocyclic pyridyl-carbene ligands (NHC; E = C in Figure 1), complexes of the type $[Ru(NHC)_2(CO)_2]^{2+}$ (L^1 = L^2 = CO in Figure 1) and $[Ru(NHC)_2(CO)(H)]^+$ (L^1 = H; L^2 = CO in Figure 1) have been prepared. The presence of L^2 = CO in the ligand

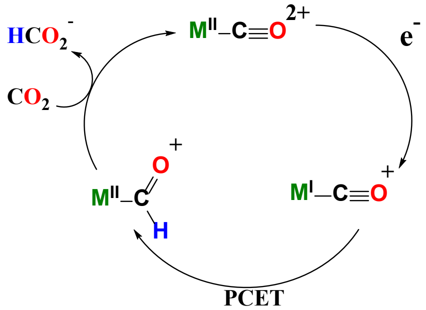

Figure 2. Ligand-based CO_2 reduction

framework enables the use of the CO stretch as a valuable IR handle for kinetic and mechanistic studies. This platform has been based on Ru complexes so far, but we have also been able to prepare the Fe and Co analogs with the same NHC ligands. The development of synthetic procedures, as well as the initial mechanistic studies using ruthenium complexes have been key to understanding the behavior of these systems before transitioning to the first-row analogues. For example, we discovered an isomerization process from C-*trans*-CO, C-*trans*-H-$[Ru(NHC)_2(CO)(H)]^+$ involving a formyl intermediate generated by insertion of CO into the Ru-H bond (to our knowledge, never before reported in the literature). The initial C-*trans*-CO, C-*trans*-H complex first undergoes isomerization to N-*trans*-CO, C-*trans*-H, followed by slower isomerization of the latter to the final N-*trans*-CO, N-*trans*-H isomer. This isomerization is completely intractable with the iron complex where ligand scrambling, CO loss and decomposition take place during the isomerization process.

$[Ru(NHC)_2(CO)_2]^{2+}$ is highly active and 100% selective in the photochemical CO_2 reduction to formate. Initial mechanistic studies indicate that the formyl intermediate $[Ru(NHC)_2(CO)(CHO)]^+$, generated by an ET-PCET mechanism involving the radical cation of the sacrificial organic hydride, is the culprit in the hydride transfer to CO_2. To our knowledge, this is the first time that such a mechanism has been invoked. The presence of the CO ligand (L^2 = CO) as an IR handle has allowed us to carry out kinetic and mechanistic studies where intermediates generated either *via* pulse radiolysis or sensitization, can be followed using TRIR. Such studies have been complemented with analogous studies using transient absorption spectroscopy. The fact that the coordination environment remains saturated during the catalytic cycle (ligand-based) is very encouraging in transitioning to first-row transition metals.

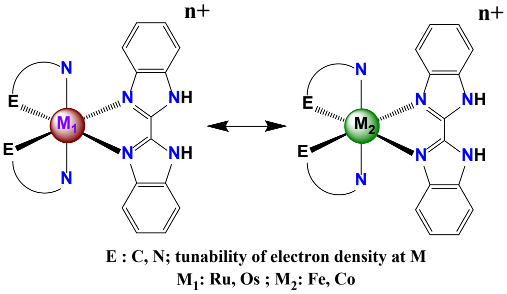

***Figure 3**. Strategy for water oxidation*

A ligand-based approach to water oxidation catalysis based on $[M(bpy)_2(bi\text{-}bimH_2)]^{n+}$ will be presented as well, Figure 3 (E = N; M_1 = Ru, Os; n = 2). This platform includes self-healing capabilities and because it is ligand-based, is amenable to first-row transition metals, a feature that we have demonstrated with cobalt-based catalyst, Figure 3 (E = N; M_2 = Co; n = 3). We have begun to explore new ligand environments based on a series of pyridyl-carbene ligands (Figure 3, E = C) that have enabled us to develop synthetic strategies for first-row transition metals such as iron. The first iron-based catalyst has already been synthesized and characterized by ^{1}H-NMR and single-crystal X-ray crystallography, Figure 4. This catalyst is also active in photochemical water oxidation.

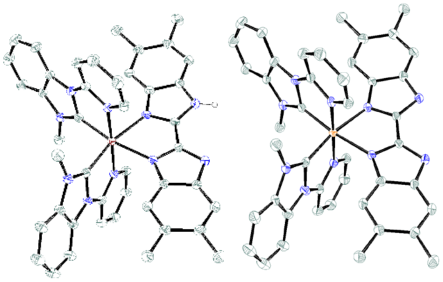

***Figure 4**. X-ray structures for Ru (left) and Fe (right) NHC-based catalysts*

In addition to ligand-based photochemical water oxidation, we are also carrying out electrochemical studies on the surfaces of planar and high-surface area electrodes with anchored catalysts. These include studies with a Ru and, for the first time, a Co-based catalyst. Using the collector-generator method, the onset potentials, turnover frequencies, and faradaic efficiencies for O_2 generation have been determined at various pH values for these ligand-based catalysts.

DOE Solar Photochemistry Sponsored Publications 2021-2024

1. Badiei, Y. M.; Traba, C.; Rosales, R.; Rojas, A. L.; Amaya, C.; Shahid, M.; Vera-Rolong, C.; Concepcion, J. J., “Plasma-Initiated Graft Polymerization of Acrylic Acid onto Fluorine-Doped Tin Oxide as a Platform for Immobilization of Water-Oxidation Catalysts”, *ACS Appl. Mater. Interfaces* **2021,** *13* (12), 14077-14090.
2. Munoz-Garcia, A. B.; Benesperi, I.; Boschloo, G.; Concepcion, J. J.; Delcamp, J. H.; Gibson, E. A.; Meyer, G. J.; Pavone, M.; Pettersson, H.; Hagfeldt, A.; Freitag, M., “Dye-sensitized solar cells strike back”, *Chem. Soc. Rev.* **2021,** *50* (22), 12450-12550.
3. Sampaio, R. N.; DiMarco, B. N.; Concepcion, J. J., “Proton-Coupled Group Transfer Enables Concerted Protonation Pathways Relevant to Small-Molecule Activation”, *Inorg. Chem.* **2021,** *60* (22), 16953-16965 (cover article).
4. Sousa, S. F.; Ertem, M. Z.; Faustino, L. A.; Machado, A. E. H.; Concepcion, J. J.; Maia, P. I. S.; Patrocinio, A. O. T., “Mechanistic investigation of the aerobic oxidation of 2-pyridylacetate coordinated to a Ru(II) polypyridyl complex”, *Dalton Trans.* **2021,** *50* (42), 15248-15259.
5. Wang, D.; Xu, Z.; Sheridan, M. V.; Concepcion, J. J.; Li, F.; Lian, T.; Meyer, T. J., “Photodriven water oxidation initiated by a surface bound chromophore-donor-catalyst assembly”, *Chem. Sci.* **2021,** *12* (43), 14441-14450.
6. Faustino, L. A.; Machado, A. E. H.; Maia, P. I. S.; Concepcion, J. J.; Patrocinio, A. O. T., “Electrocatalytic properties of a novel ruthenium(II) terpyridine-based complex towards CO_2 reduction”, *Dalton Trans.* **2023,** *52* (14), 4442-4455.
7. Zhang, L; Muller A. V.; Grills, D. C.; Polyansky, D. E.; Sampaio, R. N.; Concepcion, J. J. “Control of Selectivity in Photochemical CO_2 Reduction with the Redox Potential of the Photosensitizers” *ACS Catal.* **2024**, submitted.
8. Formiga, A. L. B.; Wang, L; Grills, D. C.; Polyansky, D. E.; Ertem, M. Z.; Concepcion, J. J. “Visible-light-driven water oxidation through ligand-based catalysis” *J. Am. Chem. Soc.* **2024**, submitted.
9. Zhang, L.; Desai, S. P.; Cappuccino, C.; Grills, D. C.; Polyansky, D. E.; Sampaio, R. N.; Concepcion, J. J. “Sustained, Selective and Efficient Photochemical CO_2 Reduction to Formate by Electron-Deficient Ruthenium Polypyridyl Complexes” *J. Am. Chem. Soc.* **2024**, submitted.

Solar-energy-driven interfacial multi-electron-transfer catalytic systems for fuels

Djamaladdin G. Musaev, Tianquan Lian, Craig L. Hill
Department of Chemistry and Emerson Center for Scientific Computation
Emory University, Atlanta, GA 30322

The overall thrust of this collaborative project is to advance in-depth understanding of key factors that impact the efficiency of polyoxometalate (POM) water oxidation catalysts (WOCs) and photoanodes composed of semiconductor (SC) electrodes and POM-WOCs. Our multidisciplinary team designs (a) stable and highly active POM-WOCs, and (b) robust visible-light-driven water oxidation photoanodes via both (i) elucidating the roles of the active-site microenvironments on [POM-WOC], and (ii) developing advanced synthetic, experimental characterization, and computational modelling tools. To date, we have made progress in the following areas:

Microenvironment effects on water oxidation catalysts. The principal WOCs used in this project are the mixed 3d-metal **M–[$\mathbf{Co_2TM_2X_2}$]** systems (where **M** is counter cation, and **TM** is 3d-metal, and **X** is heteroatom), which are derivatives of the $[Co_4(H_2O)_2(PW_9O_{34})_2]^{10-}$, **$\mathbf{Co_4P_2}$** and $[Co_4(H_2O)_2(VW_9O_{34})_2]^{10-}$, **$\mathbf{Co_4V_2}$** WOCs, previously developed by our team, and strong acid compatible **M-[$\mathbf{TM_9X_3Y_2}$]** POMs (where **X** and **Y** are heteroatoms) because their microenvironments are extensively tunable, and they are amenable to facile immobilization on electrode or photoelectrode surfaces. Through closely integrated experimental and computational collaboration: (1) we have developed and elucidated impact of the internal metals, such as **TM** = Fe and Ni (yellow balls, see Figure 1a) adjacent to the active site Co centers (purple balls). We have synthesized the $[Co_2Ni_2(PW_9O_{34})_2]^{10-}$, **$\mathbf{Co_2Ni_2P_2}$**, system and validated location of each 3d-metal in **$\mathbf{Co_2Ni_2P_2}$** using multiwavelength synchrotron X-radiation anomalous dispersion scattering (synchrotron XRAS). We demonstrated that the adjacent 3d-metals change the electronic structure and redox potentials of Co centers, and greatly impact the WO rates and stability of this family tetra-transition metal-POM WOCs; (2) We have prepared **M** = Cs^+, Ba^{2+}, La^{3+} and Y^{3+} salts of **M-**$[Co_9(H_2O)_6(OH)_3(HPO_4)_2(PW_9O_{34})_3]^{16-}$ (**M-$\mathbf{Co_9P_5}$**), and studied their X-ray structures. We find that **M-$\mathbf{Co_9P_5}$** catalysts are stable in acid down to below pH 2. We identified factors impacting structures and stabilities of these complexes; and (3) We have shown that electron-rich solvent (S) donors greatly perturb POM electronic structure and properties via donor-acceptor interactions. For example, the $(S_2H)_3[PW_{12}O_{40}]$ system (S = cyclic urea) (see Figure 1b) whose components, S and POM, are colorless and photochemically inactive, is darkly colored and photoredox active in the visible region.

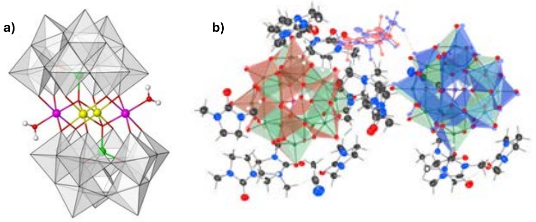

Figure 1. Structure of a) $[Co_2TM_2(PW_9O_{34})_2]^{10-}$ and b) $(S_2H)_3[PW_{12}O_{40}]$ system (S = cyclic urea)

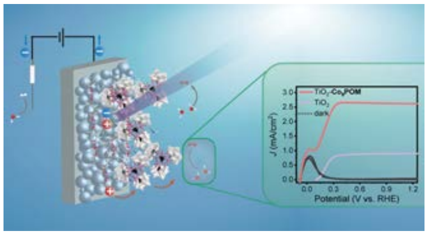

Figure 2. Schematic of TiO_2-**$\mathbf{Co_9}$POM** photoanode for water oxidation (left), and photocurrent as a function applied potential (right).

Cobalt-polyoxometalate-$\mathbf{TiO_2}$ photoanode for water oxidation in acid. We have constructed a photoanode comprising the homogeneous WOC

$Na_8K_8[Co_9(H_2O)_6(OH)_3(HPO_4)_2(PW_9O_{34})_3]$ (**Co$_9$POM**) and nanoporous *n*-type TiO_2 photoelectrodes (henceforth "TiO_2-**Co$_9$POM**") by first anchoring the cationic 3-aminopropyltrimethoxysilane (APS) ligand on a metal oxide light absorber followed by treatment of the metal oxide-APS with a solution of the POM-WOC. The resulting TiO_2-**Co$_9$POM** photoelectrode exhibits a three-fold oxygen evolution photocurrent enhancement compared to bare TiO_2 in aqueous acidic conditions (see Figure 2). Multi-component spectroscopic studies before and after use indicate that the surface-bound **Co$_9$POM** retains its structural integrity throughout all photoelectrochemical water oxidation studies. Extensive charge-transfer mechanistic studies by photoelectrochemical techniques and transient absorption spectroscopy elucidate that **Co$_9$POM** serves as an efficient water oxidation catalyst, extracting photogenerated holes from TiO_2 on the picosecond timescale.

Novel *in situ* EFISH method to probe band-bending and bend-edge unpinning of photoelectrodes. While the overall incident light-to-current conversion efficiency (IPCE) can be readily measured, identifying the microscopic efficiency loss processes remains difficult. Although transient absorption spectroscopy (TAS) is a powerful tool for probing interfacial dynamics in high surface area materials, it is often not applicable on planar electrodes because of a lack of sensitivity for interfacial processes. Our team has devoted efforts to developing *in situ* time-resolved linear and nonlinear spectroscopic tools for probing interfacial charge transfer and chemical reactions at planar photo-electrode/electrolyte interfaces. In the current funding period, we have developed a new *in situ* direct probe of the spatially varying electrostatic potential in the semiconductor space charge layer (i.e. the built-in potential) and the electric double layer at the electrode/electrolyte interface by electric field induced second harmonic generation (EFISH). We study *in situ* study of the SHG response of n-type niobium (Nb)-doped Rutile TiO_2 (100) single crystal photoanodes under applied bias. The SHG response contains the contribution of EFISH signal of the semiconductor space charge layer, the second order signal of the TiO_2 surface, and the EFISH signal of the electric double layer. We examine how these contributions depend on the azimuthal angles of the crystal surface relative to the incident light plane and the applied bias. We demonstrate that the EFISH response can be used to determine the flatband position of TiO_2 electrode, its dependence on solution pH and the open circuit photovoltage of the electrode under light illumination conditions. We observe light-induced Fermi-level pinning (band flattening) at the semiconductor/electrolyte junction caused by photogenerated hole accumulation. The extent of band flattening increases with illumination light intensity. The bias-dependence behavior of hole accumulation indicates that the reaction occurs via the surface states rather than the valence band, where the hole-trapping surface states also serve as recombination centers with conduction band electrons. Kinetic isotope experiments reveal the rate-determining step during water oxidation involves proton-coupled electron transfer (PCET). Our work shows that EFISH can be

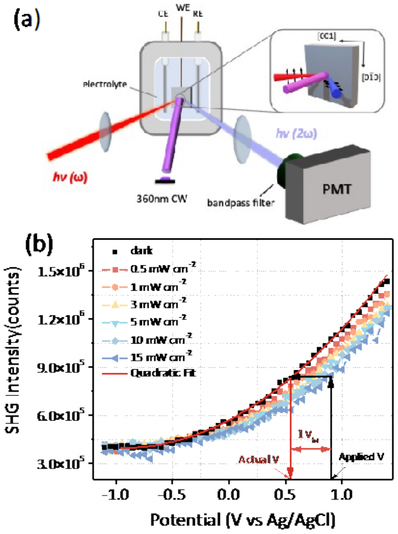

Figure 3. a) schematic of *in situ* EFISH measurement of TiO_2 photoelectrode. b) EFISH signal as a function of applied potential at indicated illumination power density, showing decreasing band bending at higher power.

a general in situ/operando technique for probing changes in band bending and Fermi-level pinning of photoelectrodes. Ongoing study is using EFISH to study the effect POM WOC modification of photoanodes.

DOE Solar Photochemistry Sponsored Publications 2021-2024

1. Xu, Z.; Hou, B.; Zhao, F.; Cai, Z.; Shi, H.; Liu, Y.; Hill, C.; Musaev, D. G.; Mecklenburg, M.; Cronin, S.; Lian, T., Nanoscale TiO_2 Protection Layer Enhances the Built-In Field and Charge Separation Performance of GaP Photoelectrodes, *Nano Lett.* **2021**, *21*, 8017–8024.
2. Yin, Q.; Xu, Z.; Lian, T.; Musaev, D.G.; Hill, C. L.; Geletii, Y.V., “Tafel Slope Analyses for Homogeneous Catalytic Reactions”, *Catalysts* **2021**, *11*(1), 87;
3. Yin, Q.; Geletii, Y.V.; Lian, T.; Musaev, D.G.; Hill, C. L. “Polyoxometalate Systems to Probe Catalyst Environment and Structure in Water Oxidation Catalysis,” *Adv. in Inorganic Chem.*, **2021**, v. 79, ch. 10.
4. Kaledin, A.L.; Lian, T,; Hill, C.L.; Musaev, D.G., “An All-Atom Theory of Electron Transfer at Nanocrystal/Molecule Interfaces: A Hybrid LCAO/DFT Approach”, *J. Phys. Chem. C*, **2021**, *125*, 5116-5126.
5. Nash, A. G.; Breyer, C. J.; Vincenzini, B. D.; Elliott, G. I.; Niklas, J.; Poluektov, O. G.; Rheingold, A. L.; Smith, D. K.; Musaev, D.G.; Grotjahn, D. B., “A Water Oxidation Catalyst with a Sulfonate Moiety in the Ruthenium Active Site is Highly Active in both Neutral and Acidic Media”, *Angew. Chem. Int. Ed.* **2021**, *60*, 1540–1545
6. Tao, M.; Yin, Q.; Kaledin, A.L.; Uhlikova, N.; Lu, X.; Cheng, T.; Chen, Y.-S.; Lian, T.; Geletii, Y.V.; Musaev, D.G.; Bacsa, J.; Hill, C.L., “Structurally precise two-transition-metal water oxidation catalysts. Quantifying adjacent 3d metals by synchrotron X-radiation anomalous dispersion scattering." *Inorg. Chem.*, **2022**, *61*, 6252 - 6262
7. Xu, Z.; Hou, B.; Zhao, F.; Suo, S.; Liu, Y.; Shi, H.; Cai, Z.; Hill, C.L.; Musaev, D.G.; Mecklenburg, M.; Cronin, S.B.; Lian, T., Direct *In Situ* Measurement of Quantum Efficiencies of Charge Separation and Proton Reduction at TiO_2-Protected GaP Photocathodes, *J. Am. Chem. Soc*. **2023**, *145*, 2860–2869
8. Ibañez, M.A.; Breyer, C. J.; Gembicky, M.; Musaev, D.G.; Grotjahn, D. B., “Electron Donating *para*-Substituent (X) Enhances the Water Oxidation Activity of the Catalyst Ru(4’-X-terpy)(phenanthroline-SO_3)$^+$.” *ACS Catalysis*, **2024**, *in revision*
9. Zhao,F.; Cheng, T.; Lu, X.; Ghora, N.; Yang, Y.; Geletii, Y. V.; Musaev, D.G.; Hill, C.L.; Lian, T., “The charge transfer mechanism on a cobalt-polyoxometalate-TiO_2 photoanode for water oxidation in acid”, *JACS*, **2024**, *under review*.
10. Zhao, F.; Xu, Z.; Lin, L.; Suo, S.; Hill, C.L.; Musaev, D.G.; Lian, T., ” In situ measurement of electrostatic potential distribution at n-TiO_2(100)-electrolyte Junction by Second Harmonic Generation”, **2024**, *to be submitted*
11. Zhao, F.; Xu, Z.; Suo, S.; Hill, C.L.; Musaev, D.G.; Lian, T., “Direct *operando* observation of surface hole build-up on TiO_2 photoanode under water oxidation conditions by EFISH”, **2024**, *to be submitted*

12. Xu, Z.; Zhao, F.; Zhao, B.; Cai, Z.; Hill, C. L.; Musaev, D.;Cronin, S.B.; Lian, T.; “The effect of electrolyte concentration on interfacial charge recombination in GaP/TiO_2 photocathodes”, **2024**, *to be submitted*.
13. Suo, S.; Zhao, F.; Xu, Z.; Shi, H.; Cai, Z.; Zhao, B.; Hill, C.L.; Musaev, D.G.; Cronin, S.B.; Lian, T.; Surface States Controlled Fluence-Dependent APCE Behavior of p-GaAs-TiO_2-Pt Water Reduction Photocathodes, **2024**, *manuscript in prep.*
14. Zhu, Z.; Zhao, F.; Yin, Q.; Kaledin, A. L.; Musaev, D. G.; Bacsa, J.; Lian, T.; Hill, C. L.; “Polyoxometalate-Based Visible-Light-Induced Intermolecular Charge Transfer System” *Inorganic Chemistry*, **2024**, *invited manuscript to be submitted*.

Kinetic Barriers to Metal Hydride Complex Formation in Fuel-forming Catalysis

Jillian L. Dempsey, Charlotte L. Montgomery, Jaruwan Amtawong, Annie McCullough, Zoe Claytor, Mehmed Z. Ertem, Léo Chevalier, Austin L. Raithel, Thomas W. Hamann, Chun-Hsing Chen
Department of Chemistry
University of North Carolina
Chapel Hill, NC 27599-3290

Fuel-forming catalytic reactions proceed via multi-step reaction mechanisms, often with alternating proton and electron transfers. The high energy, charged intermediates encountered on these reaction pathways impart energy penalties that impact catalyst efficiency. Moreover, these intermediates are susceptible to off-cycle reactivity that can decrease catalyst selectivity and lead to catalyst degradation. Concerted proton-coupled electron transfer processes can help overcome to challenges of efficiency, selectivity, and durability of stepwise proton and electron transfer steps. However, mechanistic studies undertaken in our lab show that the vast majority of catalysts operate through stepwise proton-coupled electron transfer reaction and there is only one known family of coordination complexes known to react via a concerted proton-coupled electron transfer reaction. Moreover, in several examples identified in our lab, ligands are initially protonated, followed by a tautomerization to yield the stable metal hydride product. The preference for a stepwise reaction over a concerted proton-coupled electron transfer route that circumvents the high energy, charged intermediates associated with stepwise pathways, as well as a kinetic preference for protonating the ligand over direct metal protonation, suggests multiple factors dictate the proton-coupled electron transfer reactions that form metal hydride species. Overall, the design principles needed to direct fuel-forming catalysis via concerted proton-coupled electron transfer are unknown. This talk will detail research that addresses this gap in knowledge, discussing 1) studies that correlate structural reorganization associated with metal protonation with proton transfer kinetics and 2) examples of catalysts that circumvent high barriers to metal-based protonation by leveraging metal-ligand cooperativity.

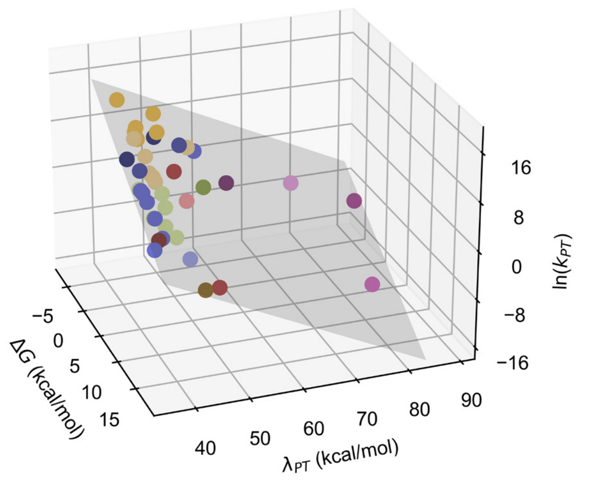

Figure 1. For the protonation of reduced metal complexes to form the corresponding metal hydride species, strong correlations between ΔG_{PT}, k_{PT} and λ_{PT} are observed.

The dominance of stepwise proton-coupled electron transfer pathways in catalysis has led to the hypothesis that an intrinsic barrier to metal protonation inhibits access to the concerted proton-coupled electron transfer pathway. High inner-sphere reorganization energies arising from the geometric changes that occur upon metal protonation may be a determining factor in this barrier. In support of this, we show a strong correlation between the isolated proton transfer reaction and associated reorganization energy for a large range of coordination complexes, including some complexes that are established catalysts for proton reduction (Figure 1). Our ongoing work is focused on examining the mechanisms by which proton-coupled electron transfer reactions proceed to test the hypothesis that a concerted proton-coupled electron transfer process is accessible for coordination complexes that have low reorganization energies for proton transfer.

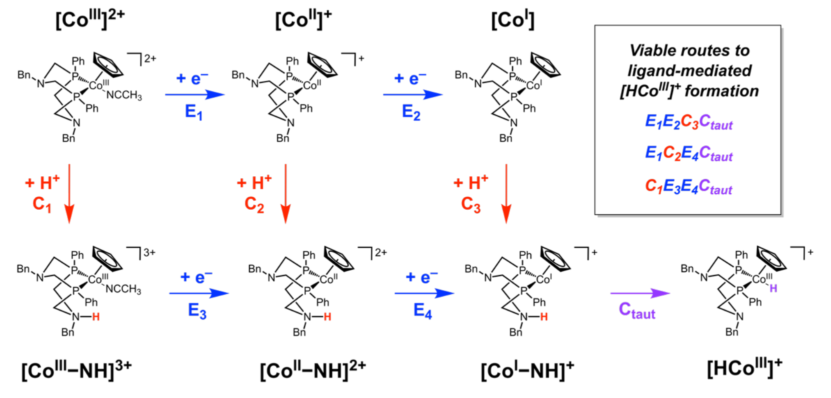

Figure 2. Possible mechanisms for the two-electron, one-proton transformation of [Co^{III}Cp(P$^{Ph}{}_2$N$^{Bn}{}_2$)(CH$_3$CN)]$^{2+}$ to [HCo^{III}]$^{+}$. [HCo^{III}]$^{+}$ reacts further with CO$_2$ to generate formate. We have shown that depending on acid strength, acid concentration, and timescale between electron transfer steps, reactivity proceeds through E$_1$E$_2$C$_3$C$_{taut}$, E$_1$C$_2$E$_4$C$_{taut}$, C$_1$E$_3$E$_4$C$_{taut}$, or some combination of the three mechanisms.

Through mechanistic studies, we have identified several catalysts and model systems that react to form metal hydride species through indirect routes that proceed through initial ligand protonation followed by tautomerization. This observation suggests that while the metal hydride species is the thermodynamic product, direct metal protonation has a high kinetic barrier, and thus ligand protonation is the kinetic product. Detailed mechanistic studies of the proton-coupled electron transfer reactivity of [Co^{III}Cp(dxpe)(CH$_3$CN)]$^{2+}$ (Cp = cyclopentadienyl; dxpe = 1,2-bis(di-x-phosphino)ethane, where x = phenyl, ethyl, cyclohexyl), [Co^{III}Cp(P$^{Ph}{}_2$N$^{Bn}{}_2$)(CH$_3$CN)]$^{2+}$ (P$^{Ph}{}_2$N$^{Bn}{}_2$ = 1,5-dibenzyl-3,7-diphenyl-1,5-diaza-3,7-diphosphacyclooctane) (Figure 2), and [CoPY5Im]$^{2+}$ (Figure 3) show that the Cp, P$^{Ph}{}_2$N$^{Bn}{}_2$, and PY5Im ligands can all be kinetically accessible protonation sites en route to formation of Co^{III}-hydride species. Through systematic studies, we have identified the thermodynamic and kinetic factors that dictate ligand-based vs. metal-based proton-coupled electron transfer reactivity. Our data show that acid strength, acid concentration, pendant amine basicity, structural rigidity, timescale between electron transfer steps dictate the mechanism of hydride formation.

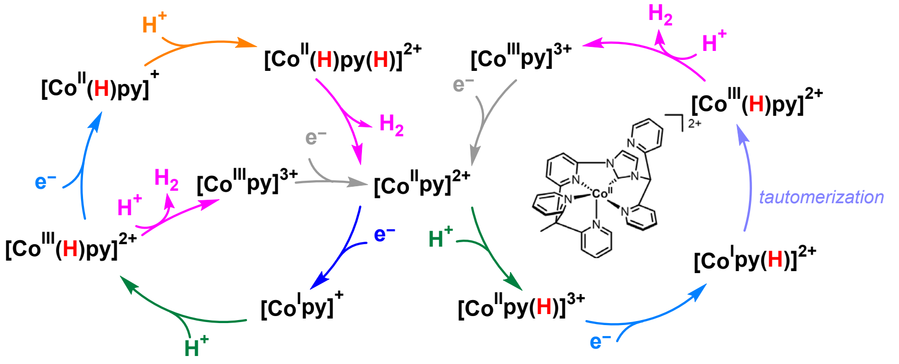

Figure 3. [CoPY5Im]$^{2+}$ can react via parallel ECEC and CECCE mechanisms to generate hydrogen, depending on the strength of the proton source.

DOE Solar Photochemistry Sponsored Publications 2021-2024

1. Montgomery, C. L.; Ertem, M. Z.; Chevalier, L.; Dempsey, J. L. Circumventing Kinetic Barriers to Metal Hydride Formation with Metal–Ligand Cooperativity. *Submitted to Journal of the American Chemical Society, revisions requested and submitted.*
2. Huffman, B. L.; Bredar, A. R. C.; Dempsey, J. L. Origins of Non-ideal Behavior in Voltammetric Analysis of Redox-Active Monolayers. *Nature Reviews Chemistry* **2024**, *In Press.*
3. Amtawong, J.; Montgomery, C. L.; Bein, G. P.; Raithel, A. L.; Hamann, T. W.; Chen, C.-H.; Dempsey, J. L. Mechanism-Guided Kinetic Analysis of Electrocatalytic Proton Reduction Mediated by a Cobalt Catalyst Bearing a Pendant Basic Site. *Journal of the American Chemical Society* **2024**, *146*, 3742–3754.
4. Huffman, B. L.; Donley, C. L.; Dempsey, J. L. Electrochemistry of Redox Active Ferrocene Covalently Attached to Glassy Carbon Electrodes. *Journal of the Electrochemical Society* **2023**, *170*, 126501.
5. Montgomery, C. L.; Amtawong, J.; Jordan, A. M.; Kurtz, D. A.; Dempsey, J. L. Proton Transfer Kinetics of Transition Metal Hydride Complexes and Implications for Fuel-Forming Reactions. *Chemical Society Reviews* **2023**, *52*, 7137–7169.
6. Kurtz, D. A.; Dhar, D.; Elgrishi, N.; Kandemir, B.; McWilliams, S. F.; Howland, W. C.; Chen, C.-H.; Dempsey, J. L. Redox-Induced Structural Reorganization Dictates Kinetics of Cobalt(III)-Hydride Formation via Proton-Coupled Electron Transfer. *Journal of the American Chemical Society* **2021**, *143*, 3393–3406.
7. Huffman, B. L.; Lee, K. J.; Geer, A. M.; McKeown, B. A.; Jia, X.; Dickie, D. A.; Gunnoe, T. B.; Dempsey, J. L. Role of Axial Ligation in Gating the Reactivity of Dimethylplatinum(III) Diimine Radical Cations. *Organometallics* **2021**, *40*, 333–345.

Mechanism of Photochemical N_2 Reduction

Peter Dahl[1], David W. Mulder[1], Lauren M. Pellows[2], Ritika Sharma[3], Florence Mus[3], Bhanu Jagilinki[3], Andrew Clinger[4], Zhi-Yong Yang[4], Gordana Dukovic[2], Lance C. Seefeldt[4], John W. Peters[3], Paul W. King[1]
[1]Biosciences Center, NREL, Golden, CO 80401; [2]Dept. of Chemistry, University of Colorado, Boulder, CO 84322; [3]Dept. of Chemistry and Biochemistry, Oklahoma University, Norman, OK 73019; [4]Dept. of Chemistry and Biochemistry, Utah State University, Logan, UT 84322

We have demonstrated that nanocrystal materials self-assemble with the Mo-nitrogenase MoFe protein into biohybrid complexes, which under illumination, support the catalytic reduction of N_2 and protons to ammonia and dihydrogen (DOI: 10.1126/science.aaf2091). The biohybrid system we have developed is a unique architecture and reporter for understanding how to direct electron transfer in a N_2 reduction catalytic system and the fundamental properties that control product formation. To understand how the components of the biohybrid system functions in photocatalysis, we have developed approaches for studying the binding thermodynamics, the interfacial electron transfer kinetics, and for analysis of the reaction intermediates and products of the nitrogenase reaction. These approaches are informing on physical properties of nanocrystals, including the dimensions and surface chemistries, that control the binding interactions and photoexcited electron transfer efficiencies. Coupling light-controlled electron delivery in the frozen state with electron paramagnetic resonance (EPR) spectroscopy, has enabled photogeneration and trapping of N_2 reduction reaction intermediates in Mo-dependent nitrogenase. The presentation will summarize our progress on understanding of the binding interactions, charge-transfer and product formation kinetics, and the reaction mechanism of nitrogenase under photochemical activation.

Mo-nitrogenase is a two-component enzyme system composed of Fe protein and MoFe protein. The Fe protein functions in ATP-dependent electron delivery to MoFe protein which catalyzes the reduction of N_2 to NH_3. In CdS-MoFe protein biohybrids, the function of Fe protein in electron delivery is replaced by CdS quantum dots (QD) and catalysis is driven by photoexcited electron delivery. Understanding the fundamental properties that control the physical arrangement of the two components is necessary for defining how binding influences the kinetics and quantum efficiencies of electron transfer. Using a microscale thermophoresis (MST) approach (Figure above), we have studied the effect of nanocrystal dimension and surface ligand chemistry on the binding thermodynamics with nitrogenase. Building from that, recent studies have probed the effect of the capping ligand on binding, electron transfer, and product yields.

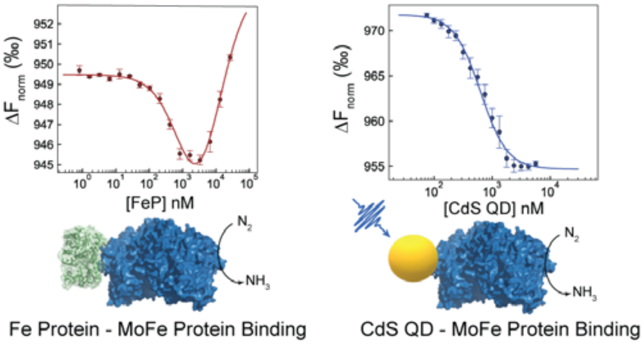

Figure. Binding curves obtained from MST for the Fe protein MoFe protein binding (left) and CdS QD and MoFe protein (right). (DOI: 10.1021/acs.nanolett.3c03205).

We have observed that the chemistry of the functional group of QD capping ligands, i.e., carboxylic acid, is critical to establishing a binding interaction. Recent investigations have been testing the effects of using an exciton delocalizing ligand, mercaptobenzoic aid, on electron transfer and photochemistry of the N_2 reduction reaction. Thus far, there are significant differences observed in the photoexcited state lifetimes and product formation rates of biohybrids that utilize QDs capped with mercaptopropionic acid (MPA) versus mercaptobenzoic acid (MBA). For example, the MBA-capped QDs have a longer excited state lifetime than MPA-capped QDs, which correlated with higher photocatalytic rates of product formation, and with higher selectivity for NH_3 over the co-product H_2.

The improvements in understanding the binding interactions and electron transfer efficiencies are also being exploited to address knowledge gaps in the understanding of the nitrogenase mechanism that have been challenging to address using the natural, Fe protein redox partner that requires ATP-driven electron transfer. We have developed techniques for illumination of QD-MoFe protein complexes in the frozen state coupled to EPR spectroscopy to resolve the role of conformational states in electron transfer and to test stability of N_2 bound reaction intermediates. The technical foundation from our work is leading to more detailed pre-steady state time-course studies to address the larger challenge of evolving a "complete" kinetic model of the N_2 reduction reaction catalyzed by nitrogenase (Figure, right top). An aim of this effort is to identify and assign each of the EPR-active E-state intermediates (Figure, right bottom) under a range of reaction conditions (i.e., with and without N_2; varying reaction temperatures) and to determine the reaction step activation energies and thermodynamics. The progress emerging from these efforts is providing unique insights into complexities of N_2 activation by evolving a tunable model system to address the grand challenge of converting solar energy into ammonia and other reduced compounds.

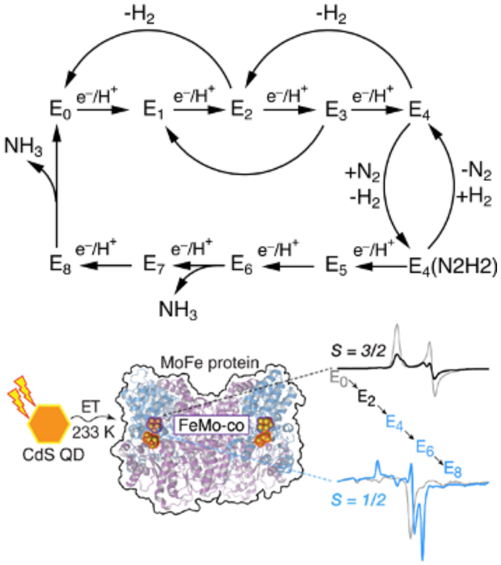

Figure. Top, N_2 reduction reaction cycle of nitrogenase. "E" refers to the oxidation states that follow successive electron transfer and reduction steps. Bottom, schematic of CdS quantum dot (QD) - nitrogenase MoFe protein complex and resulting photo-driven changes in the MoFe protein FeMo-co cofactor redox state (or E-states) measured as changes in the EPR signals. (DOI: 10.1063/5.0170405).

DOE Solar Photochemistry Sponsored Publications 2021-2024.

1. B.P. Jagilinki, M.A. Willis, F. Mus, R. Sharma, L.M. Pellows, D.W. Mulder, Z.-Y. Yang, L.C. Seefeldt, P.W. King, G. Dukovic, J.W. Peters. **2024**. "Microscale Thermophoresis (MST) as a tool to study binding interactions of oxygen-sensitive biohybrids." *Bio-protocols*. *In review.*
2. A. Clinger, Z.-Y. Yang, L.M. Pellows, P.W. King, F. Mus, J.W. Peters, G. Dukovic, L.C. Seefeldt. **2024**. "Hole-scavenging in photo-driven N_2reduction catalyzed by a CdS-nitrogenase MoFe protein biohybrid system." *J. Inorgan. Biochem.* **253**:112484. DOI:10.1016/j.jinorgbio.2024.112484.

3. L.M. Pellows, M.A. Willis, J.L. Ruzicka, B.P. Jagilinki, D.W. Mulder, Z.-Y. Yang, L.C. Seefeldt, P.W. King, G. Dukovic, J.W. Peters. **2023**. “High affinity electrostatic interactions support the formation of CdS quantum dot:nitrogenase MoFe protein complexes.” *Nano Lett*. **23**:10466. DOI:10.1021/acs.nanolett.3c03205.

4. L.M. Pellows, G.E. Vansuch, B. Chica, Z-Y. Yang, J.L. Ruzicka, M.A. Willis, A. Clinger, K.A. Brown, L.C. Seefeldt, J.W. Peters, G. Dukovic and D.W. Mulder, P.W. King. **2023**. “Low-temperature trapping of N_2 reduction reaction inter-mediates in nitrogenase MoFe protein–CdS quantum dot complexes”. *J. Chem. Phys.* **159**:235102. DOI:10.1063/5.0170405.

5. G.E. Vansuch, D.W. Mulder, B. Chica, J.L. Ruzicka, Z-Y. Yang, L.M. Pellows, M.A. Willis, K.A. Brown, L.C. Seefeldt, J.W. Peters, G. Dukovic, P.W. King. **2023**. “Cryo-annealing of photoreduced CdS quantum dot–nitrogenase MoFe protein complexes reveals the kinetic stability of the E_4(2N2H) intermediate.” *J. Am. Chem. Soc*. **145**:21165. DOI:10.1021/jacs.3c06832.

6. A. Badalyan, Z.Y., Yang, M. Hu, M., T.L. Liu, L.C. Seefeldt. **2022**. “Tailoring electron transfer pathway for photocatalytic N_2-to-NH_3 reduction in a CdS quantum dots-nitrogenase system.” *Sustain. Energy Fuels*. **6**:2256-2263. DOI:10.1039/D2SE00148A.

7. J.L. Ruzicka, L.M. Pellows, H. Kallas, K.E. Shulenberger, O.A. Zadvornyy, B. Chica, K.A. Brown, J.W. Peters, P.W. King, L.C. Seefeldt, G. Dukovic. **2022**. "The kinetics of electron transfer from CdS nanorods to the MoFe protein of nitrogenase." *J. Phys. Chem. C.* **126**: 8425-8435. DOI:10.1021/acs.jpcc.2c02528.

8. B. Chica, J. Ruzicka, L.M. Pellows, H. Kallas, E. Kisgeropoulos, G.E. Vansuch, D.W. Mulder, K.A. Brown, D. Svedruzic, J.W. Peters, G. Dukovic. **2022**. “Dissecting nitrogenase MoFe protein P-cluster P^{2+} to P^{+} conversion in CdS nanocrystal–MoFe protein complexes”. *J. Am. Chem. Soc.* **144**:5708-5712. DOI:10.1021/jacs.1c13311.

A Programmable, Non-Equilibrium Electrified Ammonia Synthesis for Efficient Hydrogen Storage

Liangbing Hu,[1] Ji Yang,[1] Qi Dong,[1] Shuke Li,[1] Yiguang Ju,[2] Emily A. Carter,[2] Ziyang Wei,[2] Zijian Sun,[2] Ziqiao Chang,[2] Bowen Mei,[2] John Mark P. Martirez,[3] Stephen J. Klippenstein,[4] Ahren W. Jasper,[4] Yuri Georgievski,[4] Dongxia Liu,[5] Zixiao Liu,[5] Akash Ajit Warty,[5] Gen Yarema[5]

[1]Department of Materials Science and Engineering, University of Maryland, College Park, Maryland 20742; [2]Department of Mechanical and Aerospace Engineering, Princeton University, Princeton, New Jersey 08540; [3]Applied Materials and Sustainability Sciences, Princeton Plasma Physics Laboratory, Princeton, New Jersey 08540; [4]Argonne National Laboratory, Lemont, IL 60439; [5]Department of Chemical and Biomolecular Engineering, University of Delaware, Newark, Delaware 19716

Overall Goal. This initiative, supported by the Department of Energy's Basic Energy Sciences (DOE BES), aims to significantly advance our fundamental understanding of the non-equilibrium chemical kinetics essential for ammonia (NH_3) synthesis from N_2 and H_2, with the ultimate goal of developing a highly efficient technique for hydrogen (H_2) storage. This innovative technique will be based on an electrified NH_3 synthesis process and novel catalysts, characterized by a minimal carbon footprint, which will help reduce the environmental impact associated with energy storage technologies.

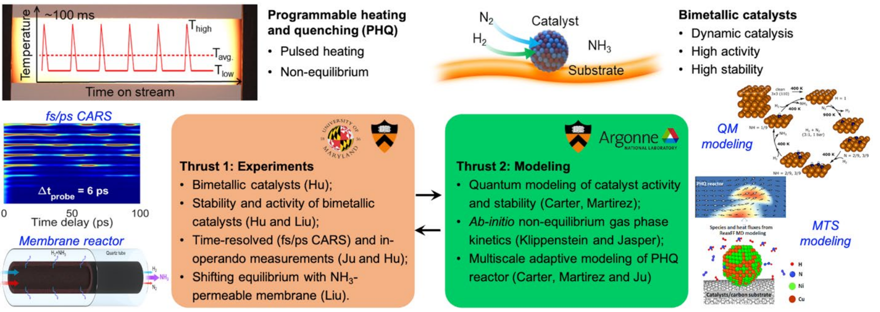

Fig. 1 *Overview of the research for the PHQ-based non-equilibrium NH_3 synthesis.*

Specific Objectives. Objective 1: Focuses on creating metastable bimetallic catalysts for the Pulsed Heating and Quenching (PHQ) process for NH_3 synthesis, employing real-time diagnostics and material characterization to assess their stability and catalytic efficiency. Concurrently, it aims to conduct time-resolved analyses of NH_3 synthesized under non-equilibrium conditions and to develop membrane separation technologies to shift chemical equilibria toward the product and enhance process efficiency. **Objective 2:** Utilizes quantum mechanical (QM) modeling to design catalysts and understand the mechanisms governing their activity and stability during non-equilibrium NH_3 synthesis via the PHQ process. It also explores non-equilibrium gas-phase kinetics using a multiscale modeling approach integrating QM, molecular dynamics (MD), and adaptive detailed chemistry and transport simulations, with the aim of achieving a comprehensive understanding of non-equilibrium kinetics for NH_3 synthesis.

Current progress and achievements: Bimetallic Catalysts: Through the screening of approximately hundreds of different bimetallic compositions, we have identified a highly active FeCr bimetallic catalyst for NH_3 synthesis. Its catalytic activity at 700 K is approximately 8000 μmol (g.metal)$^{-1}$ h^{-1}, which is four times the activity of conventional Fe catalysts. **Membrane Separation Technology**: Concurrently, we have developed new membrane separation materials to adjust the chemical equilibrium in the PHQ-based NH_3 synthesis. At present, the selectivity for the ammonia product is satisfactory and we are still improving the efficiency of separation. **Kinetic Analysis of the PHQ Process:** We have developed time-resolved spectroscopic diagnostic methods for measuring the surface temperature of the pulsed heater, as well as the gas temperature, and NH_3 concentration to unveil the kinetics of the PHQ process. **Multi-scale Simulations:** To optimize the NH_3 synthesis process, we have employed multi-scale simulations. Over the past year, led by the Jasper and Klippenstein Groups at Argonne National Laboratory, we have developed a machine-learning-based method that integrates data from various sources to accurately predict rate constants for chemical bond breaking and forming. **First-principles Calculations:** We have also conducted first-principles calculations based on density functional theory (DFT) to screen potential copper (Cu)-based catalysts suitable for NH_3 synthesis using the PHQ technique, with a focus on the thermodynamics. More specifically, we have investigated the doping of Cu (100) and (111) surfaces with first-row transition metals and molybdenum to meet the thermodynamic requirements of two elementary steps: nitrogen dissociative adsorption and the reduction of adsorbed NH_2 to NH_3 gas. We have also investigated the $NH_3 \leftrightarrow 1/2\ N_2 + 3/2\ H_2$ kinetics on Fe(110) within DFT, the results of which we also subsequently used to train machine-learned atomic force fields to enable dynamics simulations with larger system sizes and longer trajectories. **First Principles Gas Phase Kinetics:** We have mapped the PES for all NH_x and N_2H_y species with state-of-the-art ab initio electronic structure methods. For well-defined stationary points we have employed the high accuracy ANL1 composite method and for radical-radical channels we have employed multi-reference electronic structure methods. For NH_3 we have predicted the temperature and pressure dependence of the dissociation with two-dimensional master equation simulations. A new more general two-dimensional master equation code is nearly ready for production level calculations.

Future Research Objectives. Building on our current achievements, the future work of our initiative will focus on refining FeCr bimetallic catalysts and exploring new compositions for enhanced catalytic efficiency and stability, alongside advancing membrane separation technologies for improved ammonia recovery. We aim to deepen our kinetic and mechanistic understanding of the PHQ process through expanded time-resolved spectroscopic studies and advanced diagnostic tools, while leveraging quantum mechanical and multi-scale modeling to bridge atomistic insights with macro-scale process optimization. Additionally, we will assess the environmental impact of our NH_3 synthesis and H_2 storage techniques, aiming for sustainability and reduced carbon footprint through integration with renewable energy sources. The culmination of these efforts will be demonstrated in a pilot-scale PHQ reactor, in collaboration with industry partners, to validate the feasibility and scalability of our approach, setting the stage for commercialization and industrial-scale implementation of this groundbreaking technology.

DOE Solar Photochemistry Sponsored Publications

1. M. B. Bertagni, R. H. Socolow, J. M. P. Martirez, E. A. Carter, C. Greig, Y. Ju, M. E. Mueller, S. Sundaresan, R. Wang, M. A. Zondlo, A. Porporato, Minimizing the Impacts of the Ammonia Economy on the Nitrogen Cycle and Climate, Proceedings of the National Academy of Sciences U.S.A., **2023**, 120, e2311728120.
2. Shi, Z., Lele, A., Jasper, A., Klippenstein, S., Ju, Y., Quasi-Classical Trajectory Calculation of Rate Constants Using an Ab-Initio Trained Machine Learning Model (AML-MD) with Multi-Fidelity Data. *The Journal of Physical Chemistry A*, **2024** (Accepted).
3. Shi, Z., Lele, A., Jasper, A., Klippenstein, S., Ju, Y., Quasi-Classical Trajectory Calculation of Rate Constants Using Ab-Initio Trained Machine Learning Force Field (AML-MD). AIAA 2024-0797, *AIAA SCITECH 2024 Forum*, January **2024**, doi.org/10.2514/6.2024-0797.
4. Huang, Z., Li T., Fang Y., Smith J., Li B., Brozena A., Zhang Q., Dong Q., Mao S., Wang G., Chi M., Hu L., Reversible phase transition of high entropy alloy nanoparticles at elevated temperature. *Proc. Natl. Acad. Sci. U.S.A.*, **2024**, Submitted.
5. Lele, A., Shi, Z., Khetan, S., Carter, E. A., Martirez, J. M. P., Ju, Y., Development of a Machine Learning Force Field for Molecular Dynamics Simulation of Non-Equilibrium NH_3 Synthesis on Fe(110) Surface. **2024**, In Preparation.
6. Wei, Z., Martirez, J. M. P., Carter, E. A., First-Principles Insights into the Thermodynamics of Variable-Temperature Ammonia Synthesis on Transition-Metal-Doped Cu (100) and (111). **2024**, In Preparation.
7. Yang, J., Huang Z., Wei, Z., Dong Q., Li S., Martirez J. M. P., Carter E. A., Hu L., Tailoring Bimetallic Catalysts to Enhance Ammonia Synthesis Process. **2024**, In Preparation.
8. Yarema, G., Liu, Z., Yang, J., Hu, L., Liu, D., Ammonia-Permeable Membrane Reactor: Experimental and Computational Studies. **2024**, In Preparation.
9. Liu. Z., Yarema. G., Warty. A., Yang. J., Hu. J., Liu. D., Electrified Molten Salt Membrane Reactor for Ammonia Production. **2024**, In Preparation.
10. Mulvihill, C. R.; Georgievskii, Y.; Jasper, A. W.; Klippenstein, S. J. High Accuracy First Principles Kinetics for Pyrolysis of Ammonia: NH_X and N_2H_y Reactions. **2024**, In Preparation.
11. Martirez, J. M. P., Carter, E. A., First-Principles Insights into the Thermocatalytic Cracking of Ammonia-Hydrogen Blends on Fe(110). 2. Kinetics, **2024**, In Preparation.

Understanding Interfacial Phenomena for Solar H_2 Production and N_2 Reduction

Adam C. Nielander[1], Todd G. Deutsch[2], Thomas F. Jaramillo[1], Michal Bajdich[1], Amy Cordones-Hahn[1], Dimostenis Sokaras[1], Myles Steiner[2], James Young[2], Jorge Colón[3], Dino Villagrán[4], Jingjing Qiu[5], Frank Abild-Pedersen[1], Matteo Cargnello[1], Kelly Gaffney[1]

[1]SLAC National Accelerator Laboratory, Menlo Park, CA, 94025; [2]National Renewable Energy Laboratory, Golden, CO, 80401; [3]Department of Chemistry, University of Puerto Rico, San Juan, PR, 00925; [4]Department of Chemistry, University of Texas — El Paso, El Paso, TX, 79968; [5]Department of Chemistry, San Francisco State University, San Francisco, CA, 94132

Using solar energy to drive the synthesis of chemicals and fuels is a grand challenge that, if met, offers a route to sustainable production of molecules of global importance (e.g., H_2 and NH_3) from abundant feedstocks (e.g., H_2O, N_2). Fundamental insights are needed develop an understanding of the molecular, material, and interfacial phenomena that underpin these light-driven processes and will inform improved device design. To meet this need, we have brought together a team with diverse expertise in (photo)electrocatalytic characterization, molecular and materials synthesis, computational methods, and ultra-fast spectroscopic measurements. Our aim in this project is to provide basic science-level insights across the key components of integrated solar-fuels systems to enable the production of H_2 and NH_3, with a broad focus on three key tasks mapped to BES priority research opportunities:

- Task 1 – Understand the mechanisms that underpin constituent durability and performance
- Task 2 – Control catalyst microenvironment to promote selective and efficient fuel production
- Task 3 – Bridge the time and length scales of light excitation and chemical transformations

We review here our recent progress and highlight future plans.

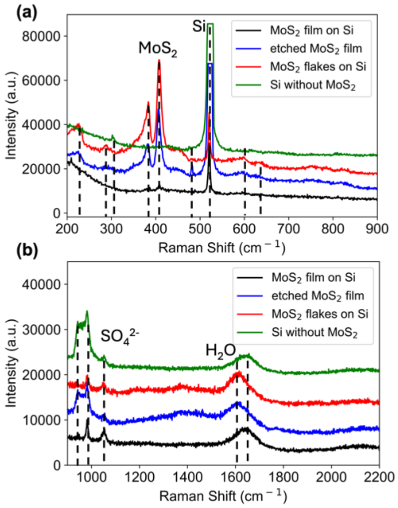

Figure 1. Raman spectra between (A) 200-900 cm^{-1}, and (B)1000-2200 cm^{-1} of various MoS_2/Si interfaces after chemical etching.

One key challenge limiting an integrated solar-fuels-based approach to chemical synthesis is realizing durable performance. It will be critical to understand the mechanisms that drive degradation pathways to match >10,000 h DOE durability goals. Further, it will be necessary to understand durability challenges that arise from the diurnal conditions that any solar-fuels device will face under deployed operating conditions. Our team is working to synthesize new, stable catalysts for both the H_2 evolution (HER) and O_2 evolution reaction (OER) based on Zr, Co, and Fe materials. We are also working to gain a deeper understanding of the relevant degradation pathways. We highlight here one recent effort, using an MoS_2/Silicon electrocatalyst/protective layer as a model system to understand how the material stability is driven by varying operational and environmental conditions. Using a complement of *in situ* electrochemical Raman spectroscopy, online inductively coupled plasma mass spectrometry (ICP-MS), and electrochemical characterization, we observe varying degradation rates and pathways as a function of (electro)chemical conditions replicating expected day/night cycles (**Figure 1**), informing the limits of MoS_2 as a catalyst and protective layer under 'on-sun' conditions.

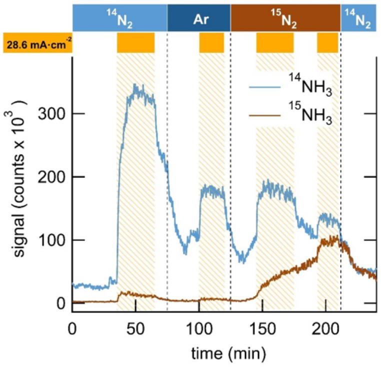

Figure 2. TOF-MS enabled observation of $^{14}NH_3$ and $^{15}NH_3$ as a function of supplied, isotope labeled N_2 reactant to an Ru surface under electrochemical conditions.

The (photo)electrochemical reduction of N_2 (N_2R) to produce NH_3 is uniquely challenging. The inert N_2 triple bond is difficult to activate, and the requirement for a proton source to also be present inherently provides a selectivity challenge. It has further been shown that there are several pernicious contamination sources that can lead to false positive observations of N_2 to NH_3 production. In response to this challenge, we have developed a tool and methodology based on multi-turn time-of-flight mass spectrometry (TOF-MS) that enables real-time quantification of $^{15}NH_3$ at ultralow concentrations (**Figure 2**). As a proof-of-concept, we report N_2R testing of a sputter-deposited Ru catalyst, showing N_2R activity of $1.7 \pm 0.1 \times 10^{-11}$ mol s^{-1} cm^{-2} and $FE_{NH3} = 0.017\%$. The reported method shows ultra-low detection limits, as well as precise and sensitive detection of multiple products on the seconds timescale. The reported protocol represents a standard for N_2R false-positive-resistant catalyst testing, and will serve as a critical component of a high-throughput testing protocol for N_2R in gas diffusion electrode (GDE)-cell architecture with varying operation conditions (e.g., voltage, temperature, N_2 partial pressure, water activity). We are also designing advanced III-V-semiconductor-based photoelectrodes that will have sufficient voltage to drive unassisted Li-mediated N_2R (Li-N_2R). Li-N_2R provides an N_2-to-NH_3 route that can be reliably executed but requires substantial cell potential (> 3 V). To meet this need, we have developed monolithic multijunction AlGaInP / AlGaAs / GaAs stacked photovoltaic structures with evaporated nickel catalyst patterned on the front surface. The best photoelectrodes generate 3.8 V at open circuit, and ~3.4 V at the light-limiting photocurrent. We are currently testing these photoelectrodes for assisted and unassisted Li-N_2R performance, informing improved semiconductor surface-electrolyte interface design.

Our team is also working to understand photo-induced charge transfer for N_2R and HER catalysis at semiconductor-catalyst-electrolyte interfaces. Using a computational catalysis approach, we have revised the activation mechanism of nitrogenese enzyme. We also plan to calculate the N_2R catalytic efficiency of the above sputter-deposited Ru catalyst. Theory is teaming up with experimentalists to investigating the facet dependence of interfacial charge injection in model HER photocatalysts, combining facet-dependent Cu_2O semiconductor nanoparticles with metallic or molecular co-catalysts. Time-resolved XPS experiments will quantify the efficiency and dynamics of electron transfer across the semiconductor-catalyst interface as a function of surface termination and environment, correlating the results with facet-dependent photocatalytic activity — we are also aiming to incorporate novel molecular catalysts in a similar approach. In March, we performed our first operando beamline measurements of III-V photocathodes to leverage spectroscopies to track interfacial chemical transformations that lead to photocorrosion. This involved designing and synthesizing representative thin III-V structures and transferring them to SiN windows that allow x-rays to probe from the back side while maintaining photoelectrode functionality. We also are developing *ps*-time resolved *operando* X-ray absorption spectroscopy (XAS) experiments to delve into photoinduced structural transformations, excited state events, and degradation mechanisms, using a Pt/TiO_2 nanoparticulate platform. In addition to yielding preliminary results, this work has laid the foundation for future operando studies across the project.

DOE Solar Photochemistry Sponsored Publications

1. Tayyebi, A.; Mehrotra, R.; Mubarok, M. A.; Kim, J.; Zafari, M.; Tayebi, M.; Oh, D.; Lee, S.; Matthews, J. E.; Lee, S.-W.; Shin, T. J.; Lee, G.; Jaramillo, T. F.; Jang, S.-Y.; Jang, J.-W. Bias-Free Solar NH_3 Production by Perovskite-Based Photocathode Coupled to Valorization of Glycerol. *Nat Catal* **2024**, 1–12. https://doi.org/10.1038/s41929-024-01133-4.
2. Schichtl, Z. G.; Carvalho, O. Q. ; Tan, J.; Saund, S. S.; Ghoshal, D.; Wilder, L. M.; Gish, M. K.; Nielander, A. C.; Stevens, M. B.; Greenaway, A. L. Chemistry of Materials Underpinning Photoelectrochemical Solar Fuel Production. *Submitted,* **2024**.

Reversible Photoinduced Ligand Detachment from CdSe Quantum Dots

McKenna N. Grega, Jianing Gan, Muhammad Noman, and John B. Asbury
Department of Chemistry
The Pennsylvania State University
University Park, PA 16802

Project Overview. The objective of this research is to understand and control the excited state surface chemistry of colloidal nanocrystals being targeted as light absorbers and catalysts in artificial photosynthetic molecular constructs. The surface chemistry of molecules known as ligands bonded to nanocrystal surfaces mediate the primary energy and electron transfer processes that underpin photochemical and photocatalytic transformations in artificial photosynthetic reactions. Such ligand layers on nanocrystals have dual and often competing roles of facilitating surface access of catalysts and charge acceptor species involved in photocatalytic processes while providing colloidal stability and protecting the nanocrystal surfaces from photodegradation. This research project is framed around the hypothesis that it is possible to design nanocrystal/ligand interactions that enhance the change in ligand bonding in the excited states of nanocrystals to create more permeable ligand shells just when they are needed – when the nanocrystals are in their excited states and ready to drive photocatalytic processes. Then, when the nanocrystals return to their ground states, the ligand surface bonding strength can be restored to protect nanocrystals until the next photoexcitation event. The research plan seeks to uncover design rules about how to control such changes in excited state surface chemistry and to reveal mechanisms by which the molecular and material components of nanocrystalline photocatalytic systems can be integrated to utilize the effect to facilitate the primary light harvesting, charge transferring, and chemical bond forming components of photocatalytic systems.

Current Progress. The research plan seeks to demonstrate the unexpected opportunity to accomplish both the synergistic coordination of the primary molecular dynamics and charge transfer processes in photocatalysis while at the same time enhancing the durability of nanocrystals in these reactions. The first step toward achieving this goal is to demonstrate that ligands can in fact be detached from nanocrystal surfaces to create a more permeable ligand shell when the nanocrystals are promoted to their electronic excited states. The second step is to show that this detachment is reversible, allowing ligands to reattach to the nanocrystal surfaces after the excited states have relaxed to restore the ground states of the nanocrystals. To date, we have successfully demonstrated both steps in CdSe colloidal quantum dot (QD) assemblies as described below.

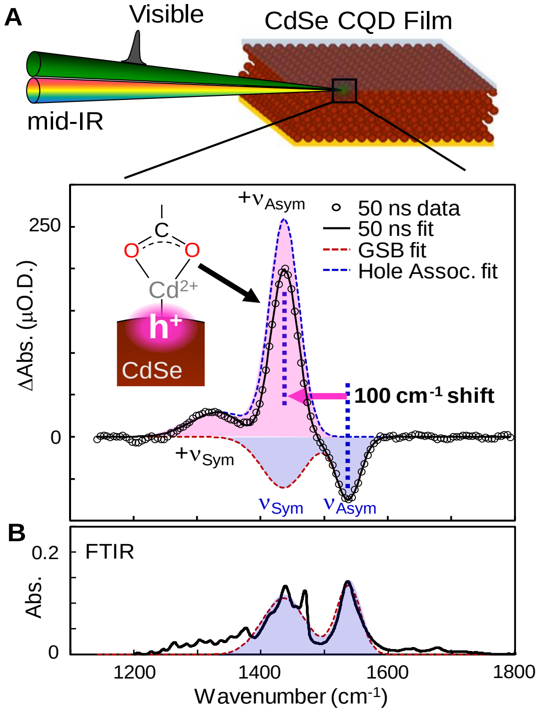

Figure 1. **A**. Diagram of the mid-IR transient absorption experiment. Transient vibrational spectrum measured at 50 ns time delay (open circles) with a best fit curve (50 ns Fit) corresponding to a hole associated carboxylate model indicating a 100 cm^{-1} frequency shift of the carboxylates features due to interactions with surface-localized holes. The ground state carboxylate features are overlaid on the FTIR spectrum of the sample in **B** for comparison.

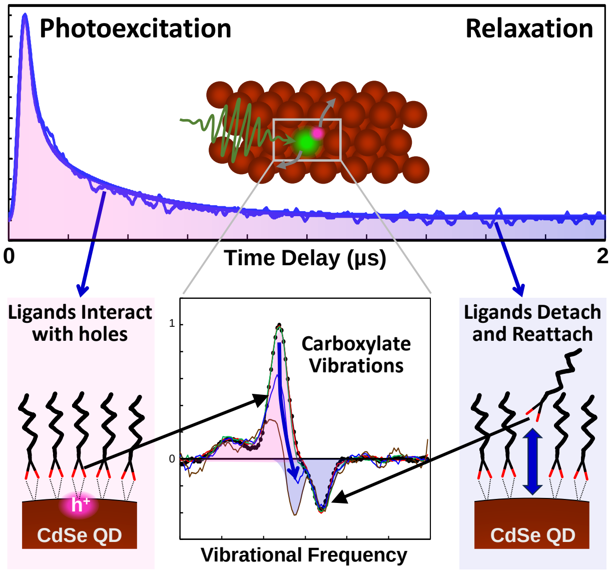

Figure 2. Top. Kinetics trace of the mid-IR transient absorption of carboxylate features interacting with surface-localized holes in CdSe QDs. **Bottom**. After photoexcitation, carboxylate groups experience ~100 cm^{-1} red-shift due to electron density being pulled out from the π-conjugated carboxylate molecular orbital. On longer time scales, the appearance of both carboxylate bleach features reveals that ~6% of ligands detach/excitation event. Longevity studies show that the ligands reattach, indicating the reversibility of the detachment/reattachment process.

To accomplish these first steps, we investigated charge and molecular dynamics at the surfaces of CdSe QDs passivated by stearate ligands following optical excitation to their excitonic excited states (**Figure 1**). We used time-resolved infrared spectroscopy to probe vibrational modes of the carboxylate anchoring groups of stearate ligands that were attached to the surfaces of CdSe QDs after optically exciting them in solid nanocrystal films. Visible transient absorption and time-resolved photoluminescence spectroscopies were used to track the dynamics of the electronic states through their optical transitions for comparison to the population dynamics read-out through the vibrational features. The vibrational frequencies of surface-bonded carboxylate groups revealed their interactions with surface-localized holes in the excited states of the QDs, leading to a 100 cm^{-1} red-shift due to reduction of electron density in the π-conjugated carboxylate molecular orbital. Furthermore, on longer time scales, the molecular and charge dynamics at the QD surfaces monitored through the transient vibrational features revealed that ~6% of stearate ligands originally attached to the QD surfaces transiently detached following each photoexcitation event (**Figure 2**). Thus, ligand detachment occurs with relatively high yield from CdSe QD surfaces following photoexcitation, even in the solid state. Importantly, we used a longevity study to show that despite the relatively high yield for photoinduced ligand detachment, CdSe QDs irradiated with nearly 10^7 photoexcitations per nanocrystal showed no signs of long-term degradation of their ligand shells, indicating that the ligand detachment was transient and reversible. Such photoinduced ligand detachment and reattachment processes have the potential to inform the design of ligand-nanocrystal boundaries that can transiently provide surface access to charge and energy acceptors within the excited states of the nanocrystals. Going forward, experimental and computational methods that allow exploration of this boundary may reveal design rules for QD architectures tailored for enhanced activity or selectivity in solar energy harvesting or photoredox catalytic applications.

Future Work. Having demonstrated that transient and reversible ligand detachment indeed occurs from CdSe QD surfaces, the next steps in the research plan are to 1) move the mid-IR transient absorption experiments into solution to allow us to demonstrate how the ligand detachment and reattachment dynamics can influence the rate and yield of charge transfer processes that underpin photocatalytic reactions. 2) we also plan to complete construction of our new ultrafast mid-IR transient absorption system that will allow us to examine the fundamental processes that occur on faster time scales and that lead to the observed changes in excited state surface chemistry of the QDs. 3) finally, we plan to explore core/shell architectures to selectively promote enhanced electron versus hole surface charge density to further explore the origins of this effect.

DOE Solar Photochemistry Sponsored Publications 2021-2024

1. “Influence of Ligand Structure on Excited State Surface Chemistry of Lead Sulfide Quantum Dots,” Eric R. Kennehan, Kyle T. Munson, Grayson S. Doucette, Ashley R. Marshall, Matthew C. Beard, and John B. Asbury, *J. Am. Chem. Soc*., **143**, 13824-13834 (2021).
DOI: 10.1021/jacs.1c06248

2. “Exciton−Phonon Coupling and Carrier Relaxation in PbS Quantum Dots: The Case of Carboxylate Ligands,” Eric R. Kennehan, Kyle T. Munson, Grayson S. Doucette, Ashley R. Marshall, Matthew C. Beard, and John B. Asbury, *J. Phys. Chem. C*, **125**, 22622-22629 (2021).
DOI: 10.1021/acs.jpcc.1c05803

3. “Electron Transfer Going the Distance: Mn-Doped ZnSe as a Model Photocatalytic System,” Kelsey M. Watson and John B. Asbury, *J. Phys. Chem. C*, **125**, 25749-25765 (2021).
DOI: 10.1021/acs.jpcc.1c08298

4. “Synthesis and Photoinduced Electron Transfer Studies of Ligand Exchanged Mn-Doped ZnSe Nanocrystals in Water,” Kelsey M. Watson and John B. Asbury, *J. Phys. Chem. C*, **126**, 4995-5003 (2022). **DOI**: 10.1021/acs.jpcc.2c00379

5. “Excited State Dynamics of 5,14- vs 6,13-Bis(trialkylsilylethynyl)-Substituted Pentacenes: Implications for Singlet Fission,” Ryan D. Pensack, Geoffrey E. Purdum, Samuel M. Mazza, Christopher Grieco, John B. Asbury, John E. Anthony, Yueh-Lin Loo, Gregory D. Scholes, *J. Phys. Chem. C*, **126**, 9784-9793 (2022). **DOI**: 10.1021/acs.jpcc.2c00897

6. “Thermal Disorder-Induced Strain and Carrier Localization Activate Reverse Halide Segregation,” Nursultan Mussakhanuly, Arman Mahboubi Soufiani*, Stefano Bernardi, Jianing Gan, Saroj Kumar Bhattacharyya, Robert Lee Chin, Hanif Muhammad, Milos Dubajic, Angus Gentle, Weijian Chen, Meng Zhang, Michael P. Nielsen, Shujuan Huang, John Asbury, Asaph Widmer-Cooper, Jae Sung Yun, Xiaojing Hao, *Adv. Mater*., **25**, 2311458 (2023).
DOI: 10.1002/adma.202311458

7. “Reversible Ligand Detachment from CdSe Quantum Dots Following Photoexcitation,” McKenna N. Grega‡, Jianing Gan‡, Muhammad Noman, and John B. Asbury, *J. Phys. Chem. Lett*., **15**, 3987-3995 (2024). **DOI**: 10.1021/acs.jpclett.4c00529

Time-resolved Studies of Photodynamic Metal Organic Frameworks

Qingyu Ye, Sajia Afrin,[a] Daniel Cairnie, Xiaozhou Yang, Erik Grumstrup,[a] and Amanda J. Morris
Department of Chemistry
Virginia Tech
Blacksburg, VA 24060

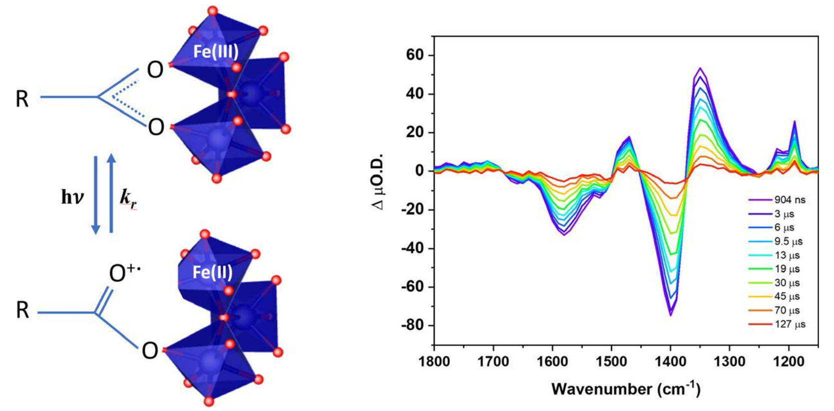

Figure. After photoexcitation, the coordination mode between the carboxylate and Fe-oxo within MIL-101(Fe) switches from bidentate bridging to monodentate configuration as probed by time-resolved infra-red spectroscopy.

The observation of structural rearrangement upon charge separation, reduction or oxidation, and catalysis within molecules is well-known. From the classic example of the transition of an iron porphyrin from a puckered to planar arrangement as it is reduced from the Fe(III) to the Fe(II) oxidation state to the photodissociation of metal-halide bonds in rhodium dimers, these events are critical in understanding the mechanism by which those catalysts promote desired chemistry. By exploiting MIL-101(Fe) as a model MOF platform, we have recently unveiled the photodynamic nature of the MOF structure. The excited state in MIL-101(Fe) was studied via time-resolved infrared (TRIR) spectroscopy. By probing the vibrational fingerprints of the carboxylate bonds upon photoexcitation, a transient change of the carboxylate-Fe bonding configuration was observed, namely, a shift from bidentate bridging coordination to monodentate counterpart. We observed clear ground state bleaches (1400 cm^{-1} and 1590 cm^{-1}), corresponding to the major ground state IR absorption peaks. Meanwhile, excited-state absorption peaks were observed at 1360 cm^{-1} and 1710 cm^{-1}, suggesting the formation of monodentate coordination mode. Over 40 ± 1 μs, the Fe-O bond reforms to regenerate the ground state MOF configuration. Interestingly, the visible time-resolved absorption investigation recorded a broad excited state absorption from 400-700 nm, previously attributed to the transient generation of Fe(II) states, which decayed with a similar lifetime. The similarity in the decay lifetimes of the vibrational and visible transients suggests the LMCT event, where an electron is injected from the carboxylate to the Fe-oxo cluster, results in a bond-breakage event and only upon reformation of that bond can the charge recombine to regenerate the ground state. Compared to the irreversible photo- deligation events in traditional photocatalysis, the observed reversible photodynamic phenomenon could potentially point out a key merit of MOFs and provide new pathways to promote efficient photocatalysis.

[a] Department of Chemistry and Biochemistry, Montana State University, Bozeman, Montana 59717

DOE Solar Photochemistry Sponsored Publications 2021-2024

1. Wang, Q.; Jin, J.; Wang, Z.; Ren, S.; Ye, Q.; Dou, Y.; Liu, S.; Morris, A.J.; Slebodnick, C.; Quan, L. “Supramolecular Metal Halide Complexes for High-Temperature Nonlinear Optical Switches.” J. Am. Chem. Soc. 2024, 2024, 146, 13, 8971–8980.

2. Afrin, S.; Yang, X.; Morris, A.J.*; Grumstrup, E.M.* “Rapid Exciton Transport and Structural Defects in Individual Porphyrinic Metal Organic Framework Microcrystals” J. Am. Chem. Soc. 2024, 146, 7, 4309-4313.

3. Ye, Q.; Cairnie, D.R; Troya, D.; Kumar, N.; Yang, X.; Morris, A.J.* “Photoinduced Dynamic Ligation in Metal-Organic Frameworks.” J. Am. Chem. Soc. 2024, 146, 1, 101-105.

4. Cairnie, D.R.; Morris, A.J.* “A Technical Guide for Performing Spectroscopic Measurements on Metal-Organic Frameworks.” JoVE, 2023, 194, e65072.

5. Vong, D.; Novak, E.C.; Ruiz-Rodrigues, M.M.; Elorfi, S.; Thomas, B.; Morris, A.J.; Moule, A.J.; Daemen, L.L.* “Compact, Portable, Automatic Sample Changer Stick for Cryostats and Closed-Ccycle Refrigerators.” Rev. Sci. Instrum. 2023, 94, 085108-1 – 085108-9.

6. Bonchio, M.; Bonin, J.; Ishitani, O.; Lu, T.; Morikawa, T.; Morris, A.J.; Reisner, E.; Sarkar, D.; Toma, F.M.; Robert, M.* “Best Practices for Experiments and Reporting in Photocatalytic CO2 Reduction.” Nat. Catal. 2023, 6, 657-665.

7. Gibbons, B.; Cairnie, D.R.; Thomas, B.; Yang, X.; Ilic, S.; Morris, A.J.* “Photoelectrochemical Water Oxidation by a MOF/Semiconductor Composite.” Chem. Sci. 2023, 14, 4672 – 4680.

8. Bryant, J.T,; Logan, M.W.; Chen, X.; Djokic, M.; Cairnie, D.R.; Vazquez-Molina, D.A.; Nijamudheen, A.; Langlois, K.R.; Markley, M.J.; Pombar, G.; Holland, A.A.; Caranto, J.D.; Harper, J.K; Morris, A.J.*; Mendoza-Cortes, J.L.*; Jurca, T.*; Chapman, K.*; Uribe-Romo, F.J.* “Synergistic Steric and Electronic Effects on the Photoredox Catalysis by a Multivariate Library of Titania Metal–Organic Frameworks.” J. Am. Chem. Soc. 2023, 145, 8, 4589-4600.

9. Fabrizio, K.; Andreeva, A.B.; Kadota, K.; Morris, A.J.; Brozek, C.K. “Guest-dependent bind Flexibility in UiO-66, a “stable” MOF.” Chem. Commun. 2023, 59, 1309–1312.

10. Gibbons, B.; Cai, M.; Morris, A.J.* “A Potential Roadmap to Integrated Metal-Organic Framework Artificial Photosynthetic Arrays.” J. Am. Chem. Soc. 2022, 144, 39, 17723–17736.

11. Benseghir, Y.; Sole-Daura, A.; Cairnie, D.R.; Robinson, A.L.; Duguet, M.; Mialane, P.*; Gairola, P.; Gomez-Mingot, M.; Fontecave, M.; Iovan, D.A.; Bonnett, B.; Morris, A.J.*; Dolbecq, A.; Mellot-Draznieks, C.* “Unveiling the Mechanism of the Photocatalytic Reduction of CO2 to Formate Promoted by Porphrynic Zr-Based Metal-Organic Frameworks.” J. Mater. Chem. A. 2022, 10, 18103-18115.

12. Ilic, S.; May, A.M.; Usov, P.M.; Cornell, H.D.; Gibbons, B.; Celis-Salazar, P.; Cairnie, D.R.; Alatis, J.; Slebodnick, C.; Morris, A.J.* “An Aluminum-Based MetalOrganic Cage for Cesium Capture” Inorg. Chem. 2022, 61, 17, 6604-6611.

13. Ilic, S.; Cairnie, D.R.; Bridgewater, C.M.; Morris, A.J.* “Investigation into Dual Emission of a Cyclometalated Iridium Complex: The Role of Ion-Pairing.” J. Photochem. Photobiol. 2021, 8,

100084.

14. Shaikh, S.; Ilic, S.; Gibbons, B.; Yang, X.; Jakubikova, E.; Morris, A.J.* "Role of 3D Structure in Energy Transfer in Mixed-Ligand Metal-Organic Frameworks." J. Phys. Chem. C. 2021, 125, 42, 22998-23010.

15. Shaikh, S.; Ilic, S.; Gibbons, B.; Yang, X.; Jakubikova, E.; Morris, A.J.* "Role of 3D Structure in Energy Transfer in Mixed-Ligand Metal-Organic Frameworks." J. Phys. Chem. C. 2021, 125, 42, 22998-23010.

Light Harvesting, Energy Transport, and Energy Conversion with Molecular Frameworks

Alice Li,[a] Boris V. Kramar,[a] Sydney Koehne,[a] Anna Bondarenko,[a] Roel Tempelaar,[a] Richard D. Schaller,[a,c] Lin X. Chen,[a,b] Joseph T. Hupp[a]
[a]Dept. of Chemistry
Northwestern University
Evanston, IL 60208
[b]Chemical Sciences and Engineering Division, and [c]Center for Nanoscale Materials
Argonne National Laboratory
Lemont, IL 60439

By analogy to light harvesting complexes in plants and photosynthetic bacteria, well-defined, porous, and chemically robust arrays of molecular chromophores offer potentially attractive starting points for artificial structures capable of absorbing visible light, transporting molecular excitons, and delivering reducing or oxidizing equivalents to remotely sited catalysts for desired, energy-relevant chemical transformations. Crystalline metal-organic frameworks (MOFs) constitute one class of structures amenable to such investigations. Indeed, we and others have shown that appropriately designed and elaborated MOFs can: a) function as antenna systems capable of enlisting up to a few hundred molecular chromophores for light collection and directional transport of molecular excitons, b) photocatalytically drive comparatively simple reactions such as reduction of CO_2 to CO, c) engage in complementary directional charge transport, and d) facilitate related electrocatalytic chemical transformations. This presentation will touch on one or two new experimental and computational findings that both advance and significantly alter our understanding of how and why some of the most promising photo-active MOFs work. The findings point, in part, to an unexpected role for remote, and seemingly innocent protons, in defining and selecting for photocatalysis-relevant electronic excited states.

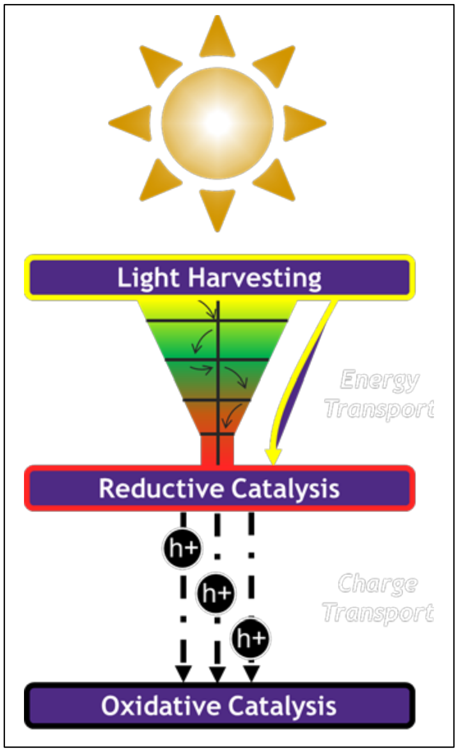

Complementary to photophysical and photochemical studies with MOFs are preliminary studies of an emerging and, as yet much less explored class of compounds termed HOFs (hydrogen-bonded organic frameworks). Of greatest interest to us are HOFs that are: a) amenable to intentional chemical and topological tuning and design, and b) characterized by well-defined (crystalline) structures, molecular-scale porosity, and prominent visible-region electronic absorption (and emission). In contrast to MOFs, which primarily assemble via formation of metal-ligand bonds, HOFs assemble via redundant, peripheral hydrogen bonding, in combination with favorable π-π stacking. The resulting compounds are often chemically and physically robust, maintaining their structural integrity, for example, when heated, when immersed in aqueous acid, when infiltrated with chemical guests, or when subjected to evacuation of water or other solvents from framework-defined channels/pores. Initial work has yielded proof-of-concept results for: a) antenna behavior based on transport of photo-generated molecular excitons over moderate distances to doped emitters, b) quantifiable dynamics for charge-transport, based on integration of HOFs with electrodes in electrochemical cells, c) photochemical generation of molecular hydrogen via sensitization of well-defined, channel-installed, transition-metal-containing catalytic clusters, and d) optical upconversion (red to green) based, in part, on diffusive transport of triplet molecular excitons, followed by triplet-triplet annihilation.

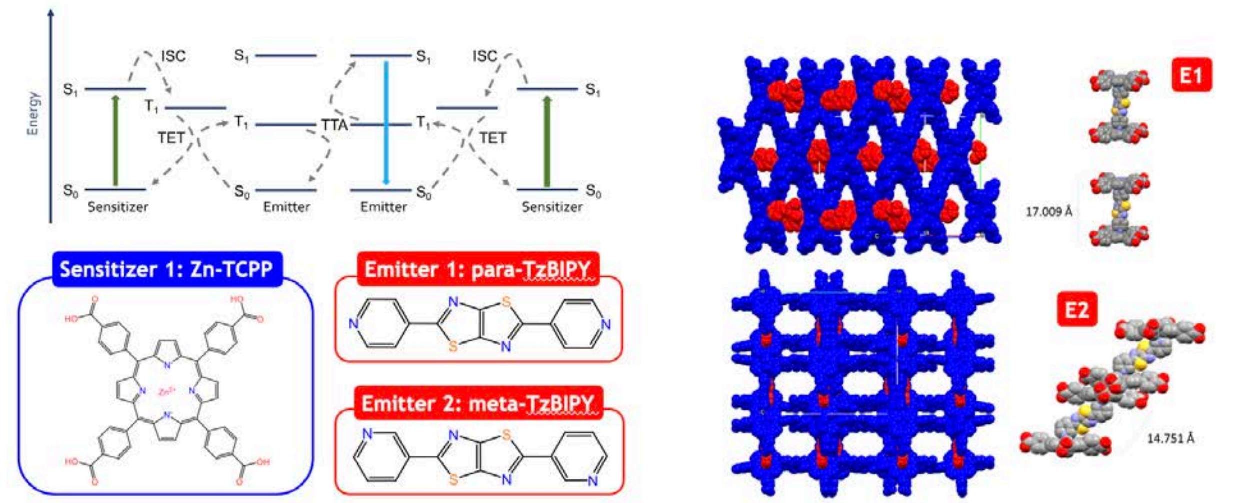

Triplet-triplet annihilation enables upconversion, thereby extending the potential utility of low-energy electromagnetic radiation. Porous HOFs provide a means of integrating sensitizers and emitters in ways that favor upconversion.

DOE Solar Photochemistry Sponsored Publications 2021-2024

1. “Photon Upconversion in a Glowing Metal-Organic Framework,” Roy, I.; Goswami, S.; Young, R. M.; Schlesinger, I.; Mian, M. R.; Enciso, A. E.; Zhang, X.; Hornick, J. E.; Farha, O. K.; Wasielewski, M. R.; Hupp, J. T.; Stoddart, J. F., *J. Am. Chem. Soc.*, **2021**, *143*, 5053-5059. DOI: 10.1021/jacs.1c00298
2. “Single-Atom Metal Oxide Sites as Traps for Charge Separation in the Zirconium-Based Metal-Organic Framework NDC-NU-1000,” Kramar, B. V.; Phelan, B. T.; Sprague-Klein, E. A.; Diroll, B. T.; Lee, S.; Otake, K.-I.; Palmer, R.; Mara, M. W.; Farha, O. K.; Hupp, J. T.; Chen, L. X. *Energy Fuels*, **2021**, *35*, 19081-19095. DOI: 10.1021/acs.energyfuels.1c02623 *invited paper*
3. “Light-Harvesting ‘Antenna’ Behavior in NU-1000,” Goswami, S.; Yu, J.; Patwardhan, S.; Deria, P.; Hupp, J. T. *ACS Energy Lett*. **2021**, *6*, 848-853. DOI: 10.1021/acsenergylett.0c02514
4. “Tuning the Conductivity of Hexa-Zirconium (IV) Metal-Organic Frameworks by Encapsulating Heterofullerenes,” Ray, D.; Goswami, S.; Duan, J.; Hupp, J. T.; Cramer, C. J.; Gagliardi, L., *Chem. Mater*., **2021**, *33*, 1182-1189. DOI: 10.1021/acs.chemmater.0c03855

5. “Photoinduced Charge Transfer with a Small Driving Force Facilitated by Exciplex-like Complex Formation in Metal−Organic Frameworks,” Li, XL; Yu, JR; Lu, ZY; Duan, JX; Fry, HC; Gosztola, DJ; Maindan, K; Rajasree, SS; Deria, P. *J. Am. Chem. Soc.*, **2021**, *143*, 15286-15297. DOI: 10.1021/jacs.1c06629
6. “Light Harvesting Antenna Properties of Framework Solids,” Kramar, BV; Flanders, NC; Helweh, W; Dichtel, WR; Hupp, JT; Chen, LX. *Accounts of Materials Research* **2022**, *3*, 1149-1159. DOI: 10.1021/accountsmr.2c00137
7. “Toward Ideal Metal–Organic Framework Thin-Film Growth via Automated Layer-by-Layer Deposition: Examples Based on Perylene Diimide Linkers,” Goswami, S; Rimoldi, M; Anderson, R; Lee, C; Li, XL; Li, A; Deria, P; Chen, LX; Schaller, RD; Gomez-Gualdron, DA; Farha, OK; Hupp, JT. *Chem. Mater*. **2022**, *34*, 9446–9454. DOI: 10.1021/acs.chemmater.2c01753
8. “Noncovalent Surface Modification of Metal–Organic Frameworks: Unscrambling Adsorption Properties via Isothermal Titration Calorimetry,” Sheridan, TR; Gaidimas, MA; Kramar, BV; Goswami, S; Chen, LX; Farha, OK; Hupp, JT. *Langmuir* **2022**, *38*, 11199–11209. DOI: 10.1021/acs.langmuir.2c01223
9. “Does the Mode of Metal–Organic Framework/Electrode Adhesion Determine Rates for Redox-Hopping-Based Charge Transport within Thin-Film Metal–Organic Frameworks?,” Duan, J.; Goswami, S.; Patwardhan, S.; Hupp, J. T. J. Phys. Chem. C, **2022**, *126*, 4601-4611. DOI: 10.1021/acs.jpcc.1c09812
10. “Encapsulating CdSe/CdS QDs in the MOF ZIF-8 Enhances Their Photoluminescence Quantum Yields in the Solid State,” Stone, A. B. E. S.; Irgen-Gioro, S.; López-Arteaga, R.; Hupp, J. T.; Weiss, E. A. *Chem. Mater*. **2022**, *34*, 1921–1929. DOI: 10.1021/acs.chemmater.1c04355
11. “Redox-Hopping-Based Charge Transport Mediated by Ru(II)-Polypyridyl Species Immobilized in a Mesoporous Metal-Organic Framework,” *Frontiers in Chemical Engineering*, Duan, Jiaxin; Goswami, Subhadip; Hupp, Joseph T. **2022**, *3*, 828266. DOI:10.3389/fceng.2021.828266.
12. “An iron-porphyrin grafted metal-organic framework as a heterogeneous catalyst for the photochemical reduction of CO_2,” Zhang, K.; Goswami, S.; Noh, H.; Lu, Z.; Sheridan, T. R.; Duan, J.; Dong, W.; Hupp, J. T. *J. Photochem. Photobiol.*, **2022**, *10*, 100111. DOI: 10.1016/j.jpap.2022.100111 *(conference themed issue)*
13. Understanding Diffusional Charge Transport within a Pyrene-Based Hydrogen-Bonded Organic Framework,” Goswami, S; Ma, K.; Duan, J; Kirlikovali, K. O.; Bai, J.; Hupp, J. T.; Li, P.; Farha, O. K. *Langmuir*, **2022**, *38*, 1533-1539. DOI: 10.1021/acs.langmuir.1c02915
14. “Identifying the Polymorphs of Zr-Based Metal–Organic Frameworks via Time-Resolved Fluorescence Imaging,” Chen, X.; Jagadesan, P.; Valandro, S.; Hupp, J. T.; Schanze, K. S.; Goswami, S. *ACS Materials Lett.*, **2022**, *4*, 370-377. DOI: 10.1021/acsmaterialslett.1c00754

15. “MOF-enabled confinement and related effects for chemical catalyst presentation and utilization,” Liu, J.; Goetjen, T. A.; Wang, Q.; Knapp, J. G.; Wasson, M. C.; Yang, Y.; Syed, Z. H.; Delferro, M.; Notestein, J. M.; Farha, O. K.; Hupp, J. T. *Chem. Soc. Rev*., **2022**, *51*, 1045-1097. DOI: 10.1039/D1CS00968K

16. Superradiance and Directional Exciton Migration in Metal–Organic Frameworks,” Rajasree, SS; Yu, JR; Pratik, SM; Li, XL; Wang, R; Kumbhar, AS; Goswami, S; Cramer, CJ; Deria, P. *J. Am. Chem. Soc.* **2022**, *144*, 1396–1406. DOI: 10.1021/jacs.1c11979

17. “Charge transfer in mixed and segregated stacks of tetrathiafulvalene, tetrathianaphthalene and naphthalene diimide: a structural, spectroscopic and computational study,” C. F. Leong, B. Chan, T. Liu, H. S. Moore, I. Hod, M. B. Solomon, P. M. Usov, Joseph T. Hupp, Omar Farha, Deanna M. D’Alessandro *New Journal of Chemistry*, **2022**, *46*, 10026-10036. DOI: 10.1039/d2nj00643j

18. “Reconstructing oxygen-deficient zirconia with ruthenium catalyst on atomic-scale interfaces toward hydrogen production,” Mansu Kim, Seung-hoon Kim, Jonghwan Park, Seongsoo Lee, Injoon Jang, Hyung Chul Ham, Joseph T. Hupp, Namgee Jung, Sung Jong Yoo, Dongmok Whang, *Advanced Functional Materials*, **2023**, *33*, 2300673. DOI: 10.1002/adfm.202300673

19. “Synthetic access to a fully sulfided analogue of an Anderson polyoxometalate that is catalytically competent for reduction reactions,” Jiaxin (Dawn) Duan, Hafeera Shabbir, Zhihengyu Chen, Wentuan Bi, Qin Liu, Pengfei Liu, Jingyi Sui, Luka Đorđević, Samuel I. Stupp, Karena Chapman, Alex B. F. Martinson, Alice Li, Subhadip Goswami, Rachel B. Getman, Joseph T. Hupp *J. Am. Chem. Soc*., **2023**, *145* (13), 7268–7277. DOI:10.1021/jacs.2c12992

20. “Post-synthetic Cyano-ferrate(II) Functionalization of the Metal–organic Framework, NU-1000,” C-W. Kung, K. Otake, R. Drout, S. Goswami, O. K. Farha, J. T. Hupp, *Langmuir*, **2023**, *39*, 4936–4942. DOI: 10.1021/acs.langmuir.2c03354.

21. “Selective Photocatalytic Reduction of Acetylene to Ethylene Powered by a Cobalt-Porphyrin Metal–Organic Framework,” Aaron E.B.S. Stone, Francesca Arcudi, Luka Đorđević, Samuel I. Stupp, Joseph T. Hupp, Emily A. Weiss *ACS Energy Letters*, **2023**, *8*, 4684-4693. DOI: 10.1021/acsenergylett.3c01995

22. “Photo-reactive CO_2 Capture by a Zr-Nanographene MOF,” Xin Zheng, Matthew C. Drummer, Haiying He, Shirin Saffar Avval, Thomas M. Rayder, Jens Niklas, Nicholas P. Weingartz, Varun Singh, Boris V. Kramar, Lin X. Chen, Joseph T. Hupp, Oleg G. Poluektov, Omar K. Farha, Brian P. Chaplin, Peter Zapol, Ksenija D. Glusac *J. Phys. Chem. Lett.*, **2023**, *14*, 4334-4341. DOI: 10.1021/acs.jpclett.3c00049

23. “Highly Active Oxygen Reduction Electrocatalysts Derived from an Iron-Porphyrin Framework,” Elvington, Mark; Ganesan, Prabhu; Ward, Patrick; Liu, Jian; Atilgan, Ahmet; Kramar, Boris; More, Karren; Cullen, David; Hupp, Joseph T.; Greenway, Scott; Adams IV, William; Colon-Mercado, Hector *PRX Energy*, **2023**, *2*, 043008, DOI: 10.1103/PRXEnergy.2.043008

24. “CO_2 Capture and Conversion to C1 Chemicals with Mixed-Metal Copper/Nickel Bis(amino)bipyrazolate Metal–Organic Frameworks,” Patrizio Campitelli, Alessia Tombesi, Corrado Di Nicola, Claudio Pettinari, Anna Mauri, Simona Galli, Tongan Yan, Dahuan Liu, Jiaxin Duan, Subhadip Goswami, Giulia Tuci, Giuliano Giambastiani, Joseph T. Hupp, Andrea Rossin *ACS Appl. Energy Mater.*, **2023**, 6, 18, 9231–9242. DOI: 10.1021/acsaem.3c00780

25. “Triplet Generation Through Singlet Fission in Metal-Organic Framework: An Alternative Route to Inefficient Singlet-Triplet Intersystem Crossing,” Surendran Rajasree, S.; Yu, J.; Fry, H. C.; Anderson, R.; Xu, W.; Krishnan, R.; Duan, J.; Goswami, S.; Gómez-Gualdrón, D. A.; Deria, P. *Angew. Chem. Int. Ed.*, **2023**, *62*, e20230532. DOI: 10.1002/anie.e20230532

26. “Framework-Topology-Controlled Singlet Fission in Metal–Organic Frameworks,” Surendran Rajasree, S.; Yu, J.; Fajardo-Rojas, F.; Fry, H. C.; Anderson, R.; Li, X.; Xu, W.; Duan, J.; Goswami, S.; Maindan, K.; Gómez-Gualdrón, D. A.; Deria, P. *J. Am. Chem. Soc.* **2023**, *145*, 17678–17688. DOI: 10.1021/jacs.3c03918

27. “Ligand Desorption and Fragmentation in Oleate-Capped CdSe Nanocrystals under High-Intensity Photoexcitation,” Samantha M. Harvey, Jacob H. Olshansky, Alice Li, Shobhana Panuganti, Mercouri G. Kanatzidis, Joseph T Hupp, Michael R. Wasielewski, Richard D. Schaller *J. Am. Chem. Soc.*, **2024**, *146*, 3732–3741. DOI: 10.1021/jacs.3c10232

28. “Unexpected Photo-driven Linker-to-Node Hole Transfer in a Zirconium-Based Metal–Organic Framework,” Boris V. Kramar, Anna S. Bondarenko, Sydney M. Koehne, Benjamin T. Diroll, Xiaodan Wang, Haofan Yang, Kirk S. Schanze, Lin X. Chen, Roel Tempelaar, Joseph T. Hupp, *ACS Energy Letters*, in revision (journal-assigned manuscript number: nz-2023-02614b); preprint available on *ChemRxiv*, DOI: 10.26434/chemrxiv-2023-9mxxc

Dye-Sensitized Semiconductor Photoelectrodes and Z-Schemes for Solar Water Splitting

Langqiu Xiao,[1] Jacob A. Spies,[2] Shunta Nishioka,[1,3] Haruka Yamamoto,[1,3] Colton J. Sheehan,[1]
Kelly Kocera,[1] Shan Yu,[1] Gary W. Brudvig,[2] Kazuhiko Maeda,[3] and Thomas E. Mallouk[1]
[1]Department of Chemistry, University of Pennsylvania, Philadelphia, PA 19119
[2]Department of Chemistry, Yale University, New Haven, CT 06520
[3]Department of Chemistry, Tokyo Institute of Technology, Tokyo 152-8550, Japan

This project investigates fundamental processes and system-level issues that underpin the development of molecule-based systems for generating hydrogen by using sunlight as an energy source. The artificial photosynthesis approach to solar water splitting has the potential to provide a carbon-neutral route to hydrogen as an energy storage vehicle and as a feedstock for fuels and chemicals. Our current research follows on recent advances in creating solar water splitting systems based on dye-sensitized semiconductor electrodes and nanoparticles. We are developing new architectures for photosystems that can improve their efficiency, and components that can enable their use in integrated solar fuel systems. Our principal goals are (1) to quantify the rates of chemical processes that occur in molecule-based water-spitting systems that utilize two light absorbers in series (so-called Z-schemes), (2) to use that information to design Z-schemes for higher efficiency and (3) to incorporate the new molecules designed for Z-schemes into water-splitting photoelectrochemical cells, and vice-versa.

Our research on molecule-based Z-schemes builds on earlier studies of light-induced charge transfer at the dye-oxide semiconductor interfaces and the strategies developed for inhibiting energetically favorable charge recombination reactions. We use transient spectroscopy to measure the kinetics of light-induced forward and back electron transfer to construct predictive models that combine individual reaction rates into rate laws that govern the overall system efficiency. We chemically tailor the hydrogen- and oxygen-evolving particles of Z-schemes as a strategy for controlling the placement of the mediator molecules that shuttle electrons between particles. We are studying molecule-based assemblies for photocatalytic water oxidation, which have not previously been tested in Z-scheme water splitting systems, as components that can in principle improve the spectral utilization of sunlight for water splitting.

In earlier studies, we used intensity-modulated photocurrent spectroscopy (IMPS) to quantify the major loss channels in water-splitting dye-sensitized photoelectrochemical cells (WS-DSPECs). With optimized core-shell electrode architectures and fast molecular catalysts for water oxidation, the main contributor to low quantum yields is the low efficiency of charge transfer from the triplet excited state of the dye to the oxide semiconductor. For water splitting with $Ru(bpy)_3$-based dyes, the photoanode must operate under mildly acidic conditinons (pH 5-6) to provide sufficient driving force for rapid catalytic water oxidation. Under these conditions, in buffered aqueous media, charge injection from phosphonate-linked dye molecules into SnO_2/TiO_2 core-shell electrodes is too slow to compete effectively with triplet MLCT decay. Our current studies show that the charge injection efficiency increases substantially in mixed acetonitrile-water solvents. Interestingly, in pure acetonitrile electrolytes, charge injection is inefficient as a result of two effects. First, there is a negative shift in the flatband potential, which lowers the driving force for charge injection. Second and most interestingly, a previously unobserved effect inhibits electron transfer from the TiO_2 shell to the SnO_2 core. A negative conductivity transient is observed on the picosecond to

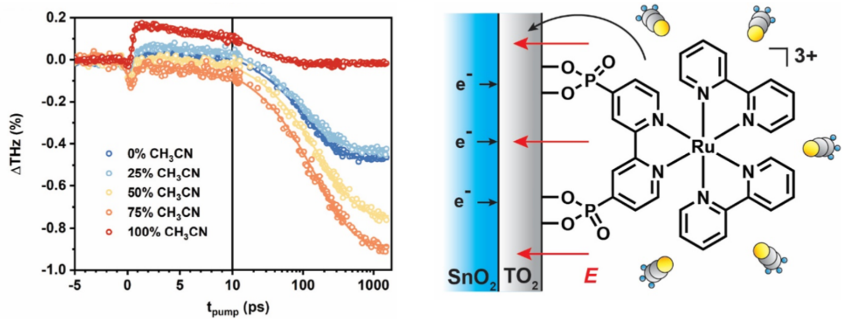

Fig. 1. A negative conductivity transient observed on the ps timescale by THz spectroscopy at dye-sensitized SnO2/TiO2 core/shell electrodes can be interpreted as field-driven trapping of conduction band electrons. This effect is minimized in higher dielectric solvent mixtures.

nanosecond timescale in the SnO_2 core by terahertz spectroscopy. This transient can be attributed to trapping of conduction band electrons at the TiO_2/SnO_2 interface by the dipolar field created upon charge injection into the TiO_2 shell. This effect is observed in mixed solvents up to about 50% water where it disappears and the charge injection efficiency is maximized. In the optimized solvent system, the ^{3}MLCT injection efficiency exceeds 80% at pH 4.5.

A second problem addressed in our current work is the stability of the dye-sensitized oxide semiconductor electrode. Typically, monomeric sensitizers functionalized with phosphonate groups have been used in WS-DPECs, and those dyes desorb on a timescale of minutes to hours under photoelectrochemical water splitting conditions in aqueous electrolytes. We have synthesized dimeric and oligomeric dyes that contain either phosphonate or carboxylate linkers, or a combination of the two. Interestingly, carboxylated dimers provide the best stability as well as the highest charge injection efficiency.

Much of the current focus of the past two years of this project has been to apply the lessons learned with dye-sensitized electrodes to particle-based Z-scheme water splitting systems. We collaborate with the Maeda group at Tokyo Institute of Techology to synthesize catalyzed oxide semiconductor nanoparticles, study photochemical water splitting by steady-state photolysis techniques, and measure electron transfer rates by flash photolysis/transient diffuse reflectance. A highlight of our recent work is the discovery that combining core-shell structure and anionic polymer modification inhibits two of the back electron transfer pathways at the hydrogen-evolving side of the system, resulting in the highest water splitting quantum yield so far seen in a dye-sensitized Z-scheme. Our current experiments are characterizing the kinetics of charge separation, recombination, and catalysis on the oxygen-evolving side of the Z-scheme. This research also involves the synthesis and characterization of new dye sensitizers, electron transfer mediators, and water oxidation catalysts.

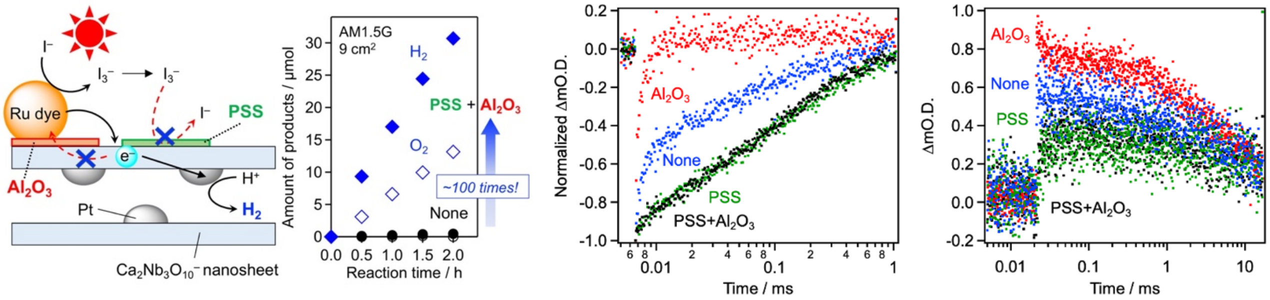

Fig. 2. A combination of chemical modifications dramatically increases the efficiency of a dye-sensitized oxide semiconductor-based water splitting Z-scheme by blocking two back electron transfer pathways.

DOE Solar Photochemistry Sponsored Publications 2021-2024

1. Z. Yan, J. L. Hitt, Z. Zeng, M. A. Hickner, and T. E. Mallouk, “Improving the efficiency of CO_2 electrolysis by using a bipolar membrane with a weak acid cation exchange layer,” Nat. Chem. 13, 33–40 (2021).

2. J. L. Hitt, Y. C. Li, S. Tao, Z. Yan, Y. Gao, S. J. L. Billinge, and T. E. Mallouk, “A high throughput optical method for studying compositional effects in electrocatalysts for CO_2 reduction,” Nat. Comm. 12, 1114 (2021).

3. S. Nishioka, T. Oshima, S. Hirai, D. Saito, K. Hoji, T. E. Mallouk, and K. Maeda, “Excited carrier dynamics in a dye-sensitized niobate nanosheet photocatalyst for visible-light hydrogen evolution,” ACS Catal. 11, 659-669 (2021).

4. Z. Yan and T. E. Mallouk, “Bipolar membranes for ion management in (photo-) electrochemical energy conversion,” Acc. Mater. Res., 2, 1156-1166 (2021).

5. K. Hojo, S. Nishioka, Y. Miseki, Y. Kamakura, T. Oshima, K. Sayama, T. E. Mallouk, and K. Maeda, “An improved Z-scheme for overall water splitting using dye-sensitized calcium niobate nanosheets synthesized by a flux method,” ACS Appl. Energy Mater., 4, 10145–10152 (2021).

6. S. Nishioka, K. Hojo, L. Xiao, T. Gao, Y. Miseki, S. Yasuda, T. Yokoi, K. Sayama, T. E. Mallouk, and K. Maeda, “Surface-Modified, Dye-sensitized niobate nanosheets enabling an efficient solar-driven Z-scheme for overall water splitting,” Sci. Adv. 8 (31), eadc9115 (2022).

7. S. Nishioka, F. Osterloh, X. Wang, T. E. Mallouk, and K. Maeda, “Photocatalytic water splitting,” Nat. Rev. Methods Primers, 3, 42 (2023).

8. H. Yamamoto, S. Nishioka, L. Xiao, Y. Miseki, K. Sayama, T. E. Mallouk, and K. Maeda, “Effects of anionic polymer modification of dye-sensitized niobate photocatalysts on solar-driven Z-scheme overall water splitting,” Solar RRL, 7, 2370231 (2023).

9. A. Kovyakh, S. Banerjee, C.-H. Liu, C. J. Wright, Y. C. Li, T. E. Mallouk, R. Feidenhans, and S. J. L. Billinge, “Towards scanning nanostructure X-ray microscopy,” J. Appl. Cryst., 56, 1221-1228 (2023).

10. H. Yamamoto, L. Xiao, Y. Miseki, H. Ueki, M. Okazaki, K. Sayama, T. E. Mallouk, and K. Maeda, “Is platinum-loaded titania the best material for dye-sensitized hydrogen evolution under visible light?” submitted.

11. L. Xiao, J. A. Spies, C. J. Sheehan, Z. Zeng, Y. Gao, T. Gao, A. Ehrlacher, M. W. Zuerch, G. W. Brudvig, and T. E. Mallouk, “Electron transfer dynamics at dye-sensitized SnO_2/TiO_2 core-shell electrodes in aqueous/nonaqueous electrolyte mixtures,” submitted.

High-Resolution Nanoelectrochemical Studies of Photoelectrocatalytic Processes

Gaukhar Askarova, Tianyu Bo, Shu Wu, and Michael V. Mirkin
Department of Chemistry and Biochemistry, Queens College-CUNY, Flushing, NY 11367

The focus of this project is on probing photoelectrochemical reactions at single particles and nanostructured interfaces by nanoelectrochemical techniques, including scanning electrochemical microscopy (SECM). We have recently reported high-resolution mapping of overall water splitting (OWS) processes on semiconductor microcrystals[1,2] by photo-SECM with the through-tip illumination of the sample.[3-6]

To extend this approach to studies of photoelectrocatalytic processes occurring at single biased microcrystals, we developed the methodology for transferring single semiconductor particles to the surface of a carbon ultramicroelectrode (UME). An SEM image of a $SrTiO_3/Rh_{2-y}Cr_yO_3$ cube (produced in Frank Osterloh's lab at UC Davis) attached to the surface of a glass-sealed 7-µm-diameter carbon fiber UME is shown in Fig. 1A. The current transients obtained at such a cube under chopped light illumination can be used to evaluate the photovoltage and investigate potential dependences of the OER (Fig. 1B) and HER (Fig. 1C) photocurrents. We are using a fiber attached cube as an SECM substrate to measure local hydrogen, oxygen and hydrogen peroxide fluxes.

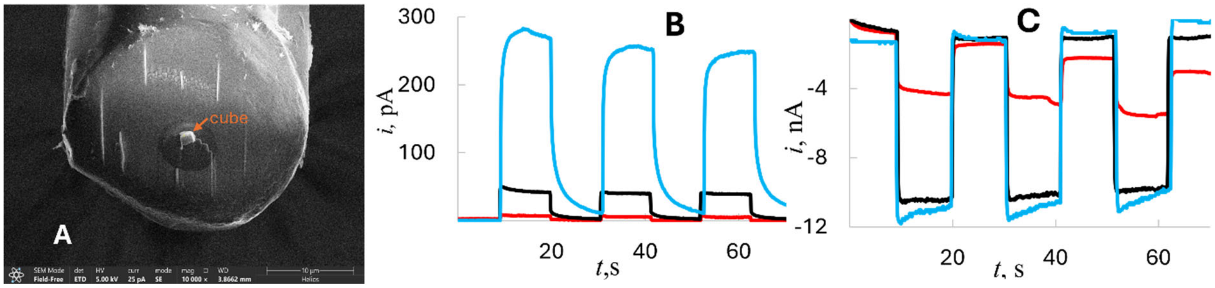

Fig. 1. Photoelectrochemical water splitting on a single $SrTiO_3/Rh_{2-y}Cr_yO_3$ cube attached to the carbon fiber UME (A). Chopped-light current transients of water oxidation (B; E, V vs. Ag/AgCl = 0.2, red; 1.0, black; and 1.6, blue) and water reduction (C; E, V vs. Ag/AgCl = -0.4, red; -0.8, black; and -0.9, blue).

A new SECM-based experimental methodology has been developed for studying photocatalyst/co-catalyst systems. We use two amperometric modes of photoSECM in combination with *in situ* measurements of local surface potential for probing charge-transfer processes and water splitting in a model system—Pt co-catalyst nanoparticles (NPs) electrodeposited on $Nb:TiO_2$ rutile (110) single crystal surface (Fig. 2). SECM experiments are performed with the same nanometer-sized probe and over the same NP (or the same spot on the semiconductor surface) to measure local rates of electron-transfer processes and photocatalytic hydrogen and oxygen evolution reactions (HER and OER).

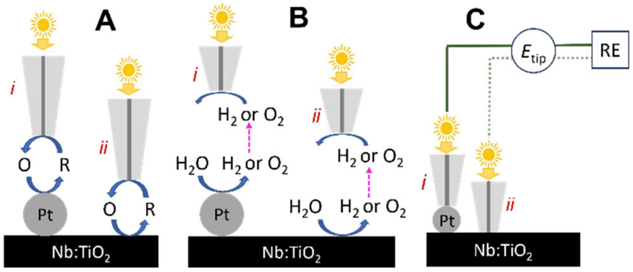

Fig. 2. Probing local charge transfer on co-catalyst particles (i) and photocatalyst surface (ii). (A) Reduction (or oxidation) of outer-sphere redox mediator is measured in the feedback mode of SECM operation. (B) The fluxes of H_2 and O_2 produced by OWS are measured in SG/TC SECM mode. (C) Local potentials of a cocatalyst NP (i) and underlying semiconductor surface (ii) are probed by potentiometric SECM. All experiments were performed under illumination and in the dark over the same Pt NP or the same spot on the TiO_2 surface.

In collaboration with the Hu group (Yale University) we are using this methodology to investigate OWS on GaN/GaInP photocatalysts with an IrOx array serving as an OER catalyst and CrOx coated Rh nanoparticles for HER. A topography SECM image of an ~0.5 µm IrOx spot is shown in Fig. 3A. The tip current vs. distance curves were obtained over IrOx (Fig. 3B) and GaN/GaInP (Fig. 3C) surface either under illumination (orange curves) or in the dark (black). A significant flux of oxygen was generated on the illuminated catalyst (Fig. 3B, orange curve) in contrast to no measurable production of oxygen on the semiconductor surface (Fig. 3C).

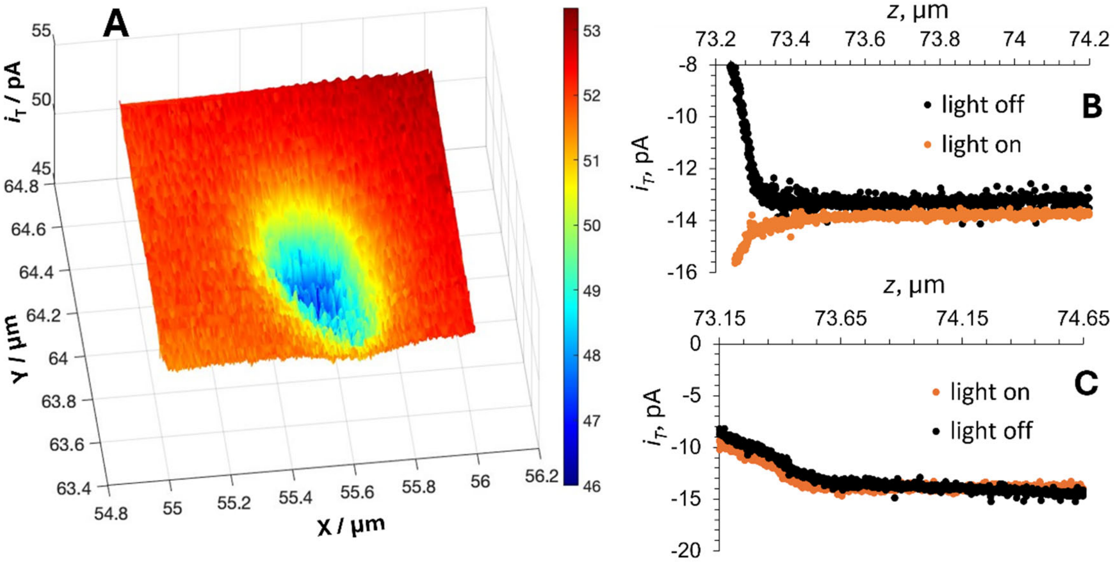

Fig. 3. SECM image of IrOx co-catalyst on the GaN/GaInP surface in 1 mm $K_4Fe(CN)_6$ solution (A) and current-distance curves obtained with an 80 nm tip approaching IrOx (B) and GaN/GaInP (C) in air-saturated solution either under illumination (orange symbols) or in the dark (black symbols). The current in (B) and (C) is due to the oxygen reduction at the tip.

DOE Solar Photochemistry Sponsored Publications 2021-2024

1. Askarova, G.; Hesari, M.; Barman, K.; Mirkin, M. V. Visualizing Overall Water Splitting on Single Microcrystals of Phosphorus Doped $BiVO_4$ by Photo-SECM. *ACS Appl. Mater. Interfaces* **2023**, *15*, 47168-47176.

2. Askarova, G.; Xiao, C.; Barman, K.; Wang, X.; Zhang, L.; Osterloh, F. E.; Mirkin, M. V. Photo-Scanning Electrochemical Microscopy Observation of Overall Water Splitting at a Single Aluminum-Doped Strontium Titanium Oxide Microcrystal. *J. Am. Chem. Soc.* **2023***, 145,* 6526−6534.

3. Askarova, G.; Hesari, M.; Wang, C.; Mirkin, M. V. Decoupling Through-Tip Illumination from Scanning in Nanoscale Photo-SECM. *Anal. Chem.* **2022**, 94, 7169–7173.

4. Wang, X.; Askarova, G.; Mirkin, M. V. Nanoscale SECM, in A. J. Bard and M. V. Mirkin (Eds), *Scanning Electrochemical Microscopy*, CRC Press, 2022, pp. 155-180.

5. Sarkar, S.; Wang, X.; Hesari, M.; Chen, P.; Mirkin, M. V. Scanning Electrochemical and Photoelectrochemical Microscopy on Finder Grids: Toward Correlative Multitechnique Imaging of Surfaces. *Anal. Chem.* **2021**, *93*, 5377−5382.

6. Wang, X.; Askarova, G.; Mirkin, M. V. Electrochemical Microscopy at the Nanoscale, in A. Wain, E. Dickinson (Eds), *Nanoscale Electrochemistry*, Elsevier Ltd., 2021, pp. 129-202.

Non-contact probes and mechanism of interface charge-carrier selectivity and photovoltage generation in semiconductor photocatalyst particles

Shannon W. Boettcher,[1,2] Aaron J. Kaufmann,[2] Meikun Shen[2]
[1]Department of Chemical & Biomolecular Engineering and Department of Chemistry
University of California, Berkeley
Berkeley, CA 94720
[2]Department of Chemistry and the Oregon Center for Electrochemistry
University of Oregon
Eugene, OR 97403

Semiconductor particles sparsely coated with nanoparticle electrocatalysts have been studied and developed for over 40 years to drive photochemical reactions such as water splitting to hydrogen and oxygen, organic pollutant degradation, and CO_2 reduction. Semiconductor photocatalysts particles, however, usually suffer from significant charge carrier recombination, are unable to generate photochemical driving forces commensurate with their bandgap, and thus have low overall efficiencies. The lack of photochemical driving force leads to the use of semiconductors with large band gaps, typically > 3 eV, to drive useful photochemical transformations. Because of this limitation, historically, sacrificial reagents have been used that are either easy to oxidize or easy to reduce thereby allowing measurements of the rates of production of, for example, hydrogen and oxygen independently in different experiments. This approach, however, masks the underlying interfacial phenomena that are governing the build-up of photovoltage in the semiconductor particles, making designing improved systems difficult.

In this project we are developing the basic interfacial science of photocatalysis, specifically targeting a fundamental understanding of how semiconductor particle surfaces and interfaces control the rates of (ideally selective) electron and hole transfer to electrocatalytic subunits. The goal of the work is to discover the quantitative design principles needed to create photochemical systems that operate at the same efficiency limits as state-of-the-art photovoltaic systems and generate useful chemical fuel from sunlight.

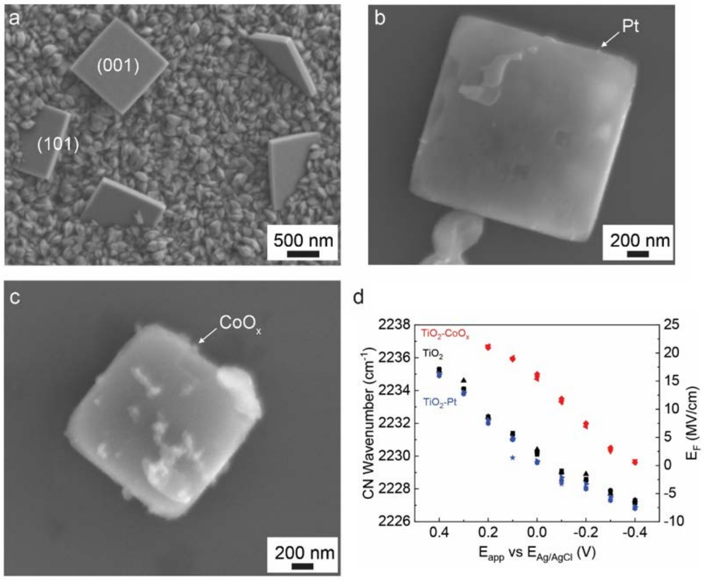

Figure 1. (a)-(c) show microcrystals of TiO_2 grown on conducting glass surfaces that serve as photocatalyst particle model system. Panel (d) shows how Raman spectroscopy of a probe molecule absorbed on the surface allows one to infer changes in the interface band bending, electric field, and hence local charge carrier selectivities.

We have developed *operando* non-contact strategies to monitor charge-transfer processes and reaction intermediates during photocatalytic reactions on semiconductor particles. First, we report a combination of *operando* conductive atomic force microscopy and electrochemical infrared spectroscopy to understand mechanisms of charge transfer at TiO_2 model catalyst surface in photocatalytic overall water splitting. We demonstrated that CoO_x-decorated TiO_2 significantly improves hole extraction compared to bare TiO_2 or Pt-decorated surfaces. We show via Raman spectroscopic probe molecules that this effect is due to larger electric fields at the TiO_2 interface and thus enhanced hole selectivity facilitated by the $CoO_x|TiO_2$ contact. Pt particles on TiO_2, however, do not increase the interface electric field (i.e. degree of band bending) and thus are expected to more-selectively collect photo-excited electrons compared to holes. We also studied reaction intermediates and radical generation, finding that CoO_x nanoparticles not only enhance hole extraction but also modulate the photocatalytic reaction pathway.

Our second model system are $SrTiO_3$ (STO) single crystals. STO has been extensively studied and shown to split water with high quantum yields under UV radiation although with poor solar-to-hydrogen conversion efficiency due to its large bandgap (3.2 eV). Despite enormous efforts transferring this model system to narrower bandgap absorbers, solar to hydrogen conversions efficiencies remain below 3%. We hypothesized this is due to the poor understanding of the mechanisms driving charge separation to carrier selective contacts. Using single-crystal STO, we show that the crystal facet asymmetry plays a much less important role than previously thought and "adaptive electrocatalysts" enable electrocatalyst work-function asymmetry larger than 1.23V, the theoretical minimum required for light to drive overall water splitting (OWS).

Using a dual-working electrode (DWE) device geometry, t*he platinum/STO barrier height was observed to be lowered at electrocatalyst potentials below that of hydrogen underpotential deposition, as it accumulates electrons*. Additionally, the CoO_x/STO barrier is observed to *increase at oxidizing potentials, as it accumulates holes*. While small work function asymmetries which we also observed here between the <100> and <110> crystal facets may initially separate electrons from holes, we show the electrocatalysts cooperatively adapt as they accumulate electrons and holes respectively, increasing their selectivity. These findings demonstrate an underlying mechanism, cooperative adaptive electrocatalysts, likely enabling OWS on photocatalyst particles. This new principle enables better design of OWS systems.

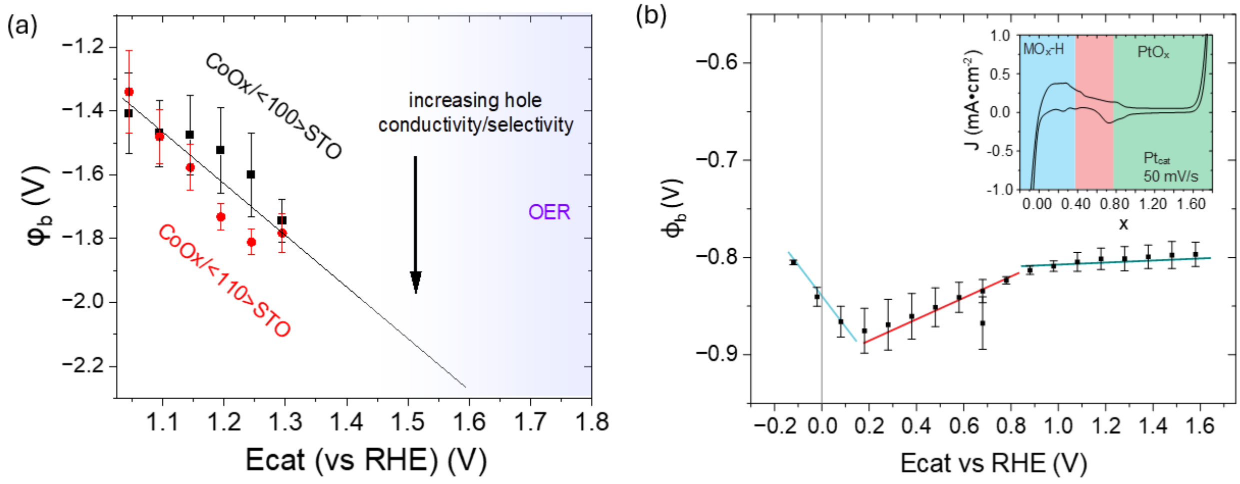

DOE Solar Photochemistry Sponsored Publications 2021-2024

1. Shen, M.; Kaufman, A. J.; Huang, J.; Price, C.; Boettcher, S. W., Nanoscale Measurements of Charge Transfer at Cocatalyst/Semiconductor Interfaces in $BiVO_4$ Particle Photocatalysts. *Nano Lett.* **2022,** *22* (23), 9493-9499.

2. Kaufman, A. J.; Krivina, R. A.; Shen, M.; Boettcher, S. W., Controlling Catalyst–Semiconductor Contacts: Interfacial Charge Separation in p-InP Photocathodes. *ACS Energy Lett.* **2022,** *7* (1), 541-549.

3. Kaufman, A.J., Nielander, A.C., Meyer, G.J., Maldonado, S., Ardo, S. & Boettcher, S.W. Absolute band-edge energies are over-emphasized in the design of photoelectrochemical materials. *Nat. Catal.* Accepted **2024**. DOI: 10.1038/s41929-024-01161-0

Exploring the Connection Between Electronic States and Surface Chemistry Using Photoelectron Spectroscopy

Sylwia Ptasinska
Notre Dame Radiation Laboratory & Department of Physics and Astronomy
University of Notre Dame
Notre Dame, Indiana 46556

Active sites present in materials can facilitate specific chemical reactions that are necessary for their enhanced photocatalytic performance. Among such materials, two dimensional (2D) atomically thin sheets have shown several promising properties, e.g., high electrocatalytic activity for hydrogen evolution reaction on top of the simplicity in their fabrication and low costs. Moreover, to enhamce their catalytic ability, several ways of active site engineering on surfaces of 2D materials have been proposed.

In our recent work, we performed characterization of water interface with two 2D materials, WS_2 and MoS_2, using photoemission techniques, near-ambient XPS and UPS. Any possible humidity efects on 2D materials is especially importnat to understand since water can cause significant issues with their performance due to changes in their electrical resistance or charge carrier concentration. In the first satge of the work, a significan time has been dedicate to find proper protocols to prepare samples for XPS studies. In the case of WS_2, liquid-phase exfoliation has been the best technique for preparing a high yield of mono- and few-layer nanosheets with defects at their edges [1]. While, in the case of MoS_2, we prepared nanosheets using electrophoretic deposition. In addition, to create defects, i.e., S-vacancies which exposed Mo sites, we removed sulfur through Ar^+ ion beam bombardment. Reactivity of the surface-engineered 2D materials exposed to water vapor up to 5 mbar at room temperature were then investigated using both photoemission techniques but also by microscopic techniques.

Our results confirmed that tungsten dangling bonds at WS_2 edges represent active site based on formation of nonstoichiometric oxides in water environment [1]. In contrast, water does not affect the W-S bonds, indicating its physisorption on the surface. Our results for MoS_2 indicated that the created active sites within nanosheets were highly reactive to water. Based on obtained comparisonal spectra of MoS_2 with and without active sites, it is evident that water undergoes a dissociative adsorption with a simultaneous hydroxide formation (Fig. 1)

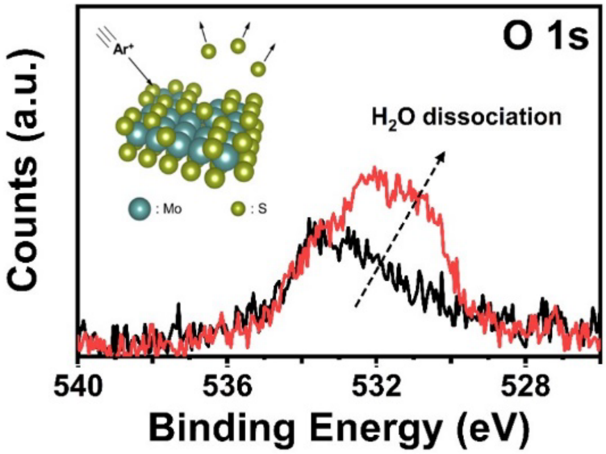

Fig. 1 Comparison of the high-resolution O 1s XPS spectra of the pristine MoS_2 before (black) and after H_2O exposure (red) with a schematic illustration of the sulfide removal from the pristine MoS_2 thin film via Ar^+ ion beam.

In addition, the first-principles calculations based on DFT have been performed to further verify our experimental findings. This type of calculations was utilized also for understanding the energy landscape associated with oxygen molecule adsorption and subsequent dissociation and penetration into the GaP surface [2].

References:
[1] J. Vujin, W. Huang, J. Ciganović, S. Ptasinska, R. Panajotović - *Direct Probing of Water Adsorption on Liquid-Phase Exfoliated WS_2 Films Formed by the Langmuir–Schaefer Technique*. Langmuir 39 (2023) 8055
[2] X. Zhang, B.C. Wood, A.J.E. Rowberg, T.A. Pham, T. Ogitsu, J. Kapaldo, S. Ptasinska, *Kinetically versus thermodynamically controlled factors governing elementary pathways of GaP (111) surface oxidation*. Journal of Power Sources 560 (2023) 232663

DOE Solar Photochemistry Sponsored Publications 2021-2024

1. D. Chakraborty, G. Kharchilava, I. Carmichael, S. Ptasinska - *Dissociative electron attachment studies of gas-phase acetic acid using a velocity map imaging technique.* Journal of Physics B: Atomic, Molecular and Optical Physics 56 (2024) 245202
2. F. Ducrozet, A. Sebastian, C.J. Garcia Villavicencio, S. Ptasinska, C. Sicard-Roselli - *Quantifying Hydroxyl Radicals Generated by a Low-Temperature Plasma using Coumarin: Methodology and Precautions*. Physical Chemistry Chemical Physics 26 (2024_ 8651-8657
3. J. Wang, T. Musall, B.A. Chen, M. Gerges, L. Riney, S. Ptasinska, X. Liu, B.A. Assaf - *Evidence of indium impurity band in superconducting (Sn, In) Te thin films.* Physical Review B 109 (2024) 014513
4. A. Paul, I. Carmichael, D. Nandi, S. Ptasinska, D. Chakraborty - *Structural rearrangements and fragmentation pathways induced by a low-energy electron attachment to ethyl acetate.* arXiv preprint arXiv:2401.02366
5. D. Chakraborty, D.S. Slaughter, S. Ptasinska - *Dynamics of resonant low-energy electron attachment to ethanol-producing hydroxide anions*. Physical Review A, 108 (2023) 052806
6. J. Vujin, W. Huang, J. Ciganović, S. Ptasinska, R. Panajotović - *Direct Probing of Water Adsorption on Liquid-Phase Exfoliated WS_2 Films Formed by the Langmuir–Schaefer Technique*. Langmuir 39 (2023) 8055
7. X. Zhang, B.C. Wood, A.J.E. Rowberg, T.A. Pham, T. Ogitsu, J. Kapaldo, S. Ptasinska, *Kinetically versus thermodynamically controlled factors governing elementary pathways of GaP (111) surface oxidation*. Journal of Power Sources 560 (2023) 232663
8. A. Sebastian, D. Lipa, S. Ptasinska - *DNA Strand Breaks and Denaturation as Probes of Chemical Reactivity versus Thermal Effects of Atmospheric Pressure Plasma Jets.* ACS Omega 8 (2023) 1663–1670
9. S. Ptasinska, M.T.N. Varella, M.A. Khakoo, D.S. Slaughter, S. Denifl - *Electron scattering processes: fundamentals, challenges, advances, and opportunities.* European Physical Journal D 76 (2022) 179

10. A. Sebastian, D. Spulber, A. Lisouskaya, S. Ptasinska - *Revealing low-temperature plasma efficacy through a dose-rate assessment by DNA damage detection combined with machine learning models*. Scientific Reports 12 (2022) 18353
11. E. Alizadeh, D. Chakraborty, S. Ptasińska - *Low-Energy Electron Generation for Biomolecular Damage Inquiry: Instrumentation and Methods.* Biophysica 2 (2022) 475-497
12. D. Danilovic, A. Milosavljevic, P. Sapkota, R. Dojcilovic, D. Tosic, N. Vukmirovic, M. Jocic, V. Djokovic, S. Ptasinska, D. Bozanic, Dusan - Electronic Properties of Silver-Bismuth Iodide Rudorffite Nanoplatelets. Journal of Physical Chemistry C 126 (2022) 13739
13. B.A. Chen, S. Ptasinska, P.V. Kamat - Metal Cocatalyst Dictates Electron Transfer in Ag-Decorated MoS_2 Nanosheets. Journal of Physical Chemistry C 126 (2022) 11907
14. S. Ptasinska - *A Missing Puzzle in Dissociative Electron Attachment to Biomolecules: The Detection of Radicals*. Atoms 9 (2021) 77
15. H.A. Suarez-Moreno, L. Eckermann, F. Zappa, E. Arthur-Baidoo, S. Ptasinska, S. Denifl - *Electron ionization of clusters containing the formamide molecule*. European Physical Journal D 75 (2021) 1-11

Enhancing the Durability and Efficiency of III-V Photoelectrodes and Structured Cu_2O Photocathodes for Solar Fuels Production

Sean T. Byrne, Dominic Covelli, Jake M. Evans, Alexandre Z. Ye, Azhar I. Carim, Nathan S. Lewis
Department of Chemistry and Chemical Engineering
California Institute of Technology
Pasadena, CA 91125

Photoelectrochemical (PEC) water-splitting using inorganic semiconductor photoelectrodes provides for direct generation of hydrogen (H_2) fuel using water and sunlight as the only inputs. We are designing photoelectrodes consisting of 3D, mesostructured semiconductor components decorated heterogeneous catalysts to drive fuel-forming electrochemical reactions at low overpotentials. Maximizing the efficiency of a water splitting cell requires the use of highly acidic or alkaline electrolytes, so photoelectrode materials must be stable in such electrochemical environments under operating conditions. Strategies to impart durability to semiconductor materials as well as the development of stable electrocatalyst materials are thus needed. Additionally, strategies to control semiconductor morphologies at the mesoscale are needed to optimize optical absorption, reactant access and product egress, and control of the bubble transport.

We have demonstrated corrosion resistance can be imparted to photoanode materials by application of thick metal oxide (e.g. TiO_2) film that is optically transparent and allows photogenerated charge carriers to reach the solution. Recent work utilizing a-TiO_2 coated GaAs microislands and planar electrodes indicated that both intrinsic and extrinsic defects limit the durability of these photoelectrodes under operating conditions. Extrinsic defects have been linked to atmospheric particulates that occlude the surface, leading to exposed GaAs. Intrinsic defects represent electrochemically active defect sites in a-TiO_2, with future work on localized electrochemistry of a-TiO_2 coated electrodes aimed at identifying and characterizing these sites.

We have systematically investigated the chemical and physical factors that limit the durability of GaAs, InP, and GaInP photocathodes, with and without decoration with hydrogen-evolution electrocatalyst materials, for solar-driven hydrogen generation in both acidic and alkaline electrolytes. From this analysis, we identified cathodic plating of In^0 and formation of As^0 as the primary chemical failure modes. We are currently working to extend the metal oxide protection layer strategy used in photoanode applications to photocathodes (**Figure 1**). We are examining conduction band alignment between candidate protection layer and semiconductor light absorber materials to identify suitable material pairs. Recent work has indicated that Nb_2O_5 films may enable stable operation of InP photocathodes in acidic electrolytes.

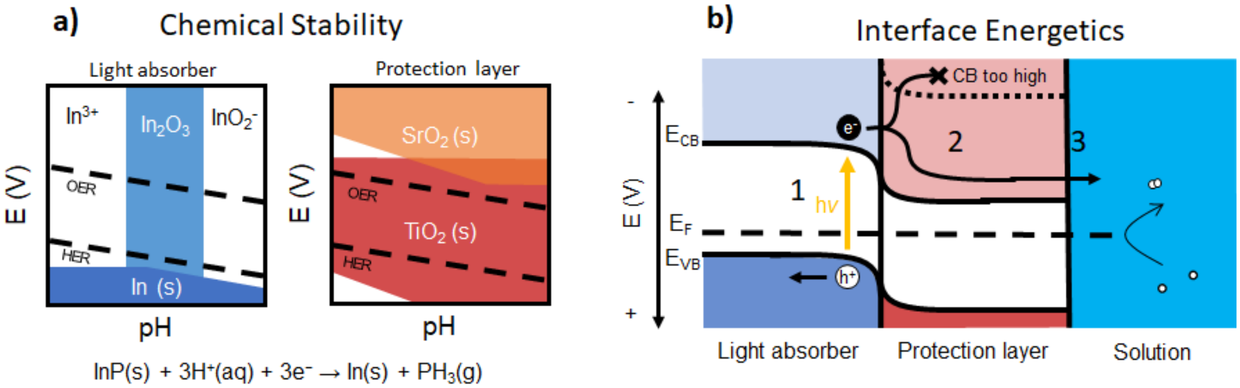

Figure 1. (a) Pourbaix diagrams showing that in acid InP is susceptible to corrosion at the potentials necessary to drive the HER and OER whereas TiO_2 is stable. (b) Simplified energy diagram illustrating the need for proper band alignment to enable facile electron flow from the semiconductor through the protection layer to solution.

We have also developed manganese antimonate electrocatalyst materials that can resist corrosion in acidic electrolytes and drive the OER and thus provide an earth-abundant alternative to Ir-based electrocatalysts. $MnSb_{1-y}O_x$ powders were synthesized by bulk powder mixing followed by annealing and ball milling. Catalyst powders that had been suspended in solutions that were pre-loaded with Ce^{4+} ions spontaneously evolved O_2(g). We also developed a chemical vapor deposition (CVD) synthesis for $MnSb_{1-y}O_x$ films and explored the activity-stability tradeoff over the Mn-Sb composition space.

We additionally have generated highly ordered mesostructures of polycrystalline p-type Cu_2O using inorganic phototropic growth via photoelectrodeposition. Arrays of anisotropic lamellar features with features pitches on the scale of 100 nm were generated using linearly polarized illumination. The feature pitch and size scaled with the illumination wavelength and the direction of the anisotropy followed the illumination polarization. Feature definition has been linked to the concentration of chemical mediators in the deposition solution that selectively passivate certain crystal facets. This approach will allow for control of the mesostructured and porosity to enable supporting catalysts on photoelectrodes to allow for controlled microenvironments that will facilitate catalysis of fuel-producing reactions while allowing for reactant access and product egress as well as controlling optical absorption and reflection of the photoelectrode in a scalable, low-energy process.

DOE Solar Photochemistry Sponsored Publications 2021-2024

1. **Primary Corrosion Processes for Polymer Embedded Free-Standing or Substrate-Supported Silicon Microwire Arrays in Aqueous Alkaline Electrolytes**
K. M. Kennedy, P. A. Kempler, M. Cabán-Acevedo, K. M. Papadantonakis, N. S. Lewis
Nano Letters, **2021**, *21*, 1056-1061.
10.1021/acs.nanolett.0c04298

2. **GaAs Microisland Anodes Protected by Amorphous TiO_2 Films Mitigate Corrosion Spreading During Water Oxidation in Alkaline Electrolytes**
P. Buabthong, J. M. Evans, K. Z. Rinaldi, K. M. Kennedy, H. J. Fu, Z. P. Ifkovits, T.-J. Kuo, B. S. Brunschwig, N. S. Lewis
ACS Energy Letters, **2021**, *6,* 3709-3714.
10.1021/acsenergylett.1c01174

3. **Investigations of the Stability of Etched or Platinized p-InP(100) Photocathodes for Solar-driven Hydrogen Evolution in Acidic or Alkaline Aqueous Electrolytes**
W. Yu, M. H. Richter, P. Buabthong, I. A. Moreno-Hernandez, C. G. Read, E. Simonoff, B. S. Brunschwig, N. S. Lewis
Energy & Environmental Science, **2021**, *14*, 6007-6020.
10.1039/D1EE02809J

4. **Investigations of the Stability of GaAs for Photoelectrochemical H_2 Evolution in Acidic or Alkaline Aqueous Electrolytes**
W. Yu, M. H. Richter, E. D. Simonoff, B. S. Brunschwig, N. S. Lewis
Journal of Materials Chemistry A, **2021**, *9,* 22958-22972.
10.1039/D1TA04145B

5. **Understanding the Stability of Etched of Platinized p-GaInP Photocathodes for Solar-driven H_2 Evolution**
W. Yu, J. L. Young, T. G. Deutsch, N. S. Lewis
ACS Applied Materials & Interfaces, **2021**, *13*, 57350-57361.
10.1021/acsami.1c18243

6. **Catalytic open-circuit passivation by thin metal oxide films of p-Si anodes in aqueous alkaline electrolytes**
H. J. Fu, P. Buabthong, Z. P. Ifkovits, W. Yu, B. S. Brunschwig, N. S. Lewis
Energy & Environmental Science, **2021**, *15*, 334-345.
10.1039/D1EE03040J

7. **Failure Modes of Platinized pn^+-GaInP Photocathodes for Solar-Driven H_2 Evolution**
W. Yu, P. Buabthong, J. L. Young, Z. P. Ifkovits, S. T. Byrne, M. Steiner, T. G. Deutsch, N. S.

Lewis
ACS Applied Materials & Interfaces, **2022**, *14*, 26622-26630.
10.1021/acsami.2c01845

8. **Powdered $Mn_ySb_{1-y}O_x$ Catalysts for Cerium-Mediated Oxygen Evolution in Acidic Environments**
Z. P. Ifkovits, J. M. Evans, P. A. Kempler, M. B. Morla, K. H. Pham, J. A. Dowling, A. I. Carim, N. S. Lewis
ACS Energy Letters, **2022**, *7*, 4258-4264.
10.1021/acsenergylett.2c01754

9. **Spontaneous Mesostructure Formation Produces Optically Transmissive Ni-P Films That are Catalytically Active for the Photoelectrochemical Hydrogen Evolution Reaction**
Z. P. Ifkovits, J. T. Reed, P. A. Kempler, M. C. Meier, S. T. Byrne, S. Lin, A. Z. Ye, A. I. Carim, N. S. Lewis
Sustainable Energy & Fuels, **2023**, *7*, 4401-4406.
10.1039/D3SE00378G

10. **Catalysis of the Oxygen-Evolution Reaction in 1.0 M Sulfuric Acid by Manganese Antimonate Films Synthesized via Chemical Vapor Deposition**
J. A. Dowling, Z. P. Ifkovits, A. I. Carim, J. M. Evans, M. C. Swint, A. Z. Ye, M. H. Richter, A. X. Li, N. S. Lewis
ACS Applied Energy Materials, **2024**, *Article ASAP.*
10.1021/acsaem.4c00135

Probing Mechanisms of Water Oxidation over Atomically Dispersed Catalysts

Tianying Liu, Hongna Zhang, Boqiang Chen, DongYoon Shin, Pengpeng Wang, Damith
Dharmapriya Lekamge, Wei Li, Matthias Waegele, Dunwei Wang
Department of Chemistry
Boston College
Chestnut Hill, MA 02467

The oxidation of water is critically important for solar fuel synthesis as it provides electrons and protons. Presently, this reaction represents a bottleneck in advancing solar fuel research due to the lack of catalysts that meet all needs for cost, efficiency, and durability simultaneously. At the heart of the issue is that the understanding of this essential reaction remains limited despite intense research efforts. The problem is particularly acute for heterogeneous catalysts, which hold great promises for practical applications but are notoriously difficult to study. This is in part due to the lack of details on the structures of the active sites. We recognized this challenge and proposed to advance the knowledge on water oxidation with a unique catalyst system which features structures that are resolved at the molecular level. Our catalyst is Ir-based, and it is derived from an organometallic precursor. Once anchored onto a support, followed by a facile photochemical treatment, this molecular precursor is transformed into atomically dispersed heterogeneous catalysts that are highly stable. We are thus presented with a heterogeneous catalyst which offers definitive information on the structure and loading density. This information serves as an importance basis for us to probe the water oxidation mechanisms of a heterogeneous catalyst as a function of photo charge density and catalyst concentration. This project is further enabled by the employment of time-resolved, surface-enhanced infrared absorption spectroscopy (tr-SEIRAS).

In this poster, we report our latest progress in two fronts. First, we show that high signal-to-noise ratios can be achieved in SEIRAS characterization of water oxidation intermediates using a phase-sensitive detection method. This approach exploits a lock-in amplification strategy that has worked well in other measurements but has not been applied to SEIRAS in the context of catalysis. By stimulating the system with a periodically varying electrode potential, we were able to detect water oxidation intermediates in the cycle of an Ir pyridinyl alkoxide complex, which is a prototypical water oxidation molecular catalyst. We observed the appearance of two distinctly different intermediates as a function of the oxidation driving force. At low driving force, the Ir=O species were prevalent, whereas the dominant species were Ir-OO at high driving force. The data imply that there is a switch of rate determining steps as a function of the driving force. Second, we show that the overall water oxidation efficiency depends on the interplays between the densities of two key factors, namely the concentrations of surface charges and the density of catalytically active sites. When there were low concentrations of surface charges, low catalytic densities appeared to favor more efficient water oxidation; when the surface charges were abundant, the benefits of high catalytic densities became more apparent. The results suggest cooperative behaviors among catalytic sites, where charge redistribution between different sites is of importance. We plan to build upon these exciting results and carry out time-resolved SEIRAS characterizations of heterogeneous catalysts and establish a relationship between surface charge concentrations and the reaction mechanisms.

Modular Nanoscale and Biomimetic Assemblies for Photocatalytic Hydrogen Generation

Kara L. Bren, Todd D. Krauss, Ellen M. Matson
Department of Chemistry
University of Rochester
Rochester, NY and 14627

This project aims to develop and understand photochemical systems for H_2 production incorporating nanocrystalline quantum dots (QDs), bioinspired cocatalysts, and metal oxide cluster charge-transfer agents. Despite the wide employment of QD-based systems for H_2 production, a fundamental understanding of structure-function relationships in these systems is lacking. Highlighted projects focus on the QD-solution interface, with specific interest in how ligand identity and density modify charge transfer and catalysis, and the pairing of new biomolecular and bioinspired catalysts with CdSe QDs for H_2 production.

Ligand Density Influences Charge Transfer from CdSe QDs. It is well established that surface capping ligands have a significant effect on the electronic properties and reactivity of CdE QDs. Comparatively, less is understood about the role that ligand density and identity play in dictating the catalytic activity of CdE QDs. We found that addition of stoichiometric equivalents of Meerwein's salt (trimethyloxonium tetrafluoroborate) to oleic-acid (OA) capped CdSe QDs result in an increase in photoluminescence (PL) quantum yield and increased formation of the anticipated methyl oleate byproduct, suggesting control over density of OA ligands at the surface of the QD. Further investigations of charge transfer with partially stripped QDs through steady-state and time-resolved transient absorption (TA) and PL spectroscopies confirm that the increased surface accessibility for the ligand-stripped QDs allows for faster hole transfer to polyoxovanadate (POV) clusters (e.g. $[V_6O_7(OCH_3)_{12}]^{1-}$).

Ligand Identity Influences H_2 Production with CdSe QDs. Photocatalytic activity was also compared between CdSe QDs synthesized with tetradecylphosphonic acid (TDPA) and OA native capping ligands. Both sets of QDs were made water soluble through exchange of the native ligands for 3-mercaptopropanoic acid. However, surprisingly, the TDPA-CdSe QDs produced 4.6 times more hydrogen compared to OA-CdSe QDs under identical photocatalytic conditions. Ultrafast TA data shows that both sets of QDs have similar excited state dynamics as synthesized, but once exchanged into water, the OA-CdSe QDs have a much faster decay compared to the TDPA-CdSe QDs. The ultrafast data suggests that the relatively poor performance of the OA-CdSe QDs is due to rapid surface trapping of the photogenerated electron.

Pairing Biomolecular and Bioinspired Catalysts with CdSe QDs for H_2 Production. To develop and understand CdSe-cocatalyst systems in water, we have been pairing bioinspired catalysts with CdSe QDs. We see excellent activity for a semisynthetic cobalt porphyrin peptide catalyst CoMP11-Ac paired with mercaptopropionic acid-capped CdSe QDs and ascorbate as an electron donor at pH 4.5, where the system with the cocatalyst yields ~100% higher activity compared to the QDs alone. This enhancement is significantly greater than what is seen for synthetic water-soluble porphyrins lacking a peptide. Future work will employ TA spectroscopy to characterize charge transfer rates in this system. Our latest work probes the H_2 production with thiomolybdate clusters, demonstrating high turnover numbers when the inorganic catalysts are paired with CdSe QDs as photosensitizers (**Fig. 1**). Ongoing studies are aimed at integrating peptide-derived ligands into these compounds, functioning as proton relays.

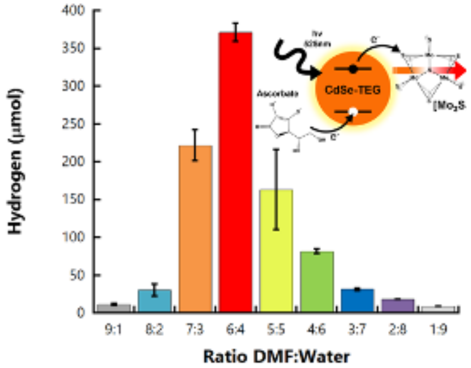

Figure 1. hydrogen evolution (48 hr) with CdSe-TEGPA (1.0 mM), $[Mo_3S_{13}]^{2-}$ (10 mM) and ascorbic acid (200 mM per equivalent of water) in DMF:water. 530 nm LED irradiation, 31 ˚C, 100 rpm.

Protonic charge separation is enhanced in bipolar membranes formed by diffusion doping

Ethan J. Heffernan,[1] Adam C. Sabatose,[2] Margherita Taddei,[2] Leanna Schulte,[2] William White,[2]
and Shane Ardo[1,2,3]
Dept. of [1]Materials Science & Engineering, [2]Chemistry, [3]Chemical & Biomolecular Engineering
University of California Irvine
Irvine, CA 92697-2025

Junctions formed at semiconductor interfaces generate space–charge regions. This can result in diode behavior, a prerequisite for efficient electronic charge separation and photoconversion. Space–charge regions also form at ion-exchange-membrane interfaces, which we are leveraging to demonstrate protonic charge separation from our new light-driven proton-pump platform.

Through a DOE Office of Science Early Career Research Program grant, we discovered that an ion-exchange membrane can be diffusion doped, converting it into a bipolar membrane. We confirmed this modification using our newly developed membrane electric potential sensing procedure. These results are important because diffusion doping is the state-of-the-art means to generate an abrupt buried junction in semiconductors, resulting in high-quality diodes and efficient charge separation. By fabricating our buried-junction bipolar membranes into membrane–electrode assemblies, analogous to fuel cells but instead driving reversible H_2 redox, we were able to measure their electrochemical properties. Results suggest that these junctions are more abrupt than those formed by drop-casting or hot-pressing bipolar membranes. Mott–Schottky analysis of potential-dependent capacitance data provides additional insight into materials properties, including potential of zero net charge, electroactive dopant density, and permittivity (**Fig. 1**).

Moreover, guided by results from our new analytical model, which assumes an abrupt junction, the depletion approximation, and the Poisson equation, we ionically associated excited-state photoacids or photobases into bipolar membranes to serve as shuttles of protonic charge between the space–charge region and the bulk of the bipolar membrane. While our model predicts photoelectrochemical behavior consistent with the superposition principle, we have yet to observe this in practice. Ongoing work aims to continue evaluating these new solar photochemical systems.

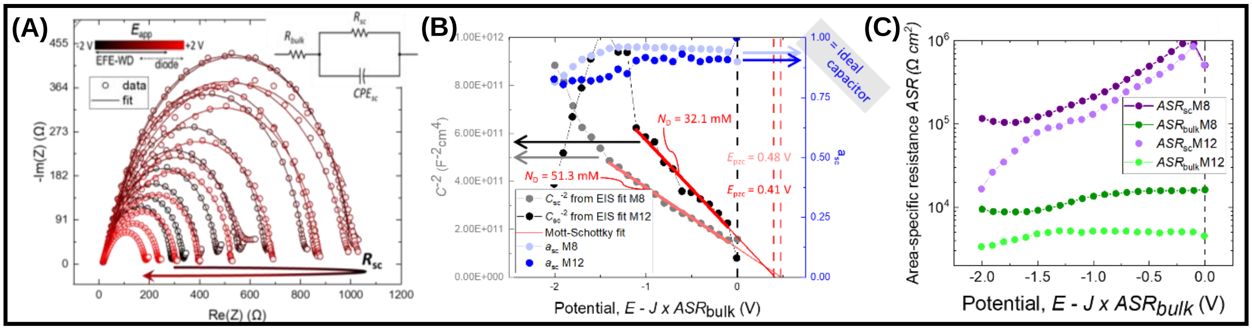

Fig. 1 | Electrochemical impedance spectroscopy data and analyses for two samples (M8 and M12) of diffusion-doped X37 buried-junction bipolar membrane shown as **(A)** a Nyquist plot with associated best fits to the indicated equivalent circuit (inset), **(B)** a Mott–Schottky plot of reverse-bias capacitance (C) as C^{-2} *versus* applied DC potential (*E*), corrected for uncompensated bulk ohmic potential drops, and capacitor ideality factor, a_{sc}, and **(C)** a semilogarithmic plot of reverse bias area-specific resistance (*ASR*) for charge transfer across the space–charge region and in the bulk *versus* *E*. Data under reverse bias suggests that Mott–Schottky analysis is suitable – because calculated dopant densities, N_D, are reasonable based on prior measurements of ion-exchange capacity and extrapolated potentials of zero net charge, E_{pzc}, are only slightly smaller than expected for polymers highly doped with fixed charges – and *ASR* values are consistent with undesired and reversible electric-field-enhanced water dissociation, as generation and recombination of mobile protonic charge carriers.

Long-lived radical ion-pairs for solar energy conversion

Matthew J. Bird, Qin Wu and John R. Miller
Chemistry Division
Brookhaven National Laboratory
Upton, NY 11973

Efficient solar energy conversion in molecular systems often comes down to preventing back electron transfer between photo-generated non-equilibrium species. There are many principles of electron transfer that could be exploited to slow down this energy loss pathway such as the inverted region, spin, electronic coupling, reorganization energy and charge delocalization.[1-3]

An obstacle to fully exploiting these principles are local triplet excited states, T_1, typically 0.5 – 1.0 V below the optically-accessible singlet excited state, S_1. These provide an additional energy loss pathway, often referred to as the "triplet drain." A recent data-driven machine learning study of 350 non-fullerene acceptor (NFA) organic solar cells showed that the parameter with the strongest (negative) correlation to overall power conversion efficiency was the S_1-T_1 energy gap.[4]

Strategies are emerging to design molecules where the lowest excited state is the one strongly optically-coupled to the ground state (e.g. TADF, open-shell molecules). To understand how to exploit these materials, we have investigated the lifetimes of coulombically-bound radical ion pairs (CBIPs) with energies lower than T_1. Historically referred to as triplet exciplexes as they can be generated by electron transfer from local triplet excited states, these pairs have lifetimes ranging from sub-nanosecond to, in some cases, microseconds.

Pulse radiolysis offers a unique opportunity to generate these CBIPs from rapid charge recombination in their mutual coulombic field. We have studied CBIPs from over 30 combinations of molecules. In this poster we discuss the formation, spectra, lifetime, energy, and deactivation pathways.

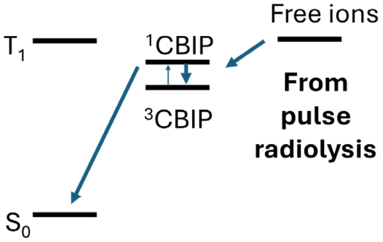

Some key findings include the lack of a clear dependence of the CBIP lifetime with either the CBIP singlet-triplet energy splitting or the CBIP energy itself and a remarkable preference for triplet ion pair formation during the recombination of separated ions.

With the support of quantum chemical calculations using constrained density functional theory-based configuration interaction we begin to explain these unexpected results with the goal of developing design rules for long-lived CBIPs to be exploited for future molecular solar energy conversion applications.

References

1. M. Myong, M. J. Bird, J. R. Miller *J. Phys. Chem. B* **2023**, 127, 13, 2881–2886
2. N Takeda, J. R. Miller *J. Am. Chem. Soc.* **2020**, 142, 42, 17997–18004
3. J. R. Miller, A. R. Cook, L. Šimková, L. Pospíšil, J. Ludvík, and J. Michl *J. Phys. Chem. B* **2019**, 123, 45, 9668–9676
4. G. Han, Y. Yi, *Angew. Chem. Int. Ed.* **2022**, *61*, e202213953; *Angew. Chem.* **2022**, *134*, e202213953.

Energy level alignment at 2D semiconductor/redox electrolyte interfaces

Rafael Almaraz, Rachelle Austin, Justin Toole, Thomas Sayer, Austin Tews, Amber Krummel,
Andrés Montoya Castillo, Justin B. Sambur*
*Department of Chemistry, Colorado State University, Fort Collins, CO, 80525

Hot carrier extraction occurs in 2D semiconductor photoelectrochemical cells.[1] Boosting the energy efficiency of hot carrier-based photoelectrochemical cells requires maximizing the hot carrier extraction rate relative to the cooling rate. One could expect to tune the hot carrier extraction rate constant (k_{ET}) via a Marcus–Gerischer relationship $\left(k_{ET} \propto \exp\frac{(-\Delta G^{0\prime}+\lambda)^2}{kT}\right)$, where λ is the reorganization energy, k is the Boltzmann constant, and T is temperature. k_{ET} depends exponentially on $\Delta G^{0\prime}$ (the standard driving force for interfacial electron transfer). $\Delta G^{0\prime}$ is defined as the energy level difference between a semiconductor's conduction/valence band (CB/VB) minima/maxima and the redox potential of reactant molecules in solution. The question is "*how does charge equilibration occur and how do the energy levels of 2D semiconductor photoelectrodes change as a function of redox species in solution* (Figure 1A)*?* In 2023, we showed that *in the absence of redox species in the electrolyte*, band edge movement in monolayer (ML)-MoS_2 is significant (0.2–0.5 eV) over a narrow range of applied potentials (0.2–0.3 V).[2] Such large band edge shifts could change k_{ET} by a factor of 10–100, which has important consequences for practical solar energy conversion applications. In the past year, we conducted in situ spectroscopy measurements on a ML-MoS_2 electrode in solutions containing redox couples whose formal potentials ($E^{0\prime}$) span 800 mV. We observed that immersing the 2D semiconductor in the redox electrolyte causes the electronic bandgap (E_g) of ML-MoS_2 to change by nearly 400 mV (Figure 1B). This phenomenon occurs due to changes in the carrier concentration of the 2D semiconductor upon Fermi level alignment with the solution phase. Our poster discusses the experimental setup, spectroscopic data and theoretical interpretation using many body theory, and discusses new directions for understanding the unique electrochemical properties of ultrathin 2D semiconductors.

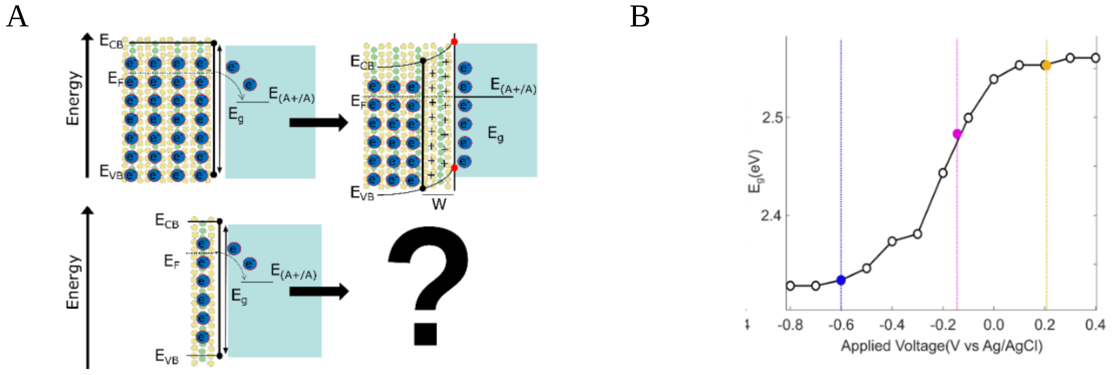

Figure 1. (A) Cartoon illustration of energy level alignment at bulk semiconductor/electrolyte interfaces and the unknown situation for 2D semiconductor/electrolyte interfaces. (B) Electronic bandgap (E_g) of ML-MoS_2 as a function of applied potential in the absence of redox species (black circles) and at open circuit but in the presence of three different redox couples with different $E^{0\prime}$ values (colored circles).

References: **(1)** Austin, R.; Farah, Y. R.; Sayer, T.; Luther, B. M.; Montoya-Castillo, A.; Krummel, A. T.; Sambur, J. B. *PNAS* **2023**, *120* (15), e2220333120. **(2)** Almaraz, R.; Sayer, T.; Toole, J.; Austin, R.; Farah, Y.; Trainor, N.; Redwing, J. M.; Krummel, A.; Montoya-Castillo, A.; Sambur, J. *Energy Environ. Sci.* **2023**, *16* (10), 4522–4529.

C-H Bond Formation with CO_2: Toward Carbon Neutral Fuel Production

Jong-Hwa Shon, Kirti Singh, Kevin Y. C. Lee, Dmitry Polyansky, David C. Grills, Yiming Liu,
Natalia D. Loewen, and Louise A. Berben*
Department of Chemistry
The University of California
Davis, CA 95616

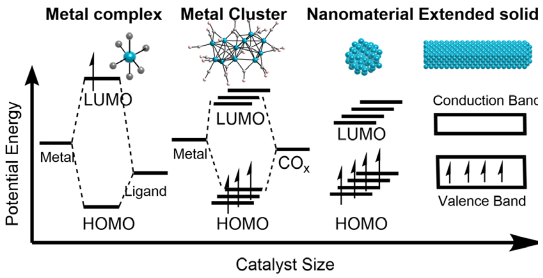

This project uses nanoscale metal clusters which have delocalized bonding, to model nanoparticle and heterogeneous (electro/photo)catalysis. The project is structured around two Specific Objectives. ***Objective 1:*** To study the structure-function relationships for CO_2 reduction by modifying the microenvironment structure. ***Objective 2:*** To study multi-electron and multi-proton chemistry on the surface of nanoscale metal clusters which are atomically defined. Initial work demonstrated a pre-equilibrium mechanism to enhance hydride transfer rates by five orders of magnitude without sacrificing product selectivity.

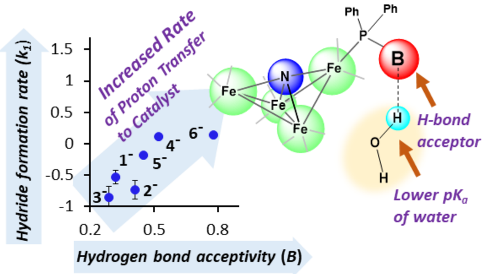

Objective 1: H-Bond Acceptors. We studied the role of hydrogen bond (H-bond) accepting functional groups in a catalyst microenvironment. This approach provided quantitative information on the rate of electrochemically driven catalyst-hydride formation from protons. Ligand substitution of Na(diglyme)$_2$[$Fe_4N(CO)_{12}$] was used to access a series of six clusters with various H-bond accepting secondary coordination sphere (SCS) functional groups that were chosen to span a wide range of H-bond acceptor strength (B). We demonstrated that the rate of formation of $[H\text{-}Fe_4N(CO)_{12}]^-$ increases linearly with B, because the H-bond acceptor modulates the pK_a of water that serves as proton source for formation of $[H\text{-}Fe_4N(CO)_{12}]^-$. Specifically, the substrate water protons have lower pK_a when the SCS functional groups are stronger H-bond acceptors. The rate of $[H\text{-}Fe_4N(CO)_{12}]^-$ formation is not correlated with pK_a of the SCS H-bond acceptor ability.

Objective 1: Protonation Modifies Rate Determining Step. We studied the effect of a proton (a cation) on the mechanism of electrochemically driven hydride transfer (HT) catalysis. Protonated, air-stable $H[Fe_4N(PEt_3)_4(CO)_8]$ (H**4**) was synthesized and its reduction potential is −1.70 V vs SCE which is 350 mV anodic of the reduction potential for **4**$^-$. Reactivity studies are consistent with HT to CO_2 or to H^+ (carbonic acid), as the chemical event following ET, when the electrocatalysis is performed under 1 atm of CO_2 or N_2, respectively. Taken together, the chemical and electrochemical studies of mechanism suggest an ECEC mechanism for the reduction of CO_2 to formate or H^+ to H_2, promoted by H**4**, which is different from the ECCE mechanism that is promoted by the less electron rich catalyst $[Fe_4N(CO)_{12}]^-$. This study included information on cluster redox potentials, obtained using Pulse Radiolysis at Brookhaven National Laboratory.

Linker Regulated Charge Transfer Pathway in COFs for Photocatalytic CO_2 Reduction with H_2O as Electron Donor

Liangji Chen, Jier Huang*
Department of Chemistry and Schiller Institute for Integrated Science and Society
Boston College
Chestnut Hill, MA 02467, United States

Charge transfer process is one of the key factors that determine the efficiency of solar-driven CO_2 reduction into renewable fuels and valuable chemicals. Most photocatalytic CO_2 reduction systems reported require the use of sacrificial electron donor to participate in the catalytic process due to undesirable charge transfer pathways and low charge separation efficiency. Working towards economical CO_2 photoreduction necessitates replacement of sacrificial donors with ones that are abundant and easily accessible like water (H_2O). To address these issues, we have been developing chemical approaches to control charge transfer pathways in covalent organic frameworks (COFs), where the wide availability of diverse functional building blocks allows the precise tuning of its structure and functional components. We hope to use this strategy as a crucial tool to make H_2O a potentially suitable electron donor which could eventually make solar-driven CO_2 photoreduction economically feasible.

Inspired by our prior findings, where reversal imine linker in Re-COF leads to different charge transfer mechanisms and photocatalytic activity due to the polarized nature of imine bond, we become interested in controlling linker chemistry for directional electron transfer process. In this presentation, I will share some of our latest efforts in linker design that can direct one-way (Figure 1a and 1b) or two-way (Figure 1c) charge transfer or short-range charge transfer (Figure 1d) in COFs and the incorporation of CO_2 reduction and/or water oxidation catalysts to COFs. We hope that this strategy will not only improve charge separation efficiency but also simultaneously achieve water oxidation and CO_2 reduction without the use of sacrificial donors.

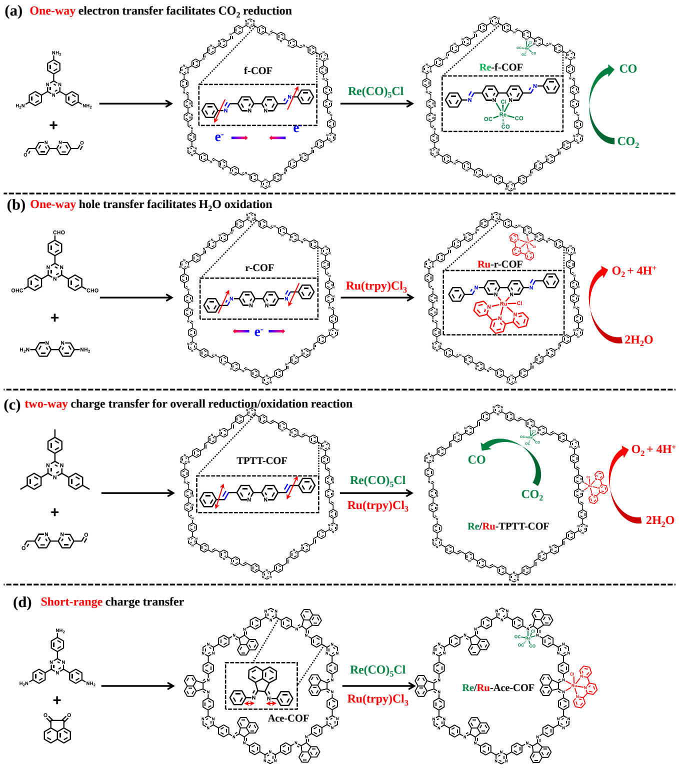

Figure 1 Illustration of synthetic scheme of COFs with different charge transfer pathways. (a) f-COF and Re-f-COF for CO_2 reduction; (b) r-COF and Ru-r-COF for water oxidation; (c) TPTT-COF for overall CO_2 reduction and water oxidation; (d) Ace-COF with short-range electron transport pathways for overall CO_2 reduction and water oxidation

Molecular regulation of charge transfer at organic semiconductor electrodes

Zhiting Chen, Spencer Yeager, Erin L. Ratcliff
Department of Chemical and Environmental Engineering
University of Arizona
Tucson, AZ 85721

The goal of this work is to seek fundamental new understanding of the mechanisms governing charge transfer and charge transport at organic semiconductor/electrolyte interfaces that underpin the development of new molecular catalysts and generation of fuels from sunlight. This poster will showcase multiple spectroscopic approaches to monitor fundamental electrochemical processes of charge transfer in the presence of significant capacitive background currents. Additional highlights will include the use of scanning electrochemical cell microscopy to evaluate spatial and temporal differences in local rate coefficients of charge transfer to outer sphere redox probes as a model system.

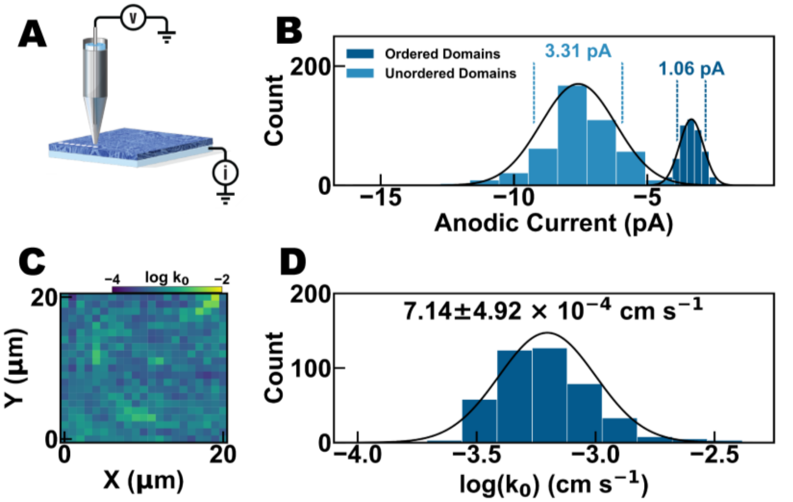

Figure. (A) Schematic of the SECCM tip at a polymer surface; (B) Current distributions for crystalline (ordered) and amorphous (unordered) domains to define spatial heterogeneity across the surface in the rrP3HT film; (C) Spatial distribution of rate coefficients (k_0) for ferrocene oxidation starting from a Butler-Volmer approximation across a 20 μm x 20 μm area on a rrP3HT film; (D) Distribution of rate coefficients from (C).

This effort focuses exclusively on the investigations of prototypical conducting polymer electrodes comprised of poly(3-alklythiophenes), which includes the highly characterized homopolymer poly(3-hexylthiophene) (P3HT). Polaron and bipolaron signals exist in the visible to near-IR region of the electromagnetic spectrum due to structural rearrangement of bonds to compensate for the presence of charges and are highly sensitive to nanometer-length scale interactions. Spectroelectrochemical methods allows one to resolve carrier motion as a function of potential, carrier density, and time to better understand underlying mechanism of charge transfer. Ongoing efforts are using electroabsorption quantifications to better understand how many charges participate in the reaction in the time/frequency domain through color impedance for a given doping density (i.e., background carrier density). Nanoscale electrochemical investigations using scanning electrochemical cell microscopy (SECCM) allow for spatial mapping of functionality (Figure A). Ongoing work considers the role of local heterogeneity on the effective rate coefficient of charge transfer (Figure C) spatially, as well as the role of the effective distribution of sites participating in the reaction on the macroscale electrode performance (Figure D).

This work was supported by the U.S. Department of Energy (DOE), Office of Science, Basic Energy Sciences (BES), under Award # DE-SC0020208.

Coupled transport-transformation phenomena in solar photoconversion systems

Frances A. Houle,[a,b] Pan Wang,[a] Thomas Cheshire,[a] Gabriel Benitez,[a] Ramzi Massad,[a,b] and Chenqi Fan[a]
[a]Chemical Sciences Division and [b]Molecular Biophysics and Integrated Bioimaging Division
Lawrence Berkeley National Laboratory
Berkeley, CA 94720

In this program, multiscale calculations that connect the molecular level events to macroscopic observables have led to new insights to the complex fundamental physical and chemical phenomena that control solar photochemical systems, with a particular focus on identifying factors that enable high-performing multicomponent systems. There are many detailed studies of important individual processes, but much less is known about how these processes influence each other when they occur in a full system. In this program, we have constructed and studied predictive reaction-transport models for photoanodes using using validated theoretical and experimental data. Starting with dye-sensitized nanoporous electrodes, we examined the role of diffusion within pores and discovered the importance of electron cycling within the electrolyte in controlling conversion efficiency.[1,2] By establishing quantitative dye photophysical kinetics, the efficiency of natural sunlight in driving excitations in these dye-sensitized systems has been examined.[3-5] The importance of the chemical state of the porous photoanode and its optical properties have been identified, revealing the influence of light scattering on photoanode efficiency. The dye-in-sunlight model has been combined with the known kinetics of water oxidation using dye-catalyst diads adsorbed on TiO_2.[6] The low efficiency of these systems had been attributed to competition by back-electron transfer, and the low density of solar photons. In fact, the simulations showed that low efficiency is attributable to the buildup of non-photochemically active intermediates that react only slowly at ambient temperature. Water oxidation by the diad system has been compared to water oxidation directly on TiO_2 to understand the complex hole concentration dependence that has been observed experimentally.[7] The simulation results show that non-photochemically active intermediates also control the kinetics, and that there is a complex interplay between hole trapping and surface reactivity that had not been previously recognized. Taken together, the results of these studies reveal a number of emergent interactions that control the chemistry in solar energy conversion systems, and provide new insights to key phenomena in integrated systems.

1. Reaction-Transport Coupling in a Nanostructured Porous Electrode, F. A. Houle Journal of Physical Chemistry C **123,** 14459-14467 (2019).
2. Adaptive Response by an Electrolyte: Resilience to Electron Losses in a Dye-Sensitized Porous Photoanode, F. A. Houle Chemical Science, 12, 6117 – 6128 (2021)
3. Ultrafast Relaxations in Ruthenium Polypyridyl Chromophores Determined by Stochastic Kinetics Simulations, T. P. Cheshire et al, Journal of Physical Chemistry B, 124, 5971-5985 (2020)
4. Ruthenium Dye Excitations and Relaxations in Natural Sunlight, T.P. Cheshire and F. A. Houle, Journal of Physical Chemistry A, 125, 4365-4372 (2021).
5. A Quantitative Model of Charge Injection by Ruthenium Chromophores Connecting Femtosecond to Continuous Irradiance Conditions. T. P. Cheshire et al. J Chemical Physics 157, 244703 (2022).
6. Water oxidation by a Dye-Catalyst Diad in Natural Sunlight: Timing and Coordination of Excitations and Reactions across Timescales of Picoseconds to Hours. R. N. Massad, T. P. Cheshire, C. Fan, and F. A. Houle, Chemical Science *14*, 1997-2008 (2023).
7. P. Wang, G. Benitez and F. Houle, manuscript in preparation (2024).

Excited-State Dynamics in Hybrid Systems with Strong Interfacial Coupling

Nick Pompetti, Ben Feingold, Melissa Gish, Marissa Martinez, Matt Beard, Justin C. Johnson
Chemistry and Nanoscience Center
National Renewable Energy Laboratory
Golden, CO 80401

Combining molecular chromophores with nanoscale semiconductors can leverage the beneficial properties of both toward unique photophysics and photochemistry. Three categories of surfaces functionalized with photoactive molecules are investigated: quantum dots (QDs), transition metal dichalcogenides (TMDCs), and mesoporous oxides (i.e., TiO_2),

PbS QDs have tunable band gaps and surface faceting, which leads to richness in their electronic behavior. We are particularly interested in tuning triplet energy transfer by creating resonance between the QD exciton and the ligand triplet, and also through changing the strength of electronic coupling through controlling ligand-surface juxtapositions. Building on our past work, we have tuned the triplet energy transfer from around 100 ns to less than 1 ns. The dramatic increase in rate seems primarily driven by flat-lying geometries where the π orbitals interact strongly with the surface Pb atoms. Steady-state spectroscopy provides hints of these interactions, while transient spectroscopy reveals strongly perturbed triplet spectra and the hastening of population flow.

TMDCs have unique spin-valley properties that lead to valley-polarized excitons in response to circularly polarized light. We have used this response to better understand charge transfer between WSe_2 and phthalocyanines, which can adopt different configurations on the surface. In much the same way as with QDs, we find that coercing the molecules to lie approximately flat on the surfaces yields a hybrid electronic state, in this case quickly destroying the spin-valley polarization. Upright orientations shuttle charges away from the surface, preserving the spin-valley polarization of the remaining hole in WSe_2, Fig 1A.

Utilizing singlet fission (SF) with dye-sensitized photoelectrochemical cells can be advantageous in photochemical transformations by providing multiple excitons simultaneously, in some cases with well-defined spin orientations of the composite charge carriers. We have monitored triplet formation in anthradithiophene (ADT) dyes on TiO_2 to determine how surface coverage influences the triplet yield for derivatives with differing intermolecular interactions. We find that tethering of molecules to the surface changes the SF behavior, resulting in a high yield of triplets in a monoacid derivative compared with the ADT diacid – opposite to what occurred in neat films. Constraining diacid geometries alters the role that hydrogen bonding plays in defining the geometries, opening an excimer pathway that competes with SF (Fig 1B).

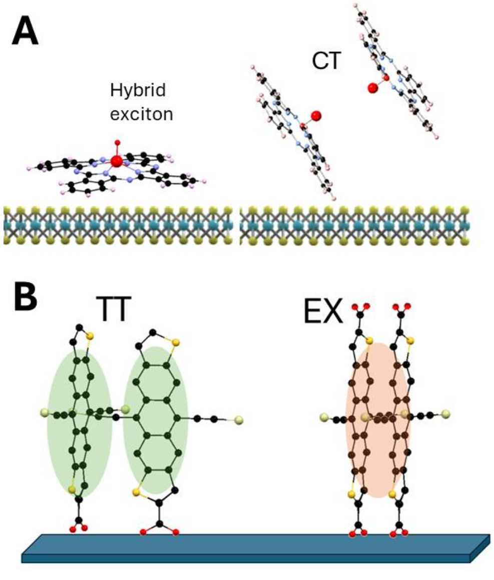

Figure 1. A, geometries and resulting states in WSe_2/VOPc bilayers. **B**, geometries and states in ADT/TiO_2 samples.

Strategies for Water Oxidation with Abundant Metals: Catalyst Design, Immobilization on Conducting Substrates, and Sensitizer Integration

Carlos Lucecki, Emerson Perry, Gibson Kirui, Neha Rani, and Cláudio Verani
Department of Chemistry
Wayne State University
Detroit, MI, 48202

In this poster, PI Verani will present current progress on the understanding of molecular catalysts containing earth-abundant 3d-metal ions for water oxidation, covering the three proposed objectives of grant DE-SC0022114, namely, (i) catalyst design and mechanisms, (ii) immobilization of catalysts on conducting substrates, and (iii) integration of catalyst/sensitizer systems. Beyond their abundance, interest in the incorporation of 3d-metal ions into catalysts for water splitting is driven by affordable free energies of activation (ΔG*) associated to smaller molecular orbitals and ligand fields than those found in 4d- and 5d-catalysts. On the other hand, these metals foster weaker M-L bonds, yielding significant challenges that remain unsolved.

We have finished a study involving the new water-soluble cobalt(II) complex **$[\mathrm{Co^{II}(QPy2)H_2O}]^{+}$** (**Figure 1a**) capable of water splitting promiscuity. The molecular and electronic structures of **$[\mathrm{Co^{II}(QPy2)H_2O}]^{+}$** were evaluated by multiple spectroscopic, spectrometric, and electrochemical methods in pre- and post-catalytic studies, and provided evidence for both $\mathrm{Co^{I}}$ and $\mathrm{Co^{IV}}$ states, respectively relevant for water reduction and water oxidation. This design is related to our 2016 catalyst **$[\mathrm{Co^{II}(Py3)H_2O}]^{+}$** (**Figure 1b**) which displayed TONs above 7000, but was prone to methylene oxidation at the singly substituted Ph-NH-MePy arm, leading to eventual demetallation. Because we noticed that the doubly substituted Ph-NH(-MePy)2 moiety was more resilient to oxidation, we added a methyl protecting group to the singly substituted amine leading to good results for water reduction (**Figure 1c**). We hypothesized that for **$[\mathrm{Co^{II}(QPy2)H_2O}]^{+}$** the incorporation of a more robust singly substituted, aromatic framework, such as a quinoline, would prevent oxygen insertion while enhancing catalytic activity by enabling electron shuffling within the framework, enabling water oxidation. Indeed, it performs both water reduction at a low onset overpotential (η) of 0.65 $\mathrm{V_{Ag/AgCl}}$, pH 7, reaching TOF = 970 $\mathrm{h^{-1}}$ at 98% Faradaic efficiency (FE), and promotes water oxidation at η = 0.34 V under pH 8, achieving TOF = 64 $\mathrm{h^{-1}}$ at 84% FE. Experimental and DFT enabled us to propose reaction intermediates and mechanisms, **Figure 1d**.

We have also finished a structural study on modular and hierarchical Ru-Co structures deposited on ITO surfaces to enhance the stability of catalysts by immobilization. We have designed new catalysts **$[\mathrm{Co^{III}L^{1}(pyrr)_2}]^{+}$** and **$[\mathrm{Co^{III}L^{2}(pyrr)_2}]^{+}$**. Monolayers of **$[\mathrm{Co^{III}L^{1}(pyrr)_2}]^{+}$** allowed us to probe the feasibility of electron transport on fabricated Au|catalyst|Au junctions. Both species were self-assembled by bilayer anchoring onto FTO decorated with J. Concepcion's chromophoric anchor **$[\mathrm{Ru^{II}(bpy^{PO3H})_2\,(bpy^{C7})}]^{2+}$** (**Figure 1e**).

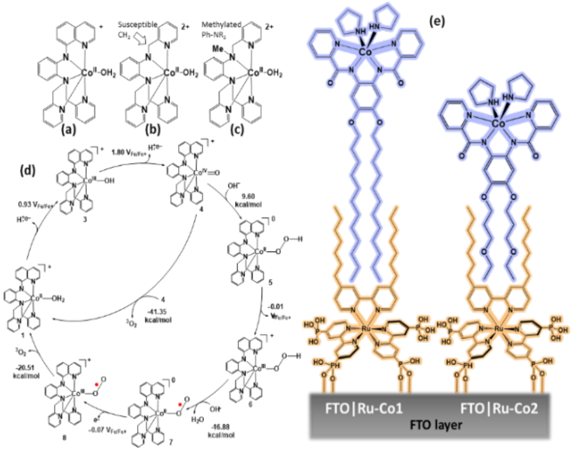

Figure 1. Systems discussed.

Excitation Dynamics in the Photosystem II Supercomplex

Shiun-Jr Yang, Cristina Leonardo, Masa Iwai, Tsung-Yen Lee, Johanna Hall, Kunyan Zhang,
Trisha Bhagde, David Wales, Esmae Woods and Graham R. Fleming

Molecular Biophysics and Integrated Bioimaging Division
Lawrence Berkeley National Laboratory
and
Department of Chemistry, University of California Berkeley
Berkeley CA 94720

The Photosystem II Supercomplexes with composition C_2S_2 and $C_2S_2M_2$ are common forms of PSII at high light and low light, respectively. Contrary to other antenna/reaction center systems and intuitive pictures of “funnel” landscapes, the PSII-SC landscape is rather flat. This is a result of the need to balance efficient charge separation at the RC with effective photoprotection against excess light to minimize formation of destructive reactive oxygen species. We use a combined 2DEV spectroscopy and modeling approach to show energy initially flows from the core antenna towards the peripheral antenna (where we assume detectable quenching sites are created). We also used the kinetic Monte Carlo method to study trajectories in the $C_2S_2M_2$-SC. By “knocking out” individual subunits in the kinetic model we were able to address the functions of the individual subunits. Next, we used 5th order nonlinear pump-probe spectra to explore the excitation motion by excitation-excitation annihilation. We are also able to calculate the 5th order signal form the C_2S_2 rate matrix and analyze it in terms of dimensionality of the motion and probability of annihilation on encounter.

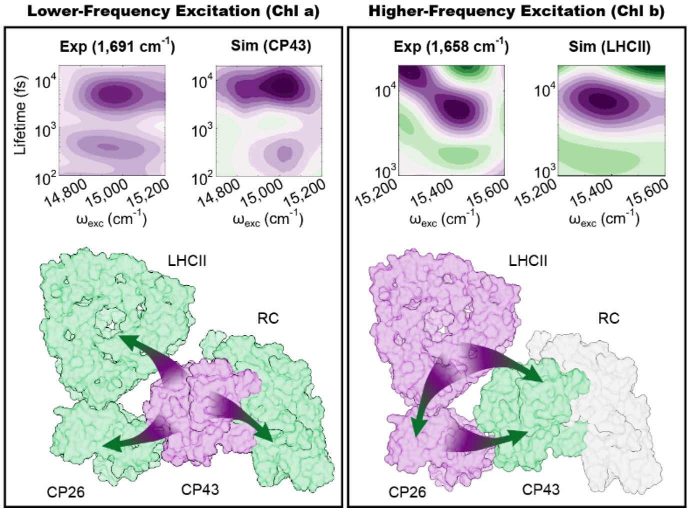

Figure 1. Left: Lower excitation frequencies lead to energy leaving the PSII core as the initial step, whereas higher excitation frequencies lead to energy

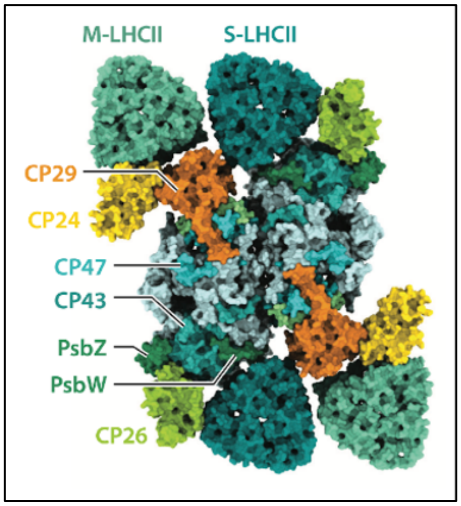

Right: $C_2S_2M_2$ Supercomplex of PSII

Tuning Energy Transfer Pathways in Halide Perovskite QD-Dye Hybrids

Akshaya Chemmangat, Jishnudas Chakkamalayath, Jeffrey T. DuBose and
Prashant V. Kamat
Radiation Laboratory, Department of Chemistry and Biochemistry
University of Notre Dame, Notre Dame, Indiana 46556, United States

The rich photochemistry of semiconductor nanocrystals has enabled their use in light harvesting and light emitting devices. Semiconductor nanocrystals, which absorb photons in the visible and infrared region, are capable of transferring singlet or triplet energy transfer to surface bound molecular dyes, which can increase excited-state lifetimes and allow for more complex excited-state interactions. We have now successfully established the key factors that dictate singlet and triplet energy transfer between excited $CsPbI_3$ and surface bound rhodamine dyes using absorption and emission spectroscopies. The pendant groups on the acceptor dyes influence surface binding to the nanocrystals, which in turn dictates the energy transfer kinetics as well as the efficiency of energy transfer.

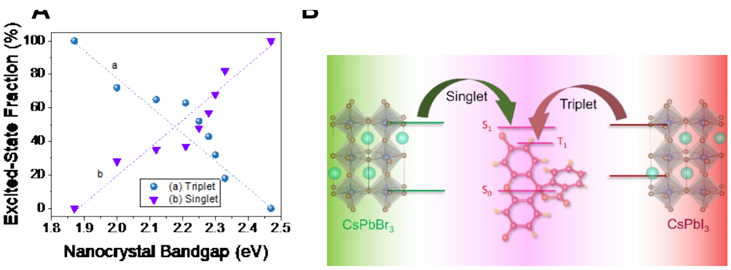

Figure 6. (A) Percentage of (a) triplet and (b) singlet excited states formed in acceptor RoseB via energy transfer as a function of donor $CsPb(Br_{1-x}I_x)_3$ bandgap. (B) Scheme illustrating the energetics of the perovskite nanocrystal–RoseB system. As donor nanocrystal bandgap is increased from that of $CsPbI_3$ to $CsPbBr_3$ composition, a progressive tunning from triplet energy transfer to mixed singlet energy transfer is achieved.

Of the three rhodamine dyes investigated (rhodamine B, rhodamine B isothiocyanate, and rose Bengal), the $CsPbI_3$ -rose Bengal hybrid with the strongest binding showed the highest triplet energy transfer efficiency (96%) with a rate constant of 1×10^9 s^{-1}. This triplet energy transfer rate constant is nearly two orders of magnitude slower than the singlet energy transfer observed for the pure-bromide $CsPbBr_3$-rose Bengal hybrid (1.1×10^{11} s^{-1}).[1] Whereas the single-halide $CsPbBr_3$ and $CsPbI_3$ nanocrystals selectively populate singlet and triplet excited states of rose Bengal, respectively, the mixed halide perovskites were able to generate a mixture of both singlet and triplet excited states. By tuning the bromide/iodide ratio and thus bandgap energy in $CsPb(Br_{1-x}I_x)_3$ compositions, the percentage of singlets vs. triplets delivered to the acceptor dye was systematically tuned from 0 to 100%. The excited state properties of halide perovskite-molecular hybrids discussed here provide new ways to modulate singlet and triplet energy transfer in semiconductor-molecular dye hybrids through acceptor functionalization and donor bandgap engineering.

References.

1. Chemmangat, A., Chakkamalayath, J., DuBose, J.T., Kamat P. V., Tuning Energy Transfer Pathways in Halide Perovskite–Dye Hybrids through Bandgap Engineering, J. Am. Chem. Soc. 2024 146, 3352-3362

Optical Gating of Spin Quantum States for Quantum Information Science

Subrata Ghosh[1], Harini Wimalasekera[1], Zachary Kehoe[1], Majid Hassan[1], Mitra Rooien[1],
Benjamin King[1], Matthew Tucker[1], Sergey Varganov[1], Joonhee Lee[2] and Natia L. Frank[1]*
Department of Chemistry[1] and Physics[2]
University of Nevada
Reno, NV 89557

The goal of our collaborative project is to understand the fundamental electronic and structural parameters that govern quantum sensing with high spatial and temporal resolution at the molecular level. Quantum sensing utilizes the exquisite sensitivity of quantum states to external field (magnetic, electric, thermal, and electromagnetic) to detect and measure physical quantities of interest with unprecedented sensitivity and accuracy. The "intrinsic" sensitivity of a quantum sensor is proportional to $1/\gamma\sqrt{Tx},$ where γ is the transduction (coupling) parameter of quantum sensor to external physical quantity, and T_x is the coherence or relaxation time. An increase in sensitivity requires strong coupling to the environment, while strong coupling to the bath (external nuclear and electronic spins, phonons) leads to rapid decoherence, presenting significant challenges in design and measurement. Understanding the interplay between spin-orbit coupling, spin-vibrational coupling, Orbach, Raman, direct processes and coupling to the bath (vibrational or spin-bath) is critical to controlling spin dynamics in molecular systems. The role of spin-orbit (SO) coupling is a major contributor to spin relaxation; the stronger the SO coupling, the faster the relaxation. Existing studies examine molecular systems with simultaneous changes in oxidation state, ligand field, and geometry. The spin dynamics in metal complexes with large changes in spin-orbit coupling and oxidation state, ligand field, and geometry held constant (*ls*-Co(II) (S = 1/2) and Cu(II)N_4Phen) reveal that spin-lattice relaxation (T_1) and decoherence times (T_m) are long (μs) and faster for Co vs Cu, despite larger single-ion SO coupling in Cu. Computational modelling by CASSCF supports the importance of the orbital reduction parameter via metal-ligand covalency as a dominant contribution to spin dynamics in molecular spin qubits.

The modulation of metal-ligand covalency is harnessed for quantum sensing applications through structurally bistable ligands that respond to external stimuli (electromagnetic (optical), thermal, pH, chemical). Structural gating induces changes in metal-ligand covalency and local magnetic field of transition-metal spin qubits, as revealed by pulsed X-band and W-band EPR experiments for first row transition metal (*ls* Co(II) S=1/2, Cu(II) S=1/2 and Ni(II) S=1) photochrome complexes. Optical gating of the resonance frequency (g-value), longitudinal relaxation (T_1) and phase-memory (coherence) time (T_m), generates a Class II magnetic quantum sensor (Fig. 1). The sensitivity depends on the change in local magnetic field at the metal center upon ligand isomerization (metal-ligand covalency), and the kinetics of isomerization vs. spin dynamics. These studies provide fundamental insight into requirements for gating of coherence and spin-lattice relaxation in spin- qubit platforms critical to molecular quantum sensing strategies.

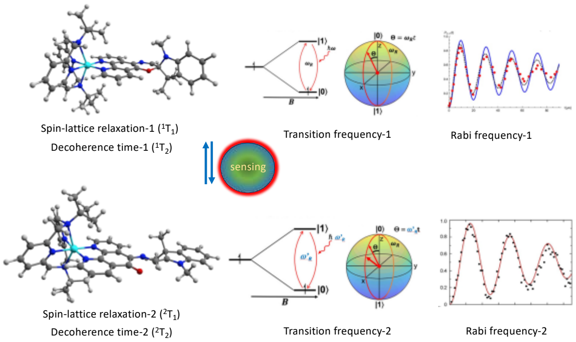

Figure 1. Modulation of metal-ligand covalency leads to local changes in magnetic field and in turn quantum states.

Functionally Active Linker Design for Photoactive Molecules at Semiconductor Interfaces

Elena Galoppini, Yang Zhang, Katherine Lloyd
Chemistry Department, Rutgers University, Newark, NJ 07102

Molecular-level control of hybrid molecule/semiconductor interfaces is one of the prerequisites to enable innovative technologies for the capture and conversion of solar energy to produce electricity and energy-rich chemicals. Our research program aims at controlling and understanding, through tunable synthetic design of chromophores, linkers, and anchor groups, the properties of the interface between nanostructured metal oxide semiconductors and photo- or redox-active compounds. The poster will illustrate our results and plans toward advanced linker-anchor designs to tune charge separation between organic/redox active groups and semiconductors and to form strong bonding to the surface.

The poster will present updates in the following areas: *(1) Linker's design to control stacking, distance, orientation, and electronic coupling at chromophores/semiconductor interfaces*. We developed perylenes with structurally different linker groups and multiple surface attachments to predictably modify electronic coupling to acceptor states, and to control stacking on surfaces, Figure 1.(1). We studied structurally and electronically different linkers, attached to ortho/peri substitution positions, and with the Gundlach group at U Delaware we demonstrated that often-neglected conformational and binding mode effects dominate IET. Once understood, these interactions can be exploited and directed through linker molecular design informed by theoretical calculations. *(2) Anchor design.* The poster will describe the systematic study of synthetically accessible Ipa-substituted anchors that provide multidentate coordination and strong binding through a third binding point. Our results point to slower desorption in basic conditions and slow recombination for the OH-Ipa, Figure 1. (2). These X-Ipa groups will be used in click (CuAAC) covalent stepwise binding approaches. *(3) IR-active linkers*. Finally, we developed IR-active linkers based on carboranes, where charge transfer can be promoted by excitation with infrared radiation. The poster will report our progress with the first donor-linker-acceptor model system (*N,N*-dimethylaniline-*m*carborane-pyrene), studied by Rubtsov at Tulane.

(1) Linker's design to control stacking, orientation, and electronic coupling

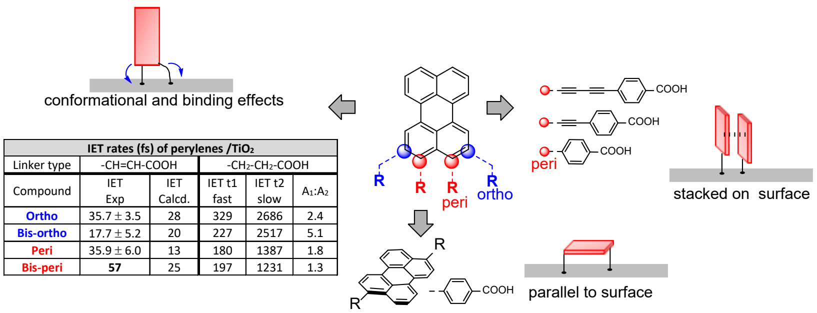

IET rates (fs) of perylenes /TiO_2					
Linker type	-CH=CH-COOH		-CH_2-CH_2-COOH		
Compound	IET Exp	IET Calcd.	IET t1 fast	IET t2 slow	A_1:A_2
Ortho	35.7 ± 3.5	28	329	2686	2.4
Bis-ortho	17.7 ± 5.2	20	227	2517	5.1
Peri	35.9 ± 6.0	13	180	1387	1.8
Bis-peri	**57**	25	197	1231	1.3

(2) Anchor groups for strong binding and inhibited recombination

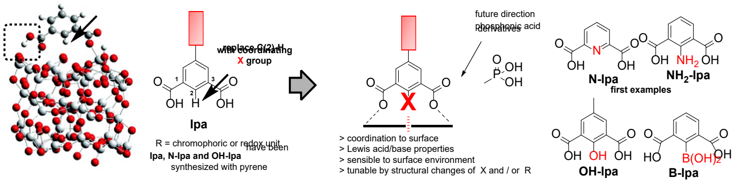

Figure 1. (1) Linker strategies pursued with perylene as chromophore. **(2)** Fully optimized, preferred binding mode of Ipa to $(TiO_2)_{46}$ and novel2-substituted isophthalic acids studied (X-Ipas).

Enhancing the Visible Light Absorption and Excited State Properties of Cu(I) HETPHENs

Michael C. Rosko, Jonathan P. Wheeler, Reem Alameh, Adrienne P. Faulkner, Nicolas Durand, and Felix N. Castellano*

Department of Chemistry, North Carolina State University
Raleigh, NC, 27965-8204

Cu^{I} chromophores have been studied over the last 50 years as substitutes for more traditional 2nd- and 3rd-row transition metal photosensitizers. However, stable heteroleptic Cu^{I} complexes constructed from diimines remain underexplored. Most architectures ubiquitously invoke the heteroleptic phenanthroline (HETPHEN) strategy in conjunction with 2,9-mesityl-1,10-phenanthroline (mesPhen), represented to the left. The current work seeks to further expand this concept by leveraging experimental results derived from decades of homoleptic Cu^{I} diimine research.

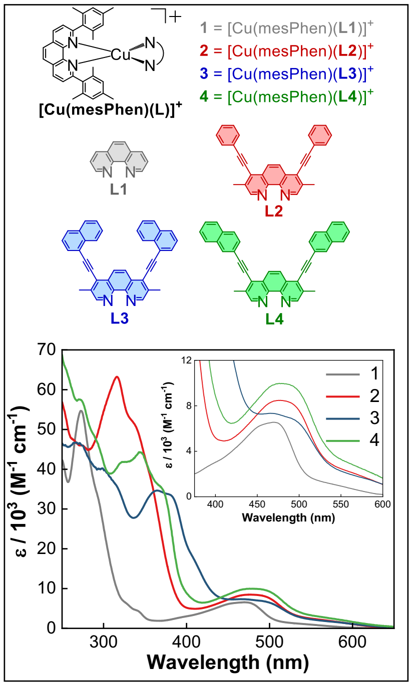

In our quest to amplify visible light harvesting, we embraced a computationally guided approach, which has yielded remarkable results. This strategy has empowered us to precisely forecast visible-light absorption across a range of CuHETPHENs and augment π-delocalization via 4,7-arylethynyl substituents, thereby fortifying MLCT oscillator strengths. The robustness of our findings was further underscored by a thorough examination of TD-DFT computations, electrochemistry, and transient absorption spectroscopy, all of which confirmed the preferential reduction of the arylethynyl-substituted ligand in these complexes.

Conversely, our synthesis of a series of CuHETPHENs by replacing the secondary phenanthroline ligand with diverse 2,9-alkyl groups and cooperative steric 3,8-methyl enhancements yielded some exceptional outcomes. These CuHETPHENs, designed to emulate their long-lived homoleptic counterparts, have generated the most prolonged MLCT lifetimes for CuHETPHENs to date (τ = 400 ns in deaerated CH_2Cl_2) (**6**) and correspondingly feature RT photoluminescence (PL). Intriguingly, the cooperative steric 3,8-methyl enhancements in the phen ligand do not significantly prolong MLCT excited state lifetimes, a stark contrast to the findings in the corresponding homoleptic species. Chromophore **11** stands out in this context, as the homoleptic species is unattainable due to its half-chair conformations within the cyclopentyl ring. Nevertheless, it forms a stable heteroleptic Cu^{I} species, underscoring the distinctiveness of this research. These findings will be compared to our recent work pioneering record-setting MLCT excited state lifetimes and PL metrics in newly conceived Cu^{I} homoleptics.

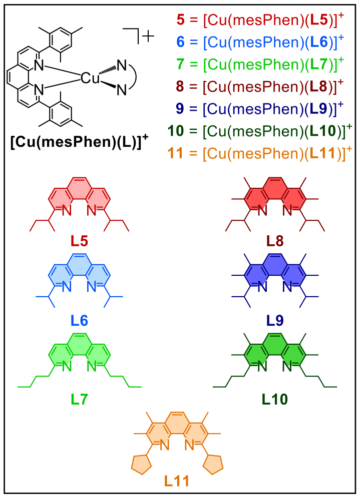

Ab Initio Quantum Dynamics of Charge Carriers in Advanced Solar Materials

Oleg Prezhdo
Department of Chemistry
University of Southern California
Los Angeles, CA 90089

Our group develops methods for modeling excited state dynamics in nanoscale, molecular and condensed phase materials, and applies them to study photoinduced processes in diverse and modern systems for solar energy harvesting, as exemplified in the figures below.

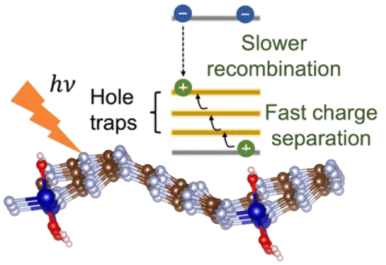

Figure 1. Doping graphitic carbon nitride with single cobalt atoms produces filled midgap states that serve as photo-oxidation centers and enable harvesting longer wavelengths. Although doping accelerates charge relaxation overall, charge recombination is significantly slower than charge separation, creating beneficial conditions for applications. [*JPCL* **15**, 2202 (2024)].

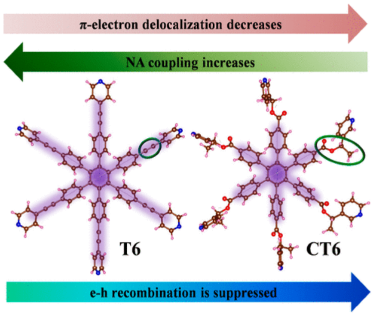

Figure 2. A short π-conjugated optically active template can control hot carrier relaxation, separation, and recombination in porphyrin nano-rings. Hot hole relaxation of hot holes is slowed by 60%, while charge recombination is suppressed 6-fold. [*JPCL* **14**, 11384 (2023)].

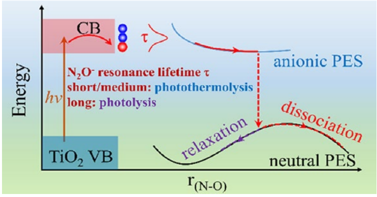

Figure 3. Even a transient injection of photogenerated charges into adsorbed molecules can initiate bond breaking in semiconductor and plasmonic photocatalysis. The chemistry is activated by a combination of excited state evolution and local heating. The contributions of photolysis and photothermolysis, and their efficiencies depend on resonance lifetime and catalytic interfacial interaction. [*JACS* **145**, 476 (2022)].

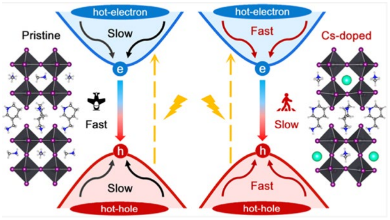

Figure 4. Spontaneous symmetry breaking in organic and mixed organic-inorganic 2D metal halide perovskites drives rapid interlayer charge separation and extends charge carrier lifetime. It occurs due to thermal fluctuations and slight structural inhomogeneity. Doping enhances the effect and provides composition-structure-dynamics-function relationships to tailor optoelectronic properties of layered perovskites [*JACS* **145**, 5297 (2023)].

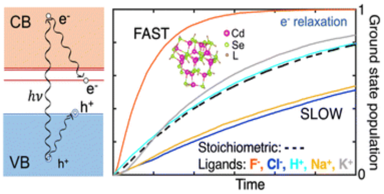

Figure 5. Non-stoichiometry is frequent in conventional nanocrystals. We confirm localized traps in anion-rich but not cation-rich CdSe. The localized states disappear with bulkier ligands. Ligand size controls crystal vibrations and electron–phonon coupling, while ligand coordination number affects electronic structure. Ligands can both increase and decrease electron relaxation time. [*J. Mater. Chem. A*, **11**, 8256 (2023)].

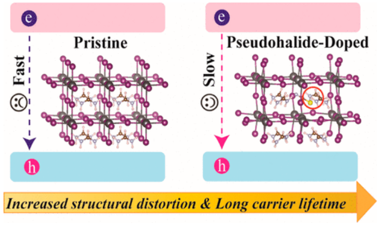

Figure 6. Nonradiative charge recombination is suppressed when iodide in FAPbI$_3$ is partially replaced with a pseudohalide (SCN$^-$, BF$_4^-$, and PF$_6^-$). The replacement breaks the symmetry and creates local distortion and dynamic disorder, decreasing electron-hole overlap and electron-phonon coupling. Carrier lifetime grows with structural distortion and is longest for PF$_6^-$. [*JPCL*, **14**, 10685 (2023)].

Mixed-Metal Oxide Catalysts for the Oxygen Evolution Reaction

Alaina C. Hartnett, Samuel S. Veroneau, Daniel G Nocera
Department of Chemistry and Chemical Biology
Harvard University
Cambridge, MA 02138

Scope of the project. Water splitting catalysis underpins all sustainable energy conversion schemes as the reaction is the source of proton and electron reducing equivalents. The first step of water splitting is the most kinetically demanding—the oxygen evolution reaction (OER)—coupling of two water molecules to produce oxygen. The four protons and four electrons formed in OER are then available to drive a reduction reaction, most popularly, the reduction of CO_2 to a fuel. Because the coupling of electrons and protons is demanded for high OER energy efficiency, we have focused on examining systems that allow proton-coupled electron transfer (PCET) in OER to be defined at a mechanistic level. This is a challenging task as the most active OER catalysts are heterogeneous. Nonetheless, we have developed a science of metallate oxygen evolution catalysts (M-OECs) that allows the mechanism of heterogeneous OER catalysts to be examined with the atomistic fidelity of molecular systems.

Recent results. Most M´M-OECs are generated by electrodeposition. However, many M´M-OECs cannot be co-deposited due to differing solubilities (K_{sp}s), deposition potentials, and redox activities of constituent metal ions and their corresponding oxides. To overcome this challenge, we have developed a synthesis based on sol-gel methods that allows a large range of M´M-OECs to be synthesized. Our method relies on formation of a homogeneous gel comprised of constituent metal ions from nitrate precursors, citric acid chelating agent, and gel-forming polymers. Subsequent annealing of the gel and exposure to oxygen plasma yield a surfactant-free polycrystalline M´M-OEC film. The sol-gel method now opens the door to obtain a variety of M´M compositions, with much to study. Exploiting this method, for instance, we have successfully synthesized the Ln-doped (Ln = lanthanide) Co-OEC systems, which are otherwise unattainable with conventional electrodeposition methods owing to the vastly different solubilities and redox potentials of Ln and Co precursors. LnCo-OECs are intriguing to us because Ln ions are highly Lewis acidic and redox inactive, thus allowing Lewis acidity to be cleanly isolated from redox-induced effects for OER under anodic bias.

Our preliminary results on LaCo-OECs, a significant drop of over 350–400 mV in overpotential is observed with La doping. The maximal effect is reproducibly observed with 10% La^{3+} loading (Figure 1, green trace).

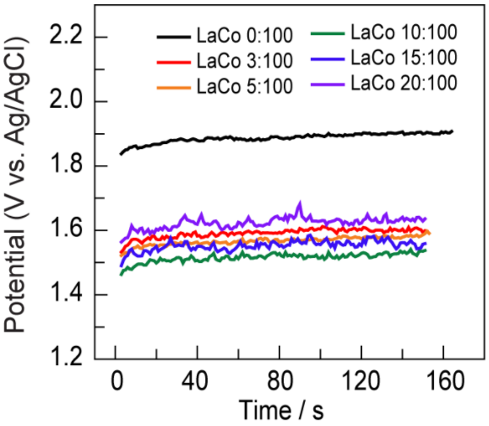

Figure 1. OER activity for LaCo-OECs prepare by sol-gel synthesis methods. OER potential measured at the constant OER current density of 10 mA/cm^2 in 100 mM P_i buffer and with 100 mM KNO_3 supporting electrolyte.

Future plans. We now wish to discover the origins of this activity enhancement. Questions that we wish to address include: How does La^{3+} doping promote OER catalysis? Does the correlation between Lewis acidity and OER activity hold across the Ln^{3+} series? Is this correlation affected by the nature of the transition metal oxide?

Nickel Hydride Photochemistry Enables Catalytic H_2 Evolution and Hydrogen Transfer

Tamara Jurado, Eamon Reynolds, Afrah Faraz, Alexander J. M. Miller
Department of Chemistry
University of North Carolina at Chapel Hill
Chapel Hill, NC 27599-3290

This project seeks transition metal hydride complexes that can be generated at mild electrochemical potentials and then react photochemically to release H_2 or undergo hydrogen transfer reactions.[1] Recent research has focused on understanding the reactivity of nickel hydride complexes and controlling reactivity between H_2 evolution and hydrogen atom transfer pathways.

Isolable nickel hydride complexes of the type $[HNi(diphosphine)_2]^+$ generate H_2 upon visible light illumination via homolysis to releases a solvated hydrogen atom.[2] Thermochemical studies predict a very weak Ni–H BDFE in the excited state. To understand the practical limits of the excited state BDFE, a series of hydrogen atom transfer (HAT) reactions varying driving force and solvent was examined. As shown in the Figure, HAT proceeds even with challenging substrates. These reactions, including some that are thermally endergonic, suggest that the Ni hydride is an extremely potent photochemical hydrogen atom donor. Electrochemical hydride regeneration enables photoelectrocatalytic anthracene reduction to dihydroanthracene. Based on interest in arenes as liquid organic hydrogen carriers (LOHCs), future work is focused on maximizing hydrogen addition and identifying other promising hydrogen carriers. In addition, we are carrying out fundamental studies of Ni hydride photochemistry to improve the photochemical quantum yield for fuel synthesis and hydrogen storage reactions.

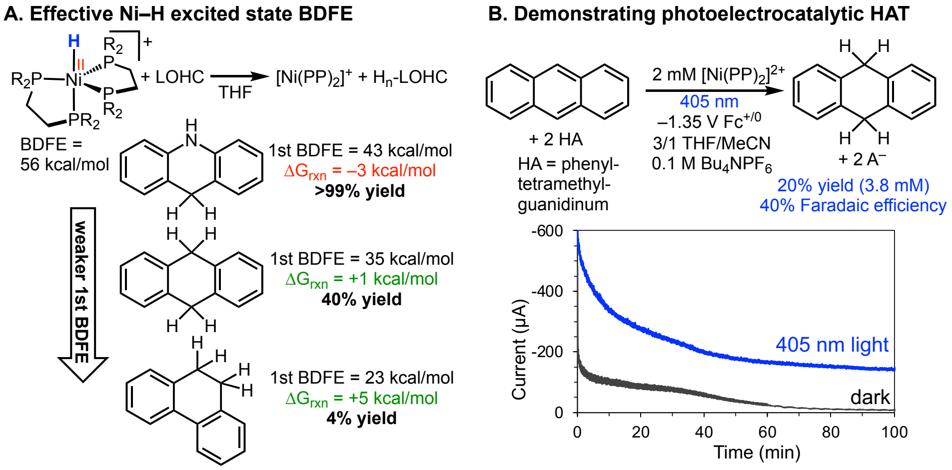

Another focus of recent research is developing comparisons between traditional semiconductor-catalyst photoelectrodes and single-component systems in which a molecular catalyst acts as both the light absorber and electrochemical mediator of bond-forming events. Access to surface-anchored photohydrides has enabled more meaningful comparisons based on external quantum efficiency. We are examining how molecular-level characteristics such as the extinction coefficient, bond-forming photochemical quantum yield, or heterogeneous electron transfer rate constant can predict the overall efficiency.

[1] Brereton, K. R.; Bonn, A. G.; Miller, A. J. M. *ACS Energy Lett.* **2018**, *3*, 1128.
[2] Stratakes, B. M.; Wells, K. A.; Kurtz, D. A.; Castellano, F. N.; Miller, A. J. M. *J. Am. Chem. Soc.* **2021**, *143*, 21388.

Energetic Tuning of Silicon Nanocrystal-Electrocatalyst Hybrid Photocatalysts

Simran S. Saund, Trung H. Le, Melissa K. Gish, Nathan R. Neale
Chemistry and Nanoscience Center
National Renewable Energy Laboratory
Golden, CO 80401

Direct coupling of light-harvesting semiconductors and molecular catalysts is an attractive approach in designing new systems for artificial photosynthesis that could enable cooperativity not possible with either system alone. We have been exploring such systems by tethering molecular electrocatalysts (ECat) to silicon nanocrystals (Si NCs). These systems offer the ability to tune energetics of both the ECat and the Si NC and probe the impacts of energetics on charge generation, charge transfer and photocatalytic activity.

In our first forray into this area, we tethered a Lehn-type rhenium carbonyl coordination complex ([Re]) to dodecyl-terminated Si NCs (Si-C_{12}). We will present full characterization of the Si-[Re] hybrid system using spectroscopic and electrochemical methods including transient absorption spectra (**Figure 1**) and photocatalysis (PC) for CO_2 to CO, which demonstrates that the Si NC-[Re] hybrid does *not* enhance photocatalytic activity compared with [Re] alone (DOI: 10.1039/d3se01512b).

To explain these results and devise strategies to generate energetically matched systems, we turned to density functional theory (DFT). We will present Jablonski diagrams from these DFT calculations showing that high reduction potential ECats are mismatched to the conduction band of the bulk Si semiconductor by ~1 eV. However, by manipulating the Si NC and/or the ECat, the DFT calculations show energetic coupling can be achieved (**Figure 2**). Our poster will describe these DFT results and initial experiments synthesizing and characterizing these new systems via TA, EPR, electrochemistry and PC.

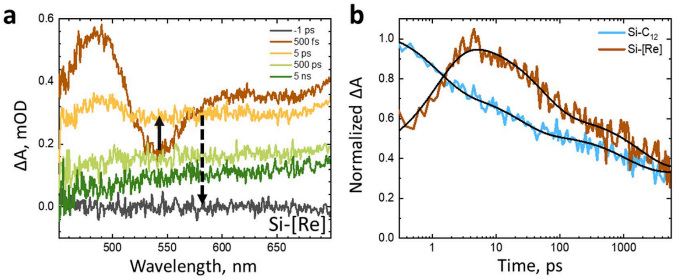

Figure 1. (a) TA spectra of Si-[Re] solutions monitored at 500 fs (brown) through 5 ns (green). (b) Normalized TA kinetics of colloidal Si-C_{12} (blue) and Si-[Re] (brown) solutions monitored at 545 nm. Fits to the data are shown as black lines.

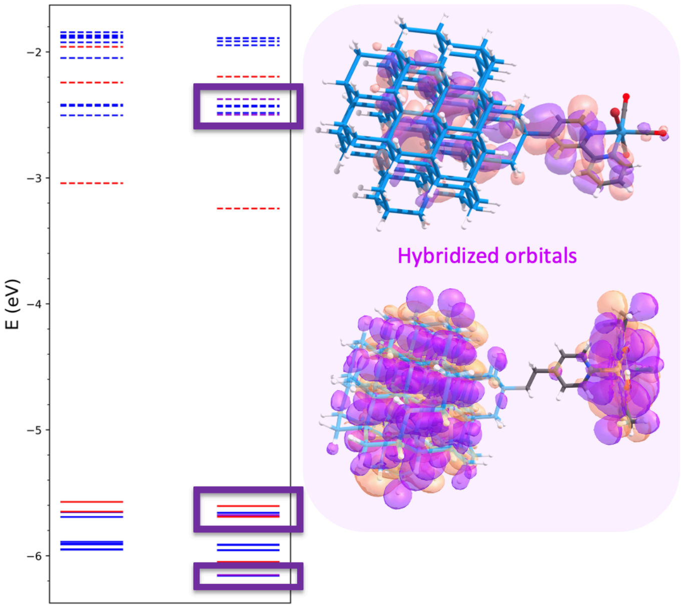

Figure 2. Jablonski diagrams of intrinsic Si-[Re] NCs hybrids showing decoupled Si NC orbitals (blue) and [Re] orbitals (red). Hybridized orbitals (purple) are found when tuning the Si NC and/or ECat structure and energetics.

Finding and Steering Reaction Coordinates in Photoinduced Electron Transfer Process in Transition Metal Superamolecular Systems

P. Kim,[1] S. Roget,[1] S. Roy,[2] A. J. S. Valentine,[3] X. Liu,[3] S. Kromer,[2] T. W. Kim,[1] W. Hanke,[1] K. L. Mulfort,[1] X. Li,[4] F. N. Castellano,[2] L. X. Chen[1,4]

[1]Chemical Science and Engineering Division, Argonne National Laboratory, Lemont, IL 60439
[2]Department of Chemistry, North Carolina State University, Raleigh, NC 27695-8204
[3]Chemistry Department, University of Washington, Seattle, WA 98195
[4]Chemistry Department, Northwestern University, Evanston, IL 60208

The goal of our research is to provide a critical knowledge base for understanding the fundamental aspects of light—matter interactions that will influence the development of molecular systems for solar photochemistry as well as emergent new science in photoredox catalysis. We explore ultrafast functional structural dynamics in photoexcited states with strongly coupled electronic and nuclear motions aiming at - A) identifying key reaction coordinates of photoinduced electron transfer (PET) in electron donor-acceptor complexes; B) steering PET processes by chemical modifications and tailored light pulse sequences.

1. Spin-Vibronic Coupling and its impact on PET trajectory Pt(II) metal-metal-to-ligand charge transfer (MMLCT) complex **1** shows spin-vibronic coupling, leading to ultrafast intersystem crossing (ISC) driven by Pt-Pt stretching along the reaction trajectories, enabling coherent vibrational wavepacket (CVWP) transfer. For the corresponding D-A complexes of covalently linked Pt(II) dimer as donor and naphthalene diimide (NDI) as the acceptors, we investigated the CVWP behaviors during PET and revealed significant coupling between the PET reactions and nuclear motion driven by spin-vibronic coupling in PET trajectories.

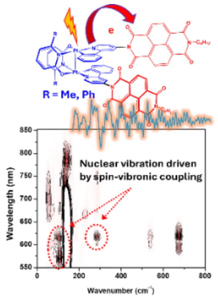

2. Pseudo Jahn-Teller distortion influencing PET dynamics The metal-to-ligand charge transfer (MLCT) state of Cu(I) bisphenanthroline undergoes photoinduced pseudo Jahn-Teller (PJT) distortion from tetrahedral to flattened geometry. We examined the impact of PJT distortions on PET in Cu bisphenanthroline-NDI D-A complexes and observed a CVWP mode of 248 cm^{-1} decohering due to the PET. An emerging 310 cm^{-1} CVWP motion accompanied the NDI radical anion formation during the PJT distortion. These findings highlights the role of PJT distortion in driving PET process.

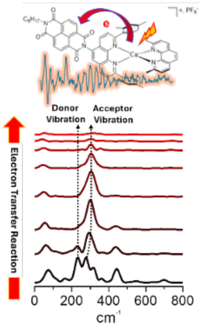

3. Influencing PET kinetics in D-B-A system by activating bridge vibrations To explore PET dynamics control via activating the vibrational mode at the bridging ligand in Cu(I) bisphenanthroline-ethynyl-anthraquinone charge separation (CS), we measured the growth of anthraquinone radical anion and ethynyl vibrational spectra synchronized with the PET dynamics. Enhanced ethynyl stretch oscillator strength and ethynyl stretch frequency down shifts in MLCT and CS states suggests potential vibrational control in PET dynamics via direct infrared excitation, currently under examination using pump (visible) – pump (IR) – probe (white continuum) spectroscopy.

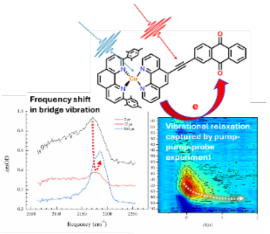

Modeling Ultrafast Excited State Dynamics in Complex Reaction Landscape

Xiaosong Li,[1] Maxwell Taub[1], Xiaolin Liu,[1]
Zach Mast,[2] Subha Chaudhuri,[2] Jason Zeman,[2] Diptesh Dey,[2] George Schatz,[2]
Lin Chen,[2,3] Karen Mulfort,[3] Michael Mara,[3] Kim, Pyosang,[3]
Amy Cordones-Hahn,[4]
Felix Castellano[5]

[1]Chemistry Department, University of Washington, Seattle, WA 98195
[2]Chemistry Department, Northwestern University, Evanston, IL 60208
[3]Chemical Sciences and Engineering, Argonne National Laboratory, Lemont, IL 60439
[4]Stanford PULSE Institute, SLAC National Accelerator Laboratory, Menlo Park, CA 94025
[5]Department of Chemistry, North Carolina State University, Raleigh, NC 27695

Modulating directional charge transfer processes in metal complexes is a critical goal in photochemical research, essential for the effective separation of photo-generated electrons and holes. Understanding the physical underpinnings underlying ultrafast photochemical processes in complex excited states is key to designing high-performance molecular photocatalysts and photoenergy converters. The theory team, led by Li and Schatz, employs electronic structure calculations to characterize homo- and hetero-bimetallic complexes and identify charge transfer pathways, supported by spectroscopic analysis from X-ray free electron laser and X-ray transient absorption experiments. We have also introduced two methodologies to model excited state dynamics within complex reaction landscapes (Figure 1). The first method extends the surface-hopping technique to simulate competing intersystem crossing and internal conversion pathways in homo-bimetallic complexes. The second method utilizes data science tools, specifically cheminformatics, to design and improve charge-transfer properties in hetero-bimetallic complexes, enhancing their photocatalytic effectiveness. This poster will demonstrate the successful application of these simulation tools to model and understand the excited state dynamics and properties of bimetallic complexes.

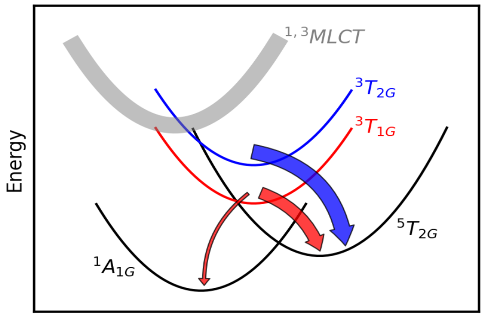

Figure 1. Illustration of complex excited-state reaction pathways driven by the competing multi-level intersystem crossing and internal conversion dynamics.

Directional Excited State Charge Transfer for Solar Energy Conversion Tracked with Element Specificity

Amy Cordones-Hahn,[1] Michael Mara,[2] Xiaosong Li,[3] Karen Mulfort,[2] George Schatz,[4] Lin Chen[2,4]
[1]Stanford PULSE Institute, SLAC National Accelerator Laboratory, Menlo Park, CA 94025
[2]Chemical Sciences and Engineering, Argonne National Laboratory, Lemont, IL 60439
[3]Department of Chemistry, University of Washington, Seattle, WA 98195
[4]Department of Chemistry, Northwestern University, Evanston, IL 60208

Solar energy conversion to fuels and electricity requires multi-step photo-redox and photochemical processes. Following light absorption, the direction of electron density migration and nuclear motions resulting from photon energy dissipation are governed by the interplay between electrons and nuclei in excited states. Thus, a detailed understanding of the light-driven electronic and nuclear response of energy conversion materials is needed to optimize photochemical reaction outcomes, minimize energy losses, and increase light energy conversion efficiency. The continued development of novel ultrafast x-ray methods provides unprecedented opportunities for tracking electronic/nuclear motions in real time along excited state trajectories.

We are applying ultrafast x-ray absorption spectroscopy (XAS) to directly detect how electronic/nuclear reorganization in the excited and intermediate states facilitate directional charge transfer towards catalytic reaction sites. Our focus is on covalently linked heterobimetallic donor-acceptor dyads that combine light absorber and catalytic sub-units. By using the elemental specificity of XAS, we track the real-time excited-state charge distribution at specific metal, ligand, and bridging ligand atoms and can fully resolve and distinguish intra- and inter-molecular electron transfer pathways. With an initial focus on tetrapyridophenazine (tpphz) bridged dyads, we have explored potential role of tpphz as an electron acceptor and investigated if this bridging ligand either facilitates or hinders long range metal-to-metal electron transfer. We've characterized the electronic structure of the tpphz bridging ligand using N K-edge XAS and also identified distinctive spectral features corresponding to the metal-bound and central bridge-located N atoms. These distinctive features have enabled real-time experiments tracking the excited state redistribution of charge from inner coordination sphere ligands to the bridge, allowing us to quantify the rate and localization of intramolecular electron transfer directly. In addition, we have probed the donor and acceptor metal atoms directly to identify the degree of long-range charge separation in Cu-Ru, Cu-Os, Cu-Ni, and Ru-Rh dyads.

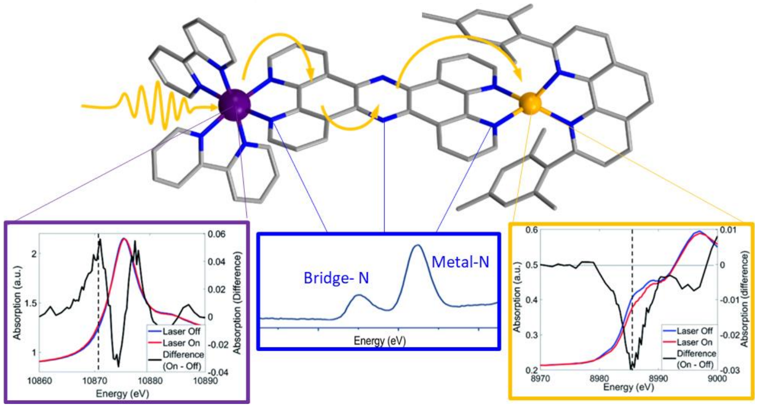

Figure 1. The combination of metal and ligand atom XAS provides an unprecedented view of excited state electron transfer processes in donor-acceptor dyads.

Harvesting Electrons and Holes from Photodriven Symmetry-Breaking Charge Separation within a Perylenediimide Photosynthetic Model Dimer

Jillian M. Bradley, Adam F. Coleman, Paige J. Brown, Yuheng Huang, Ryan M. Young, and
Michael R. Wasielewski
Department of Chemistry and Paula M. Trienens Institute for Sustainability and Energy
Northwestern University
Evanston, IL 60208-3113

Symmetry-breaking charge transfer (SB-CS) is of particular interest in solar energy conversion because photodriven charge separation occurs with minimal loss of the photon energy. While previous research has identified molecules that undergo SB-CS, as well as characterized their intrinsic properties and the environmental factors that affect the process, little effort has focused on how to transfer the photogenerated charges to adjacent molecules to store or utilize the energy.

Understanding how to utilize symmetry-breaking charge separation (SB-CS) offers a path toward increasingly efficient light-harvesting. This process plays a central role in the first step of photosynthesis, in which the dimeric "special pair" of the photosynthetic reaction center enters a coherent SB-CS state after photoexcitation. Previous research on SB-CS in both biological and synthetic chromophore dimers has focused on increasing the efficiency of light-driven processes. In a chromophore dimer undergoing SB-CS, the energy of the radical ion pair product is nearly isoenergetic with that of the lowest excited singlet (S_1) state of the dimer. This means that very little energy is lost from the absorbed photon. In principle, the relatively high energy electron and hole generated by SB-CS within the chromophore dimer can each be transferred to adjacent charge acceptors to extend the lifetime of electron-hole pair, which can increase the efficiency of solar energy conversion. To investigate this possibility, we have designed a bis-perylenediimide cyclophane (*m*PDI$_2$) covalently linked to a secondary electron donor, *peri*-xanthenoxanthene (PXX) and a secondary electron acceptor, partially fluorinated naphthalenediimide (FNDI).[1] Upon selective photoexcitation of *m*PDI$_2$, transient absorption spectroscopy shows that *m*PDI$_2$ undergoes SB-CS, followed by two secondary charge transfer reactions to generate a PXX$^{\bullet+}$-*m*PDI$_2$-FNDI$^{\bullet-}$ radical ion pair having a nearly 3 μs lifetime. This strategy has the potential to increase the efficiency of molecular systems for artificial photosynthesis and photovoltaics.

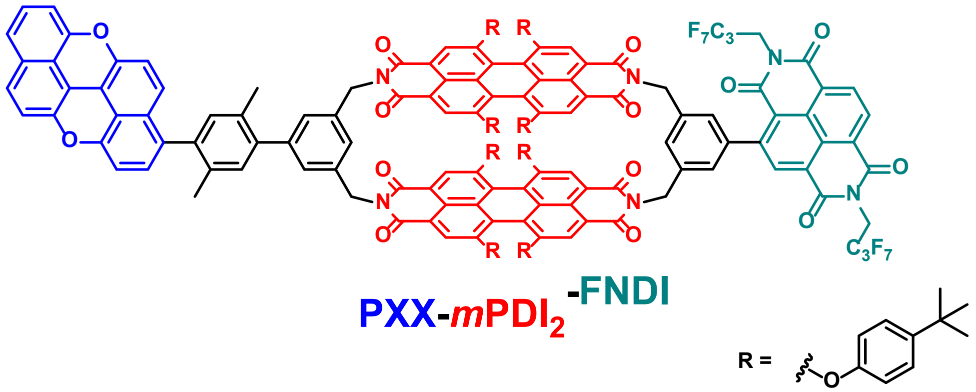

PXX-*m*PDI$_2$-FNDI

---

[1] Bradley, J. M.; Young, R. M.; Coleman, A. F.; Brown, P. J.; Huang, Y.; Wasielewski, M. R. *Proc. Natl. Acad. Sci. USA* **2023**, *120*, e2313575120.

From Captured CO_2 to Value-added Chemicals: A Photochemical Approach

Ksenija D. Glusac,† David Kaphan,† Karen Mulfort,† David Tiede,† Lin Chen,† Peter Zapol,†
Amy Cordones-Hahn,‡ Alex Martinson,†
†Chemical Sciences and Engineering Division, Argonne National Laboratory, Lemont, Illinois 60439
‡Stanford PULSE Institute, SLAC National Accelerator Laboratory, Menlo Park, California 94025

We investigate *photoreductive CO_2 capture,* an approach that combines the capture of CO_2 with its conversion into value-added chemicals, such as formate ion, using visible light as an energy input. While our work is use-inspired, we explore the fundamentals of molecular motifs that can efficiently harvest light (light-responsive MOF), capture CO_2 at low concentrations (O-capture via alkoxide ions) and catalyze target conversion (via redox-active transition metal complexes).

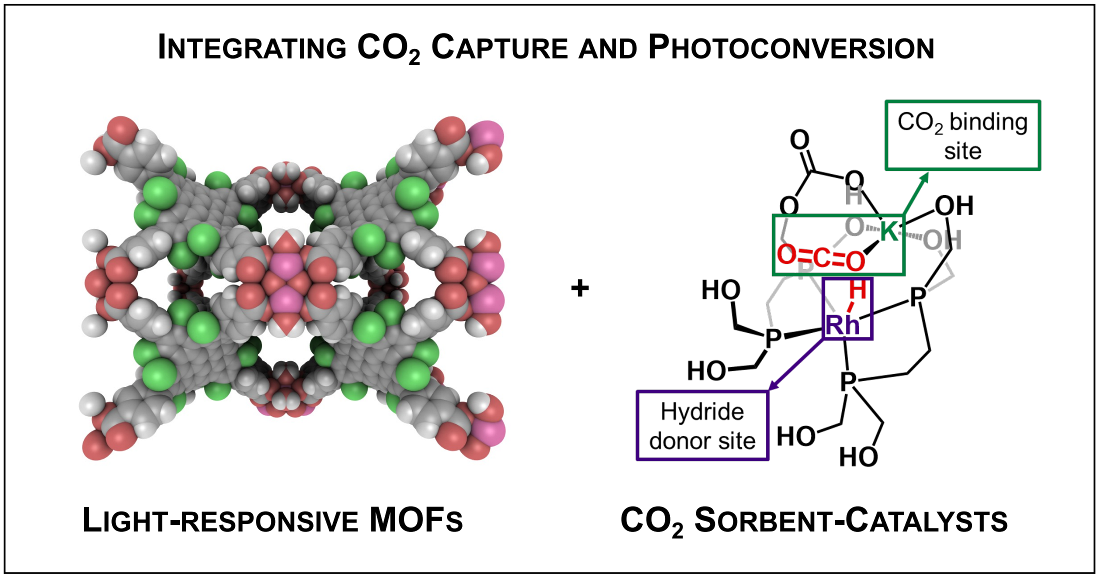

Our work with light-responsive MOFs has led to a discovery of a series of MOF structures with nanographene ligands. The UV/Vis spectra of these structures range from UU to near-IR range, illustrating the richness of their light-absorbing characteristics, while their crystal structures illustrate the diversity of their 3D architectures. So far, we investigated the behavior of three Zr-based nanographene MOFs in more detail and these studies have shown exciting photophysical and photochemical behavior of these porous crystals, including facile tunability of their optical gaps and the role of nodes in capturing CO_2 during photochemical conversion to the formate ion. In our studies on combined CO_2 capture and conversion, we explored a series of catalytic transition metal complexes with pendant oxygen and nitrogen-based functional groups for capture CO_2. For example, we discovered a rhodium complex with pendant alkoxide groups that efficiently captures CO_2, even at very low partial pressures. Furthermore, the CO_2-bound complex was found to accelerate the hydride exchange reaction between CO_2 and formate, opening the avenues of integrated capture and conversion of CO_2. Moving forward, we plan to expand these studies to include the conversion of CO_2 into value-added chemicals with C4 or more atoms using photo-carboxylation chemistry.

Tuning Solar Fuels Catalysts for Fast Rates at Low Overpotentials

Gerald F Manbeck, Mehmed Z Ertem, and Dmitry Polyansky, Zongheng Wang, Renato Sampaio, and Brian DiMarco
Chemistry Division, Energy & Photon Sciences Directorate
Brookhaven National Laboratory
Upton, NY 11973-5000

Improving photo- and electrocatalytic efficiencies by increasing rates with less energy input (i.e., a smaller overpotential) is challenging for molecular catalysts since operating near the thermodynamic potential for a given reaction is often kinetically disadvantageous. Here we present strategies to break typical scaling relationships by (1) storing extra charge in electropositive ligands, and (2) manipulating redox potentials using highly cationic ligands.

For strategy (1), a series of five Ru hydrido complexes [$(Rbpy)_2Ru{-}H^+$] were synthesized and characterized with respect to key properties relevant to the production of solar fuels. In this research, we tested our characterization and mechanistic predictions using electrocatalytic hydrogen evolution by the reduction of weak acids as a model reaction. Substituents of the bipyridine ligands (CF_3 > Cl > H > CH_3 > CH_3O) were chosen to systematically vary the electron density at the metal centers. The metal complexes were shown to be stable in three redox states, retaining the Ru−H bond and enabling analysis of hydride thermodynamics in $(Rbpy)_2Ru{-}H^+$, $(Rbpy)_2Ru{-}H^0$, and $(Rbpy)_2Ru{-}H^-$ oxidation states. The hydricities ($\Delta G°_{H-}$) of the five metal complexes spanned a substantial range of 22 kcal/mol, enabling precise control over overpotentials and mechanisms of reactivity. From these data, we *predicted* which weak acids would react with the catalysts to produce H_2 from various redox states, and experimentally *confirmed* two mechanisms of electrocatalytic hydrogen production: (i) beginning in the $(Rbpy)_2Ru{-}H^+$ state where hydride transfer from the catalyst to an H^+ in solution is rate-limiting and $(Rbpy)_2Ru{-}H^+$ regeneration is fast, and (ii) beginning from the $(R)Ru{-}H^0$ or $(R)Ru{-}H^-$ state, where the regeneration of the catalyst is slow and can be rate-limiting, especially in the case of the catalysts with electron-rich metal centers. The key finding is by using an electron poor catalyst in its doubly-reduced state (charge = –1), we realized a 350–400 mV decrease in the overpotential for H_2 production compared to an electron rich catalyst in its singly-reduced state (charge = 0). Future work will test the mechanistic and thermodynamic predictions on CO_2 (photo)electrocatalytic reduction, which is further complicated by the numerous possible products.

For strategy (2), we have evaluated self-sensitized and chromophore-sensitized photochemical CO_2 reduction catalyzed by a series of isomeric, dicationic $Re(bpy^{2+})(CO)_3I$ catalysts with pendent tetra-alkylammonio cations in the second coordination sphere. The excited states of these species are strongly oxidizing, and positive redox potentials promote efficient catalysts with or without an additional sensitizer. Exceptional turnovers for CO and formate production compared to neutral amine-substituted catalyst or the parent $Re(bpy)(CO)_3Cl$ have been observed and mechanistic details have been probed by steady-state and time-resolved UV-vis and IR spectroscopies.

(Photo)oxidation of Hydroxymethylated Polycyclic Aromatic Dyes: Mechanisms and Scope

Dugan Hayes, Omid Ghasemloo, Carson L. Hasselbrink, Douglas Cardona, and Sophia M. Tiano
Department of Chemistry
University of Rhode Island
Kingston, RI 02881

We have discovered a novel photochemical reaction wherein polycyclic organic dyes bearing hydroxmethyl groups oxidize to their corresponding aldehydes with concomitant elimination of H_2 as a byproduct. Our efforts are now focused on understanding the mechanism(s) of these photooxidations using 9-anthracenemethanol (AnMeOH) and 9-acridinemethanol (AcMeOH) as model reactants. By combining steady-state physical organic chemistry techniques (isotope labeling, kinetic studies, and photophysical characterization) with optical transient absorption spectroscopy and time-dependent density functional theory, we aim to piece together a complete picture of the reaction from the initial photon absorption event to the formation of the products in their electronic ground states. Insights from this work will then allow us to identify the requisite properties of such constructs for photochemical H_2 release and thereby develop computational screening methods to design improved materials for molecular hydrogen storage, which we will experimentally validate by synthesizing these new dyes and evaluating their performance.

In the current reporting period, we synthesized the series of anthracene, 10-methylanthracene, and acridine dyes shown below bearing $-CH_2OH$, $-CHDOH$, and $-CD_2OH$ groups in the 9-position. We have found that the 10-methyl substitution on AnMeOH affords a degree of steric protection against cycloadditive photooxygenation by trace O_2 in solution, while nitromethane is the optimal solvent for the desired photooxidation. Then, by comparing the ^1H NMR aldehyde and aromatic peaks in the photochemical product mixtures of the singly-deuterated dyes, we found a kinetic isotope effect of ~5 in each case (top row). Most notably, we performed residual gas analysis of the headspace for the reaction of the doubly-deuterated AnMeOH dye (bottom row) and observed production of HD that is entirely absent for the unlabeled dye (right), demonstrating conclusively that the H_2 produced in the reaction originates from the methylene and hydroxyl hydrogen atoms as we had hypothesized. We have also quantified intersystem crossing rates and triplet lifetimes from fs- and ns-resolved optical transient absorption and photoluminescence measurements and plan to correlate these values with directly excited and triplet sensitized quantum yield measurements to determine if the reaction proceeds from the singlet and/or triplet excited state.

Finally, we have discovered that AcMeOH undergoes spontaneous oxidation to its aldehyde in the presence of dilute, weak acid, which we believe proceeds via a 1,5-hydride shift to give a dihydroacridinium aldehyde intermediate. We are currently exploring the scope of this reaction and assessing whether it may be used for non-photochemical H_2 storage and release.

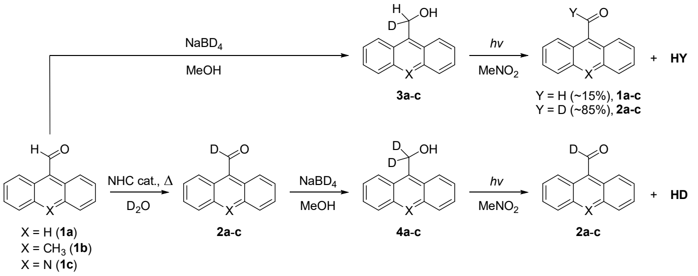

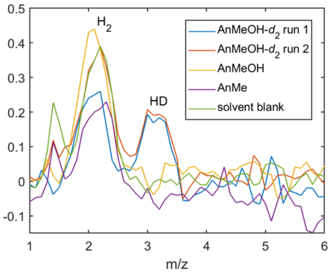

Understanding and Controlling the Physical and Chemical Characteristics of Nanoscale Metal/Semiconductor Interfaces on Functioning Photocatalysts for Solar Water Splitting

Aarti Mathur, Ahmet Sert and Suljo Linic
Department of Chemical Engineering
University of Michigan
Ann Arbor, MI 48109

Materials that are receiving increasing attention in photocatalysis (including solar water splitting) contain a semiconductor (SC) light absorber and attached metal electrocatalysts (EC). In these integrated photoelectrochemical systems, the SC provides a photovoltage that is used by the ECs to drive (electro)chemical reactions. In general, our understanding of the photocatalytic function of these EC/SC photoelectrocatalysts is based on simple models that often assume that the interface does not evolve or change under the reaction conditions and the fluxes of charge carriers between the SC and EC are controlled by their inherent, as-fabricated barrier heights. It has been recognized that these simple models cannot fully capture the behavior of EC/SC photoelectrocatalysts, particularly under reaction conditions. The overarching goal of this project is to study how the atomistic complexities associated with the functioning electrocatalyst/semiconductor (EC/SC) interfaces impact the performance of E/SC photoelectrocatalysts. We mainly focused on the water oxidation (i.e., OER) half-reaction, which usually takes place under highly oxidizing and corrosive conditions that often induce oxidative changes to the EC/SC interface.

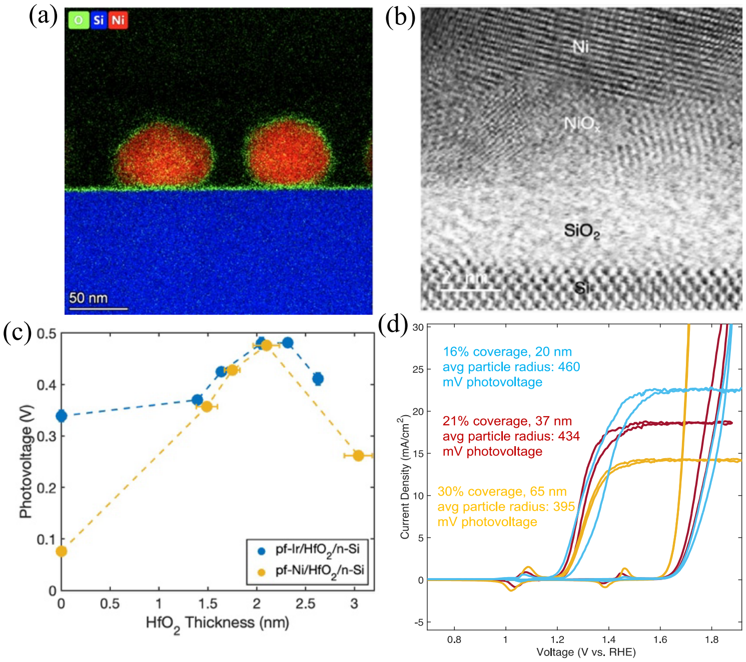

Figure 1. (a) Cross-sectional STEM images of np-Ni/n-Si after OER cycling (b) High-resolution TEM cross-section of the nanoparticle-Ni/NiO$_x$/SiO$_2$/Si interface (c) Photovoltage as a function of the interfacial oxide thickness for pf-Ir/HfO$_2$/n-Si and pf-Ni/HfO$_2$/n-Si systems (d) Photoelectrochemical OER performance of illuminated and dark np-Ni/Si with varying EC size and coverage

In a case study, we focused on describing the interface of a functioning SC(Si)/EC(Ni) photoelectrocatalyst in photoelectrochemical water oxidation. We investigated these systems in planar EC/SC and nanoparticle-EC/planar-SC form factors. We showed that when exposed to the electrochemical environment, the Ni/Si interface rapidly oxidizes under OER conditions (shown in Figure 1a). We demonstrated that the evolution of thin interfacial oxide layers (see Figure 1b) plays a critical role in modulating the electron/hole recombination rates, changing the inherent barrier height of the junction, and introducing non-idealities at the EC/SC interface. These studies that the thickness of the interfacial oxide layer is a critical factor governing the photovoltage generated by these EC/SC systems (see Figure 1c). More recently, we have been investigating how the size and coverage of the Ni nanoparticle EC impacts the performance of these photoelectrocatalysts, and how the interfacial oxide may evolve differently under reaction conditions based on the specific properties of EC (see Figure 1d). Our experimental and modeling analyses shed light on how a complex interplay between light absorbing properties of SC and electrocatalytic EC properties impacts the properties of the interface and the photoelectrocatalytic performance.

Light Harvesting in Semiconductor Quantum Dots

Warren F. Beck,[1] Benjamin G. Levine,[2] P. Gregory Van Patten,[3] Mengliang Zhang[3]

[1]Department of Chemistry, Michigan State University, East Lansing, Michigan 48824
[2]Department of Chemistry and Institute for Advanced Computational Science,
Stony Brook University, New York 11794
[3]Department of Chemistry, Middle Tennessee State University, Murfreesboro, Tennessee 37132

We are probing the light-harvesting dynamics of semiconductor quantum dots (QDs) using broadband multidimensional electronic spectroscopy (2DES/3DES) and electronic structure calculations. Our results favor consideration of a many-electron, molecular theory for the electronic structure of QDs, where the vibrations of organic surface-capping ligands serve as branching modes in a coherent nonadiabatic mechanism for nonradiative decay.

In a recent publication, the Levine group discusses how the coupling between core electronic excitations and ligand vibrations occurs through two distinct mechanisms. Lower frequency ligand modes (<400 cm^{-1}) couple directly to core vibrations, which are driven by core electronic excitations. However, higher frequency vibrations tend to be local to the ligand and are driven directly by the delocalization of core electronic excitations on the ligands.

Hetherington, C. V.; Mohan T M, N.; Tilluck, R. W.; Beck, W. F.; Levine, B. G. Origin of Vibronic Coherences During Carrier Cooling in Colloidal Quantum Dots. *J. Phys. Chem. Lett.* **2023**, *14*, 11651–11658, DOI: 10.1021/acs.jpclett.3c02384.

In on-going work, we are investigating how the photoinduced charge-transfer and triplet–triplet excitation energy transfer properties of QDs depend on the extent of mixing of the core electronic and ligand vibrational states. Recent 3DES results with methyl viologen dication acceptors adsorbed onto the surface of oleate-capped CdSe QDs show that an intermediary charge-transfer state is populated with retention of vibronic coherence following hot-carrier cooling on the <200-fs timescale. Two classes of rapidly damped coherent wavepacket motions are observed, involving mixed core lattice vibrations and out-of-plane deformations of the methyl viologen acceptors. These vibrations evidence the initial formation of a charge-separated character prior to the transfer of an electron to the methyl viologen acceptor on the ps timescale.

Coupled light absorption and mass transport improvements in a nanostructured, ‘knock out’ photonic glass photoelectrode

Ashlyn DesCarpentrie, Samuel K. Conlin, Grecia Pierina Alvarado Munoz, Trent Papenmeier,
and Robert H. Coridan
Department of Chemistry and Biochemistry
University of Arkansas
Fayetteville, Arkansas, 72701

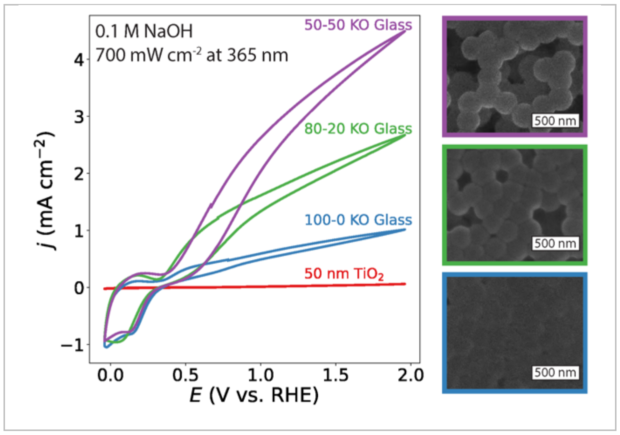

Nanostructured photonic crystal structures are often used to enhance light absorption in thin film photoelectrodes. The most common motif is the inverse opal, inspired by natural opal minerals. The inverse opal is fabricated from a template based on a self-assembled crystal of sacrificial colloidal particles. The periodicity of the colloidal crystal is chosen to enhance light trapping of a particular narrow band of wavelengths. In a photoelectrode, this stop band would correspond to light with energy near the semiconductor band edge of interest, where the material’s absorption length is the longest. A drawback for inverse opal, and for photonic crystal-based photoelectrodes more generally, is that there is a single characteristic structural length scale is determined by nanoscale light-matter interactions. It ignores what is optial for the coupled photoelectrochemical processes driving photochemical energy conversion. This can generate significant mass transport limitations quantum efficiencies in electrodes that otherwise have near unity light absorption in favorable portions of the photoelectrode.

Here, we will show that the opal structure can be selectively modified to improve both light absorption and mass transport through intentional disorder. We study the photoelectrochemical properties of ultra-thin-film TiO_2 (20 nm) photoanodes prepared by atomic layer deposition (ALD) on the SiO_2 surface of a SiO_2-polystyrene (PS) colloidal composite. PS can be removed after TiO_2 deposition by high temperature burn-out or chemical dissolution. The degree of this PS removal, or ‘knock out’, results in the formation of a hierarchical porosity that increases the mass transport through the electrode. It also disrupts the stop band associated with a photonic crystal and induces a deeper distribution of light absorption within photoelectrode structure. A counterintuitive result is that absorption in the photoelectrode increases while the volume of active material decreases. We used finite element simulations of light absorption and photoelectrochemical experiments to characterize the simultaneous photonic and mass transport effects in this 'knock out' photonic glass photoelectrode structure. We also propose to extend this strategy to improve carrier collection in photoelectrodes based on semiconductors with short minority carrier diffusion lengths. We broaden our simulation and experimental efforts to show how semiconductors that absorb in the visible part of the spectrum can be integrated into this nanostructure. We synthesize layers of semiconductor material on the surface of the sacrificial PS colloid to be integrated into the SiO_2 scaffold. The ALD-TiO_2 layers are used to generate dielectric contrast (light scattering) and act as a transparent current collector.

Non-equilibrium Methods for Tuning Photoelectrochemical Reactions

O. Quinn Carvalho, Zebulon G. Schichtl, Nicholas F. Pompetti,
Justin C. Johnson, Elisa M. Miller, Ann L. Greenaway
Materials, Chemistry, and Computational Science
National Renewable Energy Laboratory
Golden, CO 80401

(Photo)electrochemical (PEC) reactions are a promising route to capturing solar energy and storing it long-term in stable chemical bonds. However, such processes are hindered by a variety of factors; as research in PEC fuel-forming reactions continues to grow, there is increasing interest in overcoming hindrances with conditions beyond thermodynamic equilibrium. This poster will discuss multiple examples of non-equilibrium methods for tuning PEC behavior.

Strain: The oxygen evolution reaction (OER) is the prototypical multi-electron transfer reaction in PEC fuel formation. Theoretical adsorption free energy scaling relationships predict large overpotentials (>370 mV) for metal oxides performing the adsorbate evolution mechanism in OER, based on a series of four proton-concerted electron transfer steps. Surface strain is one potential mechanism to "break" those scaling relationships. We are investigating the influence of mechanically-induced strain on OER activity of polycrystalline rutile TiO_2 thin films grown on the super elastic NiTi alloy. Our work characterizes how strain manifests in these complex polycrystalline systems with complementary characterization (e.g. X-ray diffraction, X-ray photoelectron spectroscopy), relating spectroscopic information to OER performance in alkaline electrolytes.

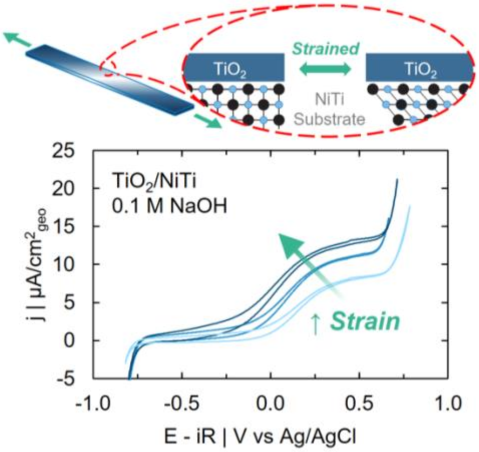

Figure 1: (Top) schematic of strain application to TiO_2. (Bottom) increasing photocurrent response for OER on TiO_2 with increasing strain.

Pressure: Carbon dioxide reduction (CO_2RR) requires a H^+ source, which has led to work in aqueous PEC environments where reaction rates are limited by reactant gas solubility competition with hydrogen evolution. Translation to high-pressure, non-aqueous (organic) environments could reduce substrate starvation, eliminate competing processes, and limit aqueous corrosion. We are establishing a high-pressure reactor which will enable investigation of CO_2RR up to supercritical pressures. This pilot reactor will be used to establish electrochemical baselines for CO_2RR on metallic surfaces with controlled H^+ concentrations, with future work focused on investigating elemental reactions under illumination in a next-gen reactor with integrated windows.

Spin selectivity: Chiral-induced spin selectivity (CISS) may enable selective generation of (photo)electrochemical products, but there has been limited fundamental research on the mechanisms underlying that selectivity. We are designing a modular system to understand how CISS manifests through different forms of chirality (stereogenic and rotational chirality) in molecular assemblies for spin selective (photo)electrocatalysis. We will investigate the influence of coupling between a molecular photosensitizer and the chiral molecular wire component, as well as how each piece should be organized in an assembly and with a semiconductor substrate to prolong spin polarized lifetimes for (photo)electrochemical fuel-forming reactions.

Evidence for Photocatalytic H_2 Evolution in Rh_2(II,II) Complexes Localized on a bncn Ligand: Design and Synthesis of Cu_2(I,I)–(bncn) Systems

Claudia Turro
Department of Chemistry and Biochemistry
The Ohio State University
Columbus, OH 43210

The photochemical proton reduction and H_2 evolution by air-stable single-molecule photocatalysts of the type *cis*–$[Rh_2(form)_2(bncn)_2]^{2+}$ (bncn = benzo[*c*]cinnoline, form = formamidinate) with red light has been shown to proceed with turnover numbers, TONs > 200 (λ_{irr} = 670 nm, 24 hours) in the presence of *p*-toluenesulfonic acid (TsOH) and BNAH (1-benzyl-1,4-dihydronicotinamide) as a sacrificial electron donor. We have recently shown that the electrocatalytic hydrogen evolution using *cis*–$[Rh_2(DPhF)_2(bncn)_2]^{2+}$ (DPhF = *N,N'*-diphenylformamidinate) that the reactivity is localized on proton-coupled electron transfer processes on a single bncn ligand. This is an important result because if this bncn-centered reactivity is also the pathway observed photochemically, then complexes with less scarce metals may have similar reactivity.

In order to investigate if the bncn-centered reactivity observed in electrocatalysis was also operative in the photocatalytic process, we designed a series of complexes with axially-caped sites to preclude the formation of a Rh–H hydride intermediate (Figure 1a). *Cis*-$[Rh_2(DTolF)_2(bpnp)(bncn)]^{2+}$ was able to photocatalytically produce H_2 under similar conditions as previous work, consistent with ligand-centered reactivity. The lower TONs observed for this complex are attributed to its shorter excited state lifetime, 1 ns. In addition, the series *cis*-$[Rh_2(DPhF)_x(OAc)_{2-x}(bncn)_2]^{2+}$ (x = 0 – 2; Figure 1b shows x = 1) was prepared to investigate the photo- and electrocatalytic production of H_2, which is also consistent with a bncn-localized reaction.

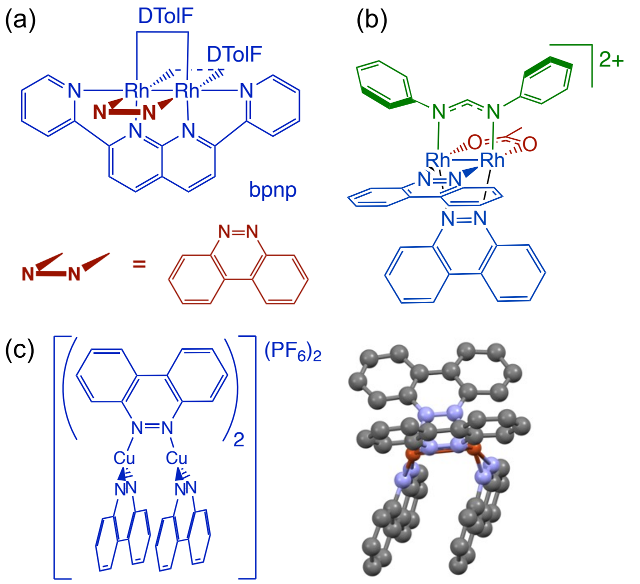

Figure 1. Molecular structures of bncn complexes with (a) blocked axial sites, (b) variation in bridging ligands, and (c) new Cu_2(I,I) complex and its x-ray crystal structure.

Very recently, we were able to synthesize and characterize a new Cu_2(I,I) complex with briding and chelating bncn ligands, *cis*-$[Cu_2(\mu\text{-bncn})_2(\kappa\text{-bncn})_2]^{2+}$, shown in Figure 1c, along with single crystal x-ray structure. This Cu_2(I,I) complex exhibits absorption in the visible range attributed to a Cu(I)→bncn metal-to-ligand charge transfer (MLCT) transition. Although the solid state structure has been determined, the temperature dependence of the ^{1}H NMR spectra show that the complex is fluctional in solution at room temperature, but not as it is cooled. We are currently using *cis*-$[Cu_2(\mu\text{-bncn})_2(\kappa\text{-bncn})_2]^{2+}$ as a precursor to exchange the two chelating ligands for a strong bridging ligand, such as acetate, formamidinate, or bpnp (Figure 1a).

Shedding More Light on Solar Photochemistry and Electrocatalysis

D. Nishiori, L. K. Hensleigh, N. Armada, I. Peterson, E. Ikediuwa, and G. F. Moore
School of Molecular Sciences, The Biodesign Institute Center for Applied Structural Discovery
Arizona State University, Tempe, Arizona 85287-1604

The immobilization of fuel-forming catalysts onto light-absorbing semiconductors provides a promising approach to producing fuels and other industrially relevant chemicals using solar energy.[1] However, realizing this strategy demands basic energy science advancements, including 1) the design of more effective electrocatalysts and 2) an improved understanding of how charge carriers (*i.e.*, the electrons, holes, and protons central to nearly all fuel-forming reactions) move within and across the phases common to solar-to-fuel assemblies. In this poster presentation, we showcase recent discoveries from our research efforts, highlighting a) evidence for breaking a molecular scaling relationship involving electrocatalysis of the oxygen reduction reaction by leveraging ligand design[2] (**Fig. 1a**) and b) experimental results showing how the mechanisms of photoelectrochemical fuel-forming reactions change with experimental conditions and reaction progress[3] (**Fig. 1b**). Our findings showcase the complexity of illumination and pH effects, including the involvement of buffer-mediated fuel formation pathways and *inverted Nernstian behavior* at high polarization. We also introduce a general yet useful formalism relating the intensity of light striking a molecular-catalyst-modified semiconductor to the turnover frequency (TOF) of the immobilized catalysts, enabling the generation of what we term *wavelength-resolved TOF plots*.

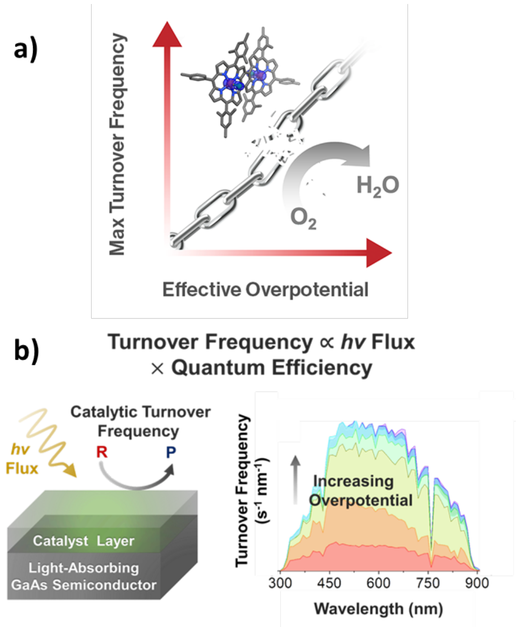

Figure 1. Depictions of (a) a catalytic Tafel plot for breaking a *molecular scaling relationship*, governing tradeoffs between kinetic and thermodynamic benchmarking parameters, (b) (left) the interplay between light absorption, charge transfer, and chemical catalysis in a photoelectrosynthetic reaction, and (right) a *wavelength-resolved turnover frequency plot.*

References

1. Reyes Cruz, E. A.; Nishiori, D.; Wadsworth, B. L.; Nguyen, N. P.; Hensleigh, L. K.; Khusnutdinova, D.; Beiler, A. M.; Moore, G. F. **Molecular-Modified Photocathodes for Applications in Artificial Photosynthesis and Solar-to-Fuel Technologies.** *Chem. Rev.* **2022**, *122*, 16051–16109.

2. Nishiori, D.; Menzel, J. P.; Armada, N.; Reyes Cruz, E. A.; Nannenga, B. L.; Batista, V. S.; Moore, G. F. **Breaking a Molecular Scaling Relationship using an Iron-Iron Fused Porphyrin Electrocatalyst for Oxygen Reduction.** *J. Am. Chem. Soc.* **2024**. DOI: 10.1021/jacs.3c08586.

3. Nishiori, D.; Hensleigh, L. K.; Nguyen, N. P.; Peterson, I.; Moore, G. F. **Shedding More Light on Solar Photochemistry**. **2024** (in preparation).

14.8% Quantum Efficient Gallium Phosphide (GaP) Photocatalyst for Hydrogen Evolution

Kathleen Becker, Chengcan Xiao, Samutr Assavachin, Anna Kundmann, Frank E Osterloh
Department of Chemistry,
University of California, Davis,
Davis, CA 95616

This renewal project ‘Photovoltage Generation at Junctions in Heterogeneous Solar Fuel Photocatalysts and Photoelectrodes’ continues investigations of photochemical charge separation at semiconductor-liquid and semiconductor-solid contacts as relevant to photoelectrochemical cells (PEC) and photocatalysts (PC) for the production of hydrogen from sunlight and water. Junctions are studied with photoelectrochemical methods and with Vibrating Kelvin Probe Surface Photovoltage Spectroscopy (VKP-SPS) to obtain the photovoltage and the electrochemical potential of the semiconductor-liquid interface. These and other parameters are used to answer fundamental questions about the workings of each electrode, incl. the effect of the redox potential of the electrolyte, the role of the kinetics of charge transfer, the impact of cocatalysts and of the light intensity, and the role of surface defects. Materials include gallium phosphide, metal oxides and oxynitrides. The poster summarizes recent results on a GaP photocatalyst for H_2 evolution.

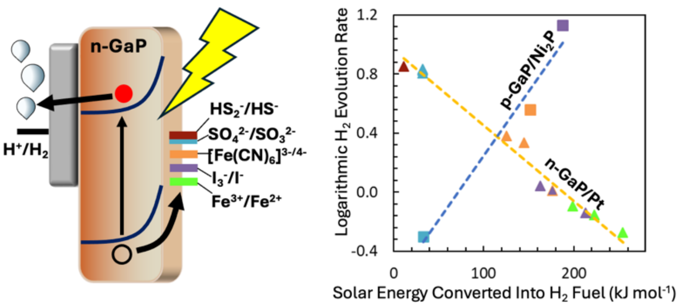

GaP is an established photoelectrode material for H_2 or O_2 evolution from water, but particle-based GaP photocatalysts for H_2 evolution are very rare. To understand the reasons, we investigated the photocatalytic H_2 evolution reaction (HER) of suspended n-type GaP particles with iodide, sulfite, ferricyanide, ferrous ion, and hydrosulfide as sacrificial electron donors, and using Pt, $Rh_yCr_{2-y}O_3$, and Ni_2P HER cocatalysts. A record apparent quantum efficiency of 14.8% at 525 nm was achieved after removing gallium and oxide charge trapping states from the GaP surface, adding a Ni_2P cocatalyst to reduce the proton reduction overpotential, lowering the Schottky-barrier at the GaP-cocatalyst interface, adjusting the polarity of the depletion layer at the GaP-liquid interface, and after optimizing the electrochemical potential of the electron donor. The work not only showcases the main factors that control charge separation in suspended photocatalysts, but it also explains why most known HER photocatalysts in the literature are based on n-type and not p-type semiconductors.

References

Becker, K., C. Xiao, S. Assavachin, A. Kundmann, and F.E. Osterloh, J. Am. Chem. Soc., **2024**. 146(11), 7723-7733. https://doi.org/10.1021/jacs.3c14545 ; Askarova, G., C. Xiao, K. Barman, X. Wang, L. Zhang, F.E. Osterloh, and M.V. Mirkin, J. Am. Chem. Soc., **2023**. 145(11), 6526-6534. https://doi.org/10.1021/jacs.3c00663 ; Assavachin, S. and F.E. Osterloh, J. Am. Chem. Soc., **2023**. 145(34), 18825-18833. https://doi.org/10.1021/jacs.3c03762 ; Cheng, Y., C. Xiao, B. Mahmoudi, R. Scheer, A.W. Maijenburg, and F.E. Osterloh, EES Catalysis, **2023**. 1, 74-83. https://doi.org/10.1039/D2EY00062H ; Daemi, S., S. Kaushik, S. Das, T.W. Hamann, and F.E. Osterloh, J. Am. Chem. Soc., **2023**. 145(47), 25797-25805. https://doi.org/10.1021/jacs.3c09546 ; Daemi, S., A. Kundmann, P. Cendula, K. Becker, and F.E. Osterloh, Energy Environ. Sci., **2023**. 16, 4530-4538. https://doi.org/https://doi.org/10.1039/D3EE02087H

Surfing the Marcus Wave: Sampling the Full Spectrum of Non-radiative Decay Regimes with the Photophysics of d^6 Polypyridyl Complexes

Mohammad Abdullah, Hayden T. Beissel, Atanu Ghosh, and James K. McCusker*
Department of Chemistry
Michigan State University
East Lansing, Michigan 48824

As part of our ongoing efforts to understand the structure-property correlations that underpin the conversion of light-to-chemical energy in first-row transition metal-based complexes, we have been able to develop isoelectronic chemical platforms that, in conjunction with our use of variable-temperature ultrafast time-resolved spectroscopy, allow us to probe excited-state dynamics in this class of chromophores in all three of the regimes defined by the Marcus relation.

Normal Region. This region is defined by the condition wherein the magnitude of the driving force for a given process (in our case, ground-state recovery) is exceeded by the reorganization energy required to accommodate the structural changes associated with that process (i.e., $|\Delta G_0| < \lambda$). We have established that polypyridyl complexes of Fe(II) generally fall into this regime. Using a series of 4'-substitued Fe(II) bis-terpyridyl complexes wherein the reorganization energy remains constant, increases in the zero-point energy difference between the lowest-energy ligand-field excited state of the compound (${}^5T_2$) and its ground state (${}^1A_1$) are accompanied by the expected increase in the rate constant for decay.

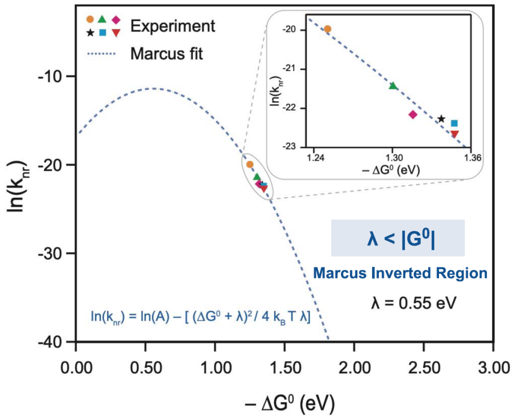

Figure 1. Plot of driving force versus rate constant for ground-state recovery in a series of Co(III) polypyridyl complexes. (Chan et al. *Science* **2023**, *382*, 191)

Inverted Region. When the driving force for a given process exceeds the reorganization energy ($|\Delta G_0| > \lambda$), Marcus Theory predicts that the rate constant for the process will begin to decrease. We have confirmed this phenomenon in the ground-state recovery dynamics of Co(III) polypyridyl complexes: as the zero-point energy for ground-state recovery increases, we observe a decrease in the rate constant for non-radiative decay (Figure 1). This shift in behavior relative to corresponding Fe(II) complexes occurs due to a change in the identity of the lowest-energy ligand-field state from ${}^5T_2$ in the latter to ${}^3T_1$ in the former. Specifically, the combined effect of a larger zero-point energy difference upon moving from Fe(II) to Co(III) and a smaller reorganization energy associated with the ${}^3T_1$ state was identified as giving rise to these observations. Its potential significance goes beyond fundamentals, as we have been able to leverage this effect to carry out photoredox reactions with Co(III) with yields that are more than an order of magnitude higher than was achieved using Ir(III)-based chromophores.

Barrierless Region. Finally, we have discovered one Fe(II) compound that, due to a fortuitous combination of driving force and reorganization energy, does not exhibit any significant temperature dependence in its excited-state lifetime in CH_3CN solution. This rare example of the barrierless region ($|\Delta G_0| \approx \lambda$) is providing us a unique opportunity to examine outer-sphere contributions to the overall reorganization energy through variations in the solvent.

High-resolution investigations of molecular catalyst microenvironment

Niklas B. Thompson, Zhu-lin Xie, Jens Niklas, Oleg G. Poluektov, David M. Tiede, Karen L. Mulfort
Division of Chemical Sciences and Engineering
Argonne National Laboratory, Lemont, IL 60439

The activity and mechanisms of molecular catalysts that facilitate small molecule transformations relevant to solar energy conversion are strongly influenced by secondary coordination sphere and solvation effects. Therefore, a prime focus of our team is to uncover these effects, and understand how they respond to synthetic modifications and solution conditions with an eye toward developing design principles for catalysts with enhanced selectivity and stability. We are focusing these efforts on a series of Co(II)poly(pyridyl) complexes (Figure 1A) from our group that are highly effective and stable H_2 evolution photocatalysts in near-neutral aqueous conditions with $Ru(II)(bpy)_3$ sensitizer and sacrificial electron donors. These catalysts are readily modified at the bpy-bridging nitrogen group, providing a handle to tune metal- and ligand-centered redox potentials, as well as introducing sites for substrate binding or solvent restructuring around the metal center. This poster will describe our group's recent work toward developing a high-resolution picture of catalyst microenvironment using high-energy X-ray scattering and pair distribution function analysis (HEXS/PDF) and pulsed EPR spectroscopy methods.

The HEXS response for Co-H and Co-pyMe was collected at 101.7 keV under catalytically-relevant conditions to investigate how the intramolecular and catalyst-solvent pairwise interactions change with pH since we observed a strong pH-dependence on catalytic activity (Figure 1B). The differences in the low-*Q* region for Co-H at pH 3 versus 7 indicate reorganization of the solvent cage; this effect is much less pronounced for Co-pyMe. The relatively dramatic alteration of solution-phase molecular structure with pH for Co-H, largely lacking for Co-pyMe, suggests that the dangling group rigidifies the molecular structure through interactions with free or Co-bound water. The ^{1}H-ENDOR difference spectra comparing Co-pyMe with 1 or 20 equivalents H^+ relative to no added acid reveals two different protonation sites at ~5 and ~3 Å from the Co(II) spin center, corresponding to protonation of the pyridine and bridging nitrogen, respectively (Figure 1C). We will interpret these complementary experimental studies with DFT calculations and molecular dynamics simulations to create a complete picture of protonation and solvation structure which will inform advanced catalyst designs.

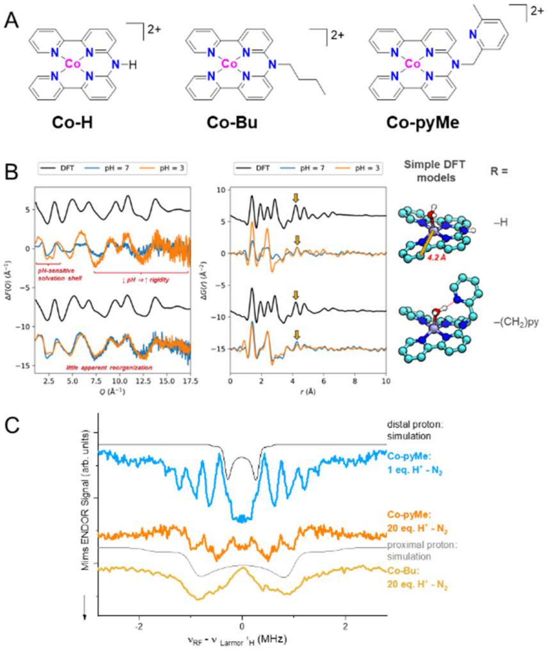

Figure 1. A) Chemical structures of Co(II)poly(pyridyl) HER photocatalysts. B) Comparison of reduced HEXS response (left) and G(r) in real space (middle) for 15 mM Co-H and Co-pyMe in aqueous solution at pH 3 or 7, and DFT models indicating relevant pairwise interactions (right). C) Mims-type ^{1}H ENDOR difference spectra for Co-R in the presence of 1 or 20 equivalents acid; spectra collected in 1:2 $CH_3CN:CH_2Cl_2$, 15 K.

Solar Energy Conversion Enabled by Ligand Exchange Reactions

E. Firestone, S. Kaushik, T.W. Hamann
Chemistry
Michigan State University
East Lansing, MI 48824

Solar photochemical systems that convert sunlight to electricity or chemical fuels involve a series of electron-transfer steps following light absorption to produce a charge separated state. Charge separation in dye-sensitized solar cells (DSSCs) occurs by injection of an electron from the excited dye molecule to the semiconductor and reduction of the oxidized dye by a redox couple dissolved in solution. These processes complete with back electron transfer (recombination) from the semiconductor to oxidized dye or redox couple. Redox couples thus must be good electron donors and poor electron acceptors, which generally comes at the cost of a significant energy penalty, and thus efficiency loss, to drive the forward reaction. The overarching goal of this project is to design first-row transition metal coordination complexes capable of controlling the kinetics of such electron-transfer reactions.

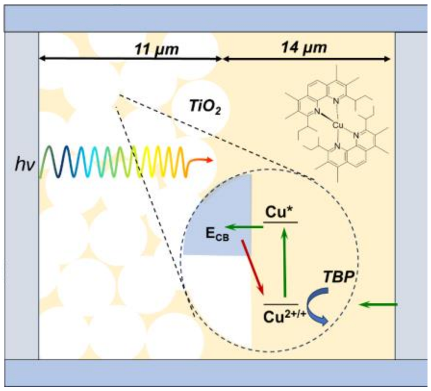

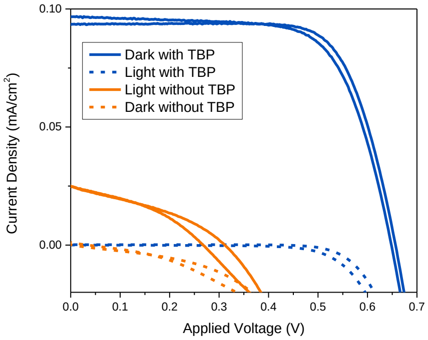

This poster will present our recent efforts investigating the use of a copper complex dissolved in solution to act as both the dye and redox couple. Such a system has many advantages including eliminating the dye regeneration electron transfer step and the associated energy penalty which can enable higher efficiencies than traditional DSSCs. There are many demands on such a complex, including adequate light absorption, long excited state lifetime to enable contact with the semiconductor surface before relaxing to the ground state, favorable energetics for charge separation, and slow recombination to allow good change collection.

$[Cu(dsbtmp)_2]^+$ (dsbtmp=bis(2,9-di(sec-butyl)-3,4,7,8-tetramethyl-1,10-phenanthroline) was shown to have excited-state lifetimes >1 μs in a variety of solvents. A molar absorptivity of 7400 M^{-1} cm^{-1} at 445 nm allows excellent visible light absorption within a ca. 10 micron TiO_2 mesoporous electrode. The excited state potential is several hundred mV negative of the conduction band edge of TiO_2, thus allowing charge separation. Charge collection is constrained by fast recombination limiting the photovoltage and charge collection, however. Introduction of tert-butyl pyridine (TBP) to the electrolyte was found to displace one dsbtmp ligand from $[Cu(dsbtmp)_2]^{2+}$ which results in a poor electron acceptor species and quantitative charge collection. A detailed analysis of the fundamental processes giving rise to the overall solar energy conversion of this system will be presented, with the rate limiting steps identified and future paths to overcome the current bottlenecks.

Mechanisms of Long-Distance Charge Separation and Efficient Plasmon Induced Hot Electron Transfer in Colloidal Nano-Heterostructures

Tianquan (Tim) Lian
Department of Chemistry
Emory University
Atlanta, Georgia 30322

The long term goal of the project is to understand fundamental charge transfer processes in colloidal quantum confined semiconductor nanocrystal/catalyst complexes for solar energy conversion. The current project objectives include: 1) understanding interaction and charge transfer between nanocrystals and adsorbed catalysts, 2) exciton and carrier dynamics in electrochemically charged nanocrystal/catalyst complexes, 3) hot electron transfer in plasmonic semiconductor nano-heterostructures. In this poster presentation, I will provide an update of our progress on these objectives.

1) Fano resonance between excited QDs and adsorbed catalysts: dependence on QD size and coupling strength. The interaction between surface adsorbate vibrations and the intraband electron absorption within nanocrystals leads to Fano resonance in the vibrational spectrum of the complex and it may influence the photophysical properties of both NCs and adsorbate molecules and the photocatalytic performance of these materials. Here, we investigate the dependence of Fano resonance on the QD size, QD shell thickness, and catalyst loading dependence using a CO_2 reduction catalyst, $Re(CO)_3(bpy\text{-}COOH)Cl$ (ReC0A), bound to CdSe and CdSe/ZnS quantum dots. We observe that the Fano resonance appears instantaneously with the conduction band electrons. The Fano resonance signal strength decreases at larger QD size, larger shell thickness, or decrease of adsorbed ReC0A molecules, reflecting its dependence on their coupling strength.

2) Charge transfer in electrochemical controlled nanocrystal/catalyst complexes. Unlike molecules, semiconductor nanocrystals have poorly characterized trap states within their band gap. The occupancy of these states depends on the conditions of the solution (such as the formal potential of the dominant redox couples) and are often poorly controlled; but it can have profound effects on the excited state and charge transfer properties of NC/catalyst complexes. In this project, we are examining the effect of applied bias on exciton dynamics in semiconductor NCs and interfacial charge transfer properties of well-characterized NC/molecule complexes, such as CdSe/methylviolgen. We will report the effect of applied bias on the static state absorption, photoluminescence and transient absorption properties nanocrystals, and discuss how they reflect the filling of the trap and band edge states.

3). Semiconductor plasmonics. Heavily doped semiconductor NCs are a new class of plasmonic materials whose properties differ significantly from their metallic counterparts and the mechanism of hot carrier generation and transfer in these materials are poorly understood. In this project, we are examining the mechanism of plasmon induced hot electron transfer in p-CuS/CdS nanorod heterostructures. We demonstrated rapid plasmon induced hot electron transfer from Cu_7S_4 to the CdS domain (faster than 200 fs) upon near-IR excitation (1400 nm) of the Cu_7S_4 plasmon band, and the lifetime of transferred electrons is 6.46 ± 0.53 ns, much longer than Au/CdS interface. Our results demonstrate promising potentials of plasmonic semiconductors for driving chemical reactions with near-IR light.

From UV to XUV: Revealing interfacial charge dynamics in semiconductor heterostructures

Conner Dykstra, Lauren Boedicker, Brandon Rasmussen, Josh Vura-Weis
Department of Chemistry
University of Illinois at Urbana-Champaign
Urbana, IL 61801

Charge separation and diffusion at interfaces is a crucial step in semiconductor photochemistry, and is often a major factor that limits their efficiency. In systems as diverse as dye-sensitized solar cells, quantum dot heterostructures, and organic photovoltaics, charge transfer across an interface first creates a bound state before full charge separation yields free carriers. There are several potential sources of this bound state even in high-dielectric materials, including intrinsic surface states, charge localization on defects, and band bending. In this work, we use a combination of femtosecond transient visible and ultraviolet spectroscopy to study the charge injection from CdSe quantum dots into ZnO nanowires. The visible probe selectively probes the CdSe band-edge bleach and reveals both the initial exciton formation and the subsequent injection of a photoexcited electron. The UV probe selectively probes the appearance of free carriers in ZnO. A delay is observed between the CdSe injection signal and the ZnO free-carrier signal, a phenomenon that has been previously attributed to a surface Charge Transfer State (CTS). However, our analysis of a range of QD sizes reveals that a band-bending model incorporating two populations of QDs matches well to the experimental result.

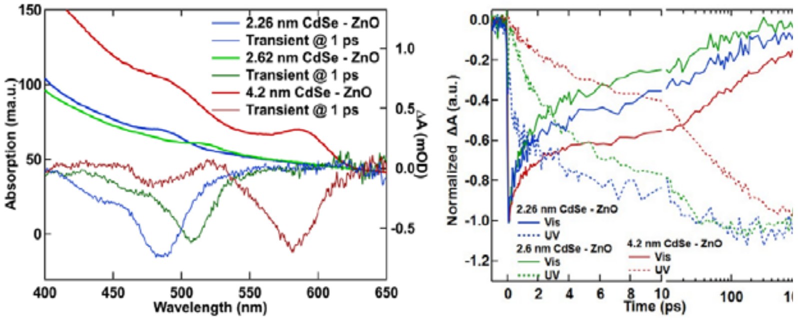

Figure 1: Optical transoent absorption of CdSe QDs on ZnO nanorods. UV and Vis probes reveal ZnO and CdSe dynamics, respectively

We will also show first results from a new tabletop femtosecond soft X-ray transient absorption instrument that will provide a new tool for the photochemistry community. This system uses high-harmonic generation to produce a broadband continuum from 100-300 eV, a range that is resonant with the core-to-valence transitions of elements such as B, C, P, S, and most lanthanides. Initial experiments will focus on mapping the element-specific charge distribution of organic photovoltaic heterostructuctures from the initial exciton, to the charge transfer state, and finally to free charges.

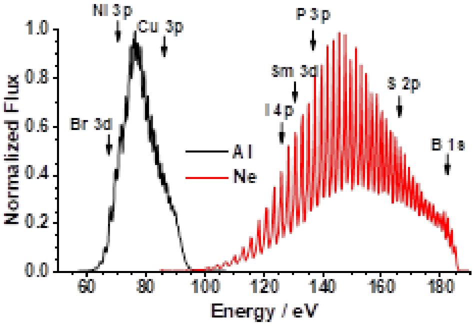

Figure 2: Soft X-ray spectrum produced via high-harmonic generation in Ar and Ne, with corresponding atomic edges

Improving and measuring water oxidation catalyst viability

Colton Breyer, Miguel Ibanez, Jake Kerkhof, Mustafa Yildirim, Nilay Kanova, Diane Smith*,
Douglas Grotjahn*, Jing Gu
Department of Chemistry and Biochemistry
San Diego State University
San Diego, CA, 92182

* Diane deceased on 24 Oct 2022 and Doug deceased on 26 Oct 2023, this presentation is in memory of them

The Overall goals of the project are to (1) slow water oxidation electrocatalyst (WOEC)'s degradation rate, (2) enable molecular WOEC activity in acid, and (3) create and refine new methods for characterizing WOEC kinetic data. Good progress has been made in all three areas.

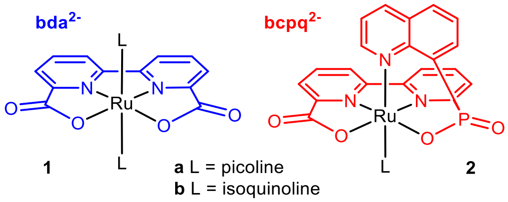

For the first goal, we discovered the benefit of employing a high valence phosphinate [P(V)] as a connecting element relative to the conventional carboxylates to increase the ligand denticity. The new bcpq ligand allows the formation of [Ru(II)(bcpq)(L)] (**2a-b**, L = picoline or isoquinoline). In comparison to [Ru(II)(bda)(L_2)](**1a-b**, L=picoline or isoquinoline), where bda ligand contains a carboxylate group, **2a-b** shows impressive rates of O_2 formation with the presence of sacrificial oxidant and under electrochemical conditions, **2b** remained completely homogeneous over 15 h electrolysis at pH 7 where **1b** was no longer homogeneous.

Ligands functionalized with an external pendent base are believed to help facilitate proton-coupled electron transfer in the water oxidation process. For the second goal, the effects of electron donor and withdrawing groups on the parent compound **3** ([Ru(X-tpy)(phen-SO_3)OTF]) were studied. Functionalization of the terpyridine ligand with an electron-withdrawing group shifted oxidation potentials more positively, whereas an electron donor group shifted the oxidation potential more negatively. Compared to X=H, taken 7 h for the full conversion of sacrificial oxidant Ce(IV), the full conversion of X=OEt occurred in 30 min with a 30 times faster TOF. DFT revealed that two sequential electron transfers along with proton transfer (ETPT), under the presence of CAN, the Ru(II)-aqua complexes [**1a-OH$_2$**], [**1b-OH$_2$**], and [**1d-OH$_2$**] are converted into the respective Ru(III)-oxyl complexes [**1a-O·**], [**1b-O·**], and [**1d-O·**].

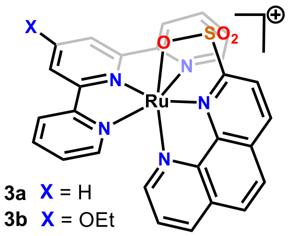

3a X = H
3b X = OEt
3c X = NO_2
3d X = CF_3

For the third goal, analysis of homogeneous water oxidation catalysts proves to be difficult via the conventional limiting current analysis and foot-of-the-wave (FOWA) analysis methods due to water acting both as solvent and substrate. We propose a method for analyzing non-ideal cyclic voltammetry waveshapes in water oxidation. This is accomplished by analyzing rate data for a large range of potentials to find the optimal potential where linear fits for plots of i_{cat}/i_p vs $v^{-½}$ and k_{cat} vs [B] may be obtained. Herein, the optimal potential E_{cat} is the potential at which catalytic current i_{cat} is nearly independent of scan rate and has a linear dependency on buffer concentration.

Dexter Energy Transfer Mechanisms

Hassan Alkhunaizi[1], Spyroulla A. Mavrommati[2], Peng Zhang[1], Spiros S. Skourtis[2]
and David N. Beratan[1]
[1]Department of Chemistry, Duke University, Durham, NC 27708
[2]Department of Physics, University of Cyprus, Nicosia 1678, Cyprus

The ability to direct the flow of triplet excitons through molecular and nanostructured assemblies is expected to have a significant impact in energy science. The migration of triplet excitons over long distances is essential for triplet fission and fusion, processes of great interest for enhancing the performance of solar cells and semiconductor materials. This project focuses on developing and applying theoretical models to understand and control Dexter mechanism energy transport (DET), the operative mechanism for triplet energy transport. We are formulating theories of Dexter coupling in molecular assemblies and establishing system design guidelines to develop novel molecular structures with the aim of transporting triplet excitons over extended distances.

Completed Studies: We have established design rules for polychromophoric structures that enable coherent long-distance triplet exciton transfer (TET) between the chromophores. As well, we developed a method to compute Dexter couplings using adiabatic energy splitting by altering molecular geometries to drive the systems into quasi-degenerate energy transport complex. We have studied the mechanism of TET between CdSe/CdS core-shell quantum dot and an organic acceptor as a function of shell thickness, and found that TET in core-shell assemblies cannot be described as the simple product of charge transfer (electron and hole transfer) steps. We have also explored unique advantages that may be derived from performing quantum simulations on quantum computers to describe key transport processes.

Ongoing Studies: 1) Building Dexter wires with efficient metal-to-metal Dexter transport channels. We are using theoretical analysis and electronic structure calculations to explain recent experiments that observed long-range DET in self-assembled wires with platinum- and palladium-based monomers. Our findings indicate enhanced DET couplings at room temperature, supporting fast metal-centered coherent DET. **2) Borrowing Förster Coupling to Drive Long-Range Dexter Transport.** We developed analytical and computational approaches to estimate the Dexter couplings between transition metal containing chromophores. We studied the use of spin-orbit coupling interactions to enhance Dexter couplings by borrowing interaction strength from the stronger Förster interaction between chromophores. **3) Realizing Excitonic Wires with Disorder: Flickering Resonance.** We combine electronic structure calculations with quantum dynamics simulations to develop a rigorous theoretical framework to assist the design of assemblies that support long-range and coherent DET via flickering resonance mechanisms.

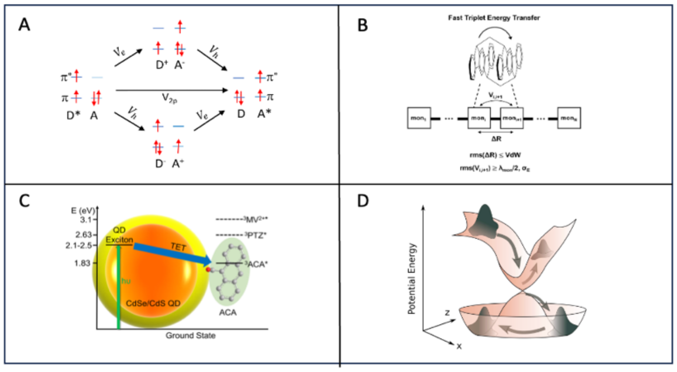

Design Principles and Effects of Semiconductor|Molecule Electronic Coupling: Symmetry, Hybridization and (Photo)Electrochemical Function

Michael J. Rose
Department of Chemistry
University of Texas at Austin
Austin, TX 78712

The interactions between surface ligands and semiconductor materials to a large extent determines properties such as charge transport, band-bending, charge separation and the function of attached catalysts. In the absence of defects, semiconductor photoelectrochemical (PEC) function is governed by (*i*) the electronic structure of the material, (*ii*) the electronic structure of interfacial molecules, and (*iii*) the communication between these two systems. We demonstrate the principles and PEC effects of surface modification by evaluating symmetry-adapted linear combinations (SALCs) between semiconductor plane-waves and molecular orbitals. Our approach utilizes Si(111) facets covalently modified with acenes (anthracene, tetracene, pyrene, etc). The formation (or not) of SALCs is determined by the following: (*a*) *symmetry* (mis)match between semiconductor plane-waves and molecular orbitals; (*b*) *energy* (mis)match between plane-waves and orbitals; and (*c*) the *connectivity* between the two systems.

We hypothesized that silicon|acene hybridization would result in higher photovoltages due to greater induced dipole at the interface, which would in turn increase the Schottky barrier height and provide more band-bending. We find portions of this hypothesis to be proven, and other portions to be disproven (*i.e*. better performance was obtained for a different reason). Both Si-Anth and Si-Tet result in valid SALCs with strong VB|HOMO coupling and induced dipoles, which increase photovoltage. However, the Tet LUMO is symmetry-incompatible with Si CB, resulting in a decoupled Tet LUMO. This generates beneficial charge accumulation in CB|LUMO surface states that are outside of the bandgap, providing additional barrier height (upon illumination). The result is our highest yet Si-R|TiO_2|Pt HER photovoltage ($V_{onset} \approx 300$ mV). Ongoing work:

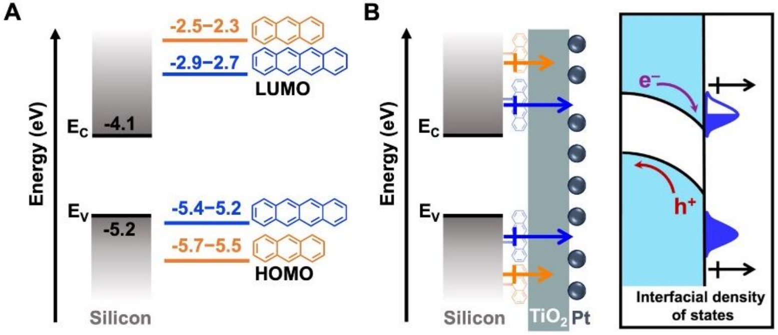

- Extent of charge-drop across hybridized interfaces like Si–Anth or Si–Tet
- Symmetry-versus-Energy effects on coupling using acenes (pyrene, phenanthrene, perylene)
- Changes in spectroscopic bandgap and DOS (UPS/LEIPS) upon surface modification
- Electrochemical impedance (EIS) investigation of band-edge-hybridized states

References

1. Rose, M. J. (*Perspective*) “Semiconductor Band Structure, Symmetry and Molecular Interface Hybridization for the Chemist”. *JACS* **2024**, *146*, 5735-5748.
2. Hallock, C. D; Rose, M. J. “EIS of Well-Passivated Silicon and Germanium Semiconductors Reveals Bandgaps, Fermi Levels & Interfacial DOS”. *In revisions*.
3. Pollok, B.; Brinker, J.; Lewis, S.; Daemi S.; Roberts, S.; Eaves, J.; Osterloh, F.; Rose, M. “Tetracene Functionalized Si(111) Achieves Enhanced Energy Conversion”. *Submitted*.

Decoding Semiconductor Voltammetry via a Convolutive Analytical Model and a Machine Learning Algorithm

Dylan Vitt, Yifan Liu, Alex Devine, Naomi Raicu, and Stephen Maldonado
Department of Chemistry
University of Michigan
Ann Arbor, MI 48109-1055

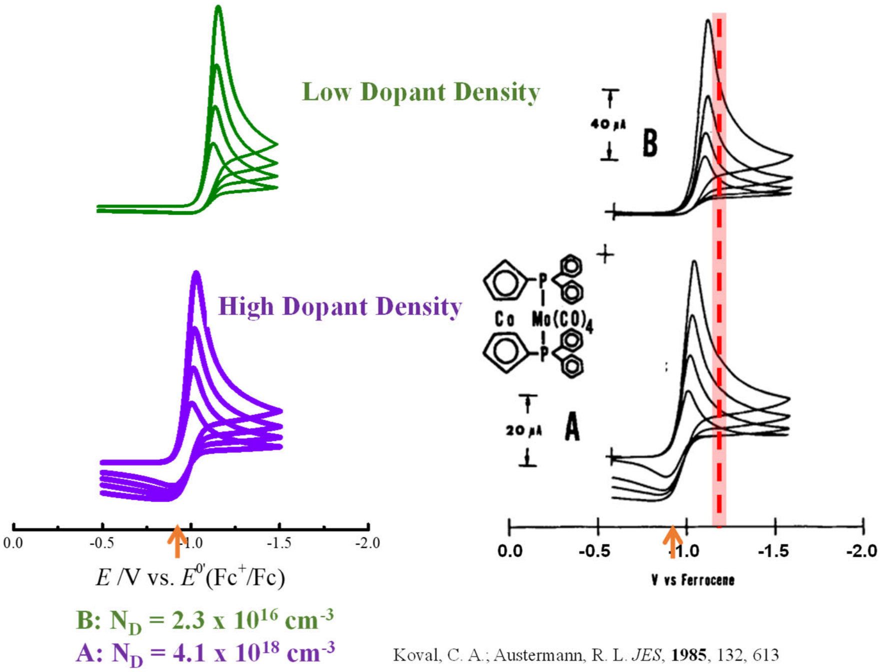

Koval, C. A.; Austermann, R. L. *JES*, **1985**, 132, 613

Figure 1. Comparison of (right) experimental voltammograms for n-InP and a cobalt-molybdenum metallocene reported by the Koval group in 1988 and (left) simulated voltammograms generated by the convolutive transform of semiconductor heterogeneous charge-transfer rate constants.

This presentation will describe the use of a convolutive transform to adapt the analytical expressions for the heterogeneous charge-transfer rate constants at semiconductor-liquid contacts developed in the prior project period. This extension of the model allows simulation of voltammograms for freely diffusing redox species to a planar semiconductor macroelectrode. Voltametric responses from this convolutive model will be presented as a function of system parameters of interest (e.g. band edge values, scan rate, standard potential of redox species, surface oxide thickness, dielectric constants of solvent, semiconductor, and surface layer(s)). The utility of this model to describe experimental data will be demonstrated on two different datasets. Voltammetric data with InP electrodes reported by the Koval group (**Figure 1**) and data with Si electrodes collected by our lab will be analyzed. A key finding is that it is possible to determine the semiconductor band edge values from sets of voltammograms with precisions comparable to or better than impedance measurements. The utility of this model to analyze sets of voltametric data with a machine learning algorithm will also be presented. Preliminary data will be presented on a methodology that allows the usage of the convolutive model without requiring a comprehensive understanding of the underlying mathematical framework.

Triplet-Pair Mediated Systems for Multiexciton-Driven Photochemistry

Matthew Y. Sfeir,[1,2,4] Luis M. Campos,[3] Guiying He,[1,2] Huaxi Huang,[3] Bernardo Salcido-Santacruz,[2,4] Daniel Malinowski[3]

[1]Department of Physics, Graduate Center, City University of New York, New York, NY 10016, USA
[2]Photonics Initiative, Advanced Science Research Center, City University of New York, New York, NY 10031, USA
[3]Department of Chemistry, Columbia University, New York, New York 10027, USA
[4]Department of Chemistry, Graduate Center, City University of New York, New York, NY 10016, USA

Exerting precise control over processes driven by singlet and triplet excitons is of paramount importance in organic optoelectronics and photochemistry. The principles underpinning energy and charge transfer have led to robust guidelines to molecularly engineer advanced excitonic materials. However, a reexamination of these principles is required to develop new paradigms for triplet-pair multiexciton-driven photochemistry. In this program, our approach is based on the molecular engineering of intramolecular singlet fission (iSF) compounds, in which a triplet-pair can be generated in isolated molecules in solution as the primary photoproduct with high yields and long lifetimes. We focus on treating the triplet-pair [T_1T_1] as a distinct excited state from a singlet or triplet exciton, with its own characteristic multi-reference wavefunction, total energy, and spin angular momentum.

Here we present a study on the efficient direct photochemical conversion of triplet-pair multiexcitons by energy and charge transfer process. For example, we describe and validate a second generation [G2] iSF chromophore design that enables the generation of a charge separated (CS) state directly from the [T_1T_1] state. We identify this process using the characteristic spectral signatures of the triplet pair and oxidized donor moiety. Importantly, we show that the CS state is not energetically accessible from an individual triplet exciton. We establish key principles for second generation iSF model systems in which the formation of CS states from [T_1T_1] depends on the dielectric environment, energetics of the building blocks, and molecular connectivity. These studies unveil the potential capabilities of the multiexciton states in an integrated molecular system to facilitate favorable energy and charge transfer processes for solar photochemical reactions.

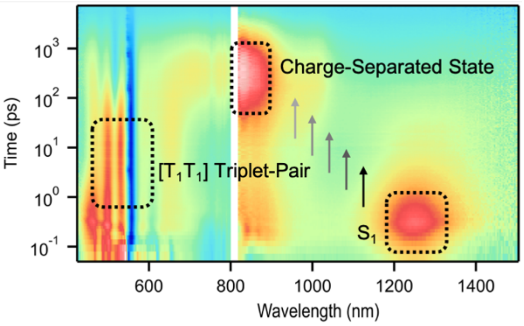

Figure: Transient absorption spectra of a second-generation singlet fission chromophore that generates a charge-separated state mediated by the triplet-pair.

Conformational Control for Photoinduced Charge Separation

Bronte Charette, Paul Griffin, Jiaqi Chen, Shuohao Wang, Lisa Olshansky
Department of Chemistry
University of Illinois, Urbana-Champaign
Urbana, IL 61820

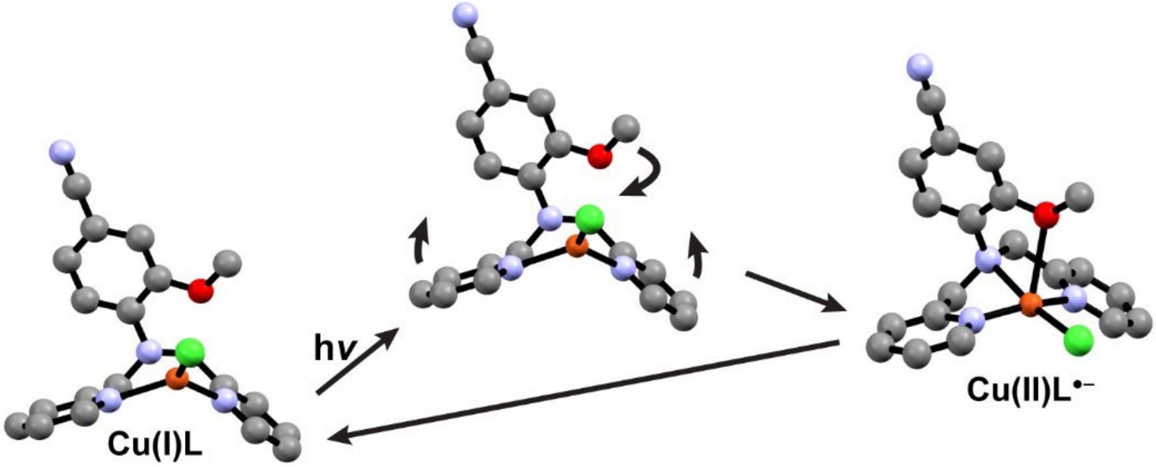

We report progress toward the development of earth-abundant coordination complexes in which light-induced conformational rearrangements enable gated electron transfer (ET). By leveraging the oxidation state-dependent changes in coordination geometry and hard-soft-acid-base properties associated with the Cu(II/I) redox couple, these complexes are designed to ue structural control to hasten charge separation (CS), and slow charge recombination (CR). A series of Cu(II/I) complexes utilizing dpa^R ligands (dpa = dipicolylaniline equipped with an *ortho*-R functional group of either OMe or SMe) have been prepared and studied. These complexes are each conformationally fluxional in one oxidation state and exhibit unexpectedly large ET self-exchange rate constants of $2.48(6) \times 10^5$ and $2.21(9) \times 10^6$ M^{-1} s^{-1}, respectively. Among the fastest reported for molecular copper coordination complexes to date, that of $[CuCl(dpa^{SMe})]^{+/0}$ exceeds all others by an order of magnitude and compares only to those observed in type 1 blue copper proteins. The dynamicity of these complexes establish pre-steady-state conformational equilibria that minimize the inner sphere reorganization energies (λ_i) to 0.71 and 0.62 eV for R = OMe and SMe, respectively. We then modified these complexes with photooxidants capable of driving CS. Initial efforts used twisted intramolecular charge transfer (TICT) fluorophores for this purpose. Investigations by time-resolved emission and transient absorption spectroscopies, as well as TDDFT calculations revealed that, though we are likely generating a transient CS state, its lifetime is fleetingly short. We hypothesize that the short lifetimes of these CS states result from a mismatch in the driving force ($\Delta G_{CS}°$) and value of λ_i for these complexes. Accordingly, new dpa^R ligands are now being prepared with acridine photooxidants, who's excited state reduction potentials that will produce $\Delta G_{CS}° \sim 0.8$ eV, well-matched with the measured values of λ_i. Upon generation and characterization, we aim to prepare a series of similar derivatives to enable the construction of a Marcus curve correlating $\Delta G_{CS}°$ with k_{CS}. Through these efforts, we aim to produce long-lived (~μs) CS states using first row transition metals and to demonstrate a new approach in photodriven CS. This approach harnesses biomimetic conformational gating to control the directionality and duration of photoinduced CS.

Relating Photochemical Pathways to Oxygen Evolution in Cobalt Oxide Materials Using Ultrafast X-ray Spectroscopy and X-ray Solution Scattering

Michael W. Mara, Zachary Mast, Justin Hoffman, Tyler Haddock, Brian Phelan, George Schatz,
Karen Mulfort, David Tiede, Lin X. Chen
Chemical Sciences and Engineering
Argonne National Laboratory
Lemont, IL 60539

CoPi, an amorphous cobalt oxide formed by anodic electrochemical deposition from aqueous phosphate buffer containing Co(II) ions, is a promising oxygen evolution reaction (OER) catalyst in solar fuels applications. Recently, photoelectrocatalytic activity of CoPi has been discovered with excitation wavelength dependent OER activity, with blue light inhibiting OER and red light enhancing it. To understand and ultimately control these photocatalytic pathways, the photogenerated excited-state trajectories that drive productive OER reactivity must be characterized. This is challenging owing to the heterogenous nature of the native cobalt oxide catalyst, motivating complementary studies on molecular cobalt–oxo cubanes that serve as atomically-precise model complexes. These cubanes are competent precatalysts for electrochemically driven OER in their own right, possessing a core structure reminiscent of that in photosystem II. We investigated the ultrafast dynamics of photoexcited CoPi and cobalt cubane using time-resolved X-ray absorption spectroscopy (XAS) and X-ray emission spectroscopy (XES). *Operando* time-resolved Co K-edge XAS of CoPi was performed at the Advanced Photon Source, where 400 nm photoexcitation was shown to prompt a photoreductive response, increasing the amount of Co(II) sites and inhibiting OER. For cobalt cubanes, the most pronounced dynamic evolution occurs within the first few ps following photoexcitation, so the cubanes were investigated by ultrafast XAS and XES using XFEL radiation following 400 nm excitation. The XES measurements indicate that the cubanes are dominated by excited-state spin changes, with the spin dynamics heavily dependent on the redox state of the Co centers. Ultrafast Co K-edge XAS spectra of cobalt cubane exhibit an edge shift consistent with a spin change, as well as difference signals in the post-edge associated with an expansion of the cubane core. Future work will utilize ultrafast X-ray solution scattering of aqueous cobalt cubane to quantify both the expansion in the cubane core and the solvent reorganization that alters H-bonding interactions between solvent waters and the cubane oxo groups. The experiments here will be coupled to computational modeling and supplementary optical measurements to elucidate the mechanism for photocatalytic enhancement of OER in amorphous cobalt oxides and reveal the role of intermolecular hydrogen bonding in stabilizing reactive intermediates in aqueous media.

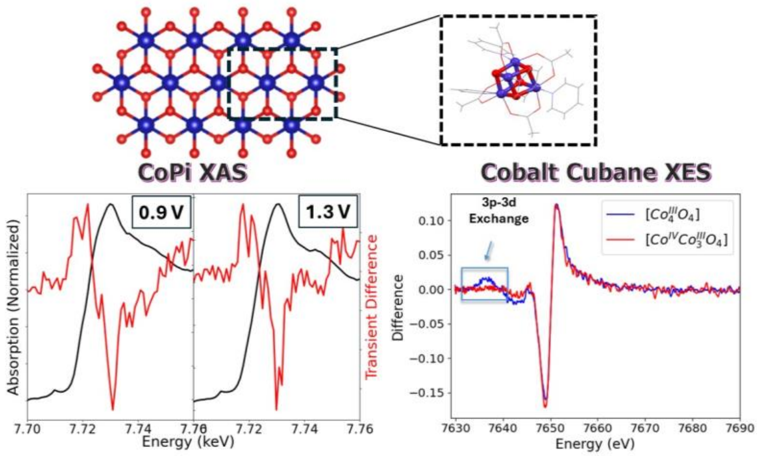

Controlling water splitting using chirality-induced spin in electrocatalysis

Jeiwan Tan, Md Azimul Haque, Demelza Wright, Debjit Ghoshal, Simran Saund, Trung Huu Le, Michelle Smeaton, Katie Jungjohann, Elisa Miller, Matthew Beard, Nathan Neale, Jao van de Lagemaat
Chemistry and Nanoscience and Materials Science Centers
National Renewable Energy Laboratory
Golden, Colorado, 80401

In this presentation, we study the effect of chiral ligands during the electrodeposition of copper electrocatalyst This leads to enantiospecific copper structures that show a remarkably strong circular dichroism (CD) response (Fig 1. Top). The chiral molecules are apparently able to impart chirality to the copper structure and induce a CD response in the surface plasmon region as well as in the higher energy band-to-band transitions. We also observe significant shifts of the onset potential of hydrogen evolution reaction (HER) on these chiral Cu catalysts to more negative potentials compared to the achiral counterparts despite otherwise identical physical and chemical properties of the catalyst films as evident from electron microscopy, photoelectron spectroscopy and other characterization methods. Electrochemical impedance spectroscopy suggests that the results are explained by an altered reaction pathway involving less facile surface diffusion of intermediates and therefore more sluggish HER kinetics on the chiral Cu catalysts owing to the electrons reaching the surface having an aligned spin. This spin alignment would be imparted by a chirality induced spin selectivity (CISS) as has been observed in other systems. The strong chiral optical response of the catalysts also implies that light could be used to further impact the selectivity. Also, the observations immediately suggest that chirality in the electrocatalysts could be used to control the selectivity during CO2R/N2R and other valuable reduction reactions.

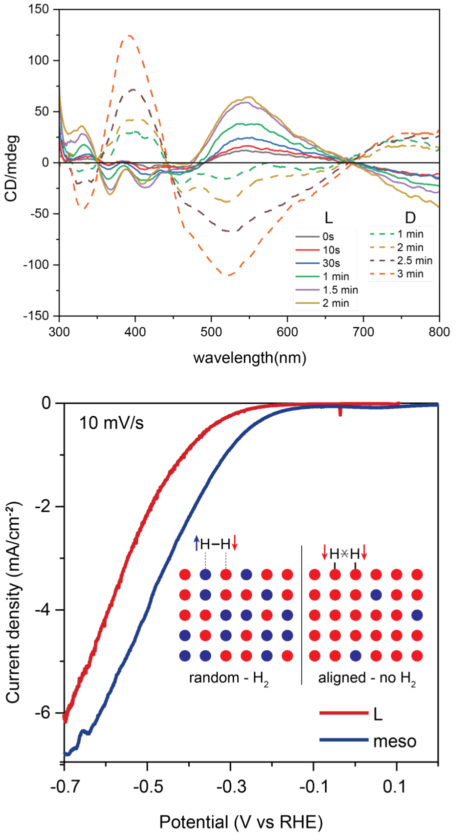

Fig1. Top: Circular dichroism observed during copper catalyst deposition on F-doped SnO_2 for the L and D form of the surface active agent. The meso variant gives negligible dichroism during deposition. Bottom: current-voltage plot for hydrogen evolution using chiral and achiral copper in pH 7.4 buffer solution. The inset shows a possible model for suppression of hydrogen evolution from the chiral copper surface.

Electrochemical carbon dioxide reduction (CO2R) to valuable products such as CO, CH_4, formic acid, ethylene and other products as well as ammonia generation from nitrogen reduction (N2R) in aqueous electrolytes suffers from low Faradaic efficiency and selectivity due in part to the competing HER reaction. We can therefore expect that using the CISS effect to suppress the HER reaction can lead to improved selectivity for CO2R, N2R and other valuable electrochemical fuel forming reactions.

Photo-induced and Spin Polarized Charge Transfer at Semiconductor/Molecular Interfaces

Xiaoyang Zhu and Colin Nuckolls
Department of Chemistry
Columbia University
New York, NY 10027

This research program aims to establish fundamental mechanisms for spin-selective photochemistry at semiconductor/molecule interfaces. Spin-polarized electrons can improve the efficiency and selectivity of photo- and electro-catalytic reactions, as demonstrated in the past with magnetic or magnetized catalysts. During the current funding period, the PIs successfully demonstrated a scheme in which spin-polarized charge separation occurs at the interfaces of nonmagnetic semiconductors and molecular films in the absence of magnetic field. The PIs take advantage of the spin-valley-locked band structure and the valley-dependent optical selection rule in group VI transition metal dichalcogenide (TMD) monolayers to generate spin-polarized electron-hole pairs. Photo-induced electron transfer from monolayer WS_2 to fullerene (C_{60}) and hole transfer from $MoSe_2$ to phthalocyanine (H_2Pc) are found to result in spin polarization lifetimes that are one order of magnitude longer than those in the TMD alone. These findings connect valleytronic properties of TMD monolayers to spin-polarized interfacial charge transfer and suggest a viable route towards spin-selective photocatalysis [1].

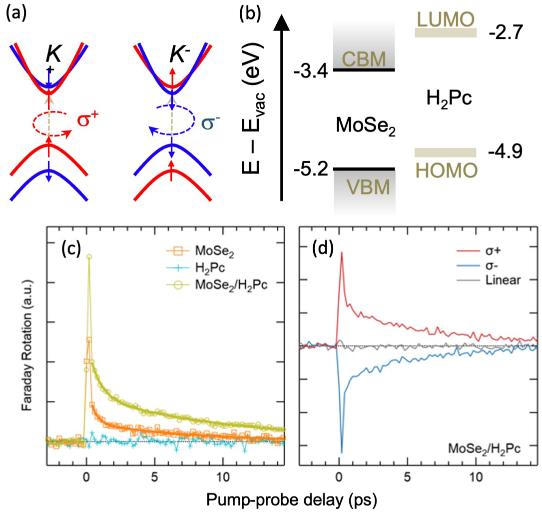

Fig. 1. (a) Photo-excitation of spin-polarized electrons/holes from spin-valley locking in transitional metal dichalcogenide monolayers; (b) Energy alignment at the $MoSe_2/H_2Pc$ interface; (c) Time-resolved Faraday rotation (FR) following resonant excitation of the A-exciton in $MoSe_2$. Hole transfer from $MoSe_2$ to H_2Pc increases the spin polarization time by one order of magnitude; (d) The sign of FR flips in accordance with the sense of circular polarization of the pump.

The PIs are coupling this experimental platform to chiral electron and hole acceptors for further spin selection and filtering in photo-induced interfacial charge transfer based on the chiral induced spin selectivity (CISS) effect. The PIs have developed a new class of electron acceptor molecules with unmatched chiro-optical properties based on helically perylene diimides (PDI) oligomers [2,3]. Experiments are underway to combination of spin-selective photoexcitation with CISS in electron transfer dynamics.

[1] Liu, et al. "Spin-Polarized Charge Separation at Two-Dimensional Semiconductor/Molecule Interfaces," *J. Am. Chem. Soc.* **2024**, *146*, 10.1021/jacs.4c00956\

[2] Bao, et al. "Remote control of dynamic Twistacene chirality," *J. Am. Chem. Soc.* **2022**, *144*, 18772-18777.

[3] Xiao, et al. "Single-handed Helicene nanoribbons via transfer of chiral information," *J. Am. Chem. Soc.* **2022** *144*, 20214-20220.

Modeling Electrochemical Vacancy Regeneration in Single-Walled Carbon Nanotubes

Jana Jelušić, Jan Paul Menzel, Quentin C. Bertrand, Robert H. Crabtree, Hailiang Wang, Gary W. Brudvig, Victor S. Batista
Department of Chemistry
Yale University
New Haven, Connecticut 06520

Synthesis-induced surface defects enable single-walled carbon nanotubes (SWCNTs) to catalyze a variety of useful reactions. However, the exact nature of the catalytic intermediates, their reactivity, and how the active species regenerate is still poorly understood. Here, we employ a quantum mechanics/molecular mechanics (QM/MM) hybrid methodology based on density functional theory (DFT) and a classical force-field, to investigate the reactivity of a single-carbon vacancy on the surface of a zigzag SWCNT and its subsequent electrochemical regeneration.

Our findings indicate that the single-carbon type of defect (structure **1** in **Fig. 1**) undergoes hydrolysis, resulting in the formation of a ketone group on one carbon and C—H bonds on two other carbons, all three carbons being immediately adjacent to the defect (structure **2** in **Fig. 1**). Applying an electrochemical potential of E_{SHE} = -0.740 V induces a proton-coupled electron transfer (PCET) to the ketone, forming a hydroxyl group (structure **3** in **Fig. 1**). Further reduction at a potential of E_{SHE} = -1.08 V induces a PCET that expels the hydroxyl group as water, thereby regenerating carbon **1** for further reactions. The hydrogen atoms on the remaining two carbons are retained, preventing further water dissociation, and maintaining the vacancy with catalytic function. In addition to the observed reactivity with water, we find that hydrogen peroxide and perchlorate can also react with the restored nanotube vacancy.

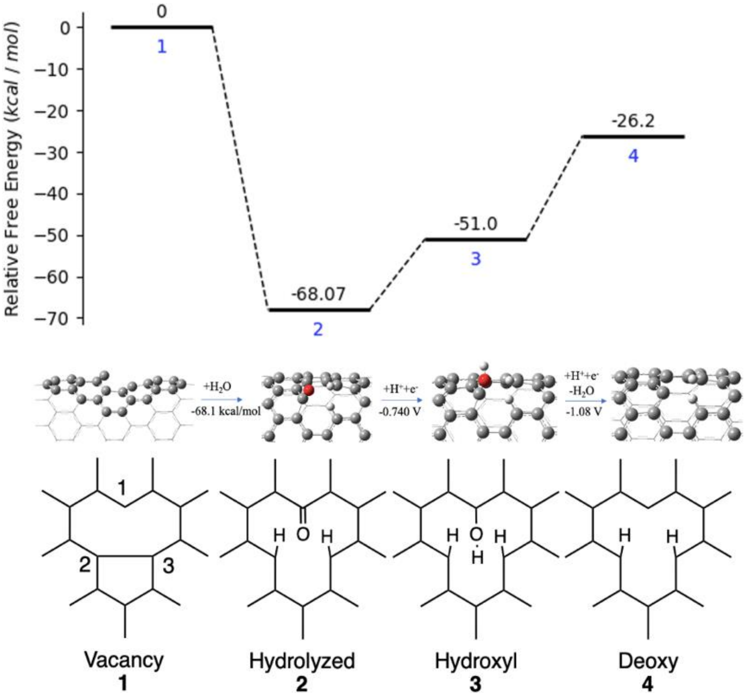

Fig. 1: Structural defects of SWCNT: **1** is the initial form of the vacancy, including the carbon atom numbering, **2** is the hydrolyzed form with two C—H bonds and a keto group, **3** is the one-electron, one-proton reduced hydroxyl form, and **4** is the deoxy form that has retained the two C—H bonds.

In future work, we aim to expand the scope of this electrochemically active carbon-based system towards photochemical applications by further functionalizing the vacancies with molecular organic chromophores, which will allow for light-driven vacancy regeneration and subsequent catalytic conversions.

Voltage-induced Inversion of Band Bending and Photovoltages at Semiconductor/liquid Interfaces Using *In Situ* Spectroscopy

Ruoxi Li, Marcos Gabriel Yoc-Bautista, Sizhe Weng, Zhi Cai, Bofan Zhao
and Stephen B. Cronin
Departments of Chemistry, Physics, and Electrical Engineering
University of Southern California
Los Angeles, CA 90089

At semiconductor/liquid interfaces, the surface potential and photovoltages are produced by a combination of band bending and quasi-Fermi-level splitting at the semiconductor surface, which are usually treated in a qualitative fashion. As such, it is important to develop quantitative metrics for the band energies and photovoltages at these interfaces. Here, we present a spectroscopic method for monitoring the photovoltages produced at semiconductor/liquid junctions.[1] Surface reporter molecule mercaptobenzonitrile (MBN) is functionalized on the photoelectrode surface (*p*-type silicon) and is measured using *in situ* surface enhanced Raman scattering (SERS) spectroscopy with a water immersion lens under electrochemical working conditions. In particular, the vibrational frequency of the C≡N stretch mode (ω_{CN}) around 2225 cm^{-1} is sensitive to the local electric field in solution at the electrode/electrolyte interface via the vibrational stark effect. Over the applied potential range from -0.8 V to 0.6 V vs Ag/AgCl, we observe ω_{CN} to increase from 2220 to 2229 cm^{-1} (at low laser power). As the incident laser power is increased from 83.5 µW to 13.3 mW, we observe additional shifts of $\Delta\omega_{\mathrm{CN}} = \pm 1$ cm^{-1}, corresponding to photovoltages produced at the semiconductor/liquid interface $\Delta V = \pm 0.2$ V. Based on Mott-Schottky measurements, the flat band potential (FBP) occurs at -0.39 V vs. Ag/AgCl. For applied potentials above the FBP, we observe $\Delta\omega_{\mathrm{CN}} > 0$ (i.e., blueshifts ~1 cm^{-1}) corresponding to positive photovoltages, whereas, for applied potentials below the flat band potential, we observe $\Delta\omega_{\mathrm{CN}} < 0$ (i.e., redshifts ~1 cm^{-1}) corresponding to negative photovoltages. These spectroscopic observations indicate a voltage-induced inversion in the band bending at the semiconductor/liquid junction which, thus far, have been difficult to measure.

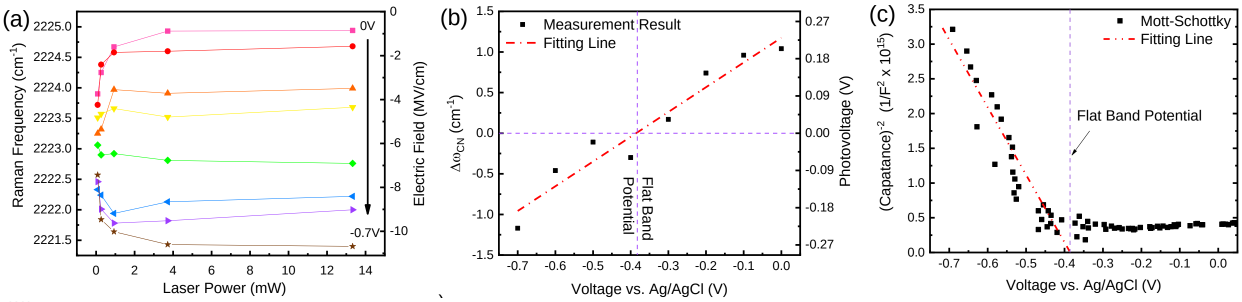

Figure 1. (a) Raman shifts of the C≡N stretch mode taken under various applied potentials plotted as a function of laser power on *p*-type silicon. (b) Maximum photoinduced change in Raman shift ($\Delta\omega_{\mathrm{CN}}$) and corresponding photovoltage plotted as a function of applied potential. (c) Mott-Schottky plot and linear fit, indicating the flat band potential at -0.07V.

1. Li, R., M.G. Yoc-Bautista, S. Weng, Z. Cai, B. Zhao and S.B. Cronin, "Voltage-induced Inversion of Band Bending and Photovoltages at Semiconductor/liquid Interfaces". **ACS Applied Materials & Interfaces**, DOI:10.1021/acsami.3c14116 (2024).

Probing Hole QFLs and Redox-Site Distance in Oxide Photocatalysts

Haoqing Su, Devan Solanki, Shu Hu
Department of Chemical and Environmental Engineering
Yale University
New Haven, CT 06510

Particulate photocatalysts, usually in a powder suspension or immobilized on a panel, coevolve H_2 and O_2. The reduction and oxidation sites, supported on photocatalyst surfaces, are in nanoscale proximity. While co-evolving H_2 and O_2 is unsafe, instead, the field is moving on to redox-mediated water splitting: H_2-evolving photocatalysts will produce hydrogen while selectively oxidizing, e.g., I^- to IO_3^- in solutions; a dichroic mirror splits the solar spectrum to allow O_2-evolving photocatalysts to absorb the solar light unused by the H_2-evolving photocatalysts; and the O_2-evolving catalysts produce oxygen while selectively reducing, e.g., IO_3^- back to I^- in a second solution.

In all cases of, e.g., H_2/O_2 coevolution, redox-mediated source-separated water splitting, or other fuel-forming reactions coupled to water oxidation via redox couples, photocatalysts involve light absorption, charge separation, charge transfer with trapping or accumulations at surfaces, surface catalysis, and chemical transport across multiple scales. Furthermore, neutral pH or vapor-phase photocatalysis opens up opportunities to repair pinhole defects with molecular materials, thus expanding durability.

O_2-evolving photocatalysts have deep O 2p or N 2p levels at the valence band maxima. Typically, their potentials (vs. RHE) are too positive to impose a challenge for electrochemical contact probing. On the materials front, we first developed a hole-selective back contact for oxide photocatalysts. This contact is a thin-film oxide with a deep O 2p level to probe hole (quasi-)Fermi levels (QFLs) of commonly studied photocatalysts such as Al:$SrTiO_3$ or $BiVO_4$. The hole-selectivity was achieved by alloying $SrTiO_3$ with Rh to make Rh:$SrTiO_3$. This thin film can make metallurgical contacts with particle and model thin-film photoabsorbers. Using this hole-selective back contact and open-circuit potential (OCP) measurements in H_2/O_2 gas mixtures as a characterization framework, we studied different photocatalyst/water interfaces. We show that even Ir dinuclear molecular co-catalysts and colloidal IrO_x co-catalysts show high water oxidation activity. When these co-catalysts are supported on $SrTiO_3$ photocatalysts, the water-oxidation activity is not the best under the same light intensity, wavelength, and local H_2/O_2 concentrations.

Last but not least, we collaborate with Prof. Mike Mirkin to probe the spatial distribution of H_2-evolving and O_2-evolving rates, because these re-dox reactions are coupled at the nanoscale. We hypothesize that the distance between electron-accumulating reductive sites and hole-accumulating oxidative sites sensitively controls the quantum efficiency of solar photochemistry. The location away from active sites shall exhibit varying redox reaction rates, which can be probed by scanning electrochemical microscopy (SECM). During co-evolution, the reduction rates vary as SECM probes move away from the IrO_x or CoO_x O_2-evolving sites. Finally, we will generate a digital model to quantify and visualize the QFLs, band edge positions, and catalyst potentials that are spatially distributed under steady-state light illumination. Our immediate next step is to perform light-dependent and wavelength-dependent studies to validate our digital model.

Triplet Energy Transfer and Dissociation at Organic-Inorganic Interfaces

Angana De, Qiushi Ma, and Libai Huang
Department of Chemistry, Purdue University, West Lafayette, IN 47907

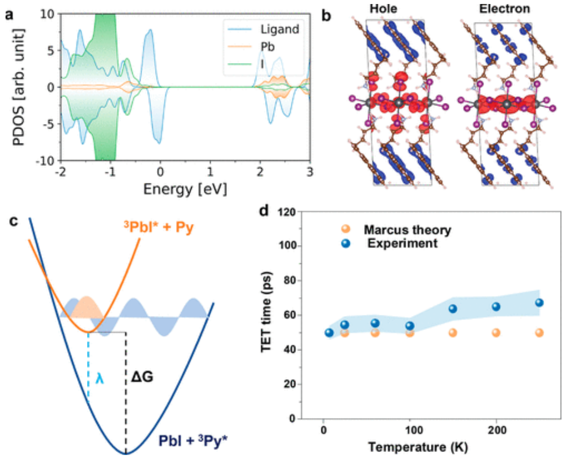

Figure 1. Energy transfer from 2D lead iodide perovskite to the triplet excitons in pyrene ligands. (a) Spin-polarized projected density of states (PDOS) for the $(PyBA)_2PbI_4$ system. (b) Charge density difference between the final and initial orbitals of hole (left) and electron (right) involved in TET. (c) Schematic of the Gibbs free energy surfaces as a function of the nuclear configuration of TET from Pb-I to pyrene in the Marcus inverted regime ($\lambda < -\Delta G^{\circ}$), depicting the enhanced vibrational overlap between the donor-acceptor wavefunctions. (d) Plot showing the theoretically predicted (orange) and experimentally extracted (blue) TET timescales as a function of temperature, depicting the tunneling induced weak T- dependence of the triplet transfer rate.

Scope of the Project. In this project, we focus on investigating exciton transfer, transport, and dissociation at organic-inorganic Interfaces, which can play a critical role in converting light into electricity and fuels. Here, we discuss our results exploiting heterostructures that combine two-dimensional semiconductors with organic triplet excitonic materials which offer new opprtunities for designing efficient triplet exciton transfer and dissociation functionalities.

Tunneling driven Marcus-inverted triplet energy transfer in a two-dimensional perovskite. Triplet energy transfer (TET) is a crucial, and often, the rate determining step in processes such as photon upconversion and phosphorescence based light emitting diodes. Quantum tunneling, a phenomenon that allows particles to pass through potential barriers, can play a critical role in energy transfer processes. In collaboration with Prof. Oleg Prezhdo, we demonstrate that the proper design of organic-inorganic interfaces in two-dimensional (2D) hybrid perovskites allows for efficient triplet energy transfer (TET), where quantum tunneling of the excitons is the key driving force (**Fig.1**). By employing temperature-dependent and time-resolved photoluminescence and pump-probe spectroscopy techniques, we establish that triplet excitons can transfer from the inorganic lead iodide sublattices to the pyrene ligands with rapid and weakly temperature-dependent characteristic times of approximately 50 ps. The energy transfer rates obtained based on the Marcus theory and first-principles calculations show good agreement with the experiments, indicating the efficient tunneling of triplet excitons within the Marcus inverted regime is facilitated by high-frequency molecular vibrations.

Triplet energy transfer at 2D-acene Interfaces. In collaboration with Dr. Justin Johnson, we demonstrate that 2D layers of transition metal dichalcogenides (TMDCs), such as WS_2, can serve as effective triplet acceptors and donors for singlet fission occurring pentacene derivatives. We performed temperature-dependent transient absorption spectroscopy to probe the energy and charge transfer pathways, tracking the dynamics of ^{1}[TT]. By tuning the acene molecular structures and energy band alignment, we show that exciton transfer to ^{1}[TT] as well as dissociation of ^{1}[TT] can occur at TMDC-acene interfaces on the sub-nanosecond timescale.

References: 1. Angana De, et al., *J. Am. Chem. Soc.* **146**, 6, 4260–4269, (2024).

Intermediate Transport Pathways in Electrochemical CO Reduction on Cu

Joel W. Ager, Peter Agbo, Frances A. Houle, Junko Yano,
Chansol Kim, Sydney Hemenway, Helen J. Zeng
Chemical Sciences Division, Material Sciences Division,
Molecular Biophysics and Integrated Bioimaging Division
Lawrence Berkeley National Laboratory
Berkeley, California 94720

Single electrocatalysts and photocatalysts cannot selectively convert CO_2 into a specific reduced product more complex than CO. To achieve this functionality, one must use multiple catalysts organized into a tandem cascade (**Figure 1**), which offers a means of generating complex chemicals with improved specificity by providing a channel for the reduction of CO and similar intermediates.[1] The rules for how to select catalysts for this purpose and design systems that have a high degree of chemical control using them are not known however. The efficiency and selectivity for individual catalysts may be optimized, but the resulting efficiency of an entire system will depend on how well the timings of all the chemical steps in the cascade as well as transport between the catalysts are managed.

Figure 1. Structure of a typical higher-plant chloroplast with green chlorophyll contained in stacks of disk-like thylakoids. Inset: Illustration of a two-step catalytic cascade using CO as an intermediate for the conversion of CO_2 to form higher hydrocarbons.[1]

Our project is inspired by the ways in which control is exerted in natural photosynthetic systems which use cascaded reactions to convert CO_2 from the air into sugars using sunlight as the sole source of energy. These cascades take place within complex architectural elements that ensure that the chemistry is as efficient as possible. Interestingly, photosynthetic organisms counteract the nonproductive photorespiration process by adopting a CO_2 concentration mechanism (CCM), whereby the encapsulation of the Rubisco enzyme maximizes turnover and outcompetes oxygenase activity. A prime example is the *chlamydomonas* (green alga) that utilizes three compartments (matrix, thylakoid and stroma) to increase the concentration of CO_2 in the matrix and activate the Rubisco. This multicompartment strategy presents a synchronous interplay of capture, intermediate transport, and conversion events, with rate matching of sequential events and maintaining the delicate balance of CO_2 and HCO_3^- supplies. Understanding the functions of these natural design elements is the key and extending them to artificial photosynthetic systems will prove to be useful, as the latter are subject to the same constraints.

An analogous inorganic system which could store the simplest building blocks (C_1) would be a promising candidate to employ as part of the tandem cascade. Our recent findings reveal that copper, in particular, oxide-derived Cu nanoparticles (OD-Cu NPs), is able to perform this storage action.[2] In an adaptation of chemical transient kinetics to electrocatalysis, the dynamic response of a gas diffusion electrode (GDE) cell was measured when the feed gas is abruptly switched between Ar (inert) and CO. After CO supply ceases, CO reduction (COR) is maintained for several seconds (t_{delay} = ~5 s). A three-site microkinetic model (**Figure 2a**) captures the observed dynamic

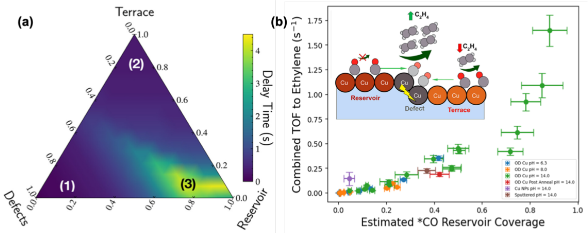

Figure 2. (a) Ternary phase diagram of predicted delay time with *CO coverage on three major sites and **(b)** scheme of the proposed three-site model (inset) with a plot showing a positive correlation between the estimated reservoir *CO coverage and the combined TOF to ethylene, based on different Cu samples and electrolyte pH.[2]

behavior and shows that Cu catalysts exhibiting delay times have a less active *CO reservoir linked by an efficient diffusion channel to active C-C coupling sites (**Figure 2b, inset**).

Moreover, the *CO reservoir sizes can be controlled by different catalyst preparation, applied potential, and microenvironment (electrolyte cation identity, electrolyte pH, and CO partial pressure). Notably, the OD-Cu NPs had the longest delay time and thus highest estimated *CO reservoir surface coverage (~88%) at high overpotentials (−1.52 V vs. SHE), followed by the post-annealed OD-Cu NPs, sputtered Cu and lastly, as-purchased (Cu NPs) as displayed in **Figure 2b**. The increase in reservoir coverage also coincides with increased turnover frequencies to ethylene, further exemplifying the importance of the reservoir sites and its role in promoting formation of higher-order carbon products. Clearly, the active C–C coupling sites by themselves do not control selectivity to C_{2+} products in electrochemical COR; the supply of CO to those sites is also crucial.

Considering all of the above, the overall activity of Cu electrocatalysts cannot simply be approximated from linear combinations of individual site activities. Instead, one must consider the diversity of the sites in the catalyst network and account for inter-site transportation pathways. For example, we estimate that in the most active electrocatalysts we studied, CO travels substantial distances (up to 10s of nm), and encounters 10-100 active C-C coupling sites, before its eventual conversion. The Sabatier-based argument for the design of active sites should also be reconsidered. That is, a higher than optimal binding energy for a reactant can be beneficial if it can fuel the activity of other sites in the network.

Focusing on the local concentrating mechanisms and the mobility of reactants, we identify two key guidelines for the design of tandem catalytic systems for CO_2 reduction:

(1) Incorporate a reservoir region. The reservoir will be useful if the reactant being stored is part of the rate determining step, and not competing for surface coverage.
(2) Explicitly optimize for diffusion and multiple adsorption/desorption events and the resultant diffusion pathways.

In our ongoing work, we are using these guidelines to investigate CO_2R and COR electrocatalysts and are developing concepts to manage the reaction intermediates as a function of time to tune selectivity.

DOE Solar Photochemistry Sponsored Publications

1. Houle, F. A.; Yano, J.; Ager, J. W. Hurry Up and Wait: Managing the Inherent Mismatches in Time Scales in Natural and Artificial Photosynthetic Systems. *ACS Catal.* **2023**, *13* (11), 7139–7158. https://doi.org/10.1021/acscatal.3c00355.
2. Kim, C.; Govindarajan, N.; Hemenway, S.; Park, J.; Zoraster, A.; Kong, C. J.; Prabhakar, R. R.; Varley, J. B.; Jung, H.-T.; Hahn, C.; Ager, J. W. Importance of Site Diversity and Connectivity in Electrochemical CO Reduction on Cu. *ACS Catal.* **2024**, *14* (5), 3128–3138. https://doi.org/10.1021/acscatal.3c05904.

Photoconversion Quantum Efficiencies of ca. 160% due to Spin-Exchange Carrier Multiplication in Manganese-Doped ‘Inverted’ CdSe/HgSe Quantum Dots

Jungchul Noh, Clément Livache, Valerio Pinchetti, Donghyo Hahm, Ho Jin, Victor I. Klimov
Nanotechnology and Advanced Spectroscopy Team, C-PCS, Chemistry Division
Los Alamos National Laboratory, Los Alamos, New Mexico 87545, USA

Carrier multiplication (CM) is a process whereby a single absorbed photon generates multiple excitons. CM can potentially benefit solar photovoltaics (PV), photochemistry, and photodetection. In a standard scenario, CM occurs due to a Coulombic collision of an energetic, *hot* carrier with a valence-band electron promoting it across the bandgap. A competing energy-relaxation pathway is fast phonon-assisted cooling, which is the major factor limiting CM yields.

Here, we show that this limitation can be overcome by employing not direct but *spin-exchange (SE) Coulomb interactions* in Mn-doped core/shell CdSe/HgSe quantum dots (QDs). Previously, we realized SE-type CM (SE-CM) using Mn-doped PbSe/CdSe QDs (H. Jin *et al.*, *Nat. Mater.* **22**, 1013, 2023). In the present study, we enhance this effect by exploiting a ~10-fold enhancement in exchange coupling in a Mn-HgSe system *vs*. that in Mn-PbSe structures. Furthermore, we ‘invert’ a core/shell structure by placing a lower bandgap material in the shell region. This makes both an electron and a hole electrically accessible - a beneficial distinction from PbSe/CdSe QDs wherein holes are core-localized and, therefore, are not readily extractable.

In the developed Mn:CdSe/HgSe structures, SE-CM occurs via two steps (Fig. 1a): (1) SE-energy transfer from a ‘hot’ exciton generated in the CdSe core to an interfacial Mn ion, followed by (2) energy- and spin-conserving relaxation of the excited Mn ion to create two excitons (bright and dark) in the HgSe shell. Due to extremely short SE time scales (<300 fs; C. Livache et al., *Nat. Phot.* **16**, 443, 2022), both SE steps occur without considerable interference from phonon emission, which leads to high SE-CM efficiencies.

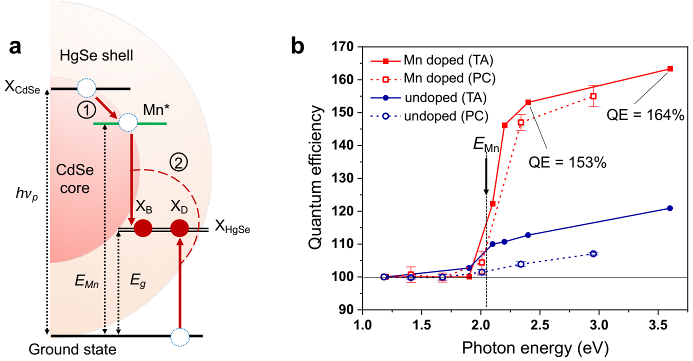

Figure 1. (a) Two-step SE-CM in Mn:CdSe/HgSe QDs and (b) resulting QEs derived from TA (red solid symbols) and photocurrent (PC; red open symbols) measurements. Blue symbols are QEs obtained for a reference undoped QD sample.

Transient absorption (TA) measurements with spectrally tunable pump pulses indicate a sharp onset of SE-CM near the energy of the Mn spin-flip transition (E_{Mn} = 2.1 eV; Fig. 1b). The measured quantum efficiency (QE) of photon-to-exciton conversion exhibits a step-like growth and reaches ~160%. Importantly, due to an ‘inverted’ architecture of our CdSe/HgSe QDs, SE-CM also leads to a considerable enhancement of a photocurrent in close-packed QD films. The QEs obtained from photocurrent measurements are in excellent agreement with those inferred from the TA studies (Fig. 1b).

In our future work, we plan to employ SE-CM to drive a model photochemical reaction such as conversion of H_2S (waste gas) to H_2 and sulfur. Since H_2 generation requires 2 electrons, we expect favorable changes in reaction kinetics due to *pair-wise production of excitons via SE-CM*.

Elucidating the Dynamic Surfaces of Solar Photocatalysts

Karthish Manthiram, Benjamin Moss; Division of Chemistry and Chemical Engineering
John M. Gregoire, Kevin Kan, Ryan J. R. Jones, Dan Guevarra; Division of Engineering and Applied Science
California Institute of Technology
Pasadena, CA 91125

Operational durability of solar fuels materials is poorly characterized by traditional (photo)electrocatalyst discovery workflows, creating a barrier to both fundamental understanding and technology deployment. We present 3 phases of program development to elucidate the dynamic surfaces of electrochemical materials: 1) the establishment of a high throughput screening system, the accelerated durability screening system (ADSS), which was completed this year; 2) the development of artificial intelligence (AI) for on-line decision making in the operation of durability characterization instruments, as demonstrated on a system that uses optical detection of corrosion; and 3) the development of a spectroelectrochemistry instrument to characterize the evolution of electrode surfaces en route to their realization as active (photo)electrocatalysts, which is the planned focus for next year.

Corrosion is a prominent degradation mechanism whose thermodynamics depend on the concentration of corrosion products in electrolyte. The ADSS [Kan et al., ChemCatChem 2024, doi: 10.1002/cctc.202301300] is an automated system for characterizing the equilibration of (photo)electrodes with dissolved metals in electrolyte for a given electrode, pH, and electrochemical potential. Automation of electrode selection, electrolyte preparation, and electrolyte aliquoting enables rapid identification of self-passivating electrodes and estimation of the equilibrium dissolved metals concentrations. The technique is demonstrated for metal oxide photoanodes in alkaline electrolyte, where $BiVO_4$ is found to continually corrode, in agreement the literature. An amorphous Ni-Sb-O photoanode is found to passivate with a Ni-rich coating on the order of 1 monolayer with less than 1 μM total dissolved metals in electrolyte, demonstrating its suitability for durable photoelectrochemical operation. The automation and throughput of the instrument are designed for incorporation in accelerated electrocatalyst discovery workflows so that durability can be considered on equal footing with activity.

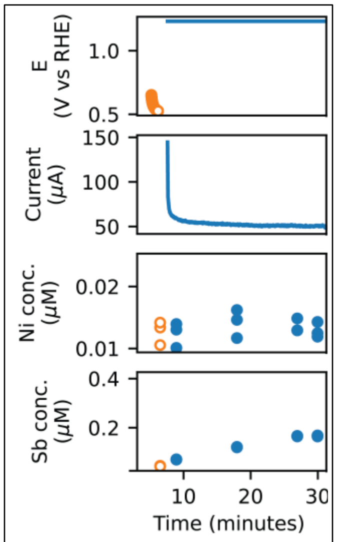

ADSS characterization of a Ni-Sb-O electrode under illumination, showing equilibration at ca. 1 μM total dissolved metals.

To build toward AI control of the ADSS, we are prototyping active learning algorithms on a complementary instrument that measures optical transmission during electrochemical operation to detect the onset of changes to the electrode, which are typically due to corrosion. By choosing the electrode material, the starting potential, and the potential sweep direction, the AI algorithm can rapidly map the voltage stability windows of solar fuels materials. Bolstered by this combination of spectroscopy, electrochemistry, and AI, we will seek to realize a new instrument with sufficient sensitivity of optical transmission detection to observe subtle changes to electrode surfaces.

Coherence as a Probe for Dynamics of Excitons, Exciton-Polarons, and Electron Transfer

Somnath Biswas, Yuanheng Wang, Alfy Benny and Gregory D. Scholes
Department of Chemistry
Princeton University
Princeton, NJ 08540

There are a rich variety of ways molecules can interact with each other and their environment, and the span of possible timescales—from femtoseconds to nanoseconds. Surely details beyond an equilibrium picture occasionally matter! Clearly, experiments need to reveal another "layer" of information—beyond kinetics—to inform sophisticated theoretical models. We have been developing methods in this program that have succeeded to reveal new mechanistic detail about photoinduced dynamics. In the poster, experimental examples will be discussed with support from relevant quantum dynamics calculations.

In a recent study [1], we established the robust polaronic nature of the excitons in two-dimensional Dion-Jacobson-type materials at room temperature by combining ultrafast spectroscopy and electronic structure calculations, figure below. The work answers an open question about the functional role of exciton-phonon interactions. We show that polaronic distortion is associated with low-frequency lead iodide lattice motions. More importantly, we discover how targeted ligand modification of this two-dimensional perovskite structure can modify exciton-phonon coupling, exciton-polaron population, and carrier cooling. At high excitation density, stronger exciton-phonon coupling increases the hot carrier lifetime, forming a hot-phonon bottleneck.

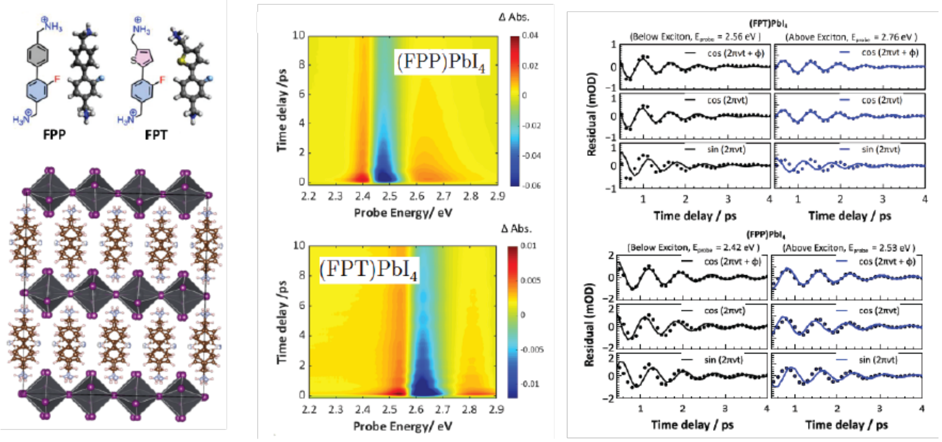

We will conclude by reporting new quantum dynamics simulations based on the time-dependent density matrix renormalization group method. The method enables realistic calculations of the interplay of all vibrational modes in the reaction coordinate of the electron transfer reaction we reported previously. We thus obtain new insights into the spontaneous development of vibrational coherence and nature of ballistic electron transfer in the Marcus inverted regime. Our work suggests open questions and new experimental directions.

[1] S. Biswas, F. Alowa, R. Zhao, M. Zacharias, S. Sharifzadeh, D.F. Coker, D.S. Seferos, G.D. Scholes, *Nature Materials* (accepted, 2024).